FSTC-HT-23-118-70

ARMY MATERIEL COMMAND

U.S. ARMY
FOREIGN SCIENCE AND TECHNOLOGY CENTER

METHODS AND DEVICES FOR THE CONVERSION OF GRAPHIC DATA

by

V. P. SIGORSKIY

COUNTRY: USSR

This document is a rendition of the original foreign text without any analytical or editorial comment.

Approved for public release; distribution unlimited.

748

UNCLASSIFIED
Security Classification

DOCUMENT CONTROL DATA - R & D

(Security classification of title, body of abstract and indexing annotation must be entered when the overall report is classified)

1. ORIGINATING ACTIVITY (Corporate author)
Foreign Science and Technology Center
US Army Materiel Command
Department of the Army

2a. REPORT SECURITY CLASSIFICATION
Unclassified

2b. GROUP

3 REPORT TITLE

Methods and Devices for the Conversion of Graphic Data

4 DESCRIPTIVE NOTES (Type of report and inclusive dates)
Translation

5 AUTHOR(S) (First name, middle initial, last name)

V. P. Sigorkiy

6 REPORT DATE	7a. TOTAL NO. OF PAGES	7b. NO. OF REFS
18 May 1972	244	N/A

8a. CONTRACT OR GRANT NO.

b. PROJECT NO.

c. T702301 2301

d. Requester AMXST-GET Mr. Smith

9a. ORIGINATOR'S REPORT NUMBER(S)
FSTC-HT-23- 118-70

9b. OTHER REPORT NO(S) (Any other numbers that may be assigned this report)
ACSI Control Number J-8547

10 DISTRIBUTION STATEMENT

Approved for public release; distribution unlimited.

11 SUPPLEMENTARY NOTES

12. SPONSORING MILITARY ACTIVITY
US Army Foreign Science and Technology Center

13 ABSTRACT

This book considers a wide range of questions relating to the theory and design of graphic data converters, as well as converter design and graphic converters.

This collection fo articles is intended for scientific workers and engineers interested in the technology of computer-aided, graphic-data processing.

DD FORM 1 NOV 65 1473 REPLACES DD FORM 1473, 1 JAN 64, WHICH IS OBSOLETE FOR ARMY USE.

UNCLASSIFIED
Security Classification

14. KEY WORDS	LINK A		LINK B		LINK C	
	ROLE	WT	ROLE	WT	ROLE	WT
Graphic data Processing Data processing Computer application Computer component Digital computer Computer circuit Computer aided design COSATI Subject Code: 09 COUNTRY CODE: UR						

TECHNICAL TRANSLATION

FSTC-HT-23-118-70

ENGLISH TITLE: METHODS AND DEVICES FOR THE CONVERSION OF GRAPHIC DATA

FOREIGN TITLE: METODY I VSTROYSTVA PREOBRAZOVANIYA GRAFICHESKOY INFORMATSII

AUTHOR: V. P. SIGOVSKIY

SOURCE: "Naukova Dumba,", 1968, 220 pages

Translated for FSTC by ACSI

NOTICE GRAPHICS NOT REPRODUCIBLE

This translation was accomplished from a xerox manuscript. The graphics were not reproducible. An attempt to obtain the original graphics yielded negative results. Thus, this document was published as is, in order to make it available on a timely basis.

NOTE

The following pages from the original manuscript were missing:

Pages: 58, 112, 113, 144, 145

METHODS AND DEVICES FOR THE CONVERSION OF GRAPHIC DATA

[Collection of works edited by Doctor of Technical Sciences V. P. Sigorskiy: Kiev, Metody i Ustroystva Preobrazovaniya Graficheskoy Informatsii (English as above), Russian, "Naukova Dumka," 1968, 270 pp]

CONTENTS

SUMMARY

Metody i Ustroystva Preobrazovaniya Graficheskoy Informatsii (Methods and Devices for the Conversion of Graphic Data), 1968, page 2

The book considers a wide range of questions relating to the theory and design of graphic-data converters as well as converter design and describes graphics converters, their components and circuit elements.

Questions relating to the improvement of the operating characteristics of devices for the recording and conversion of graphic information are also covered, as well as questions concerning information output from electronic computers in graphic form.

This collection of articles is intended for scientific workers and engineers interested in the technology of computer-aided graphic-data processing, and is useful for graduate and undergraduate students specializing in the field of automation, computer technology and technical electronics.

GRAPHIC-DATA CONVERSION AS A SCIENTIFIC AND TECHNICAL PROBLEM

Metodi i Ustroystva Preobrazovaniya
Graficheskoy Informatsii (Methods
and Devices for the Conversion of
Graphic Data), 1968, pages 3-7

V. P. Sigorskiy

Graphic information plays an important role in many fields of science and technology. Contributing to this is the fact that, of all the modes of data representation, the graphic form is the most vivid, assuring the quickest human perception of studied phenomena. Naturally, in the pursuance of various scientific investigations and design and planning projects wide use is made of the paper or photographic film records of recording and control devices (one- and two-coordinate, single- and multichannel), design graphs, drawings, charts and a variety of half-tone graphic images (aerial photographs, photographs in the visual field of a microscope, bubble and spark chambers, detection and guidance systems etc.).

Weather satellites transmit information on the thermal state of the atmosphere and its cloud cover, which is recorded subsequently on motion picture film and projected on a screen. The processing of this information requires its representation in digital code. The field of construction and architecture displays increased interest in computer-aided designing. Seismic prospecting has at its disposal extensive archives of photographic recordings of earth tremors, which are constantly augmented with new experimental material. These recordings must be represented in digital form in order to be processed.

The list of fields of human activity in which the processing of information represented in graphic form plays a leading part could be extended even further. The problem of processing such information on an electronic computer can be solved if the computer is supplied with data input and output devices.

An indication of the great interest in the problem under consideration is the success of the Symposium on Methods and Devices for the Conversion of Graphic Data for Input into Electronic Computers, held in Kiev 28-30 November 1966 by the Scientific Council on Cybernetics of the Academy of Sciences Ukrainian SSR, the Ukrainian Board of the Scientific and Technical Society of Radio Engineering and Telecommunications imeni A. S. Popov in conjunction with the Republic "Znaniye" (Knowledge) Society and the Kiev Polytechnic

Institute Participants in the symposium included 376 delegates from 173 organizations and enterprises in 42 Soviet cities.

The symposium heard and discussed 67 papers (most of which are presented in the present collection), in which the following questions were considered.

1. Methods for the information assessment of graphs and algorithms for their processing by computer (graphic-data recording equipment, information attributes of graphs and their relation to parameters of described processes, methods for the functional and statistical analysis of graphs, coding the output information of conversion devices and their relation to the computer, the formation and rearrangement of an initial data file, requirements for conversion accuracy, sampling rate etc.).

2. Methods for the conversion of graphic data (optoelectronic converter (OEC) for graphic-data sampling, automatic recognition of colors of curves and carriers, automatic and semiautomatic graph converters, the follow, scanning and combined methods for conversion of graphs of single-valued functions, reading of graphs with line gaps, equipment and algorithmic methods for separation of intersecting curves, reading of graphs of non-single-valued functions and graphic two-dimensional mappings of functions of two or more variables etc.).

3. Devices for the conversion of graphic data and their use (converters of recordings of single- and multichannel self-recorders, converters of recordings of two-coordinate self-recorders; devices for input of drawings, bubble chamber photographs, topographical and geophysical maps etc. into computers, as well as examples of the use of such devices in commercial geophysics, medicine, chemistry, nuclear physics and other fields of scientific and experimental research).

The following organizational and coordination measures seem advisable in order to expand operations in the field of computer graphic peripherals. First of all, there should be a speed-up in the development of requirements and specifications for the complex of peripheral graphic equipment necessary for computers (devices for the coding of graphs and their construction, for reading and obtaining images on a CRT screen, for microfilm coding and reproduction etc.). It is advisable here that external input devices be developed in conjunction with output devices for the purpose of obtaining closed graphic data input-output systems from the computers necessary for the automation of planning and design work. Often the transition from an input regime to an output regime in an external device is accomplished by comparatively simple means (changing the program, replacing photohead with a printing head etc.).

Special-purpose graphic-data input and output devices make use of standard elements adopted in specific computers, as well as coding and input systems. General-purpose devices are capable of working in conjunction

with any computer, but they may also prove considerably more complex because of a significant difference in the organization of data input in the computers which are being produced.

Together with manufacturers, careful revision must be made of the technical requirements for graphic-data recording equipment which is now being produced, and changes made in them to simplify the subsequent automatic processing of the recordings obtained (for example, eliminating the monochromatism of metric grid and graph line, revising the system of notations for the intersection points of graphs and making auxiliary inscriptions in another color etc.). This way is doubtless more rational and economically advantageous than the creation of complex graph converters to sense poorly made recordings. However, the requirement laid down by the developers of input devices that the metric grid be eliminated altogether leads, in our view, to a disturbance of normal operating conditions since visual evaluation and automatic processing are often combined.

The prospects for the development of computer graphic peripherals are naturally estimated on the basis of needs today, when the graphic form of recording measurement results is most popular. Consideration is given here to the wide use of recording equipment and the fact that it does not require much care and its production has been debugged, as well as the relatively low production cost of the instruments.

The rapid improvement in measuring devices with digital readout and magnetic recording, which began in the last few years, raises the legitimate question of the possibility of the future discontinuance of visual data-recording methods. This apparently will come about with the development of fully automated measuring systems in which a paper carrier is used merely as an intermediate long-term memory (and, what is more, not the best one). However, complex control and organization systems, whose duty cycle provides for human participation, will make wide use of the graphic form of recording in the future as well, owing to its visuality. Specifically, it will prove to be a rapid and convenient mode of man-computer communication, a unique graphical universal language.

At present, newly developed measuring equipment usually provides for two outputs: 1) on magnetic carrier for communication with the computer and 2) on paper tape for the research operator. Such a solution, in our view, is due in many respects to the lack of improved graphics converters which are as simple and reliable as magnetic readers.

The above remarks are true only of graphic information obtained in measurements. The volume of other types of graphic information (design, reference etc.) used in computer calculations will increase steadily within the visible future. As examples let us consider the possible operation of a complex of graphic peripherals together with a computer in the pursuance of calculation-and-drawing and design work. Thus, an engineer first makes a sketch of an article and inputs drawings and diagrams into a computer, and

the computer performs the necessary calculations (usually by the method of successive approximations) according to a given program and technical specifications. The result of the solutions at one (or each) of the stages is derived in graphic form, and the design developer can, by using a special "light pencil," correct a drawing or diagram, as well as enlarge any part of the output image or reproduce it in perspective at any angle, which significantly accelerates the designing or drafting process. The use of such an input regime is possible in the computer-aided planning of electronic circuits.

Another plan envisages the creation of a large graphic data system which contains a multitude of blueprints, plans and other documents on microfilm and permits, at the operator's option, the retrieval of a needed document, its digital coding for use in calculations, or its duplication.

Thus, the problem of creating external graphic devices for man-computer communication is more extensive and important than it may seem from the viewpoint of the current urgent problem of converting graphic measuring information. Effective solution of this problem requires the common efforts of all scientific institutions which are working on the automatic input of graphic data into computers, as well as industrial enterprises interested in the production and operation of the equipment being developed. In this case it can be expected that in the very near future several new models of converters of graphs of all types (including devices for the coding of non-single-valued functions and potential field maps) will be completed and put into series production, and in subsequent years computers will come complete with general-purpose external attachments and a library of microprograms for reading and mapping information in graphic form.

THE STATUS OF AND PROSPECTS FOR THE DEVELOPMENT OF METHODS AND DEVICES FOR THE CONVERSION OF GRAPHS FOR INPUT INTO COMPUTERS

Metody i Ustroystva Preobrazovaniya Graficheskoy Informatsii (Methods and Devices for the Conversion of Graphic Data), 1968, pp 8-29

A. I. Petrenko

Computer-aided automatic graphic data processing requires that the peripheral equipment of a computer incorporate several devices for the reading and recording of data in graphic form (these may be devices for the digitizing of graphs and their plotting, for obtaining microfilms and reading finished microfilms, for the reading and recording of text with letters and digits, for obtaining pictures on the screen of a cathode-ray tube and for reading them from the screen etc.). The input of graphic information into a computer and the receipt of output information, likewise in graphic form, will, evidently, in the not too distant future become as ordinary as input from punched cards.

Most of the work being done in this field is devoted to the input of graphs into a computer. Automation of this process, if possible, permits a substantial rise in the accuracy of data sampling, a significant increase in the processing rate and an improvement in the operator's working conditions in comparison with manual or semiautomatic input. Let us dwell briefly on the results achieved and the near-term problems to be solved.

Graphics converters can be subdivided according to the type of functions being transformed [26]: single-valued functions of one argument (recordings of ordinary single- and multichannel self-recorders), multiple-valued functions of one argument (recordings of two-coordinate self-recorders, letters and digits, drawings), functions of two or more arguments (topographical and geophysical maps etc.).

Each type of converter is a special-purpose device distinguished by its structure and operating principle. Common to all types of converters is the presence of an optoelectronic assembly for the sampling of graphic data, in which electric signals are formed which vary according to the value of the reflection coefficient or optical density of the individual elements isolated in turn on the carrier.

Optoelectronic Assembly

The isolation of the raster element to be studied on the carrier itself or its image, just as in television and photoelegraphy, is accomplished by electromechanical (a scanning disk with apertures or a photohead) or electronic means (CRT luminous spot, camera tube etc.). The design for an optoelectronic assembly is shown in Figures 1-3.

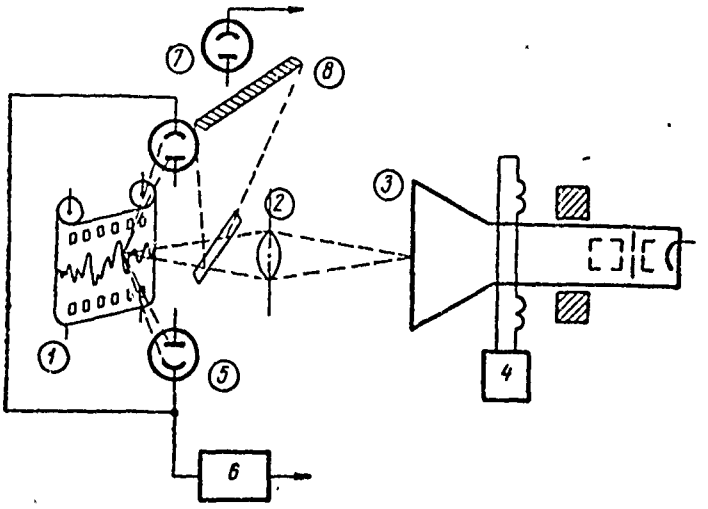

Figure 1. Optoelectronic assembly using CRT and photomultipliers:
1) carrier; 2) objective; 3) cathode-ray tube; 4) sweep generator;
5), 7) photomultipliers; 6) amplifier; 8) calibration scale.

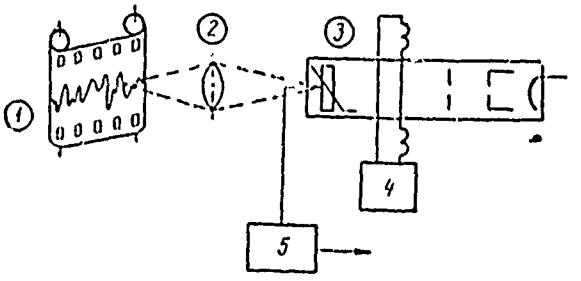

Figure 2. Optoelectronic assembly using Vidicon:
1) carrier; 2) objective; 3) vidicon; 4) sweep generator;
5) amplifier.

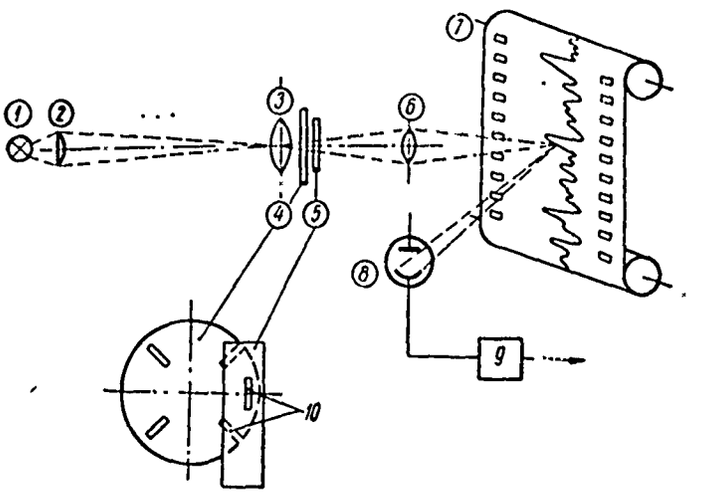

Figure 3. Optoelectronic electromechanical assembly:
1) light bulb; 2) condenser; 3) lens; 4) rotating disk;
5) fixed slit; 6) objective; 7) carrier; 8) photomultiplier;
9) amplifier; 10) slits 20 microns in width.

The quality of an optoelectronic assembly is determined by its resolution, speed of response, signal-to-noise ratio and operating characteristics. The resolution of an optoelectronic assembly using a CRT or vidicon depends on the resolution of the tube itself and the coefficient of linear magnification of the optics used, which in turn is determined by the size of the graph carrier. Tables 1 and 2 give the principal parameters of vidicons with magnetic control and cathode-ray tubes designed for black-and-white and color television flying-spot pickups. However, it should be borne in mind that the data of the manufacturer's certificate and operating and servicing manual must be employed with care, since the use of CRTs and vidicons in graph converters (and in a television automaton in general) has its own specifics, which can be seen graphically from the frequency and contrast response (aperture) characteristic of the instrument (Figure 4). The data-sheet resolution characteristic of television broadcasting systems, as a rule, is determined at a modulation level of 15-25 percent and amounts, say for the 13LK5L ("Onega") tube, to N = 2000 lines. In automatic television systems the modulation factor M is set at not less than 80 percent (to realize the necessary signal-to-noise ratio) [21], the realizable resolution therefore declines to 500 lines.

Table 1

Principal Parameters of Vidicons

Type of tube	Image size, mm	Resolution, number of lines	Illumination, luxes
LI-23	9.5x12.7	600	100
LI-401	12 x 100	500	10
LI-404	9.5x12.7	500	100
LI-409	18 x 18	800	8
LI-412	4.5x6.0	300	3
LI-411	9.5x12.7	550	1

Table 2

Parameters of Cathode-Ray Tubes

Type of tube	Resolution, number of lines	Tube diameter mm	Brightness, nits
18LK5L	2000	130	—
13LK5A	1800	130	—
13LK3B	800	130	—
18LK7B	1000	132	10,000
18LK9A	800 - [illegible]	180	300
18LK13L	800 - [illegible]	180	—
18LK14T	625 - 800	180	350

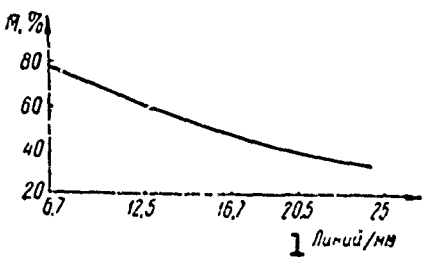

Figure 4. Frequency and contrast response characteristic of CRT

Key: 1. Lines/mm

Analogously, when vidicon LI-23 is used, only 180-200 lines can be realized instead of the data-sheet resolution of 600. Such a low resolution of present-day electron-beam tubes is holding back, in particular, the development of electronic photoelegraphy.

Maximum resolution is realized with the isolation of the raster element by electromechanical means in the optical image plane of the carrier, since the size of the diaphragm isolating the element can be very small. For example, in the "Frankenstein" device, designed to process photographs 35 mm wide obtained in a bubble chamber and Wilson cloud chamber [37], the absolute error of measurement does not exceed 5 microns, i.e., a resolution of about 700 lines. Such a method is most advisable for processing graphs recorded on wide carriers; the resolution of the optoelectronic assembly in this case is practically independent of carrier size.

Table 3

Parameters of Facsimile Transmitters

Type of apparatus	Maximum size of blank, mm	Resolution, number of lines/mm	Transmission spacing, mm	Scanning rate, rpm	Type of scanning
"Neva"	200 x 300	5	0.2 0.265	60 120 150	Circular
FTA-K	480 x 690	3.8	0.265 0.4	60 90 120	
FTA-P	200	5	0.2	120	Two-dimensional
"Prizma" (Prism)	110	4	0.25	300	
"Ladoga"	480	2.5	0.265 0.53	60 90 120	

In the development of graph converters use is often made of the scanners of series-produced facsimile apparatuses, the basic parameters of which are given in Table 3.

It should be noted, however, that because of peculiarities of the receiving apparatus (low resolution), optical magnification is not used in the plane of the diaphragm of the facsimile transmitter, i.e. the capabilities of the electromechanical scanning method are not utilized to the utmost.

The use of a fiber-optic converter in the optoelectronic assembly shows great promise [34]. Since manufactured fibers may have a diameter less than 0.025 mm, devices using such fibers possess high resolution and accuracy. An example is the optoelectronic assembly shown in Figure 5 with a fiber-optic coder, whose fibers on the entrance pupil are packed into one line close to each other, and on the exit pupil into a rectangular raster. The resolution of the converter is increased m-fold (m is the number of lines on the exit pupil). The measurement accuracy here, even if pickup tubes which are not optimal in resolution are used, is determined by the number of light guides, which can be reduced to 10^4.

The microminiaturization of electronic apparatus has raised the problem of replacing the unwieldy cathode-ray tube in the optoelectronic assembly with some light-deflection system utilizing the properties of optical crystals [35]. One possible variant of such a system is given in Figure 6. Here, in order to deflect a beam on one or two coordinates to any position out of a total number 2^n, use is made of n cells, consisting of the combination of a uniaxial crystal (for example, calcite), which possesses birefringence, and an optical switch (for example, potassium dihydrogen phosphate (KDP) crystal), which controls the direction of polarization of the light beam. Each cell can send a beam in only one of two possible directions; each subsequent cell doubles the number of possible positions of the beam.

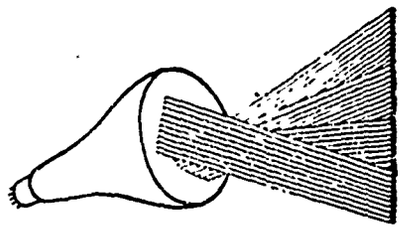

Figure 5. Optoelectronic assembly with fiber-optic coder.

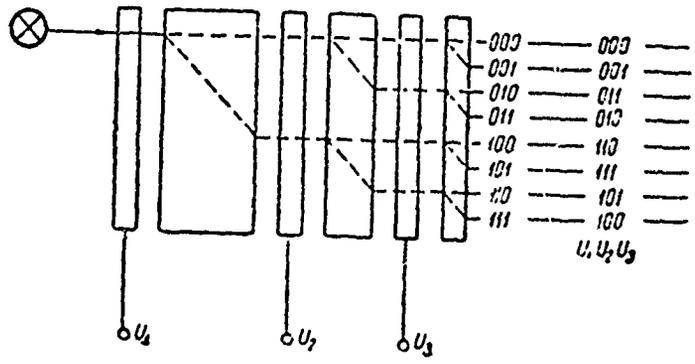

Figure 6. System of light deflection by crystals.

When a control voltage is applied to semitransparent electrodes on a KDP crystal support, there is a change in the plane of polarization of the beam. Depending on the direction of polarization, a beam passing through a calcium crystal is not deflected or is deflected by an amount proportional to the thickness of the crystal. The system described can be used with any light source. But in view of the fact that each crystal cell absorbs part of the luminous energy, it is convenient to use a high-power continuously operating helium-neon laser. The deflection rates which can be achieved are several megahertz at an acceptable power requirement level; the spot diameter is of the order of tens of microns.

Interesting possibilities for the improvement of graphic data converters are opened up by the use of scanistors in an optoelectronic assembly [20]. Scanistors are semiconductor devices with discrete or continuously distributed p-n junctions, which convert an image projected on their surface into time-variant current or voltage respectively. Figure 7,a gives the equivalent circuit of a scanistor. Each "target" element of the scanistor consists of a photodiode-diode pair, connected in series in reversed polarity. One end of each pair is hooked up to upper conducting bus 1, the second end to a resistance voltage divider. If alternating voltage is connected up to such a circuit, then at the moments of time when the voltage applied to it passes through zero and changes polarity, there is a sharp increase in the circuit current, the magnitude of the jump in current being determined by the illumination of the photodiode.

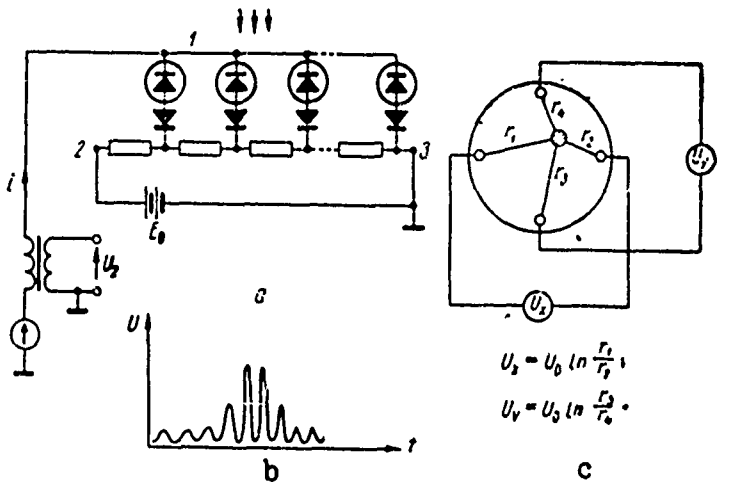

Figure 7. Semiconductor photosensitive elements:
a) equivalent circuit of scanistor; b) output signal of scanistor; c) position-sensitive photocell.

Owing to the fact that each "target" element is fed general sawtooth voltage (between outputs 1 and 3), as well as constant voltage which varies along the layer and is created by the voltage of battery E_0, connected to outputs 2 and 3, the jump in current will not take place simultaneously over the entire semiconductor layer, but will travel along it according to the applied sawtooth voltage. The variation in the currents of individual photodiode-diode pairs in turn results in a stepped variation in the current of upper bus 1. The differentiation of this step signal gives a series of pulses (Figure 7,b), whose amplitudes are proportional to the intensity of the light falling on the corresponding photodiode-diode pair. Discrete scanistors with a resolution equal to N = 10 lines/mm and a length of 2.0-3.5 cm are now in production.

There is also great promise in the use of position-sensitive photocells [12], which are characterized by a wide linearity range in two directions oriented at a right angle to each other, high sensitivity and resolution, zero stability and low persistence. The operating principle of the position-sensitive photocell is based on the fact that in the case of irregular or localized illumination of the p-n junction, in addition to the transverse photovoltage usually observed, voltage parallel to the junction also appears. This longitudinal photovoltage can be measured by placing ohmic contacts on one and the same side of the junction. It equals zero if the light spot is in a symmetric position relative to the ohmic contacts and is positive if the spot is positioned on one side and negative if placed on the other side of the relative zero position (Figure 7,c). The position-sensitive cell can be successfully used as a transducer in servo systems which reproduce complex curves with the necessary degree of accuracy.

From among the above-enumerated optoelectronic assembly variants the greatest speed of response is shown by assemblies with a cathode-ray tube and photomultipliers, a discrete system of beam deflection by crystals, fiber optics, as well as the vidicon. The principal factor limiting the speed of response of the device using a CRT and photomultipliers is the screen persistence of the CRT. The speed of response of graphic converters using the vidicon is limited by the photoelectric lag of the tube. If up-to-date CRTs with a short screen persistence are used, the speed of response is greater for an optoelectronic assembly using CRT and photomultipliers than the vidicon (several thousand readouts compared to several hundred). The speed of response of an electromechanical reader is less although it likewise is sufficient with the use of up-to-date tape punchers at maximum speed. It should be noted that the appearance of step-by-step motors with a processing frequency of up to several kilohertz and the step-pulse drive based on them is significantly changing the former idea regarding the speed of response of electromechanical systems, especially of the closed-loop type [29].

In view of the fact that recordings (graphs) are usually made on coordinate paper, the construction of graph converters requires the proper selection of recording line thickness and its color. Special research has established that colors can be effectively separated by means of light filters which make possible "suppression" of one of the colors and "intensification" of the other.

An input device with electromechanical scanning and an external illuminating source, unlike devices using a CRT and vidicon, assures data sampling from the carrier regardless of the color of the grid. The reading of a curve of any color with any metric grid is solved as a problem in automatic color determination, which resembles pattern recognition. The recognition device serves to convert signals received from the photoelectric assembly into a code description of the pattern, as well as to compare the code description with a given standard and to receive recognition signals in the coding system adopted. The code description of a color pattern may be given by a set of spectral radiation components. Work [33] describes an optoelectronic assembly which permits the certain isolation of a graph line plotted in one of the basic colors (black, red, orange, blue, azure, green and yellow) on a carrier with preliminary training in the recognition of this color.

The choice of optoelectronic assembly variant is determined by the type of graph converter and its purpose. Electromechanical readers have recently been successfully used for autonomous coding devices, and assemblies employing cathode-ray tubes for computer-aided programmed control devices.

Methods of Graph Reading

The problem of automatic graph reading reduces to the determination of carrier elements belonging to a graph line and the generation of signals in analog or digital form, the magnitudes of which are proportional to the coordinates of the isolated elements. Graph conversion devices of various types are based on two fundamental methods: 1) the tracking and 2) the scanning method [26]. In the first case carrier elements belonging to the graphic image or situated near it are interrogated, in the second case all carrier elements.

Tracking readers operating according to a closed control system scheme use a compensation method of measurement based on matching a graph curve with the position of the reading organ (raster element); used as the latter is an electron or light beam, a photosensitive head, reticle etc. In the last case the feedback loop of the device is closed via a human operator, who manually brings the finder into coincidence with the line.

Automatic servo systems are subdivided into two- or one-coordinate systems depending on the single-valuedness or multiple-valuedness of the graphic functions to be transformed. Noteworthy among the multitude of suggested variants for the construction of such systems are follow scanning systems, in which some supplementary local scanning is used for the generation of correcting signals of the servo system channels (centering signal and inner home signal); local search and line bypass are sometimes combined here [27]. The reading raster-element may rotate along a circle intersecting the graph line [9], along arcs of the circle osculating at the intersection points [14], or move in steps of equal length in certain fixed directions [17] etc. (Figure 8). The technical characteristics of such systems (speed of response, tracking accuracy etc.) are determined by the mode of obtaining phasing signals according to the coordinates of the points of intersection of local scanning

with graph curve, viz. in the form of analog signals proportional to the scanning voltage amplitude at intersection moments [9], in the form of phase relations of the first and second harmonics of the sequence of received notch pulses relative to reference voltage [1], in the form of control pulses which restructure system components [13], etc.

For single-valued graphic functions whose scanning on one of the axes must be performed by means of a tape transport or horizontal deflection of the reading beam, the inner home signal in the above-described system is disconnected together with one of the tracking channels. Figure 9 presents the realizable paths of the scanning raster element of a one-coordinate servo system. The real possibility arises here of scanning a curve in the direction of the normal to it [26].

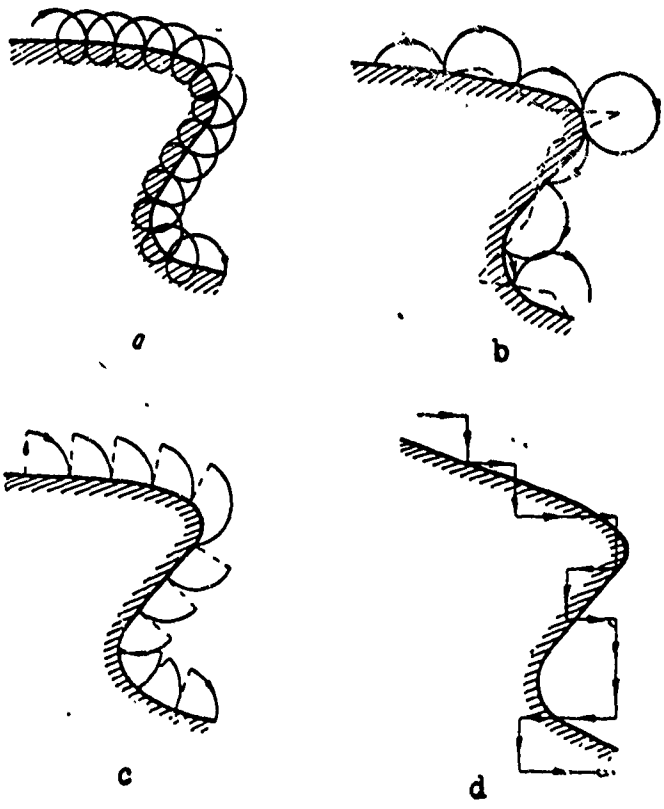

Figure 8. Path of raster element in two-coordinate servo system:
a) movement along circle intersecting graph line;
b) movement along circle arcs osculating at intersection points;
c) movement along segments of circle arcs;
d) movement in mutually perpendicular directions.

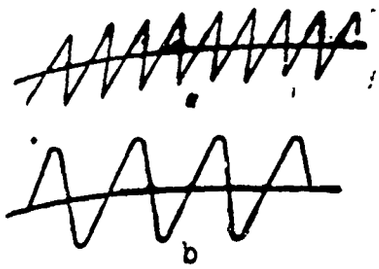

Figure 9. Path of raster element in one-coordinate servo system:
a) linear scanning; b) sinusoidal scanning.

It must be emphasized that follow reading can be performed using an optoelectronic assembly of any design, viz. based on a CRT and photomultipliers (easiest), a vidicon, by means of an electromechanical scanning head. Until recently, rotating prisms or mirrors were used in such heads to obtain local scanning [26]. The appearance of position-sensitive photocells, fiber-optic structures and photomatrices has made it possible to dispense with mechanically rotating elements. The last two cases assume parallel interrogation of the carrier elements nearest the graph line with simultaneous investigation of all received signals. An example is a multisector (for example, three-sector) photosensitive head [36]. An image of the portion of the curve approximately equal to the line thickness is partitioned into three sectors, which are connected with isolated photosensors. The signals of photosensors 1 and 3, as well as 2 and 3 are summed, and the difference of these two sum signals in quantity and sign determines the correcting signal of the servo system (Figure 10). The admissible emergence of the photohead outside the line is controlled by the minimum permissible value of the difference signal.

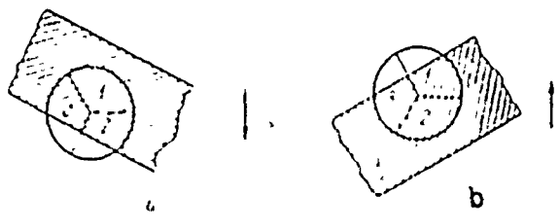

Figure 10. Relative position of sectors of multisector head and graph line:
a) downward motion; b) upward motion.

Of course, in principle a mechanically tracking photohead can be dispensed with if the entire field of vision of the graph converter is covered with a multielement photomatrix and, by comparing the signals of individual elements, those which belong to the graph line are isolated in series.

Output signals of follow graph converters can be obtained with equal success in analog or digital form without intermediate interconversions [25].

In the case of electromechanical heads this is facilitated by the use of a step-pulse drive. Follow conversion is also realized by means of special computer control signal programs [10].

Follow readers operating according to a scheme of open-loop control systems use the method of dynamic compensation measurement, in which the value of the graph curve ordinate is compared with an auxiliary scanning function which maps the motion of the reading organ (raster element) along the carrier. At moments of equilibrium states, when the scanning raster element intersects the line of the graphic image, notch pulses are generated whose time position relative to the start of the measurement cycle is proportional to the ordinates of the measured graph. The measured time interval is filled with range markers for obtaining the output signal in digital form or is converted into the amplitude of the continuous output signal.

As in follow scanning systems, the measurement cycle period is chosen on the basis of information theory theorems for obtaining the necessary data on the graph to be converted [22, 26]. Any variant of optoelectronic assembly can also be used here, and in the case of parallel interrogation of carrier elements by means of a photomatrix (bar of photocells or light guides) scanning is achieved by series commutation of the output signals of individual elements of such a matrix.

According to scanning system theory [32], a graph converter may use sweeps of arbitrary form, but not necessarily linear. The measurement error here is reduced to practically zero if a function identical to the scanning function is used to obtain analog output and calibration scales, to be scanned by the raster element simultaneously with the graph carrier, to obtain digital output (see Figure 1).

Scanning- and tracking-method devices will make it possible to process the recordings of recording instruments without preliminary preparation; the graphs here may have line omissions and fractures. In the case of a graph line omission the output of the device is given an ordinate value corresponding to the preceding value. Tracking converters make it possible to process graphs on a contaminated carrier. Scanning converters permit simultaneous reading of several graphs, the graph converter being constructed as a multiplied scanning system. Despite the fact that the scanning method is hardly suitable for the conversion of multivalued functions and graphs with a large value for the first derivative (maximum angle of inclination of graph line less than 87°), it is often technically simpler to realize than the tracking method.

In the general case of multichannel recordings individual curves may intersect or touch, and their input into a computer is considerably complicated. The main problem in the reading of intersecting curves is to recognize curves when they intersect or touch. The entire process of automatic initial data processing reduces to two stages (carrier reading and mathematical-logic processing of the results obtained), which can be carried out either by the

converter itself or by the converter in conjunction with a computer (the first processing stage is performed by the converter, the second by the computer [15]).

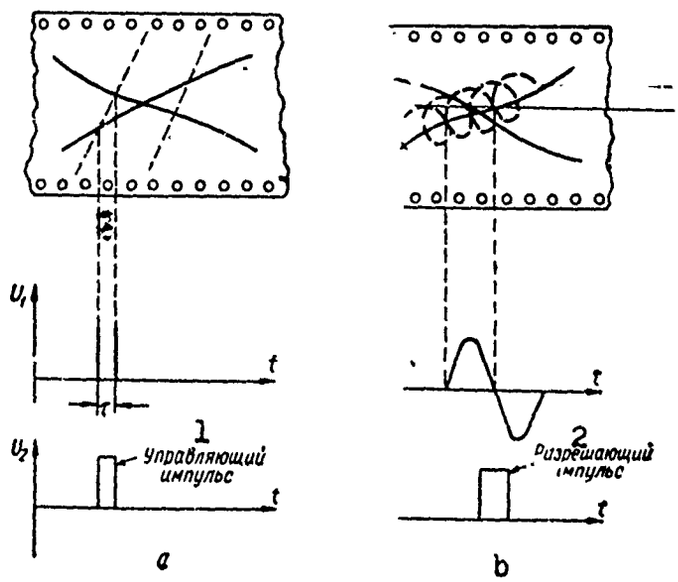

Figure 11. Equipment methods for the separation of intersecting curves:
a) in scanning systems; b) in systems with follow circular sweeps.

Key: (1) control pulse
(2) Gate pulse

In scanning systems the time interval between notch pulses from neighboring lines is used to determine curve intersections (Figure 11,a) [28, 30]; in converters with circular follow sweeps reading of intersecting curves is achieved by gating the amplifier link for the expected time that a sweep encounters the traced line (Figure 11,b); in tracking converters with a multisector head this is done by analysis of the signals of individual sectors. The cases of curve tangency and intersection can be separated in the analysis of the first and second derivatives of the functions to be read.

There is very great promise in extrapolative processing algorithms, according to which the graph ordinate value that is being measured at some moment of time is compared with the value determined from its preceding values. A conclusion as to the shape of the graph after the intersection point is drawn from the agreement between the extrapolated value of the ordinate and the actual value [24].

At the present time variants of such extrapolative algorithms are being tested at the Institute of Cybernetics of the Academy of Sciences Ukrainian SSR, Kiev Polytechnic Institute and the Institute of Technical Cybernetics

of the Academy of Sciences Belorussian SSR. In view of the fact that many graphs to be converted represent [sets] of statistical processes, on the one hand, while, on the other hand, certain extrapolation expressions (those of Newton, Lagrange etc., for example) do not [completely] assure convergence of the extrapolation process, it will apparently not be easy to obtain a dependable algorithm for the separation of intersecting curves.

The problems of the input of the coordinates of the points of intersecting graphs and their separation over individual channels can be combined if the carrier lines differ from one another in some physical attribute (width, optical density, auxiliary dash lines, color etc.). Most convenient, in our view, is the separation of curves on the basis of color discrimination, in which event the input device can be compact and reliable.

Graphs of functions of two or more variables (topographical or geophysical maps etc.) can be converted with the aid of scanning or tracking conversion methods. In this case the information available as maps of lines of equal values of some function can be represented by the matrix of values of this function in the nodes of a square grid plotted on the initial map.

In a scanner the carrier is read line by line, with the assignment of coordinates for the points of intersection of scanning lines with isolines of the map and the sign of the corresponding function increment. Information about the sign is given by additionally outlining the isoline in color from the direction of the larger value for the function that is to be read (Figure 12,a). Function values in the nodes of a uniform grid are calculated by interpolation of the read data in computers [8, 32].

In a tracker one makes the circuit of the separate isolines of the map in turn, assigning the current value of one of the coordinates (say Y) at the given step of variation along the other coordinate (Figure 12,b). The result is the formation of the section of a family of isolines given $\overline{X}$ = const, analogous to the section obtained on the scanning line in the first case. Unfortunately, the transition from isoline to isoline cannot be automated by simple means with this method.

Graph converters can be regarded as an intermediate link between the graphic data carrier and computer. A direct hook-up of the graph converter to computer can be conveniently effected at computer centers, while a converter with intermediate output data recording (on magnetic tape, perforated tape and punched card) can be used for the preparation of calculation data in organizations which do not have their own computer pool. In a direct connection the graph converter is hooked up to the connector of the computer photoinput and, in addition to the code of the graph ordinates, forms a series of control signals: pulses for the shift of word positions in the magnetic memory, for clearance of the receiving register etc.

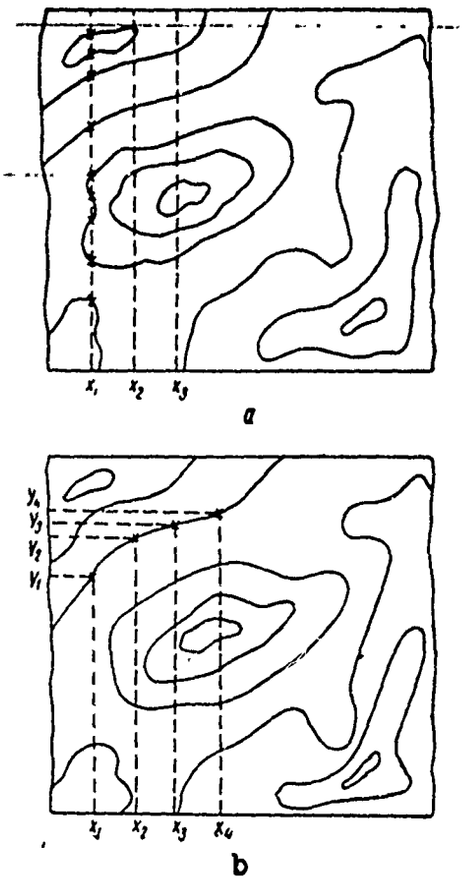

Figure 12. Methods for reading graphic images of function of two variables:
a) scanning; b) tracking.

The theory of the design of various types of graph converters has, in the main, been worked out. It includes such questions as the rational choice of the optoelectronic assembly, optimal regimes for the electronic instruments used in it, the stabilization of their characteristics; questions relating to the processing of output signals of the optoelectronic assembly; methods for the construction of special types of converters; questions regarding the connection of converter to computer (direct, via a buffer storage); error analysis and ways of increasing conversion accuracy etc.

The scientific and technical principles are now provided for the development of a general-purpose converter for input into a computer of information given on coordinate paper or motion picture film by individual and intersecting curves with possible fractures and colors of curves and carriers which represent single-valued and multiple-valued functions of one or several variables.

Graph Conversion Devices

Some organizations engaged in the development of external graphic devices for computers have already constructed and are successfully operating laboratory prototypes of various classes of graph converters, viz.: for semiautomatic input of graphs with the aid of an operator [2, 5], coding and reproduction of geological and geophysical maps [18, 23], coding of multichannel recordings [3, 6], coding of colored multichannel recordings [31], reading of arbitrary graphs [5, 27], coding of half-tone images [11] etc.

However, it must be noted that theoretical and practical results are still being inadequately introduced. As a result, only a complex of three graph input devices has been prepared for series production, viz. the "EASP-S," "Gamma" and "Silhouette," developed by the Special Design Bureau at the Vil'nyus Calculating Machine Plant. These devices have the common design of a vidicon-based optoelectronic assembly, but different purposes and technical characteristics (Table 4).

The complex of instruments being manufactured in Vil'nyus covers only the input of individual and nonintersecting (up to three) graphs of single-valued functions subject to certain restrictions imposed on line thickness, color and inclination, as well as coordinate paper. But the demand for devices for the input of multiple-valued curves and the coding of intersecting graphs, maps, drawings and photographs remains unsatisfied, as before.

The further development of automatic graphic data processing in our country requires the creation of a series of new external graphic devices for computers with due regard for the results of research which has been done on optoelectronic assembly designs and realizable parameters, methods for the color separation of graphs, the elimination of fracture and omission effects, as well as the algorithmization of the machine separation of intersecting curves. Even now many laboratory prototypes have been prepared for rapid mastery by industry. The high technical and economic indicators of Soviet developmental projects, which are at the level of the best foreign firms, indicate that many instruments can be put into experimental series production. Let us mention some of them.

1. The "Karta" (Map) device for the coding and reproduction of potential field maps (Kiev Polytechnic Institute), which makes it possible to obtain a numerical model of a field function from an initial map and to punch the resultant data for subsequent input into a computer, as well as to construct a transformed potential field map from the computer perforated-tape data. This device was demonstrated at the "USSR Education" pavilion at the Exhibition of Achievements of the National Economy of the USSR and was rated highly by representatives of interested organizations.

Table 4

Principal Parameters of Some Graph Converters

Type or Brand	Manufacturer	Optoelectronic Assembly	No. of channels	Carrier width	Line Requirements			Error %	Output
					Thickness mm	Color	Is there a grid		
EASP-S	Special Design Bureau of Vil'nyus Calculating Machine Plant	Vidicon	1	35-305	0.2-0.3 or 0.5-0.6	Black, red, green	No	5	Analog, voltage
"Gamma"	Special Design Bureau of Vil'nyus Calculating Machine Plant	Vidicon	1	35-305	0.2-0.3 or 0.5-0.6	Black, red, green	No	2	Perforated tape, telegraphic code No. 2
"Siluet" (Silhouette)	Special Design Bureau of Vil'nyus Calculating Machine Plant	Vidicon	2	35-305	0.2-0.3 or 0.5-0.6	Black, red, green	No	2	Perforated tape, telegraphic code No. 2
MASK	Institute of Technical Cybernetics, Academy of Sciences Belorussian SSR	Electromechanical	6	170	0.2	Black, red, green	No	0.2	Digital code
"Luch" (Beam)	Kiev Polytechnic Institute	Electromechanical	3	220	0.3-0.5	Any basic tone	Yes	0.25	Perforated tape

Table 4
(continued)

Type or Brand	Manufacturer	Optoelectronic Assembly	No. of channels	Carrier width mm	Line requirements			Error %	Output
					Thickness mm	Color	Is there a grid		
"Grafik" (Graph)	Kiev Polytechnic Institute	Electromechanical	9	220	0.2	Any basic tone	Yes	0.1	Perforated tape
"Ostsillogramma" (Oscillogram)	Institute of Cybernetics, Academy of Sciences Ukrainian SSR	Electromechanical	4	35	0.12	Black	No	1	Digital code
MP	Institute of Mathematics of the Siberian Department of the Academy of Sciences USSR	Electromechanical	1	210	0.2	Black, red	No	1	Perforated tape
PG	Institute of Electronics, Automation and Telemechanics, Academy of Sciences Georgian SSR	Electromechanical	1	35-230	0.5	Black, red	No	1	Perforated tape

2. The "Luch" (Beam) multichannel log reader (Kiev Polytechnic Institute) for the sequential reading of intersecting colored graphs, perforation of the resultant data and input into "Minsk-2" and "Minsk-22" computers. The device easily learns to recognize an arbitrary line color, including the color blue, which is usually difficult to perceive [31]. In a modification called "Grafik" (Graph), the device permits parallel reading and coding of nine-channel graphs (for example, medicobiological) for input into an "M-220" computer. It affords the possibility of choosing or reading any graph or any group of graphs from among those available on the carrier, it being possible to plot the graphs in one of the basic colors, whatever the color of the metric grid. In the event of intersection of the curves their ordinates are separated by a computer according to a special program.

3. Multichannel oscillogram converters, developed at the Institute of Technical Cybernetics of the Academy of Sciences Belorussian SSR, the Institute of Cybernetics of the Academy of Sciences Ukrainian SSR. the Institute of Mathematics of the Siberian Department of the Academy of Sciences USSR, the Institute of Electronics, Automation and Telemechanics of the Academy of Sciences Georgian SSR, code either all nonintersecting graphs available on the carrier or any of them by sampling. The first two devices are designed for direct connection to a computer (digital or analog), the last two are designed for connection via a perforated tape. These devices, like the Vil'nyus complex of equipment, have restrictions on the color shades of the carrier and curves.

BIBLIOGRAPHY

1. Abakumov, V. G., and Petrenko, A. I., Trudy Vtoroy Vsessoyuznoy Konferentsii po Avtomatizatsii Obrabotki Nauchnoy Informatsii -- Sbornik (Transactions of the Second All-Union Conference on the Automation of Scientific Data Processing -- Collection of Works), Publishing House of the All-Union Institute of Scientific and Technical Information, Moscow, 1963.

2. Alekserov, S. A., and Aliyev, T. A., Vychislitel'naya Tekhnika v Upravlenii -- Sbornik (Computer Technology in Control -- Collection of Works), "Nauka" (Science), Moscow, 1966.

3. Afanas'yev, G. K., and Chegolin, P. M., Vychislitel'naya Tekhnika -- Sbornik (Computer Technology -- Collection of Works), Minsk, 1965.

4. Afanas'yev, G. K., and Chegolin, P. M., Vychislitel'naya Tekhnika v Mashinostroyenii -- Sbornik (Computer Technology in Machine-Building -- Collection of Works), No. 1, Minsk, 1965.

5. Afraymovich, E. N., and Yegorov, Yu. A., Geomagnetizm i Astronomiya (Geomagnetism and Astronomy), 1965, 4.

6. Bartkus, T., Budryunas, A., Meshcheryakov, V., and Tel'ksnis, L., Avtomatizatsiya Vvoda Pis'mennykh Znakov v Elektronnyye Vychislitel'nyye Mashiny -- Sbornik (Automating the Input of Written Signs into Electronic Computers -- Collection of Works), Vil'nyus, 1965.

7. Bosyakov, A. N., Afanas'yev, G. K., Shpakovskiy, G. I., and Rudakovskiy, A. V., Analogovaya i Analogo-tsifrovaya Vychislitel'naya Tekhnika -- Sbornik (Analog and Analog-Digital Computer Technology -- Collection of Works), "Mashinostroyeniye" (Machine-Building), Moscow, 1965.

8. Budnyak, A. A., and Petrenko, A. I., Mekhanizatsiya i Avtomatizatsiya Upravleniya (The Mechanization and Automation of Control), 1966, 6.

9. Germash, V. A., Pereverzev-Orlov, V. S., and Tsirlin, V. M., Izvestiya AN SSSR (Energetika i Avtomatika) (Bulletin of USSR Academy of Sciences (Power Engineering and Automation)), 1964, I.

10. Glushkov, V. M., Avtomatika (Automation), 1962, 1.

11. Glushkov, V. M., Kovalevskiy, V. A., and Rybak, V. I., Printsipy Postroyeniya Samoobuchayushchikhsya Sistem -- Sbornik (Principles of the Construction of Self-Learning Systems -- Collection of Works), State Publishing House of Technical and Theoretical Literature of the Ukrainian SSR, Kiev, 1962.

12. Gorbakh, T. Ya., Krolevets, K. M., and Savelov, V. N., Avtomatika i Priborostroyeniye (Automation and Instrument-Building), 1964, 4.

13. Grinnas, Ye., Miger, P., Norman, R., and Iziiger, P., Zarubezhnaya Radioelektronika (Foreign Radioelectronics), 1964, 2.

14. Zaborovskiy, Yu. A., Vestnik KPI -- Seriya Radioelektroniki (Herald of Kiev Polytechnic Institute -- Radioelectronics Series), No. 1, 1965.

15. Kapshuk, O. A., Petrenko, A. I., and Fesechko, V. A., Problemy Peredachi Kvazistatsionarnykh Signalov -- Sbornik (Problems in the Transmission of Quasistationary Signals -- Collection of Works), "Naukova Dumka" (Scientific Thought), Kiev, 1966.

16. Karyshev, Ye. I., Avtomaticheskiy Kontrol' i Metody Elektricheskikh Izmereniy -- Sbornik (Automatic Control and Methods of Electrical Measurements -- Collection of Works), Vol. I, Siberian Department of the Academy of Sciences USSR, Novosibirsk, 1964.

17. Kovalevskiy, V. A., and Semenovskiy, A. G., Avtomatika i Priborostroyeniye, 1960, I.

18. Kolesnikov, Yu. A., et al., "A Device for the Conversion of Graphs into Electrical Quantities and the Measurement of Ordinates with Automatic Entry of Numbers on Punched Cards and 'Print,'" Peredovoy Nauchno-tekhnicheskiy i Proizvodstvennyy Opyt (Advanced Scientific-and-Technical and Production Experience), 5-64-441/12, Moscow, 1964.

19. Kondakov, V. F., Priborostroyeniye (Instrument-Building), 1966, 1.

20. Kochergin, S. I., and Darvinskaya, V. K., Obmen Opytom v Radioelektronnoy Promyshlennosti (Exchange of Experience in the Radioelectronic Industry), 1964, 7.

21. Krasil'nikov, N. N., Pomekhoustoychivost' Televizionnykh Ustroystv (Noise Immunity of Television Sets), State Scientific and Technical Power-Engineering Publishing House, Moscow, 1961.

22. Lebedev, D. V., and Tsukkerman, I. I., Televideniye i Teoriya Informatsii (Television and Information Theory), "Energiya" (Energy), Moscow, 1965.

23. L'vov, V. A., and Parinov, N. D., Trudy Uchebnykh Institutov Svyazi (Transactions of Educational Communication Institutes), No. 25, 1965.

24. Parkhomenko, I. T., Avtomatika i Priborostroyeniye, 1964, 4.

25. Polyakov, V. G., Problemy Peredachi Informatsii -- Sbornik (Problems in Information Transmission -- Collection of Works), No. 20, 1965.

26. Petrenko, A. I., Preobrazovaniye Grafikov v Elektricheskiye Signaly (The Conversion of Graphs into Electric Signals), State Publishing House of Technical and Theoretical Literature of the Ukrainian SSR, Kiev, 1964.

27. Petrenko, A. I., and Zaborovskiy, Yu. A., Problemy Peredachi Kvazistatsionarnykh Signalov -- Sbornik, "Naukova Dumka" (Scientific Thought), Kiev, 1966.

28. Petrenko, A. I., Abakumov, V. G., Zaborovskiy, Yu. A., and Fesechko, V. A., Avtomatika i Priborostroyeniye, 1965, 4.

29. Ratmirov, V. A., et al., Sistemy s Shagovymi Dvigatelyami (Systems with Step-by-step Motors), "Energiya" (Energy), Moscow, 1964.

30. Rubekin, L. V., Shushkov, Ye. I., Pudkov, G. Ya., Zherbin, M. F., and Ivashkov, G. L., "Authors' Certificate No. 154,084," Byulleten' Izobreteniy (Bulletin of Inventions), 1963, 8.

31. Sigorskiy, V. P., Petrenko, A. I., Abakumov, V. G., Budnyak, A. A., Fesechko, V. A., and Zaborovskiy, Yu. A., Vestnik KPI -- Seriya Radioelektroniki, No. 2, 1966.

32. Temnikov, F. Ye., Teoriya Razvertyvayushchikh Sistem (Scanning System Theory), State Scientific and Technicel Power-Engineering Publishing House, Moscow, 1963.

33. Fesechko, V. A., and Petrenko, A. I., Vestnik KPI -- Seriya Radioelektroniki, No. 4, 1966.

34. Grim, E. D., Electrotechnology, 1965, 4.

35. Neison, T. J., BSTJ, 1964, XLIII, 3.

36. Rawling, E., and Purhiser, U.S. Patent No. 3,135,904, 1964, 2, VI.

37. Rosefeld, A. N., Nuclear Instruments and Methods, 1963, 20.

GENERALIZATION OF CHARACTERISTICS IN THE PROCESSING OF GRAPHIC DATA

Metori i Ustroystva Preobrazovaniya Graficheskoy Informatsii (Methods and Devices for the Conversion of Graphic Data), 1968, pages 30-33

F. Ye. Temnikov

Nature of Generalization

There can be various problems in the processing of graphic data [1-6], including those which do not require complete retrieval of the originally recorded information. In this case, only that portion of the graphic information is usually extracted which characterizes certain secondary parameters and data.

Let us stipulate that we shall designate as generalization that information processing in which correlation and consolidation of data takes place on the basis of certain guiding principles, criteria, tags and algorithms.

Generalized Characteristics

The following data can be taken as generalized characteristics: representative parameters; extreme values; derivative values; integral values; averaged values; dynamic characteristics; spectral characteristics; statistical characteristics; data projections; data charts; data formulas; patterns; concepts.

Hierarchic Generalization

We can approach the problem of generalization more strictly if we are guided by the principles of the theory of coding and the elimination of redundant information. Let us note six forms of signals and messages corresponding to the six basic phases of data generation: observed and controlled object; primary data generation; structural enrichment of data; statistical enrichment of data; semantic enrichment of data; generation of decisions and actions.

"Raking" of Points along T Axis

A simple method of generalization consists in "raking" the points of a diagram along the T axis (time axis). The term "raking" means the shifting and close arrangement of the "points" of a recording either at one edge of the diagram or in a zone specially designated for the purpose.

In its broad sense, "raking" can be understood as the formulation of the density function characteristic of quantity X during its realization in time T. This procedure can be performed by any method: by "raking" the scattered particles in the full sense of this word; by the exhibition of light-sensitive material along one line; through the "envelopment" of points by a discrete series of light-sensitive cells with subsequent integration or summation of the readings for each series; by appropriate scanning of the television image of a graph; by multilevel summation of discrete equilibrium marks in the "Tsentrotekhnika" system etc.

"Raking" of Points along the X Axis

An analogous procedure can be performed by moving the "raking" element along the X axis of parameter values. Obtained as a result is a unique T-set distribution with respect to the realizations along the X axis of values.

"Raking" of Points along the N Axis

An analogous procedure can be performed by moving the "raking" element along the axis of parameter numbers in the so-called XTN data complex [1-6].

Generalization of Distribution Methods

The above-indicated methods of simple generalization by "raking" the points of graphs are particular cases of the obtaining of a posterior functions of the statistical distribution density of the values of quantities, moments of time and points in space.

In practice, however, these generalized characteristics in the form of statistical distributions are more conveniently represented as data projections.*

The figure shows the initial solution of the generalized characteristic of set N of quantities X at time T in the form of three plane data projections (XT, XN and NT) and six linear data projections (reducible to three), as well as six point projections, reducible to three, which are of purely theoretical interest, though.

Formation of Generalized Characteristics Prior to Recording

Generalization can, and in some cases must, be performed prior to the recording of data, i.e. during measurements and the transmission of quantities to a central point. This can most easily be accomplished by means of the

---

* Such projections were suggested by the author and worked out by him with the participation of V. P. Savin and Yu. A. Ivashkin at MEI [Moscow Power Engineering Institute].

"Tsentrotekhnika" centralized monitoring and control system (devised by the author at MEI [Moscow Power Engineering Institute]). This ease is especially striking in the generalized variant of the "Tsentrotekhnika" system in which the whole set of values of monitored variables is represented by pulse streams. Pulses are then accumulated and visualized in any relation.

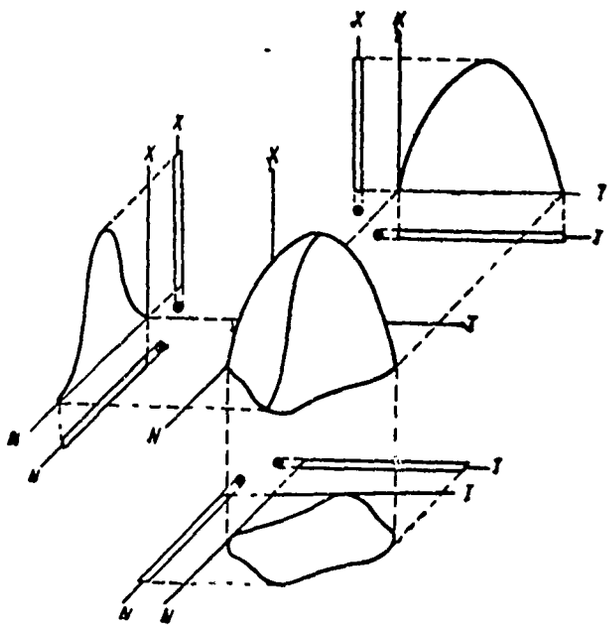

Data projections

BIBLIOGRAPHY

1. Dyssa, O. F., Statisticheskoye Predstavleniye Massovoy Informatsii (Statistical Representation of Mass Information), Dissertation, Moscow Power Engineering Institute, 1967.

2. Temnikov, F. Ye., Teoriya Razvertyvayushchikh Sistem (Theory of Scanning Systems), State Scientific and Technical Power-Engineering Publishing House, Moscow, 1963.

3. Temnikov, F. Ye., "Automatic Control Systems," Entsiklopediya Izmereniy, Kontrolya i Avtomatizatsii (Encyclopedia of Measurements, Control and Automation), No. 3, "Energiya" (Energy), Moscow, 1964.

4. Temnikov, F. Ye., in the collection of works, Avtomaticheskiy Kontrol' i Metody Elektricheskikh Izmereniy (Automatic Control and Methods of Electrical Measurements), Vol. II, Publishing House of the Siberian Department of the Academy of Sciences USSR, Novosibirsk, 1964.

5. Temnikov, F. Ye., Tekhnicheskaya Informatsiya (Technical Information), Publishing House of the Moscow Power Engineering Institute, Moscow, 1951.

6. Temnikov, F. Ye., Avtomaticheskiye Registriruyushchiye Pribory (Automatic Recorders), 2nd edition, State Scientific and Technical Publishing House of Literature on Machine Manufacture, Moscow, 1960.

PECULIARITIES OF THE DISCRETE REPRESENTATION OF RANDOM SIGNALS

Metody i Ustroystva Preobrazovaniya Graficheskoy Informatsii (Methods and Devices for the Conversion of Graphic Data), [illegible] 38, [illegible] 34-40

V. I. Chaykovskiy

Often in cases of practical importance an investigated random signal undergoes time quantization, which results in an irremediable loss of information about its st[illegible]. The magnitude of the error arising in interpolation of the signal may characterize this loss.

Existing estimates of the interpolation error of deterministic signals [3, 4, 6] are, unfortunately, completely useless for random signals. The explanation is that such concepts as spectral density, energy, maximum possible instantaneous value etc., which are used in the analysis of deterministic signals, are inapplicable to random signals.

Error in the interpolation of a stationary random signal is customarily estimated by root-mean-square value

$$\sigma^2(t) = M\{|x(t) - X(t)|^2\}, \tag{1}$$

where x(t) is the random signal in question; X(t) is its copy restored according to Kotel'nikov*

$$X(t) = \sum_{k=-\infty}^{\infty} x(k\Delta t)\,\mathrm{sinc}\,\frac{\pi}{\Delta t}(t - k\Delta t). \tag{2}$$

In Appendix I the following relations are obtained:

$$M\{x^2(t)\} = D\{x\};$$
$$M\{X^2(t)\} = D\{x\};$$
$$M\{x(t)X(t)\} = \sum_{k=-\infty}^{\infty} \Delta P_k e^{jk\frac{2\pi}{\Delta t}t}.$$

---

* Here and hereinafter a function of the form $\frac{\sin X}{X}$ is designated as sinc X.

Here ΔP_k is the power of the spectral components of the random signal in question in the frequency range

$$(2k-1)\frac{\pi}{\Delta t} < \omega < (2k+1)\frac{\pi}{\Delta t}.$$

If

$$\sum_{k=-\infty}^{\infty} \Delta P_k = D[x],$$

then

$$\sigma^2(t) = 2\left[\sum_{k=-\infty}^{\infty} \Delta P_k - \sum_{k=-\infty}^{\infty} \Delta P_k e^{j k \frac{2\pi}{\Delta t} t}\right].$$

The property of symmetry of the energy spectrum of a real random signal makes it possible to write the resultant expression as:

$$\sigma^2(t) = 4\left[\sum_{k=-\infty}^{\infty} 2\Delta P_k \sin^2\left(k\frac{\pi}{\Delta t}t\right)\right]. \qquad (3)$$

From expression (3) it follows that:

1) the mean-root-square value of restoration error is a periodic even time function with a period equal to quantization interval

$$\sigma^2(t) = \sigma^2(t \pm n\Delta t) \qquad n = 1, 2, 3, \ldots;$$

2) the maximum possible value of restoration error does not exceed quadruple value of the power of spectrum components outside the Nyquist range $\left(-\frac{\pi}{\Delta t}; \frac{\pi}{\Delta t}\right)$

$$\sigma^2_{max} \leqslant 4\sum_{k=1}^{\infty} 2\Delta P_k;$$

3) the mean value of quadratic restoration error on the quantization interval equals the doubled power of spectrum components outside the Nyquist range,

$$\frac{1}{\Delta t}\int_0^{\Delta t} \sigma^2(t)\,dt = 2\sum_{k=1}^{\infty} 2\Delta P_k;$$

4) the time-dependence of the error in the restoration of a random signal indicates the nonstationarity of a signal restored according to Kotel'nikov;

5) a random signal restored according to Kotel'nikov converges (in the sense of the root-mean-square value) to the signal in question only if the components of the energy spectrum outside the Nyquist range equal zero.

$$\sigma^2(t) = 0 \text{ given } \sum_{i=1}^{\infty} 2\Delta P_i = 0.$$

Interpolation error equals zero for random signals with a finite spectrum in the case where interpolation is performed with an untruncated Kotel'nikov series (2), which takes into consideration an infinite set of readings. In practice the investigator has at his disposal only a finite number of readings, and interpolation is performed with a truncated Kotel'nikov series

$$X_N(t) = \sum_{k=-N}^{N} x(k\Delta t)\,\mathrm{sinc}\,\frac{\pi}{\Delta t}(t - k\Delta t). \tag{4}$$

Here, regardless of the character of the spectrum of the interpolated signal, error arises which is customarily called truncation error.

The root-mean-square value of truncation error

$$\sigma_\gamma^2(t) = M\{|x(t) - X_N(t)|^2\}, \tag{5}$$

given a large enough number of readings to be taken into consideration, can be estimated approximately by using the relations obtained in Appendix II:

$$M\{x^2(t)\} = D[x];$$

$$M\{x(t)\,X_N(t)\} = D[x]\sum_{k=-N}^{N}\mathrm{sinc}\,\frac{\pi}{\Delta t}(t - k\Delta t),$$

$$M\{X_N^2(t)\} = D[x]\sum_{k=-N}^{N}\mathrm{sinc}\,\frac{\pi}{\Delta t}(t - k\Delta t).$$

By comparing the above-cited expressions with (5) we obtain

$$\sigma_\gamma^2(t) = D[x]\,\gamma_N(t), \tag{6}$$

where

$$\gamma_N(t) = 1 - \sum_{k=-N}^{N}\mathrm{sinc}\,\frac{\pi}{\Delta t}(t - k\Delta t) \tag{7}$$

denotes the generalized truncation error function.

The investigation of the generalized truncation error function, made in Appendix III, permits the following conclusions to be drawn: 1) truncation error is a function of time and increases towards the edges of the existence interval of the readings; 2) truncation error is maximal at the edges of the interpolation interval and does not exceed the value

$$\sigma_{\gamma\,\max}^2 \leqslant 0{,}21D[x].$$

Thus, the Kotel'nikov interpolation series makes possible exact (in the sense of the mean-root-square interpolation error being equal to zero)

restoration only in the event of a finite energy spectrum of the signal and the use of an infinite number of readings. In the general case, neither condition is fulfilled, which results in the appearance of the interpolation errors considered above.

Appendix I

1. By definition the statistical mean of the square of a stationary centered random process equals the variance of this process

$$M\{x^2(t)\} = D\{x\}.$$

2. Quantity $M\{X^2(t)\}$ can be represented as

$$M\{X^2(t)\} =$$

$$= \sum_{k=-\infty}^{\infty} \sum_{p=-\infty}^{\infty} R(k\Delta t - p\Delta t) \operatorname{sinc} \frac{\pi}{\Delta t}(t - k\Delta t) \operatorname{sinc} \frac{\pi}{\Delta t}(t - p\Delta t),$$

where $R(\tau)$ is the autocorrelation function of the interpolated signal. If $k - p = q$, then

$$M\{X^2(t)\} =$$

$$= \sum_{q=-\infty}^{\infty} R(q\Delta t) \sum_{p=-\infty}^{\infty} \operatorname{sinc} \frac{\pi}{\Delta t}(t - q\Delta t - p\Delta t) \operatorname{sinc} \frac{\pi}{\Delta t}(t - p\Delta t).$$

Through the use of the familiar Slepian equality [1], we obtain

$$M\{X^2(t)\} = \sum_{q=-\infty}^{\infty} R(q\Delta t) \frac{\sin q\pi}{q\pi} = R(0) = D\{x\}.$$

3. Let us consider quantity $M\{x(t)X(t)\}$, which after performance of the operation of statistical averaging can be written as

$$M\{x(t)X(t)\} = \sum_{k=-\infty}^{\infty} R(t - k\Delta t) \operatorname{sinc} \frac{\pi}{\Delta t}(t - k\Delta t).$$

Every factor under the summation sign can be expressed by a Fourier transform. If Fourier transform $R(\omega)$ corresponds to $R(\tau)$, and Fourier transform $\Pi(\omega)$ to $\operatorname{sinc} \frac{\pi}{\Delta t} t$, then

$$M\{x(t)X(t)\} =$$

$$= \frac{1}{4\pi^2} \int_{-\infty}^{\infty} \int_{-\infty}^{\infty} P(\omega_1)\Pi(\omega_2) e^{j\omega_1 t} e^{j\omega_2 t} \sum_{k=-\infty}^{\infty} e^{-j(\omega_1 - \omega_2)k\Delta t} d\omega_1 d\omega_2.$$

According to work [5]

$$\sum_{k=-\infty}^{\infty} e^{-j(\omega_1 - \omega_2)k\Delta t} = \frac{2\pi}{\Delta t} \sum_{k=-\infty}^{\infty} \delta\left(\omega_1 + \omega_2 - \frac{2\pi}{\Delta t} k\right)$$

and

$$\left.\begin{aligned} \Pi(\omega) &= \Delta t \text{ given } |\omega| \leqslant \frac{\pi}{\Delta t}; \\ \Pi(\omega) &= 0 \text{ given } |\omega| > \frac{\pi}{\Delta t}, \end{aligned}\right\}$$

$$M\{x(t)X(t)\} =$$

$$= \frac{1}{2\pi} \int_{-\frac{\pi}{\Delta t}}^{\frac{\pi}{\Delta t}} e^{j\omega_2 t} d\omega_2 \sum_{k=-\infty}^{\infty} \int_{-\infty}^{\infty} P(\omega_1)\, \delta\left(\omega_1 + \omega_2 - k\frac{2\pi}{\Delta t}\right) e^{j\omega_1 t} d\omega_1,$$

where $\delta(\omega)$ is the Dirac delta function.

Performing integration and introducing the symbol

$$\frac{1}{2\pi} \int_{-\frac{\pi}{\Delta t}}^{\frac{\pi}{\Delta t}} P\left(\omega - k\frac{2\pi}{\Delta t}\right) d\omega = \Delta P_k,$$

we obtain in final form

$$M\{x(t)X(t)\} = \sum_{k=-\infty}^{\infty} \Delta P_k e^{jk\frac{2\pi}{\Delta t}t}.$$

Appendix II

Using the representation $X_N(t)$ in the form of series (4) after averaging, we obtain

$$M\{x(t)X_N(t)\} = \sum_{k=-N}^{N} R(t - k\Delta t)\,\mathrm{sinc}\frac{\pi}{\Delta t}(t - k\Delta t).$$

On the basis of spectral interpolation theory [7] it can be proved that given $N\Delta t$, which significantly exceeds the correlation interval of the random signal under investigation, and given a small value of Δt in comparison with the correlation interval, the expression for $M\{x(t)X(t)\}$ can be written approximately in the form

$$M\{x(t)X(t)\} \cong D[x] \sum_{k=-N}^{N} \mathrm{sinc}\frac{\pi}{\Delta t}(t - k\Delta t).$$

Taking into consideration the resultant equality, and assuming a priori that $X_N(t)$ on the existence interval of readings differs little from the interpolated signal, we can write

$$M\{X_N^2(t)\} \cong M\{x(t)\,X_N(t)\} \cong D\{x\}\sum_{k=-N}^{N}\operatorname{sinc}\frac{\pi}{\Delta t}(t-k\Delta t).$$

Appendix III

Let us consider the behavior of generalized truncation error function $\gamma_N(t)$. It is known that

$$\lim_{N\to\infty}\sum_{k=-N}^{N}\operatorname{sinc}\frac{\pi}{\Delta t}(t-k\Delta t)=1.$$

Consequently, the series

$$\gamma_N(t)=\sum_{k=N+1}^{\infty}\left[\operatorname{sinc}\frac{\pi}{\Delta t}(t-k\Delta t)+\operatorname{sinc}\frac{\pi}{\Delta t}(t+k\Delta t)\right]$$

defines the generalized truncation error function on the interval $|t|<N\Delta t$. After reduction to a common denominator and replacement of the sines of the sum of two angles by trigonometric functions of the components of the angles, this series can be represented as

$$\gamma_N(t)=2\operatorname{sinc}\frac{\pi}{\Delta t}t\sum_{k=N+1}^{\infty}\frac{(-1)^{k-1}}{\left[k-\frac{\Delta t}{t}\right]^2-1}.$$

For any $|t|\leqslant N\Delta t$ series $\gamma_N(t)$ is an alternating convergent series, satisfying the conditions of the Leibniz theorem [2]. The sum of this series can be estimated by its first term

$$|\gamma_N(t)|<2\operatorname{sinc}\frac{\pi}{\Delta t}t\,\frac{(-1)^N}{\left|\frac{(N+1)\Delta t}{t}\right|^2-1}.$$

Analysis of this expression determines the fluctuating character of the truncation error function. Given $N\geqslant 10$ with error not exceeding 10 percent, it can be assumed that the maximum $|\gamma_N(t)|$ occurs given $t=(N-0.5)\Delta t$. The value of this maximum equals

$$|\gamma_N|_{\max\max}\leqslant 0{,}21\,\frac{N-0{,}5}{N+0{,}25}\approx 0{,}21.$$

BIBLIOGRAPHY

1. Bennet, W. R., Osnovnyye Ponyatiya i Metody Teorii Shumov v Radiotekhnike (Basic Concepts and Methods of Noise Theory in Radio Engineering), "Sovetskoye Radio" (Soviet Radio), Moscow, 1967.

2. Lyusternik, L. A., and Yanpol'skiy, A. R., Matematicheskiy Analiz, Funktsii, Predely, Ryady, Tsepnyye Drobi (Mathematical Analysis, Functions, Limits, Series, Continued Fractions), State Publishing House of Literature on Physics and Mathematics, Moscow, 1961.

3. Turbovich, I. T., Metod Blizkikh Sistem i yego Primeneniye dlya Sozdaniya Inzhenernykh Metodov Rascheta Lineynykh i Nelineynykh Radiotekhnicheskikh Sistem (Method of Proximate Systems and Its Use to Create Engineering Methods of Calculating Linear and Nonlinear Radio-Engineering Systems), Publishing House of the Academy of Sciences USSR, Moscow, 1961.

4. Kharkevich, A. A., Radiotekhnika (Radio Engineering), 1958, 13, 8.

5. Schwartz, L., Matematicheskiye Metody dlya Fizicheskikh Nauk (Mathematics for the Physical Sciences), "Mir" (World), Moscow, 1965.

6. Helms, H. D., and Thomas, J. B., PIRE, 1962, 2, 50.

7. Kohlenberg, A., J. Appl. Phys., 1953, 24, 12.

DETERMINATION OF THE SPECTRAL DENSITY OF A DETERMINISTIC SIGNAL FROM A DISCRETE SEQUENCE OF SIGNAL READINGS

Metody i Ustroystva Preobrazovaniya Graficheskoy Informatsii (Methods and Devices for the Conversion of Graphic Data), 1968, pages 41-44

V. I. Chaykovskiy and L. Ya. Yalovenko

In the experimental determination of signal spectral density f(t) the analyzer of any type of spectrum approximately realizes functional transforms of the form

$$c(\omega) = \int_{-\infty}^{\infty} f(t)\cos\omega t\,dt$$

or

$$s(\omega) = \int_{-\infty}^{\infty} f(t)\sin\omega t\,dt, \qquad (1)$$

corresponding to the determination of the cosine or sine component of the spectrum.

If the signal under investigation is given in the form of a discrete sequence of signal readings $f(k\Delta t)$, then in order to determine the spectrum we can use the copy restored according to Kotel'nikov

$$F(t) = \sum_{k=-\infty}^{\infty} f(k\Delta t)\,\frac{\sin\frac{\pi}{\Delta t}(t-k\Delta t)}{\frac{\pi}{\Delta t}(t-k\Delta t)}. \qquad (2)$$

The transforms

$$C(\omega) = \int_{-\infty}^{\infty} F(t)\cos\omega t\,dt;$$

$$S(\omega) = \int_{-\infty}^{\infty} F(t)\sin\omega t\,dt \qquad (3)$$

only approximately define the cosine and sine spectrum components since the restored copy F(t) of the real signal only approximately corresponds to the signal itself f(t) [1].

Let us determine the error which arises in calculating the spectrum when the signal is replaced by its restored copy

$$\Delta_c(\omega) = C(\omega) - c(\omega);$$

$$\Delta_s(\omega) = S(\omega) - s(\omega). \qquad (4)$$

For this purpose let us use the familiar expression for the spectrum of a signal restored according to Kotel'nikov [3]:

$$\left.\begin{aligned} C(\omega) &= \sum_{k=-\infty}^{\infty} c\left(\omega - k\frac{2\pi}{\Delta t}\right) \text{given } |\omega| \leqslant \frac{\pi}{\Delta t}; \\ C(\omega) &= 0 \qquad\qquad \text{given } |\omega| > \frac{\pi}{\Delta t} \end{aligned}\right\} \tag{5}$$

or

$$\left.\begin{aligned} S(\omega) &= \sum_{k=-\infty}^{\infty} s\left(\omega - k\frac{2\pi}{\Delta t}\right) \text{given } |\omega| \leqslant \frac{\pi}{\Delta t}; \\ S(\omega) &= 0 \qquad\qquad \text{given } |\omega| > \frac{\pi}{\Delta t}. \end{aligned}\right\} \tag{6}$$

From expressions (5) and (6) it follows that the spectral density obtained from the restored copy of the signal differs on any frequency ω from the idealized spectral density due to the presence of additional components ($k \neq 0$). The sum of these additional components equals the sought error

$$\begin{aligned} \Delta_C(\omega) &= \sum_{k=-\infty}^{\infty}{}' c\left(\omega - k\frac{2\pi}{\Delta t}\right); \\ \Delta_S(\omega) &= \sum_{k=-\infty}^{\infty}{}' s\left(\omega - k\frac{2\pi}{\Delta t}\right). \end{aligned} \tag{7}$$

In expression (7) the prime affixed to the summation sign signifies that summation is performed for all values of k except k = 0.

The resultant expression defines the error in calculating the spectrum from the restored signal realization. An analogous result can be obtained without preliminary restoration of the signal by making direct use of signal readings for determination of the spectrum.

As a matter of fact, equalities (3) are equivalent to equalities

$$\begin{aligned} C(\omega) &= \Delta t \sum_{k=-\infty}^{\infty} f(k\Delta t)\cos k\Delta t\omega; \\ S(\omega) &= \Delta t \sum_{k=-\infty}^{\infty} f(k\Delta t)\sin k\Delta t\omega. \end{aligned} \tag{8}$$

We can readily satisfy ourselves of this by replacing F(t) in (3) by its expression in the form of series (2) and performing integration. The identity of equalities (3) and (8) confirms the assumption stated above.

Both of the above-considered cases of spectral density determination are in practice realized only approximately by virtue of the limited analysis time. In fact, the spectral density of truncated signal $f_T(t)$ is estimated here

$$c_T(\omega) = \int_{-\infty}^{\infty} f_T(t)\cos\omega t dt = \int_{-T}^{T} f(t)\cos\omega t dt;$$
$$s_T(\omega) = \int_{-\infty}^{\infty} f_T(t)\sin\omega t dt = \int_{-T}^{T} f(t)\sin\omega t dt. \quad (9)$$

Here

$$\left.\begin{aligned} f_T(t) &= f(t) \text{ given } |t| \leqslant T; \\ f_T(t) &= 0 \text{ given } |t| > T. \end{aligned}\right\} \quad (10)$$

The quantities $c_T(\omega)$ and $s_T(\omega)$ are the practically attainable estimates of idealized spectral characteristics of real signal $c(\omega)$ and $s(\omega)$ and are linked with them by the simple dependence [2].

$$c_T(\omega) = \frac{T}{\pi}\int_{-\infty}^{\infty} c(\nu)\frac{\sin T(\omega-\nu)}{T(\omega-\nu)}d\nu;$$
$$s_T(\omega) = \frac{T}{\pi}\int_{-\infty}^{\infty} s(\nu)\frac{\sin T(\omega-\nu)}{T(\omega-\nu)}d\nu. \quad (11)$$

Obviously, $c_T(\omega)$ and $s_T(\omega)$ can be considered idealized spectral densities $c(\omega)$ and $s(\omega)$, smoothed by a sliding spectral slit of the form $\frac{\sin\omega T}{\omega T}$.

The limitation of analysis time in the determination of spectral density from readings shows up in the limitation of the number of readings taken into consideration. Spectral density in this case is determined by the truncated sum

$$C_N(\omega) = \Delta t\sum_{k=-N}^{N} f(k\Delta t)\cos k\Delta t\omega;$$
$$S_N(\omega) = \Delta t\sum_{k=-N}^{N} f(k\Delta t)\sin k\Delta t\omega. \quad (12)$$

Truncation of the sum is the source of additional error, which results from the smoothing effect considered above.

Total error (error occurring by reason of the discretization of the signal and by reason of the limitation of the number of readings taken into consideration to the quantity 2N + 1) can be determined relative to the estimate thereof $c_T(\omega)$ or $s_T(\omega)$, attainable in practice during the selected analysis time $2T = 2N\Delta t$

$$\Delta_{C_N} = C_N(\omega) - c_T(\omega);$$
$$\Delta_{C_N} = S_N(\omega) - s_T(\omega). \quad (13)$$

It can be assumed that expression (12) formally corresponds to the determination of spectral density by infinite sum (8) for signal $f_T(t)$, truncated in interval $(-N\Delta t; N\Delta t)$, the spectral density of which $c_T(\omega)$ (or $s_T(\omega)$) is characterized by expression (11). Therefore, in order to estimate the error, let us make use of expressions analogous to (7). Therefore, the unknown error equals

$$\Delta_{S_N} = \sum_{k=-\infty}^{\infty}{}' c_T\left(\omega - k\frac{2\pi}{\Delta t}\right);$$
$$\Delta_{S_N} = \sum_{k=-\infty}^{\infty}{}' s_T\left(\omega - k\cdot\frac{2\pi}{\Delta t}\right). \qquad (14)$$

Here $c_T(\omega)$ and $s_T(\omega)$ are components of the spectral density of the investigated signal, truncated in interval $2T = 2N\Delta t$.

BIBLIOGRAPHY

1. Kharkevich, A. A., Radiotekhnika (Radio Engineering), 1958, 8.

2. Kohlenberg, A., J. Appl. Phys., 1953, 24, 12.

3. Bauman, R. H., Ann. de Radioelectricite, 1965, XX, 79.

ERROR IN SIGNAL RESTORATION BY MODIFIED KOTEL'NIKOV SERIES

Metody i Ustroystva Preobrazovaniya Graficheskoy Informatsii (Methods and Devices for the Convertion of Graphic Data), 1968, pages 45-48

G. I. Vasyuk

Generally, a real signal is expressed by the segment of a function having an infinite expanse and possessing an indefinitely broad spectrum. In the instrumental restoration of such signals from discrete readings, theoretical restoration error is represented in the form of two components. One of these, usually called quantization error, is due to the fact that only a finite frequency of readings of instantaneous signal values can actually be assured. The second component (truncation error) results from the fact that in signal restoration allowance cannot be made for approximating function values lying outside the signal existence sector.

However, the expression of restoration error can be simplified somewhat for some classes of signals. This simplification is based on the theorem [2]: "Whatsoever the function f(t) which is continuous on segment $(-T, +T)$, and whatsoever $\xi > 0$, there exists a function $f_\xi(t)$, belonging to class W_α * and differing from f(t) on the indicated interval by less than ξ."

In conformity with the above-cited theorem, every signal which is continuous on the existence segment can be approximated with as great accuracy as desired by a function with a limited spectrum. In this case theoretical restoration error reduces solely to truncation error.

There are several works [1, 3, 4] devoted to the reduction of truncation error which suggest some modifications of the Kotel'nikov series. A signal-approximating function with a limited spectrum is expanded in a series with respect to composition functions which decrease more rapidly than the function $\frac{\sin x}{x}$.

Such a composition function can be represented in the form of the product

---

* W_α is a class of integral functions of finite degree $\leq \alpha$, square-integrable on the entire real axis.

$$b(t) = \frac{\sin \pi \frac{t}{\Delta t}}{\pi \frac{t}{\Delta t}} \varphi(t), \tag{1}$$

where φ (t) is a certain even, decreasing weighting function; and Δ t is the quantization interval.

The rapid decrease of composition functions of form (1) causes a decline in the influence of each disregarded reading on restoration error, which in some cases results in a decline in error.

It is easy to show [1] that in the absence of additional conditions a weighting function is not uniquely defined, i.e. it can have an infinite number of variants. Therefore, the problem arises of finding weighting functions which most significantly decrease restoration error for the broadest class of signals.

The restoration error of a function with a limited spectrum can be expressed as follows:

$$\delta(t) = \sum_{k=-\infty}^{-M} f(k\Delta t)\, b(t - k\Delta t) + \sum_{k=N}^{\infty} f(k\Delta t)\, b(t - k\Delta t), \tag{2}$$

where M is the number of readings taken into account to the left of point t ; and N is the number of readings taken into account to the right of point t .

Generally, discrete readings f(kΔ t) can have arbitrary absolute values and signs. Therefore, analysis of the dependence of error δ (t) on variation in the form of the weighting function is an exceedingly complex problem, to which no solution has been obtained.

The literature presents only estimates of error variation: decrease in upper error limit is determined by using a series with a concrete form of weighting function. Thus, by using a Cauchy inequality an estimate of the upper limit of squared error can be obtained:

$$\delta^2(t) \leqslant \left[\sum_{k=-\infty}^{-M} f^2(k\Delta t) + \sum_{k=N}^{\infty} f^2(k\Delta t)\right] \times \left[\sum_{k=-\infty}^{-M} b^2(t - k\Delta t) + \sum_{k=N}^{\infty} b^2(t - k\Delta t)\right].$$

The estimate of mean-squared error in interval 0 — Δ t of the restoration sector equals

$$S = \frac{1}{\Delta t} \int_0^{\Delta t} \delta^2(t)\, dt$$

Let us use an example to illustrate the possibility of reducing restoration error by employing series with composition functions of form (1).

In the event of the use of weighting function

$$\varphi(t) = \frac{\sin \Delta\omega t}{\Delta\omega t},$$

where $\Delta\omega = \frac{\pi}{\Delta t} - \omega_b$; and ω_b is the upper limit of the spectrum of function f(t), the decrease in the upper limit of mean-square error in the extreme interval (M = 1) given $N \gg 1$ and $\frac{\omega \Delta t}{\pi} = \frac{1}{2}$ amounts to

$$\frac{S_{кот}}{S_{wt}} \simeq 16.$$

Analysis of the variation in restoration error when various weighting functions are used is hampered by the fact that a weighting function with growth $|t|$ can be nonmonotonically increasing and even alternating. Therefore, let us limit ourselves to a consideration of error variation in the event of the use of weighting functions which decrease monotonically, at least in the interval which anywhere significantly defines restoration error [1].

Let us indicate a class of functions f(t), for which the use of expansion with weighting monotonically decreasing functions results in a decrease in error at any point on the restoration sector.

For nonalternating functions f(t), series (2) is alternating. If the rate of growth of functions f(t) outside the restoration region does not exceed $|t|$, then by pairwise summation series (2) reduces to a nonalternating series. The use of weighting functions which are monotonically decreasing reduces the magnitude of each term in such a nonalternating series and, hence, the total sum in absolute magnitude. Thus, through using a Kotel'nikov series expansion with monotonically decreasing functions, we reduce restoration error in the case where the signal is expressed by a segment of a nonalternating function with a limited spectrum, with this function growing no more rapidly than $|t|$ outside the restoration region.

Further analysis will probably permit considerable expansion of the class of signals which the Kotel'nikov series with weighting functions can rationally be used to restore.

BIBLIOGRAPHY

1. Vasyuk, G. I., Vestnik KPI. Seriya Radiotekhniki (Herald of Kiev Polytechnic Institute: Radio-Engineering Series), No. 3, 1966.

2. Khurgin, Ya. I., and Yakovlev, V. P., Metody Teorii Tselykh Funktsiy v Radiofizike, Teorii Svyazi i Optike (Integral Function Theory Methods in Radiophysics, Communication Theory and Optics), State Publishing House of Literature on Physics and Mathematics, Moscow, 1962.

3. Haber, F., IEEE Trans. on Comm. Systems, 1964, 1.

4. Helms, H. D., and Thomas, J. B., PIRE, 1962, 50, 2.

THE CONVERSION OF CONTINUOUS GRAPHIC DATA INTO DISCRETE

Metody i Ustroystva Preobrazovaniya Graficheskoy Informatsii (Methods and Devices for the Conversion of Graphic Data), 1968, pages 49-56

V. G. Dolotov

The process of converting continuous messages represented in the form of graphs, oscillograms, electric signals etc. into discrete messages reduces to discretization operations (sampling of readout points) and to the quantization of messages at the readout points.

Figure 1 presents a classification of discretization methods for continuous messages. Questions of uniform discretization are considered in [1], and questions of nonuniform (adaptive) discretization in [4-6].

It is of great interest to investigate the feasibility of uniform and adaptive discretization based on orthogonal systems of Haar and Walsh functions.

Let us consider certain questions in the discretization of continuous messages $\{f(t)\}$. A priori information about these messages includes data regarding the ranges of variation in messages and the maximum modulus of the first derivative M_1.

We shall estimate reproduction accuracy by the criterion of maximum deviation. As reproducing (approximating) functions let us adopt power polynomials of zero and first degree.

The interval between readings in the event of uniform discretization with reproducing polynomial P(t) of zero degree for $\lambda_{max} = 1$ [4] is

$$\Delta_1 t = \frac{\varepsilon_0}{M_1}. \tag{1}$$

Given $\lambda_{max} = 2$, the interval between readings is

$$\Delta_2 t = 2\frac{\varepsilon_0}{M_1}. \tag{2}$$

λ designates the number of points in the discretization interval, where the difference f(t) - P(t) reaches maximum permissible error ε_0 with subsequent alternation of signs.

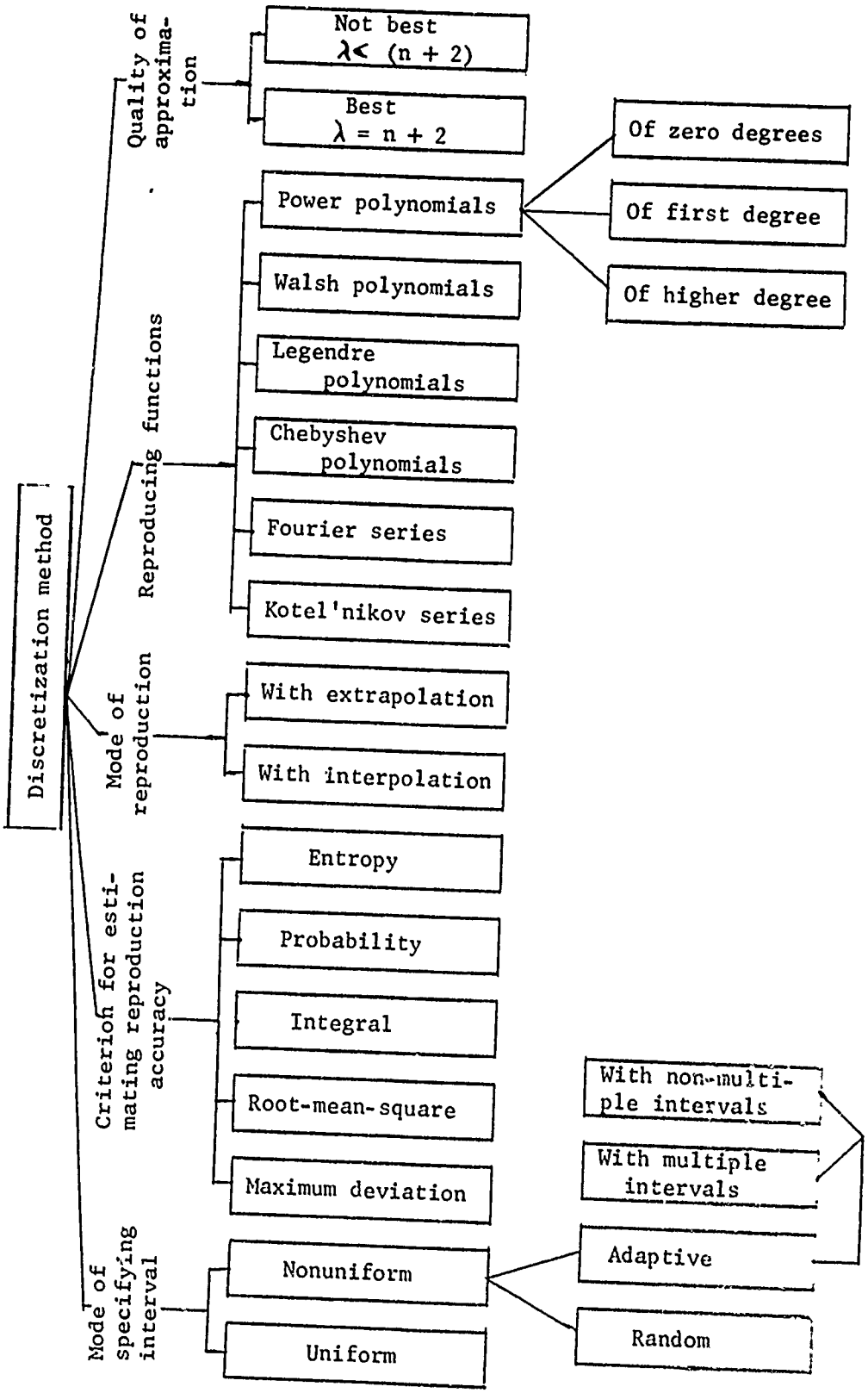

Figure 1. Classification of methods for the discretization of continuous messages.

The entire aggregate of possible messages $\{f(t)\}$ in the interval $\Delta_k t = k\Delta_1 t$ can be replaced by a finite number of catalog functions $P_q(t)$ with an error not greater than ε_0. Figure 2,a shows the existence domain of messages $\{f(t)\}$, bounded by lines $f_{11}(t)$ and $f_{12}(t)$ with angular coefficients $\pm M_1$, and the grid of approximating functions $P_{\mu 1}$ and $P_{\nu 2}(t)$, where $\mu, \nu = 1, 2, \ldots, k-1$.

The number of catalog functions S coincides with the number of unidirectional routes from the point of intersection of lines $P_{11}(t)$ and $P_{12}(t)$ to the nodes of the line $t = \Delta_k t$ (Figure 2,b). According to Pascal's triangle [3] in Figure 2,c we shall find

$$S = \sum_{i=0}^{k-1} C_{k-1}^{i} = 2^k.$$

The message discretization process in this case reduces to the reading of the values of the message at the initial points of the intervals and the determination of the catalog numbers q = 1, 2, ..., S or the characteristics of the message from which the catalog number q can be restored. Let us illustrate this with the example of uniform discretization given k = 3 and k = 4. The catalog functions take the following form:

$$\text{given } {}^{t\in\Delta_1 t,\ \Delta_k t} P_{1,2}(t) = \begin{cases} f(t_H), & t_H \leqslant t \leqslant \Delta_1 t, \\ f(t_H) \pm M_1 (t - \Delta_1 t) & \Delta_1 t \leqslant t \leqslant t_k; \end{cases} \tag{3}$$

$$\text{given } {}^{t\in\Delta_1 t,\ \Delta_k t} P_{3,4}(t) = \begin{cases} f(t_1), & t_H \leqslant t \leqslant \Delta_1 t, \\ f(t_1) \pm M_1 (t - \Delta_1 t), & \Delta_1 t \leqslant t \leqslant 2\Delta_1 t, \\ f(t_H) \pm \varepsilon_0 \mp M_1 (t - 2\Delta_1 t), & 2\Delta_1 t \leqslant t \leqslant t_k; \end{cases} \tag{4}$$

$$\text{given } {}^{t\in\Delta_k t} P_{5,6}(t) = \begin{cases} f(t_1), & t_H \leqslant t \leqslant \Delta_1 t; \\ f(t_H) \pm M_1 (t - \Delta_1 t), & \Delta_1 t \leqslant t \leqslant 3\Delta_1 t, \\ f(t_H) \pm 2\varepsilon_0 \mp M_1 (t - 3\Delta_1 t), & 3\Delta_1 t \leqslant t \leqslant t_k; \end{cases} \tag{5}$$

$$\text{given } {}^{t\in\Delta_k t} P_{7,8}(t) = \begin{cases} f(t_H), & t_H \leqslant t \leqslant \Delta_1 t, \\ f(t_H) \pm M_1 (t - \Delta_1 t), & \Delta_1 t \leqslant t \leqslant 2\Delta_1 t, \\ f(t_H) \pm \varepsilon_0 \mp M_1 (t - 2\Delta_1 t), & 2\Delta_1 t \leqslant t \leqslant 3\Delta_1 t, \\ f(t_H) \pm M_1 (t - 3\Delta_1 t), & 3\Delta_1 t \leqslant t \leqslant t_k. \end{cases} \tag{6}$$

The upper of the binary digits in (3)-(6) correspond to functions $P_q(t)$ with odd q, the lower to functions with even q. t_H and t_k denote the starting and end points of intervals.

Block diagrams of discretizers are given for one of the variants of the organization of message processing. Given k = 3 in the discretizer (Figure 3,a) the sign of the difference $f(2\Delta_1 t) - f(t_H)$ is determined. Given k = 4 (Figure 3,b) the discretizer additionally includes blocks for the determination of $|f(3\Delta_1 t - f(t_H)|$ and the comparison of this quantity with ε_0.

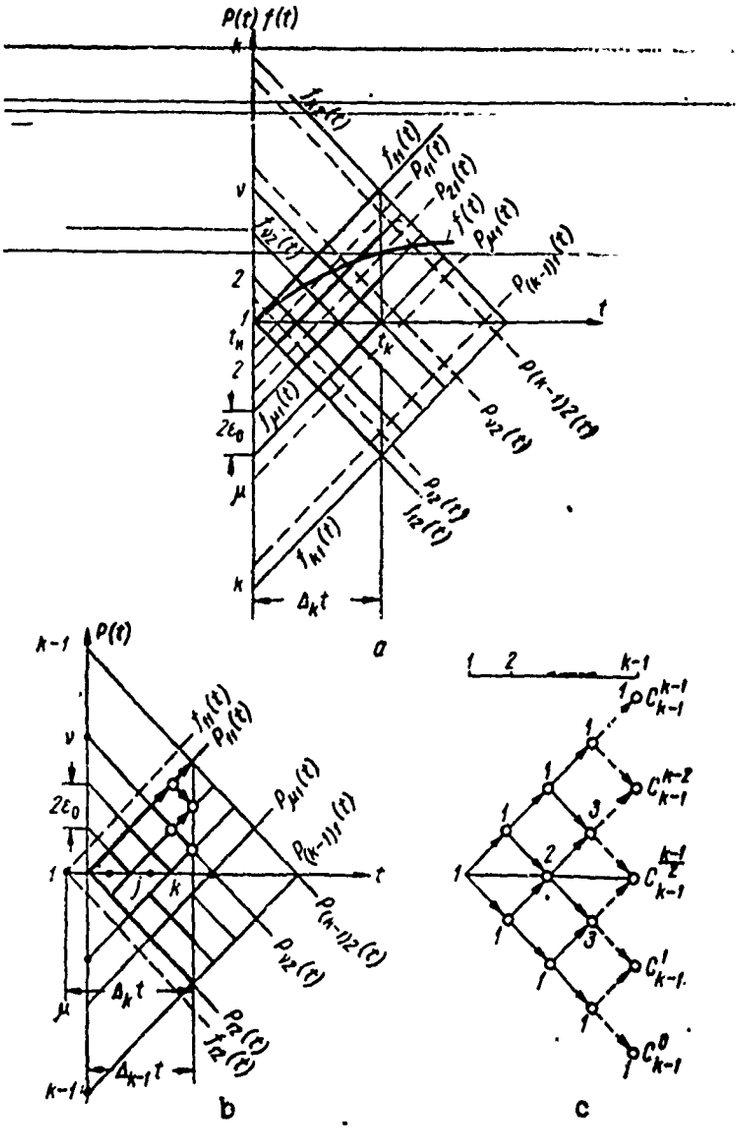

Figure 2. Replacement of aggregate of messages with a finite number of catalog functions:

a) domain of existence of messages and grid of approximating functions;
b) choice of number of catalog functions;
c) Pascal's triangle.

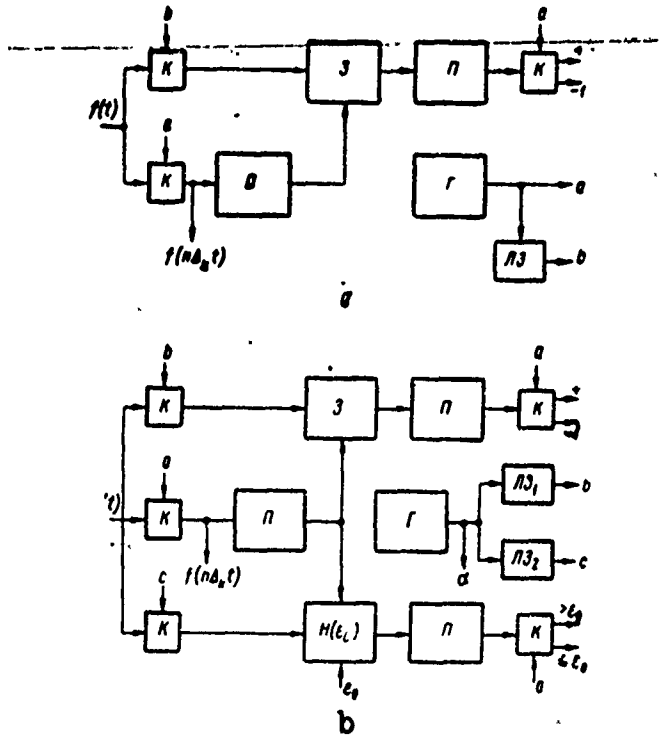

Figure 3. Block diagram of discretization devices: given k = 3 (a) and 4 (b):

П) memory block;
З) block for sign determination;
Н) comparator;
Г) pulser;
ЛЗ) delay line;
К) keys.

Let us give the logic circuits of restoration programs for k = 3 and k = 4:

1) $\overset{1}{\downarrow} p_1 \overset{2}{\uparrow} p_2 \overset{1}{\uparrow} B_1 A\omega \overset{4}{\uparrow} \overset{1}{\downarrow} B_2 A\omega \overset{4}{\uparrow} \overset{2}{\downarrow} p_2 \overset{3}{\uparrow} B_3 A\omega \overset{4}{\uparrow} \overset{3}{\downarrow} B_4 A\omega \overset{4}{\uparrow}$;

2) $\overset{5}{\downarrow} p_3 \overset{1}{\uparrow} p_4 \overset{2}{\uparrow} B_1 A\omega \overset{8}{\uparrow} \overset{2}{\downarrow} B_2 A\omega \overset{8}{\uparrow} \overset{1}{\downarrow} p_5 \overset{3}{\uparrow} p_6 \overset{4}{\uparrow} p_4 \overset{5}{\uparrow} B_5 A\omega \overset{8}{\uparrow} \overset{5}{\downarrow} B_4 A\omega \overset{8}{\uparrow} \overset{4}{\downarrow}$
$\overset{5}{\uparrow} \overset{4}{\downarrow} p_6 \overset{6}{\uparrow} B_7 A\omega \overset{8}{\uparrow} \overset{6}{\downarrow} B_6 A\omega \overset{6}{\uparrow} \overset{3}{\downarrow} p_4 \overset{5}{\uparrow} B_3 A\omega \overset{5}{\uparrow} \overset{5}{\downarrow} B_4 A\omega \overset{6}{\uparrow}$.

The letters A and B_q denote the operators for entering message $f(t_H)$ and catalog number q in the memory cells.

Logical conditions:

$$p_1(|f(t_n)-f(t_k)|>\varepsilon_0)=1;$$
$$p_2(\operatorname{sign}|f(2\Delta_1 t)-f(t_n)|=+1)=1;$$
$$p_3(|f(t_n)-f(t_k)|>2\varepsilon_0)=1;$$
$$p_4(\operatorname{sign}|f(t_k)-f(t_n)|=+1)=1;$$
$$p_5(p_2=p_4)=1;$$
$$p_6(|f(3\Delta_1 t)-f(t_n)|>\varepsilon_0)=1.$$

The symbol ω denotes the transition to the beginning of a line [2]. The final restoration of the message is performed according to (3)-(6).

Let us consider adaptive discretization on the basis of a combined algorithm. Let us isolate several of the simplest algorithms, each of which considers one of the possible tendencies in the variation of a message (periodicity, rate of change close to the maximum possible rate, invariability etc.), and on the basis of these algorithms construct a combined algorithm for adaptive discretization.

The block diagram of a discretizer with a combined algorithm is given in Figure 4.

The operation of the program block of such a discretizer is described by the line

$$\overset{0}{\downarrow} F(n)\,|n\to E_n|\,|n\to G_n|\,|n\to H_n|\,C_1C_2C_3E_nG_nH_n\,(p_7\wedge p_9\,(p_4\vee$$
$$\vee p_5))\overset{3}{\uparrow}|1-m,l|\overset{3}{\downarrow}(p_{11}\vee p_{12})\overset{4}{\uparrow}|2\to m,l|\overset{4}{\downarrow}p_{14}\overset{0,1,2}{\uparrow}p_7\overset{5}{\uparrow}|1\to$$
$$\to f(t_0)|\overset{6,1}{\downarrow}|(n-1)\to D(f(t_n))|\,D(t_0)\,D(t_n)\,\omega\overset{0}{\uparrow}.$$

The letters C_1, E_n, G_n, H_n denote the operators for the subtraction of the quantities $\Delta f(t) = f(t) - f(t_0)$, $(2n-1)\varepsilon_0$, $(n+1)\varepsilon_0$, $(n-1)\varepsilon_0$; the letters C_2, C_3, D operators for measuring the first nonzero value of $\operatorname{sign}_1 \Delta f(t)$ which entry in the memory, and for measuring the quantities $\operatorname{sign} \Delta f(t)$ and $f(t)$; and the symbols F_n and $[4 \to Q]$ operators for the input of the number n and the quantity r^n into Q or memory cells m, l.

Logical conditions:

$$p_7(|\Delta f(t)|>\varepsilon_0)=1;$$
$$p_9(|\Delta f(t)|>2\varepsilon_0)=1;$$
$$p_9(|\Delta f(t)|<(2n-1)\varepsilon_0)=1;$$
$$p_{10}(|\Delta f(t)|\geq(n-1)\varepsilon_0)=1;$$
$$p_{11}(|\Delta f(t)|<(n-1)\varepsilon_0)=1;$$
$$p_{12}(\operatorname{sign}_1\Delta f(t)\neq\operatorname{sign}\Delta f(t))=1;$$
$$p_{13}(\operatorname{sign}_1\Delta f(t)=+1)=1;$$
$$p_{14}\begin{pmatrix} l=0\\ l=1\\ l=2\end{pmatrix}=\begin{matrix}0;\\1;\\2.\end{matrix}$$

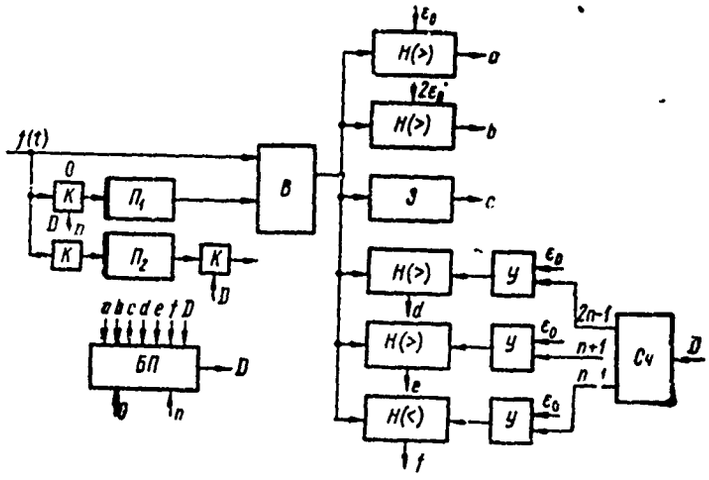

Figure 4. Block diagram of adaptive discretization device:
П) memory block;
Н) comparator;
З) sign determination block
В) subtracter;
У) multiplier;
Сч) counter;
К) keys;
БП) program block.

During restoration the quantities n, $\Delta f(t)$, sign $\Delta f(t)$ are calculated. The discretization intervals for the considered combined algorithm $\tau_i = h\Delta_2 t$, where h = 1, 2, 3...

Preliminary estimates show that the effectiveness of the catalog methods of uniform discretization (in comparing relative ξ -- entropy) is at least one and a half to two times higher than the effectiveness of uniform discretization with the interval $\Delta_1 t$.

The effectiveness of adaptive discretization with a combined algorithm (according to an estimate of the lower limit of the mathematical expectation of the number of readouts) is approximately two times higher than the effectiveness of adaptive discretization based on one of the component algorithms and six times higher than the effectiveness of uniform discretization with the interval $\Delta_1 t$.

BIBLIOGRAPHY

1. Kotel'nikov, V. A., O Propusknoy Sposobnosti Efira i Provoloki v Radiosvyazi (The Capacity of Ether and Wire in Radio Communication), Publishing House of the All-Union Power-Engineering Committee, Moscow State University, 1933.

2. Lyapunov, A. A., Problemy Kibernetiki -- Sbornik (Problems in Cybernetics -- Collection of Works), No. 1, State Publishing House of Literature on Physics and Mathematics, Moscow, 1958.

3. Ryser, H. J., Kombinatornaya Matematika (Combinatorial Mathematics), "Mir" (World), Moscow, 1960.

4. Temnikov, F. Ye., Avtomaticheskiye Registriruyushchiye Pribory (Automatic Recording Instruments), State Scientific and Technical Publishing House of Literature on Machine-Building, Moscow, 1960.

5. Temnikov, F. Ye., Teoriya Razvertyvayushchikh Sistem (Scanning System Theory), State Scientific and Technical Power-Engineering Publishing House, Moscow-Leningrad, 1963.

6. Fridrikh, Z., Izvestiya Vuzov, Radiofizika (Bulletin of Higher Educational Institutions: Radiophysics), 1960, 3, 2.

NEW FORMULAS FOR CALCULATING THE AMOUNT OF INFORMATION (MISINFORMATION) RECEIVED IN THE MEASUREMENT AND TRANSFORMATION OF QUANTITIES

Metody i Ustroystva Preobrazovaniya Graficheskoy Informatsii (Methods and Devices for the Conversion of Graphic Data), 1968, pages 61-64

A. Ye. Kulinkovich

The processes of the measurement and transformation of quantities at present are regarded as informational. Such an approach permits, on the basis of Shannon's theory [4], a quantitative estimate of the volume of information obtained during measurement, which is of great interest in determining the number of positions necessary to store the results of a measurement (transformation) and in estimating the absolute and relative effectiveness of a measurement (transformation) method.

Widely known is Brillouin's formula [1], which connects the amount of information I with the measurement range of a measured quantity $x_2 - x_1$ and the measurement error Δ

$$I = \log_2 \frac{x_2 - x_1}{\Delta}. \tag{1}$$

(the error Δ in [1] is considered constant).

Of interest is the case where the error depends on the quantity to be measured. The corresponding generalization of Brillouin's formula gives the expression

$$I = \frac{1}{x_2 - x_1} \int_{x_1}^{x_2} \log_2 \frac{x_2 - x_1}{\Delta(x)}\, dx. \tag{2}$$

Formula (2) can be written as an expression analogous to (1),

$$I = \log_2 \frac{x_2 - x_1}{\Delta_{ef}}, \tag{3}$$

where Δ_{ef} is a certain mean error, said by us to be <u>effective</u>.

The latter is determined from the formula

$$\Delta_{ef} = \exp\left(\frac{1}{x_2 - x_1} \int_{x_1}^{x_2} \log_2 \frac{1}{\Delta(x)}\, dx \right). \tag{4}$$

The concept of effective accuracy becomes most clear in using a multiplicative integral, which differs from an ordinary Riemann definite integral in that there is a limit not of the sum $\sum_{i=1}^{n} f(\xi_i)\Delta x_i$, but rather of the product $\prod_{i=1}^{n} f(\xi_i)^{\Delta x_i}$.

A multiplicative integral within the limits $x_1 x_2$ of the function f(x) will be designated as $\int_{x_2}^{x_1} [f(x)]^{dx}$.

The following relation exists between the Riemann and multiplicative integral:

$$\int_{x_1}^{x_2} [f(x)]^{dx} = \exp\left(\int_{x_1}^{x_2} \ln f(x)\right) dx. \tag{5}$$

Just as a Riemann definite integral, divided by the integration integral, represents a generalization of the concept of the arithmetic mean in the case of a continuum, the radical of a multiplicative integral with the index of the radical equal to the integration interval is a generalization of the concept of the geometric mean. From (5) we obtain:

$$\frac{1}{\Delta_{ef}} = \sqrt[x_2-x_1]{\int_{x_1}^{x_2} \left[\frac{1}{\Delta(x)}\right]^{dx}}. \tag{6}$$

If the dependence $\Delta = f(x)$ is represented as a step function, then

$$\frac{1}{\Delta_{ef}} = \sqrt[x_n-x_0]{\prod_{i=1}^{n} \left(\frac{1}{\Delta i}\right)^{x_i-x_{i-1}}}. \tag{7}$$

In many cases it is convenient to consider the relative effective error

$$\tilde{\Delta}_{ef} = \frac{\Delta ef}{x_2 - x_1}.$$

The amount of information I is connected with $\tilde{\Delta}_{ef}$ by the relation

$$I = -\log_2 \tilde{\Delta}_{ef} \tag{8}$$

In practice, cases often occur where the relative error $\delta = \frac{\Delta}{x}$ can be considered constant. In such case

$$\tilde{\Delta}'_{ef} = \frac{\delta k^{\frac{k}{k-1}}}{e(k-1)}, \tag{9}$$

where e is the base of natural algorithms and $k = \frac{x_2}{x_1}$ is the coefficient of differentiation.

If the error Δ weakly depends on x, so that the arithmetic mean proves sufficiently close to the geometric mean, then the following expression can be used for $\tilde{\Delta}_{ef}$:

$$\frac{1}{\tilde{\Delta}_{ef}} \cong \int_{x_1}^{x_2} \frac{dx}{\Delta(x)}. \tag{10}$$

In particular, if δ does not depend on x, it follows from (10) that

$$\tilde{\Delta}_{ef} \cong \frac{\delta}{\ln k} = \frac{\delta}{\ln \frac{x_2}{x_1}}. \tag{11}$$

Formulas (9) and (11) are important for choosing the optimal variant under those conditions where an increase in the coefficient of differentiation entails an increase in measurement error, and vice versa.

The coefficient r is connected with the amount of information I by the relation [2, 5]

$$|r| = \sqrt{1 - 2^{-2I}}. \tag{12}$$

Hence follows the simple dependence between $\tilde{\Delta}_{ef}$ and r

$$|r| = \sqrt{1 - \Delta^2_{ef}} \tag{13}$$

or, considering that in many cases $\tilde{\Delta}^2_{ef} \ll 1$,

$$|r| \approx 1 - \frac{\tilde{\Delta}^2_{ef}}{2}. \tag{14}$$

Expressions (13) and (14) make it possible to estimate according to the statistical connection test the accuracy of determination of one quantity x from a certain quantity y statistically connected with x.

For estimating the informativeness of measurement methods the a priori entropy H_{apr} is first calculated. For this purpose, given a specified sufficient error of measurement $\Delta_{spec}(x)$ $\tilde{\Delta}_{ef}$ and I are found. Obviously, H_{apr} equals the amount of information which is necessary to solve a given problem. Then, on the basis of actual error $\Delta_{act}(x)$ the amount of information received I_{rec} is calculated. The absolute measure of effectiveness is the a posteriori effectiveness (residual indeterminacy)

$$H_{apost} = H_{apr} - I_{rec}. \tag{15}$$

If $H_{apost} = 0$, the given method of measurement completly solves the posed problem, but if $H_{apost} > 0$, the given method is insufficiently informative. For example, a residual entropy of 1 bit means that the methods gives an accuracy twice as bad as necessary. Given $H_{apost} < 0$, the method possesses redundant informativeness.*

The relative estimate used for the measurement (transformation) method should be the increment of information -- the difference in the amount of information received by competing methods.

$$\Delta I = I_{rec}^{(1)} - I_{rec}^{(2)} = H_{apost}^{(1)} - H_{apost}^{(2)}. \qquad (16)$$

It should be noted that use of the increment of information proves very convenient in practice. Being in a certain sense a generalization of the concept of Shannon's amount of information, this quantity may be a measure of both information and misinformation. At the same time, in using this quantity we actually do not go beyond the limits of Shannon's theory (as is known, a shortcoming of Shannon's determination of the amount of information is that it is substantially a positive quantity and cannot serve as a measure of misinformation [3]).

The increment of information can also be used to estimate the misinformation received during a transformation. If $\Delta_1(x)$ and $\Delta_2(x)$ are errors taking place respectively before and after a transformation, and I_1 and I_2 are the corresponding values for the information received (in devices which do not provide "enrichment" of the information $I_1 \geqslant I_2$), then the misinformation equals

$$\Delta I = I_1 - I_2 = H_{apost}^{(2)} - H_{apost}^{(1)}. \qquad (17)$$

BIBLIOGRAPHY

1. Brillouin, L., Nauka i Teoriya Informatsii (Science and Information Theory), State Publishing House of Literature on Physics and Mathematics, Moscow, 1960.

2. Kulinkovich, A. Ye., in the collection of works, Metodika Geofizicheskikh Issledovaniy (Methods of Geophysical Research), "Naukova Dumka" (Scientific Thought), Kiev, 1965.

---

* The aforesaid is valid if in the interval $x_1 - x_2$ for any x the inequality $\Delta_{act}(x) \leqslant \Delta_{spec}(x)$ is valid. Otherwise, the calculation of I_{rec} and H_{apost} is more complicated.

3. Kharkevich, A. A., Problemy Kibernetiki (Problems in Cybernetics), 1960, 4.

4. Shannon, C., in the collection of works, Teoriya Peredachi Signalov pri Nalichii Pomekh (Theory of Signaling in the Presence of Noise), Foreign Literature Press, Moscow, 1953.

5. Linfoot, E. H., Information and Control, 1957, 1, 1.

METHODS FOR THE RECORDING OF QUANTIZED FUNCTIONS AND DEVICES FOR INPUT INTO SPECIAL-PURPOSE DIGITAL COMPUTERS

Metody i Ustroystva Preobrazovaniya Graficheskoy Informatsii (Methods and Devices for the Conversion of Graphic Data), 1968, pages 65-70

Ye. N. Karyshev

Wide use is now being made of various methods for the automatic recording of measurement results. One of the main properties of these methods is their graphicness, assuring speedy and reliable communication between instrument and man.

The introduction of recording methods in various fields of science and technology has had as a result that at the present time a large volume of recorded information has already been accumulated and it continues to increase. In order to reduce the volume and represent recorded information in a form more convenient for use by man or machine, primary processing of recorded measurement results is necessary.

In recent years wide use has been made of statistical processing methods, for which the accuracy requirements set for the recording of primary information can be significantly lowered and the processing of this information simplified [1-3]. In the machine processing of recorded data questions arise involving the speed of response, accuracy of conversion and simplification of the device for data input into the machine. Certain limitations are imposed on the form of a graph (thickness, slope of curve line) which hinder the reading of arbitrary recordings without preliminary processing [5]. In addition, serious requirements are set for the stability of converter parameters. All this considerably complicates the devices. For the most part the complexity springs from the fact that the existing methods for recording in the form of a continuous curve on tape, for all their graphicness, are completely unsuited for input into computers. It should also be noted that two types of error occur in machine processing: 1) the error of recording and 2) the error of reading values during input. To increase the ease of reading and to simplify digital computer input devices, it is advisable to change the form of recording, bring it as close as possible to machine "language." The following are the requirements for new forms of recording: 1) graphicness; 2) ease of reading the recorded data and of inputting them into computers; 3) high accuracy and speed of operation. We believe that to satisfy these requirements, it is best to use the following methods for the recording of quantum functions:

1. A method for recording in the form of a quantized function (Figure 1,a) [4].

2. A method for recording the results of the number-pulse conversion of the ordinates of an analog signal in the form of a sequence of bands (Figure 1,b).

3. A method for recording the results of the conversion of the ordinates of an analog signal in binary code (Figure 1,c).

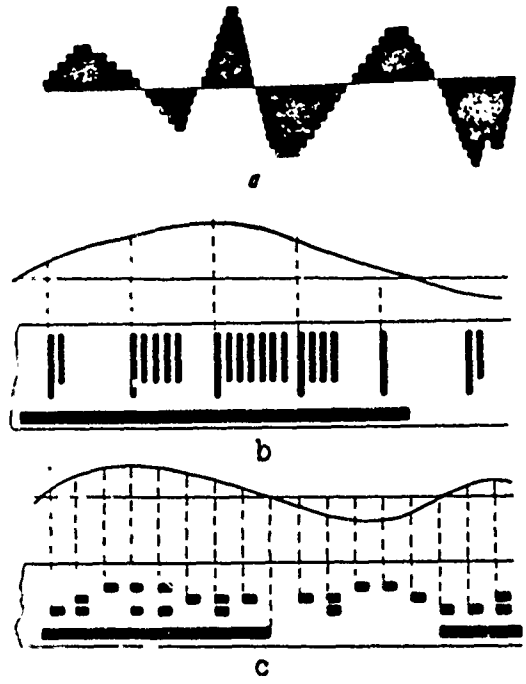

Figure 1. Materials for the recording of quantized functions:
a) in the form of a quantized function;
b) in the form of a sequence of bands;
c) in the form of binary code.

Now let us dwell on several examples of input devices which use the aforecited methods for the recording of quantized functions. We shall consider the input devices with application to the discrete measuring correlation system DMCS, developed at the Institute of Automation and Electrometry of the Siberian Department of the Academy of Sciences USSR. The input of this system must be fed four-digit binary numbers. The operation of the input device has to be synchronized by the memory cell markers CM of the DMCS memory.

Device for the Input into DMCS of Information Recorded in the Form of a Quantized Function on Photographic Film

The block diagram of the device is presented in Figure 2. A bar of 16 FD-2 type photodiodes is situated along the width of the photographic film. On the other side of the film are light bulbs. The film is drawn by a tape transport at a constant speed. The cell marker of the DMCS memory goes simultaneously to all the photodiodes and runs onto univibrators 0 if the photodiodes are blacked out. The resultant "packet" of pulses develops into a train with the aid of noncoincident delay lines. The univibrators are used as the latter. Then via the OR circuit this pulse train corresponding to the ordinate goes into binary countery BC, whose output receives the binary code. The sign of the ordinate is formed in the sign flip-flop T_{sign}. The latter is controlled by pulses coming from the first levels of the positive or negative value of the quantized function.

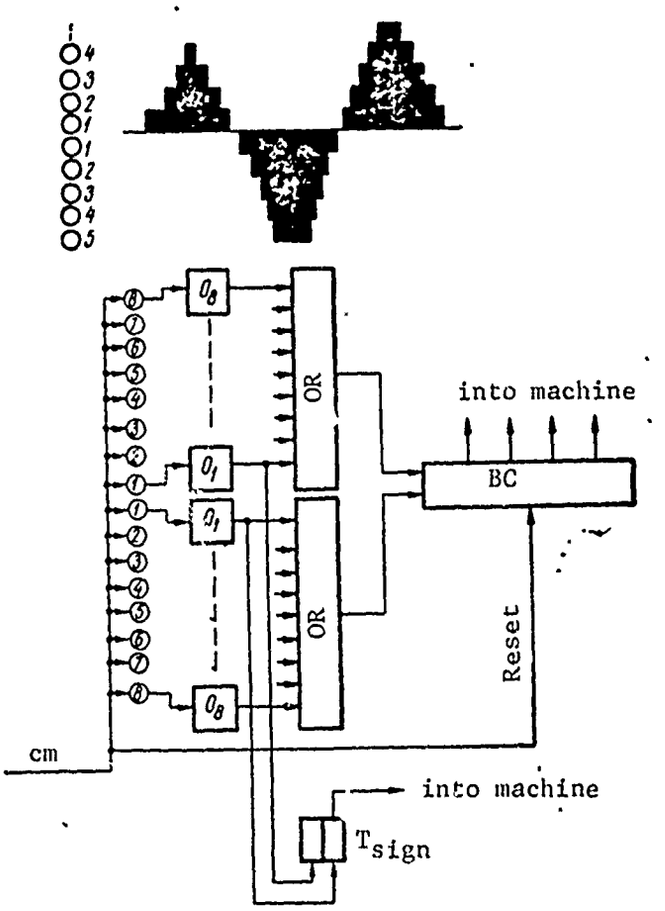

Figure 2. Block diagram of device for input of information recorded on photographic film in the form of a quantized function.

Input Device for the Results of Number-Pulse Conversion, Recorded on Photographic Film

The block diagram of the device is presented in Figure 3.

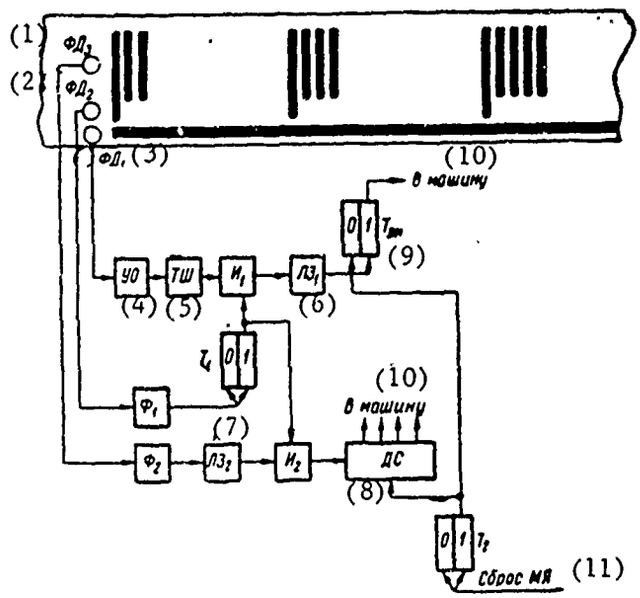

Figure 3. Block diagram of input device for the results of number-pulse conversion, recorded on photographic film.

Key: (1) PD_3
(2) PD_2
(3) PD_1
(4) Unknown; possibly, limiting amplifier
(5) Unknown; possibly, Schmitt trigger
(6) DL_1
(7) DL_2
(8) BC
(9) T_{sign}
(10) into machine
(11) CM reset

The device works as follows. Flip-flops T_1, T_2, T_{sign} and the binary counter flip-flop are first set to zero position. A signal received from PD (photodiode)$_2$ is shaped with the aid of shaper Φ_1 and converts flip-flop T_1 to the one state. The potential from the one output of T_1 goes to coincidence circuit $И_2$, preparing it for operation, and via the differentiating circuit to circuit $И_1$. The second input of $И_1$ is fed square pulses corresponding to the positive values of the process. A signal from the $И_1$ output through delay line DL_1 over the one input controls the operation of the flip-flop T_{sign}, whose return to zero position is effected by each odd cell marker. With a slight delay created by delay line DL_2, the pulse train from PD_3 via shaper Φ_2 goes to coincidence circuit $И_2$ and passes into the binary counter if T_1 is in the one state. Binary code is formed at the output of the binary counter. Machine readout of the resultant code is performed after receipt of even cell markers.

Thus, over the course of a single tape run in the input device all odd ordinate values are recorded in the memory. The input of the even ordinate values requires one more tape run, as well as changing the initial states of flip-flop T_1 and T_2 to the reverse states, i.e. they must be set to the one position.

Input Device for Information Recorded on Photographic Film in Binary Code

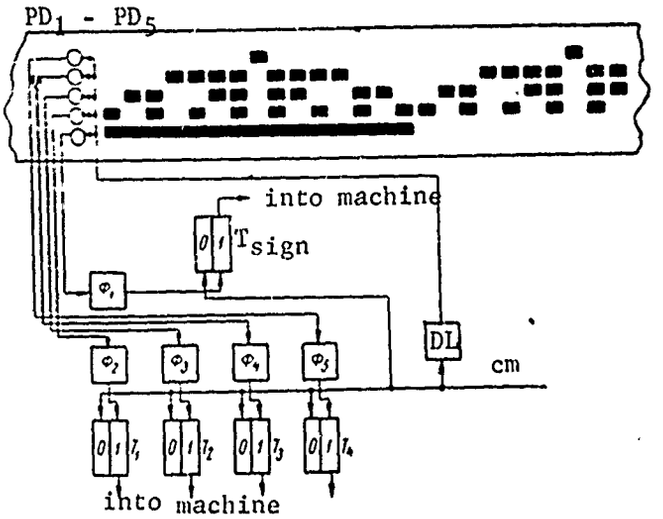

Figure 4. Block diagram of input device for information recorded on photographic film in binary code.

The block diagram of the device is presented in Figure 4. Here, as in the preceding device, it is necessary to coordinate the drawing speeds for the tape of the input device and the magnetic tape of the DMCS memory. The cell marker puts the register flip-flops T_1-T_4 and the flip-flop T_{sign} in the zero position and via the DL goes simultaneously with a short delay time to all photodiodes PD_1-DP_5. The delayed MC passes only through those photodiodes which have been blacked out. The pulse after PD_1 is shaped by ϕ_1 and acts on the one input of T_{sign}, throwing it into the one position. Pulses from photodiodes PD_2-PD_5 corresponding to the ordinate digits go simultaneously through shapers into flip-flops T_1-T_4 of the register. From here the ordinate code is transferred into the memory of the DMCS.

In order to simplify the use of recorded data in machine processing, it is necessary to change the form of recording. It is advisable to record quantized functions. The inclusion of subsequent statistical processing permits the recording of quantized functions with a small number of quantization levels. The carrier consumption here is slight, and the accuracy and speed of response adequate. The use of recorded quantized functions makes it possible to simplify the input devices and to eliminate reading errors at the same time.

BIBLIOGRAPHY

1. Anan'yev, Yu. F., Izvestiya Vuzov, Elektromekhanika (Bulletin of Higher Educational Institutions: Electromechanics), 1961, 9.

2. Voloshin, G. Ya., Vychislitel'nyye Sistemy (10) -- Sbornik (Computer Systems (10) -- Collection of Works), "Nauka" (Science), Siberian Department of the Academy of Sciences USSR, Novosibirsk, 1964.

3. Domaratskiy, A. N., Ivanov, L. N., Karyshev, Ye. N., and Sinitsyn, B. S., Diskretnaya Izmeritel'naya Korrelyatsionnaya Sistema (DIKS) (Discrete Measuring Correlation System (DMCS)), "Nauka" (Science), Siberian Department of the Academy of Sciences USSR, Novosibirsk, 1965.

4. Karyshev, Ye. N., "Method for the Conversion of an Analog Signal," Author's Certificate No. 174,842, Byulleten' Izobreteniy (Bulletin of Inventions), 1965, No. 18.

5. Petrenko, A. I., Preobrazovaniye Grafikov v Elektricheskiye Signaly (Conversion of Graphs into Electric Signals), State Publishing House of Technical and Theoretical Literature of the Ukrainian SSR, Kiev, 1964.

FUNCTIONAL ANALYSIS AND CLASSIFICATION OF GRAPHIC DATA DECODERS

Metody i Ustroystva Preobrazovaniya Graficheskoy Informatsii (Methods and Devices for the Conversion of Graphic Data), 1968, pages 71-77]

G. K. Afanas'yev and P. M. Chegolin

Most complex objects have an incomplete mathematical description or no description at all. Therefore, they are usually analyzed from the results of experiments, recorded in the form of graphs or tables. However, such an analysis is of a selective character, depends on the trend of the experiment, is very fatiguing, fails to give information on the general properties of the object and does not make it possible to predict its behavior in the face of a substantial change in external influences.

Multichannel oscillograms of processes in control systems and power engineering, chemistry and medicine, structural mechanics and other fields of science and technology carry specific information (reaction rate, frequency spectrum, displacement, energy etc.), although time variation is common to all graphs.

Consideration is given below only to plane curves, when time is plotted on one of the coordinate axes. The problem of functional analysis is solved as follows. There is a visual graph; it is necessary to automate the derivation of the law which the graph follows with time. This problem includes questions of the automatic input of graphic information into a computer, the calculation of approximating functions and the output of the initial and approximating curves on a visual display. Observing both curves on the display, an operator tries to achieve the best agreement between them by controlling the choice of coefficients of the approximating expressions.

Various graph decoders (GD) can be used for the input of the initial information; these can be conveniently classified according to the form of the curves to be converted and according to the technical principles of their construction.

The number of graphs on one tape, their intersection or closure are responsible for certain requirements for GDs. In all cases except closed loops the GDs reproduce the ordinate x_1 as a function of abscissa ξ_1, by which is usually meant time t. If $\xi_1 = (U)t$, the graph ordinate at the GD output will be an implicit function of t, i.e.

$$x_i = \psi_i(\xi) = \psi_i[\dot{U}(t)]. \qquad (1)$$

where i = 1, 2, ..., m is the number of the graph.

For reading closed loops arbitrarily oriented on the carrier, GDs should have two output channels, viz. one for the ordinate, the other for the abscissa. The curve is reproduced in the parametric form

$$\xi = m_\xi U(t); \quad x = m_x v(t), \tag{2}$$

where m_ξ, m_x are scale factors.

The classification of GDs according to the character of the information to be reproduced is useful and should be considered in developmental projects. Such a classification reflects primarily a geometric interpretation. GDs constructed according to a certain technical principle can be used to read different types of curves. Therefore, the classification of GDs as special-purpose automata is done according to the technical principles of their construction.

All GDs are divided into three basic groups: follow, scanning and matrix (Figure 1). Such a division is completely justified, since matrix GDs differ from scanning automata by the parallel method of interrogating the elements of the carrier or its image with a mosaic of sensors. A scan, which manifests itself here in veiled form, is achieved by the placement of individual elements of the mosaic and the sequential commutation of their output signals. In addition, it becomes possible in principle to create the logical structure of the simultaneous sampling of data from all elements of the mosaic and their entry in the memory. The bottom rectangles principally characterize the uniqueness of the technical implementation. The end of the diagram indicates the character of the output information received from the output of the corresponding type of GD without additional conversion by code-analog or analog-code devices.

1. Follow GDs are closed-loop type negative-feedback systems. They are used as functional converters (photoformers), which play an especially important role in problem solving on real-time analog devices. The main advantage of this group of GDs is the ability to reproduce functions with a large frequency band (up to 300 kHz).

The method of follow conversion of a function given in graphics into electrical voltage is based on measuring the position of a certain recording element PO as it is brought into coincidence with the curve x(t). The PO used may be a reticle of two lines, a controlled light spot, a photosensitive head etc.

The position of the PO on the curve is maintained through the feedback circuit OC by a control device YY. The current value of the mismatch δ between the PO position and the given curve is determined by the sensor ЧЭ. Figure 2 gives the block diagram of a follow curve-conversion device.

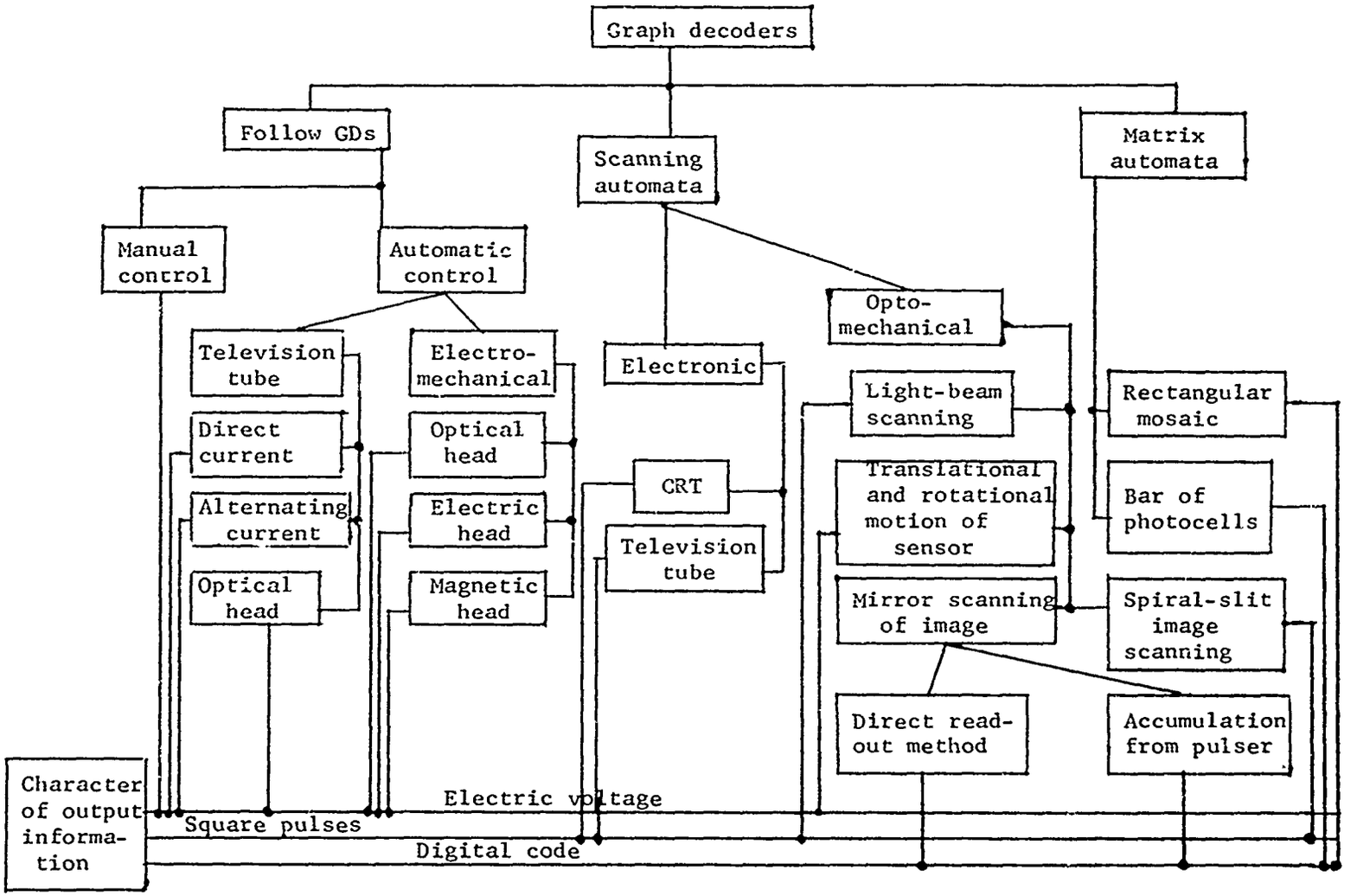

Figure 1. Classification of GDs.

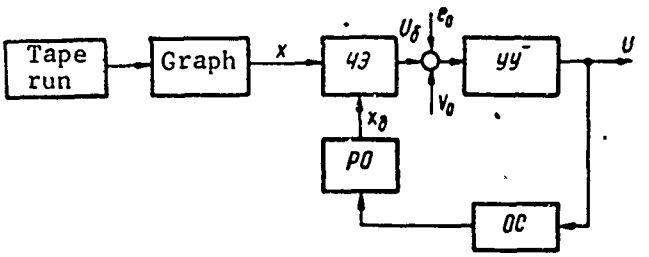

Figure 2. Block diagram of a follow GD:
ЧЭ) sensor; ОС) feedback circuit; УУ) control device;
РО) recording element

The output voltage of the follow converter in the ideal case is proportional to the ordinate of the curve to be converted.

Follow GDs may use direct- or alternating-current elements (amplifiers). In the second case the scanning frequency is practically unlimited, there are no errors caused by drift, so that a higher quality of following can be achieved. A serious hazard to follow GDs is the possible break-up of a beam from a recording line. Automatic retrieval of the lost graph is rather complex. Therefore, a pulse follow system is of considerable interest.

2. Scanning automata are open-loop type pulse devices. Scanning is the cyclically repetitive coverage of the carrier tape along its width at a certain quantization step in the direction of the length. During scanning of the reading field notch pulses are formed, whose time position relative to the base pulse is proportional to the graph ordinates. The scanning frequency can be brought up to 2.5 Mhz. This group of GDs permits the reading of m graphs from one carrier. The problem is to determine with sufficient accuracy during scanning the location of a recording in a given cross section of the tape relative to some base. For this purpose photosensitive cells are used, through which flows an electric current which varies by jumps in the transition from tape background to recording line and back. Almost the same effect is obtained in scanning the immediate reading field or its image before the inlet window of the photosensitive cell.

The scanning can be performed by means of a cathode-ray and a television (electronic scanning) tube, a rotating mirror and a polyhedral mirror drum (electromechanical scanning) or a rotating disk with a spiral slit.

3. Matrix automata. These contain a matrix or bar of photosensitive cells as the sensing unit. They are used for computer input of printed (alphabetic, digital, sign) and graphic information. When an image of a carrier sector with a plotted curve is projected onto the matrix, its cells, on which the image of the recording line falls, are excited. The coordinates or numbers of the excited cells are information regarding the curve ordinates. It remains only to take these coordinates in a certain order and enter them in the machine's memory.

The resolution δ of matrix GDs is determined by the size of the photocells and the coefficient k of magnification of the objective used to project the carrier field on the matrix. If the distance between the centers of the inlet windows of the photocells equals r, then

$$\delta = \frac{r}{k} .$$

Let us note that the electronic blocks of matrix GDs, including the system of logic circuits, amplifiers, comparison and interrogation units, are cumbersome and require a large amount of hardware. Thus, for a matrix 100 x 100 the number of adjoining elements

$$N = 2(A - 1)(2A - 1) \cong 4 \cdot 10^4,$$

where A is the number of elements in a row.

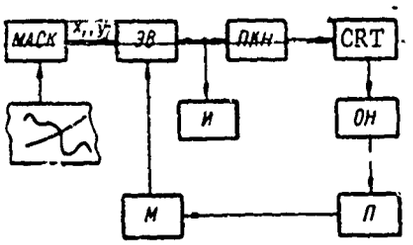

Figure 3. Block diagram of functional graph analyzer.

In graph reading it is advisable to replace a rectangular matrix with a bar of photocells and to project successive cross-sections of the carrier tape onto it.

The block diagram of a functional analyzer (Figure 3) contains a multichannel curve reading automaton МАСК, an electronic computer ЭВ, an indicator И, a code-to-electric voltage converter П КН, a cathode-ray tube with a scanning system CRT, an optical system with a negative frame of the initial graph ОН, a charge-storage tube with a scanning system П and a manipulator М.

МАСК reproduces the coordinates x_i and y_i of each oscillogram in binary code and transmits them in the form of the number i of quantization step h along the axis $x(x_i = ih)$ and the corresponding ordinate y_i to the electronic computer ЭВ. The latter uses this information to calculate Lagrange's coefficients of an approximating polynomial

$$L_n(x) = (-1)^n \frac{\tau(\tau-1)\dots(\tau-n)}{n!} \sum_{i=0}^{n} (-1)^i \frac{C_n^i y_i}{\tau - i}, \quad \text{where} \quad \tau = \frac{x - x_0}{h}; \; h = x_1 - x_0 = x_2 - x_1 = \dots = x_n - x_{n-1} \tag{3}$$

is the quantization step;

$$y_i = f(x_i); \; (-1)^{n-i} C_n^i \frac{\tau(\tau-1)\dots(\tau-n)}{(\tau-i)\,n!}$$

are complete Lagrange coefficients; C_n^i are binomial coefficients.

The sought function can be reproduced by the uniform approximation or least-squares method, using known interpolating polynomials.

The ГЦ КН converts the values of these coefficients into electrical voltage and controls one pair of deflection plates of the CRT; the other pair of plates is fed scanning voltage

$$U_x = flt - a\cos(2\pi ft - \varphi_0) + b. \quad (4)$$

Here f is frequency; a, l, ϕ_0, b are control parameters, which depend on the character and site of the curve to be reproduced and are subject to determination.

On the CRT screen elementary sectors of a curve (particularly a piecewise-linear curve) are intensified, which are components in the reproducing polynomial. The optical system projects an image of the approximating curve on the negative frame of the actual process, and then a composite image of them on the screen of the charge-storage tube. The electron beam of the charge-storage tube makes a horizontal sweep over the field of the screen; at the moment that the image of the approximating and real curve is encountered voltage pulses are issued. The time interval between the pulses in the manipulator M is compared with the permissible standard deviation, and the result of the comparison is entered in a digital computer for correction of the coefficients, the new values of which are again transmitted to the ГЦ КН. The process continues until the approximating polynomial reproduces the initial graph with the prescribed accuracy.

The analytic reproduction of a graph in the above-described system is accomplished point by point at a certain quantization interval. Naturally, a smooth curve is represented by a piecewise-linear function.

The indicator of the device serves to show the operator the values of the Lagrange coefficients. The operator can remove the corresponding addends manually via manipulator M, increasing the role of the dominant coefficients.

THE SIMULTANEOUS READING OF TWO OR MORE INTERSECTING GRAPHS

Metody i Ustroystva Preobrazovaniya Graficheskoy Informatssi (Methods and Devices for the Conversion of Graphic Data), 1968, pages 78-86

V. A. Fesechko,
A. I. Petrenko and
V. G. Abakumov

Information on variations in different parameters is recorded on several channels on a single carrier during the solution of automatic control problems, the control of complex production processes, and the processing of well-logging and seismic research data, as well as in medicobiological and other experiments. Graphs are positioned arbitrarily and it is possible for them to intersect.

In the automatic reading of such recordings the problem arises of separating the signals according to channels. Machine separation programs exist, based on the extrapolation of functions and the comparison of predicted with actual values. For the complex curves of, say, geophysical logging, medicobiological research and others of a random character, the separation programs are complex and not effective enough.

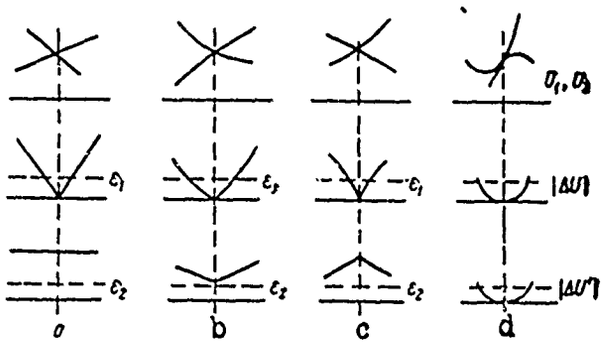

Figure 1. Reading to two graphs:
a), b), c) intersecting; d) tangent.

Considered infra are equipment methods for the separation of monochromatic records which are worth while and which can be recommended for the reading of curves with a small number of channels when there is no computer or it is impossible to use one.

As the curves of graphs converge, it is possible for them to intersect, touch or intersect at inflection points (Figure 1). If the recorded functions are continuous, monotonic and have a limited spectrum, the channel separation is effected by an analysis of the convergence process. Figure 1 shows variations in the module of the difference between readout values and the module of the derivative of this difference. At the points of curve intersection the convergence Δ U equals zero, the derivatives of the convergence are nonzero and greater than a certain level ε_2. At the points of curve tangency the convergence and its derivative are close to zero. In addition, by analogy with the foregoing the second derivative of the convergence also equals zero at the inflection points. However, since statistically such points are very rare, we shall not consider the second derivatives.

Figure 2,a gives the block diagram for the separation of signals in the reading of two-channel intersecting recordings. Pulse signals from two lines are formed in photoassembly PA, which includes any reading camera and shaping networks. These signals go to the output of the device through a commutator on channels I and II. The remaining elements form a commutator control circuit, which switches the channels of the signals as they pass through the intersection points.

The reading is performed by the scanning method; further processing is done in analog or digital form. Pulses from the photoassembly go to the ordinal separation circuit OSC and then to the block for the separation of the nearest curves BSNC.

The first pulse 1 triggers the delayed sawtooth generator STG. The pulse length τ_1 (Figure 2,b; position 1) is proportional to the convergence of curves ε_1 (see Figure 1) at which analysis of their shape begins. The second pulse 2 briefly opens the input of holding circuit HC_1, and the latter the voltage existing at the given moment in the STG. At the end of a line the end-of-reading pulse EORP transfers the voltage from HC_1 to holding circuit HC_2 (Figure 2,b; position 3), which holds the voltage until the arrival of data from the next line.

The first pulse again triggers the STG, and its voltage goes not only to HC_1, but also to comparison circuit CC, whose second input receives the voltage from HC_2. At the moment when they are equal block ϕ_1 generates a pulse (Figure 2,b; position 4, 5) whose delay relative to the first pulse of the second line equals the time shift between the pulses of the first line. Obviously the delay relative to the second pulse of the second line is proportional to variations in the curve spacing on the scanning step, i.e. the first convergence derivative.

If it is assumed that the convergence rate for the intersecting curves should not exceed a certain quantity ε_2 (see Figure 1), it is possible to establish the time interval τ_2 with which the resultant pulse shift should be compared. If it is greater than τ_2 it indicates intersection, if it is less than τ_2 it indicates tangency.

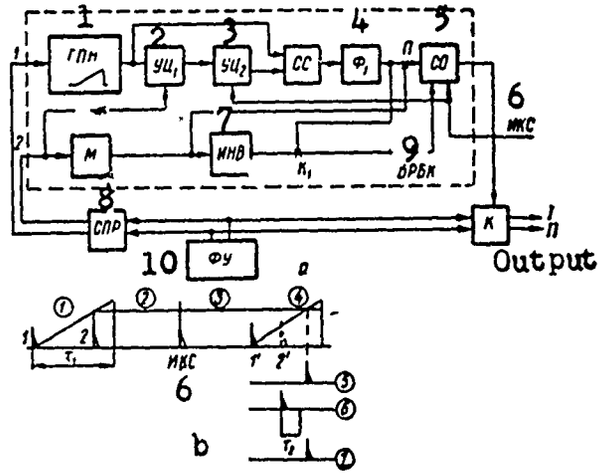

Figure 2. Arrangement for the separation of signals in the reading of intersecting two-channel recordings;
a) block diagram; b) voltage diagrams.

Key: (1) STG
(2) HC_1
(3) HC_2
(4) Shaper
(5) SC
(6) EORP
(7) INV
(8) OSC
(9) BSNC
(10) PA

For this purpose, in the circuit depicted in Figure 2 every second pulse on a reading line triggers delayed multivibrator M. The latter generates a pulse of duration τ_2 (Figure 2,b; position 6), which as inhibit pulse goes into the pulse-potential coincidence circuit and as permissive pulse through inverter INV into analogous circuit K_1. These pulse-input circuits are fed a pulse from shaper Φ_1. If it is delayed relative to the second pulse of a given line for a time greater than τ_2, it appears at the output of the circuit Π and corresponds to an intersection. If it is delayed for a time less than τ_2, it appears at the output of circuit K_1 and corresponds to a tangency. Both these pulses are fed to the intersection pulse separation circuit SC, which performs the following function. If intersection is noted for several lines in a row, for example at small curve convergence angles, then only one signal appears at its output -- at the end of the entire series which corresponds to one intersection (Figure 3). The circuit also receives a tangency recognition pulse. If it appears right after the intersection pulses, passage of the output intersection pulse in inhibited. Inhibition is necessary in case the curves converged but did not intersect.

The inputs of flip-flops T_1, T_2 are connected in parallel with respect to intersection pulses IP, i.e. each of these pulses sets both flip-flops to one state. The EORPs are received in series by the first T_1, and then, if its state is maintained on the next reading line, by the input of T_2. Thus, flip-flop T_2 is set to zero position only after the second EORP, which follows the end of the series of intersection pulses. Voltage from the one output of

T_2 is used for permission for the transmission of EORPs to the output. In addition, only one output pulse is cut off by means of flip-flop T_3. If the series of output IP pulses is followed at once by a tangency pulse TP, an additional inhibition is imposed on output pulse transmission by means of flip-flop T_4.

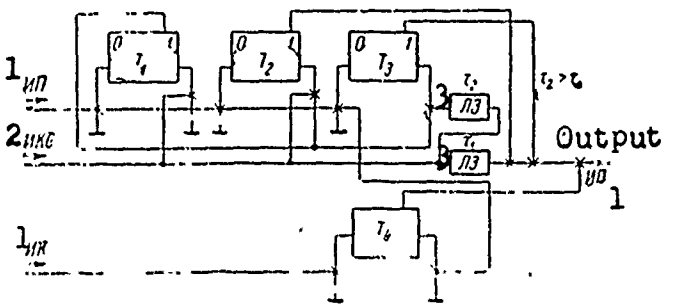

Figure 3. Functional diagram of intersection pulse separation block SC.

Key: (1) IP
(2) EORP
(3) DL

In the diagram shown above, an increase in channel separation reliability requires the proper selection of the scanning step and the use of pulses corresponding to the middle of a graph line.

Another variant for the construction of a device for the separation of two intersecting curves is considered in [1].

If the number of intersecting graphs is greater than two, the problem of channel separation becomes more complicated. However, considering that it is sufficient to study the convergence of only neighboring curves for an analysis of the intersections, methods for the separation of two curves can be used to solve this problem. Figure 4,a and b presents two block diagrams for multichannel converters, particularly for six channels.

Input signals are formed and shaped in photoreading assembly PA. They go to the ordinal separation block OSB, at whose output signals 1, 2, ..., 6 (according to the order of their appearance in the PA) occur on the individual buses. In the circuit shown in Figure 4,a these signals are transmitted to a signal commutator SC, in which they are distributed over the channels and the channels are switched in the case of intersection. Switching is performed according to a signal from the BSNC. Output device OD converts the information, reducing it to a form convenient for further processing; the train of pulses I, II, ..., VI in general differs from the pulse sequence of the PA.

In the circuit shown in Figure 4,b signals 1, 2, ..., 6 go directly to the output device. Each output signal 1*, 2*, ..., 6* is assigned a certain index or code corresponding to its channel. This code goes from the code

commutator KK, in which there is a set of code standards. Switching is effected by means of intersection signals from the BSNC. Signals are grouped by individual channels in a computer or a supplementary decoder according to channel code tags. Both circuits (Figure 4, a and b) provide for the initial and repeat periodic sending of an initial position pulse IPP on graph sectors with a known curve distribution. This controls the operation of the converter.

Let us consider in somewhat greater detail the individual blocks of the converters.

The OSB circuit is not especially complicated and represents a circuit of flip-flops which trigger in series.

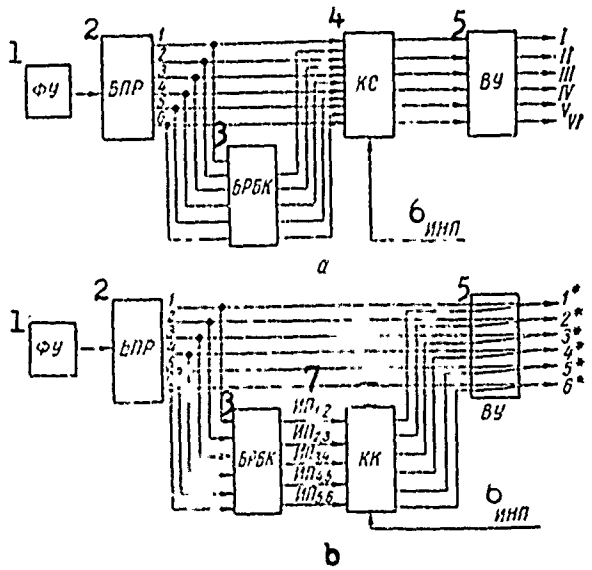

Figure 4. Block diagram of multichannel converters:
a) with signal commutator; b) with code commutator.

Key: (1) PA
(2) OSB
(3) BSNC
(4) SC
(5) OD
(6) IPP
(7) $IP_{1,2}$ $IP_{2,3}$ $IP_{3,4}$ $IP_{4,5}$ $IP_{5,6}$

The BSNC can be based on the circuit for the separation of two intersecting curves, considered previously. The number of separation circuits in the BSNC is one less than the total number of graphs: the circuit inputs receive signals from the two nearest curves, for example curves 1 and 2, 2 and 3 etc. Pulses occur at the BSNC outputs at the moments of intersection of lines $IP_{1,2}$, $IP_{2,3}$ etc. The ODs are the same as in single-channel converters and differ only in the number of channels. The KK serves for channel switching

after passage through the intersection point. Figure 5 shows a switching matrix (a) and its control circuit (b). The horizontal buses receive pulses in the order designated in the figure as 1-6; the vertical buses correspond to the output of channels I-VI. The sending of signals to the requisite channels is accomplished by switching the horizontal and vertical buses, i.e. by connecting them in nodes (these points are shown in black in the figure). For example, if the numbers of signals correspond to the numbers of their channels, the buses are switched in the nodes on the main diagonal.

Suppose that lines 5,6 intersect and the order of signal receipt by channels V, VI is subject to change. Obviously, this requires changing the switching of nodes 5, V and 6, VI to 6, V and 5, VI, i.e. with respect to the horizontal between the fifth and sixth buses. Analogously, if a line of the sixth channel, the pulse from which is numbered 5, subsequently intersects with a line of the fourth channel, there must be switching between the fourth and fifth horizontal buses. Thus, the correct channel distribution of pulses, considering the possibility of the intersection of only neighboring curves, can always be achieved by the switching of neighboring horizontal buses, which is accomplished by the control matrix (Figure 5,b).

Corresponding to each node of the switching matrix is a control cell. Running between the horizontal rows of these cells are the buses which receive a pulse from the BSNC on the intersection of the corresponding lines IP_{i-j}. On the appearance of an intersection pulse on any bus there is an exchange of states in the vertical pairs of cells along the entire bus. The outputs of the cells control the corresponding nodes of the switching matrix. Therefore, a change in the states of the cells is equivalent to channel switching. Let us note that different states and, hence, changes in them as well, can be only in the two pairs of cells along one bus of an intersection pulse.

The switching and control matrices can be technically realized in various ways. For example, the switching matrix uses diode-transformer coincidence systems and the control matrix standardized flip-flops of any computer.

Figure 6 presents the schematic circuit diagram of two flip-flops $T_{n,m}$ and $T_{(n+1)m}$, which form a vertical pair with respect to the bus with intersection pulse $IP_{n,n-1}$. In the initial state the position of the flip-flops is set manually with the aid of the initial position voltage IPV and the initial position pulse IPP. The IPV is fed to the potential inputs of the flip-flops and is retained for the time it takes to process one graph. The IPP is generated in the passage of carrier sectors with a certain graph and output signal sequence corresponding to the initial state. Additional marks may be applied to the carrier for the shaping of such a pulse. The flip-flop connections are made in such a way that the intersection pulses go to them via the counting input. The potential inputs are connected to the zero inputs of their flip-flop and the nearest two neighboring flip-flops, which assures switching of the states of the flip-flops only if one of them is in the one state. The zero outputs of the flip-flops send voltages into the switching

matrix to the potential inputs of the diode-transformer coincidence circuits, and these voltages are used as permissive signals.

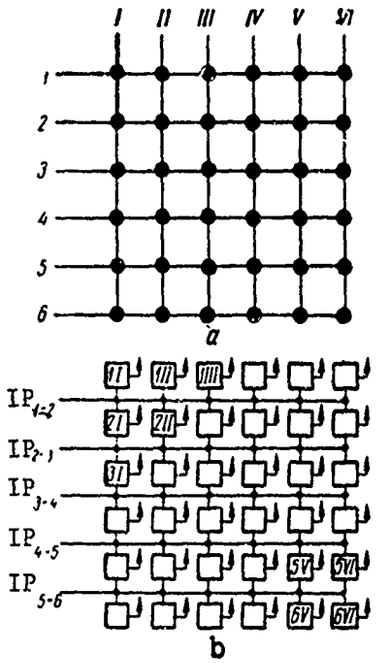

Figure 5. Switching (a) and control (b) matrices.

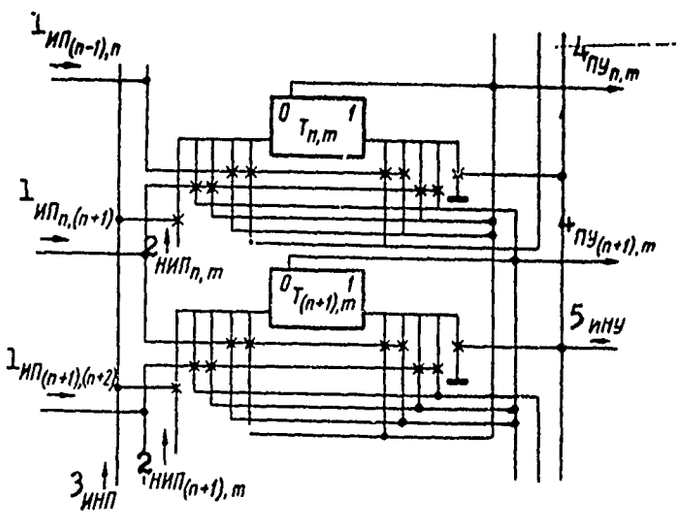

Figure 6. Circuit diagram of control matrix flip-flops.

Key: (1) IP
(2) IPV
(3) IPP
(4) PU [transliterated from the Russian. Unknown; not mentioned in text]
(5) INU [transliterated; possibly, initial setting pulse]

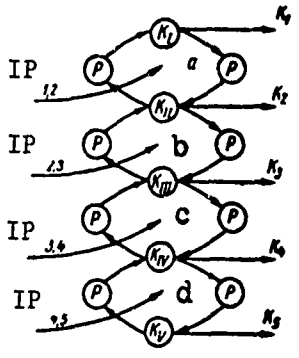

Figure 7. Functional diagram of code commutator.

In a multichannel recording converter, the block diagram of which is shown in Figure 4,b, the code tags of the channels are switched. The KK can take various schemes. In particular, Figure 7 shows the functional diagram of such a commutator which is based on loop code reversals. On the receipt of an intersection pulse by the loop there is an exchange of codes K through intermediate registers P. The codes are then sent to the output device. The circuit can also provide for the initial setting and periodical check of states. The aforecited circuits have been considered for the case of the intersection of only two curves at one point. In the intersection of three curves at one point, proper switching is possible by supplying intersection pulses with a delay relative to each other, as well as by repeating the first IP.

The simplest way to read multichannel intersecting recordings, in our opinion, is by using certain physical attributes of graph lines, for example color, thickness, structure etc. Thus, the operating reliability of the input device increases significantly and its design is considerably simplifed if curves are separated according to the color attribute [2].

BIBLIOGRAPHY

1. Petrenko, A. I., Abakumov, V. G., Zaborovskiy, Yu. A., and Fesechko, V. A., Avtomatika i Priborostroyeniye (Automation and Instrument-Making), 1965, 4.

2. Fesechko, V. A., and Smeshko, V. F., in the instant collection of works.

AN ALGORITHM FOR THE SEPARATION OF INTERSECTING CURVES

Metody i Ustroystva Preobrazovaniya Grafieheskoy Informatsii (Methods and Devices for the Conversion of Graphic Data), 1968, pages 87-91

N. D. Vashchenko, L. V. Krupskaya and I. T. Parkhomenko

If several curves are situated on one carrier, the mathematical analysis of the curves with the aid of a digital computer is preceded by separation of the curves.

Such separation is, of course, performed automatically with the aid of a computer.

The algorithm which the present article offers for the separation of curves consists in the following: the ordinates of the points of the curves at a given step on the time axis are distributed with respect to the curves in such a way that the "best correspondence" is achieved between them and the extrapolation points calculated for the particular step from preceding sectors of the curves [2]. "Best correspondence" denotes the minimum sum of the squares of the differences between extrapolation and real points of curves at a given step in the sorting of all combinations of the pairwise grouping of these points. The number of such combinations in the case of n curves is expressed by the number of permutations of n things, i.e. n!

Particularly noteworthy is the question of the mode of curve extrapolation. In view of the fact that curves are distorted by noise fluctuations and certain errors occur in their measurement and coding, agreement must be achieved in general between an approximating curve and a curve which is approximable without the repetition of local deviations. Each curve is approximated according to sliding sectors by the corresponding polynomial

$$y_e = a_0 + a_1 x + a_2 x^2 + \cdots + a_m x^m.$$

The coefficients a_0, a_1, ..., a_m are chosen from the condition of minimal difference between approximable and approximating curves by the least-squares method [1].

The algorithm presented here was checked under the following conditions: number of curves on a carrier -- five; arrangement of curves -- arbitrary (intersections and tangencies are possible, as well as the breaking off or appearance of curves); the number of simultaneously intersecting curves is

not limited, nor is the number of intersections at a given step on the time axis; the length of an intersection sector does not exceed 8h (h is a step on the time axis approximately equal to the line thickness).

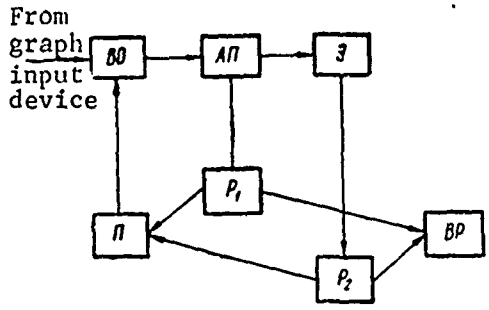

Block diagram of algorithm for the separation of curves.

БО) block for the assignment of curve ordinates at the step under study;

АП) analyzer of curve behavior;

P_1) block for the distribution of ordinates in the absence of singular points at a given step (intersections, break-offs, etc.);

P_2) block for the distribution of ordinates in the presence of singular points at a given step;

Э) extrapolator (block for obtaining extrapolation points);

ВР) block for the issuance of results;

П) block for preparing arrays for curve processing at the next step.

The figure presents the algorithm in the form of a block diagram.

It is assumed that curve ordinate codes have been entered in a certain memory array from the graph input device. The function of block БО is to isolate from the array a routine group of ordinates obtained in one scanning step and to transmit them to block АП. Block АП makes a preliminary analysis of the behavior of the curves, i.e. it checks whether singular points on a graph (fusion of lines, break-off or appearance of new curves) are absent at a given step. Actually this process consists in counting the number of ordinates obtained at a given step and comparing it with the number of ordinates of the preceding step. Inequality indicates the presence of singular points.

In view of the fact that a line fusion sector, however small it may be, is always greater than the scanning step, which is approximately equal to the width of a line, it cannot be omitted in such a check. The curve behavior analyzer is idle only when both the break-off and the appearance of a new curve are simultaneously observed at a given step. If one or more curves occur here between the broken-off curve and the appearing curve, the distribution of the curves will not be accurate. However, such a case is unlikely.

If there are no singular points the transition is made to block P_1, whose function is to distribute ordinates in the same order in which they were distributed in the preceding step. This essentially ends the creative work of the algorithm. Next is the transition to block П (here the segment array for finding extrapolation points through new points is updated and other preparatory operations are performed) and block BP, which transfers ordinates of a given step to the curve arrays for subsequent mathematical processing or puts them in print.

If there are singular points, their character must be established (break-off or appearance of a curve, fusion) and the ordinates distributed according to it. Since this required the extrapolation points of curves, there is a transition to block Э. As has already been noted, the least-squares method is used. The optimal curve segment length for calculating the extrapolation points depends on the character of the curve. Extrapolation points are found with greater accuracy on smooth curves if longer segments are used. But if there are high-frequency harmonics, it is advisable to shorten a segment. In practice satisfactory results are obtained with the use of segments five to eight scanning steps in length.

After the extrapolation points have been found, there is the transition to block P_2, whose operation also constitutes the main essence of the algorithm.

As has already been noted, the transition to block Э and then to block P_2 is made if

$$k_i \neq k_{i-1},$$

where k_i and k_{i-1} respectively are the number of ordinates at the current and preceding step.

This condition is determined by block АП.

Given $k_i < k_{i-1}$, fusion of the curves is possible, as well as the break-off of some of them.

In block P_2 a break-off check is made for the separation of such cases according to the condition

$$|y_e - y_r| \leqslant d. \tag{1}$$

Here y_e and y_r are respectively the ordinates of the extrapolation point and real point at a given step, and d is the maximum possible error in calculating the extrapolation point.

The check is made for each of the extrapolation points by sorting all real points.

Nonfulfillment of condition (1) indicates the absence of a real point in the neighborhood of a given extrapolation point, i.e. a break-off. The numbers of the broken-off curves are stored in block P_2. Entered in the array of the broken-off curve are zeros or its extrapolation points (for several steps). Small line fractures are compensated for in this way.

Fulfillment of condition (1) for all extrapolation points indicates the fusion of lines.

The optimal distribution of points is determined from the minimum sum of the squares of the differences between real and extrapolation points in all combinations of pairwise grouping. Substituted for missing real ordinates here are extrapolation points (the corresponding differences, of course, will equal zero).

The number of minimal equal sums depends on the "behavior" of the curves at a given step. In the case of a break-off one minimal sum is chosen and the ordinates are distributed according to the permutation corresponding to it. In the case of intersections the number of these sums will be one more than the difference between the number of curves processed at the preceding step and the step under study.

Having determined the permutations corresponding to these sums, we compare them term by term. Equality of the corresponding permutation terms indicates that the curve whose ordinate is also this general permutation term does not participate in an intersection; in the case of inequality the given curve is one of those that intersect. All curves which participate in a given intersection are assigned an ordinate common to them.

Particular attention should be given to the fact that in the course of overcoming an entire intersection sector the segment array for counting the extrapolation points of intersecting curves is updated through extrapolation points rather than real points. Otherwise, the proper distribution of points on completion of a curve fusion sector is impossible, since the extrapolation points of the fusing curves will coincide on a rather long sector.

Finally, a third case of curve behavior is possible -- the appearance of a new curve whose attribute will be the inequality $k_i > k_{i-1}$, determined by block AП. In order to establish the place (number) of this curve, condition (1) is checked for each of the real points by sorting all extrapolation points.

A real point for which this condition is not fulfilled is also a new one. The value of the ordinate of this new curve is entered in the curve segment array for the counting of extrapolation points. The distribution of the points is done analogously to the intersection variant, but with the simplification that, since in this case the minimum sum of the squares of the differences of the ordinates is one, the points are distributed according to the permutation which corresponds to it.

From blocks P_1 and P_2 the ordinates, being distributed in the order corresponding to the real slope of the curves, go to block BP for assignment. This algorithm is repeated at each step of curve ordinate counting.

The distribution process in the case where there are no singular points is limited to a comparatively small number (30-40) of simple operations (transfer, addition) and is accomplished very rapidly. When there are singular points, rather cumbersome operations are necessary, the volume of which increases with an increase in the number of curves. The time required for the distribution of five curves at one step in the case of intersection is of the order of 0.1 sec. However, since the number of steps which have singular points is relatively small, the effective speed of operation is rather high.

BIBLIOGRAPHY

1. Milne, W. E., Chislennyy Analiz (Numerical Analysis), Foreign Literature Press, Moscow, 1951.

2. Parkhomenko, I. T., Avtomatika i Priborostroyeniye (Automation and Instrument-Making), 1964, 4.

ALGORITHM FOR THE COMPUTER PROCESSING OF GEOLOGICAL AND GEOPHYSICAL INFORMATION WITH THE USE OF MAP CODER AND REPRODUCER

Metody i Ustroystva Preobrazovaniya Graficheskoy Informatsii (Methods and Devices for the Conversion of Graphic Data), 1968, pages 92-98

R. G. Bas, A. A. Budnyak, V. A. Dyadyura, L. P. Kalikhman and S. Ya. Shereshevskaya

The most important task at the present time in the automatic processing of geological and geophysical data is to create an automatic communication device: "geological and geophysical information carrier -- electronic computer -- carrier of resultant information," a version of which has been created at the Chair of Technical Electronics, Kiev Polytechnic Institute [1, 2].

This device makes it possible, on the one hand, to obtain a numerical field model from the source map and punch it for subsequent computer processing and, on the other hand, from the calculation results transferred to perforated tape, to construct a map of the converted field in the form of points belonging to individual isolines.

The coding of a map for subsequent computer input consists in the raster reading on an electromechanical (drum) scanner and the transferring out of the coordinates of the intersection points of scanning lines with isolines of the map, together with information about the increment of function Z on the transition from one isoline to another along a scanning line. Additional map coloring is used in order to give information about the sign of the increment of a parameter; an auxiliary red line is plotted along an isoline from the direction of the larger value of function Z.

During the automatic reading process individual map elements are singled out in turn on the map along a scanning line -- 43 vertical lines for every 10 mm of map scale. In successive rounds of map elements along one of the lines the appearance of a black element indicates that at the given point the field has a value which is a multiple of ΔZ. The device punches coordinate ξ_{ij}, to which a "plus" sign is ascribed if there is a white element in front of a black element, or a "minus" sign if there is a red element in front of a black element. The index i denotes the number of the black element appearing on the reading line, and j the number of the reading line. After scanning the map, the device impresses on a perforated tape a matrix of quantities $\{\xi_{ij}\}$ carrying information about the coordinates of isoline intersection with scanning lines and the character of field increment on the transition from one isoline to another.

By turning the map 90° it is possible to stamp a matrix of quantities $\{\eta_{ji}\}$ carrying the same information about the field, but while reading along lines perpendicular to the first ones.

During printing the device reads data from a perforated tape, on which are stamped arrays of values of the coordinates of points of intersection of the vertical grid with isolines of the map of counting results. When the code of this coordinate coincides with the code of a drum point under the printing head, a single point is printed, with the points printed with three tags for convenience in the subsequent construction of the contour.

In order to reduce to generally accepted form the digital data coded by the device, i.e. to determine field values in nodes of the square grid, a special algorithm for the "Minsk-22" computer was devised, which performs the following operations: 1) the values $\{\xi_{ij}\}$ and $\{\eta_{ij}\}$, which are entered in the working storage, are assigned the values of the area coordinates (x'_i, y'_j) and $x''_j, y''_i)$; 2) each point with the coordinates (x'_i, y'_j) or $x''_j, y''_i)$ is assigned field values Z'_{ij} of Z''_{ji} which are multiples of ΔZ at this point; 3) field values at points of the square grid are determined from found field values at arbitrarily situated area points (x'_i, y'_j) and $x''_j, y''_i)$.

Coordinates (x'_i, y'_j) and $x''_j, y''_i)$ are connected with the set of values $\{\xi_{ij}\}$ and $\{\eta_{ji}\}$ by the following relations:

$$\left.\begin{aligned} x'_i &= |\xi_{ij}| \\ y'_j &= 10_j \end{aligned}\right\} j = \overline{0, m}; \qquad (1)$$

$$\left.\begin{aligned} x''_j &= 10_j \\ y''_i &= |\eta_{ji}| \end{aligned}\right\} j = \overline{0, m}. \qquad (2)$$

As can be seen from expressions (1) and (2), one of the coordinates is easily determined by the number of the reading line. Therefore, it is not advisable to keep it in the computer's working storage, for it can always be found given an ordered arrangement of the modules of quantities ξ_{ij} and η_{ji}.

Henceforth, the ordered arrangements of modules of quantities ξ_{ij} (let us designate them x_{ij}) which have the same index number j we shall call rows; and the ordered arrangements of modules of quantities η_{ji} (let us designate them y_{ji}) we shall call columns.

To determine a function at points of rows (Z'_{ij}), we must have at our disposal the field value at the beginning of row Z_{0j}. If Z_{0j} is known, Z'_{ij} is determined by the expression

$$Z'_{ij} = \Delta Z\left[\frac{Z_{0j}}{\Delta Z}\right] + \sum_{k=1}^{i} \delta_k \Delta Z, \tag{3}$$

where ΔZ is a cross section of isolines; $\left[\frac{Z_{0j}}{\Delta Z} -\right]$ is the integer part of ratio $\frac{Z_{0j}}{\Delta Z}$, and $\delta_k = \frac{\text{sign } \xi_{i-1j} + \text{sign } \xi_{ij}}{2}$, where sign ξ_{0j} = sign Z_{0j}.

Analogously for columns, if Z_{j0} is known,

$$Z'_{ji} = \Delta Z\left[\frac{Z_{j0}}{\Delta Z}\right] + \sum_{k=1}^{i} \delta_k \Delta Z, \tag{4}$$

where $\delta_k = \frac{\text{sign } \eta_{ji-1} + \text{sign } \eta_{ji}}{2}$ with sign η_{j0} = sign Z_{j0}.

As can be seen from expressions (3) and (4), quantities Z_{0j} and Z_{j0} can be replaced by certain fictitious values $\bar{Z}_{0j}$ and $\bar{Z}_{j0}$ which satisfy the inequalities

$$\Delta Z\left[\frac{Z_{0j}}{\Delta Z}\right] < \bar{Z}_j < \Delta Z\left(\left[\frac{Z_{0j}}{\Delta Z}\right] + 1\right); \tag{5}$$

$$\Delta Z\left[\frac{Z_{j0}}{\Delta Z}\right] < \bar{Z}_{j0} < \Delta Z\left(\left[\frac{Z_{j0}}{\Delta Z}\right] + 1\right). \tag{6}$$

Quantities $\bar{Z}_{0j}$ and $\bar{Z}_{j0}$ are determined from a given field value in upper corner of the map $Z_{0\,0}$ according to the following logic arrangement:

$$\bar{Z}_{0i} = \Delta Z\left[\frac{Z_{0\,0}}{\Delta Z}\right] + \sum_{k=1}^{e} \delta_k \Delta Z + \frac{\Delta Z}{2} \text{sign } \eta_{0e+1}. \tag{7}$$

Here $\delta_k = \frac{\text{sign } \eta_{0k-1} + \text{sign } \eta_{0k}}{2}$ where $\eta_{0\,0}$ = sign $Z_{0\,0}$ and e is the index of η_{0i}, given which the difference $10_j - \eta_{0i}$ has the minimum positive value.

Analogously $\bar{Z}_{j0} = \Delta Z\left[\frac{Z_{j0}}{\Delta Z}\right] + \sum_{k=1}^{e} \delta_k \Delta Z + \frac{\Delta Z}{2} \text{sign } \xi_{e+10}$,

where $\delta_k = \frac{\text{sign } \xi_{k-10} + \text{sign } \xi_{k0}}{2}$; sign $\xi_{0\,0}$ = sign $Z_{0\,0}$; and e is the index of ξ_{i0}, given which difference $10_j - \xi_{i0}$ has the minimum positive value. (8)

If $\bar{Z}_{0j}$ and $\bar{Z}_{j0}$ are known, from expressions (3) and (4) we determine Z'_{ij} and Z''_{ji}, which are replaced by the ratios $\frac{Z'_{ij}}{\Delta Z}$ and $\frac{Z''_{ji}}{\Delta Z}$ and are assigned to orderly arranged sets $\{x_{ij}\}$, $\{y_{ji}\}$.

Numbers $\frac{Z'_{ij}}{\Delta Z}$, $\frac{Z''_{ji}}{\Delta Z}$ and associated numbers x_{ij} and y_{ji} are arranged in specially allotted blocks of cells (four per cell). This is feasible since x_{ij} and $y_{ji} \leq 420_{10} = 644_8$, and condition

$$\max\left[\frac{Z}{\Delta Z}\right] < 255_{10} = 377_8.$$

is superimposed on field values.

The field values at the beginning and end of rows Z'_{0j} and Z'_{mj}, j = 0, m, are added to the set of values Z'_{ij}, and the field values at the beginning and end of columns Z_{j0} and Z_{jm}, j = 0, m, are added to the set of values Z''_{ji}. These values can be obtained from the field values in map corners ($Z_{0\,0}$, Z_{0m}, Z_{mm} and Z_{m0}) from the relations

$$\begin{aligned}
Z'_{0j} &= Z^{*}_{0k} + \frac{10j - y_{0k}}{y_{0k+1} - y_{0k}}\left(Z^{*}_{0k+1} - Z^{*}_{0k}\right);\\
Z'_{mj} &= Z^{*}_{mk} + \frac{10j - y_{mk}}{y_{mk+1} - y_{mk}}\left(Z^{*}_{mk+1} - Z^{*}_{mk}\right);\\
Z^{*}_{j0} &= Z'_{k0} + \frac{10j - x_{k0}}{x_{k+10} - x_{k0}}\left(Z'_{k+10} - Z'_{k0}\right);\\
Z^{*}_{jm} &= Z'_{km} + \frac{10j - x_{km}}{x_{k+1m} - x_{km}}\left(Z'_{k+1m} - Z'_{km}\right).
\end{aligned} \tag{9}$$

Here $Z''_{0\,0} = Z'_{0\,0} = Z_{0\,0}$; $Z''_{0m} = Z'_{0m} = Z_{0m}$; $Z''_{m0} = Z'_{m0} = Z_{m0}$; $Z''_{mm} = Z'_{mm} = Z_{mm}$; $y_{0\,0} = x_{0\,0} = 0$; $y_{m0} = y_{0m} = x_{m0} = x_{0m} = 10m$; $y_{0\,0} = x_{0\,0} = 0$; k is the index of y_{0i}, y_{mi}, x_{0i} or x_{mi}, given which the differences $10j - y_{0j}$, $10j - y_{mi}$, $10j - x_{0i}$ or $10j - x_{mi}$ have minimum positive values.

To determine a field at an arbitrary point of a square grid with coordinates $(10\mu, 10\nu)$, from set of quantities $\{x_{ij}\}$ we select $x_{k-1\nu}$, $x_{k\nu}$, $x_{k+1\nu}$, $x_{k+2\nu}$ and associated field values $Z'_{k-1\nu}$, $Z'_{k\nu}$, $Z'_{k+1\nu}$, $Z'_{k+2\nu}$, and from set of values $\{y_{ij}\}$ $y_{\mu\ell-1}$, $y_{\mu\ell}$, $y_{\mu\ell+1}$, $y_{\mu\ell+2}$ and associated values $Z''_{\mu\ell-1}$, $Z''_{\mu\ell}$, $Z''_{\mu\ell+1}$, $Z''_{\mu\ell+2}$; here k is the index of $x_{i\nu}$, and ℓ is the index of $y_{\mu i}$, given which the differences $10\mu - x_{i\nu}$ and $10\nu - y_{\mu i}$ have minimum positive value.

After this selection the field value at point $(10\mu, 10\nu)$ can be obtained from one of the following relations:

1) $$Z_{\mu\nu} = Z'_{k\nu} + \frac{10\mu - x_{k\nu}}{x_{k+1\nu} - x_{k\nu}}\left(Z_{k+1\nu} - Z_{k\nu}\right),$$

if $$Z'_{k\nu} = Z'_{k+1\nu} \text{ и } Z''_{\mu\ell} = Z''_{\mu\ell+1}, \text{ а } \frac{x_{k+1\nu} - x_{k\nu}}{y_{\mu\ell+1} - y_{\mu\ell}} \leq 1 \tag{10}$$

or $Z'_{kv} \neq Z'_{k+1v}$, a $Z''_{\mu l} = Z''_{\mu l+1}$;

$$2)\ Z_{\mu v} = Z'_{\mu l} + \frac{10v - y_{\mu l}}{y_{\mu l+1} - y_{\mu l}} (Z''_{\mu l+1} - Z''_{\mu l}),$$

if $Z'_{kv} = Z'_{k+1v}$ и $Z''_{\mu l} \neq Z''_{\mu l}$, a $\frac{x_{k+1v} - x_{kv}}{y_{\mu l+1} - y_{\mu l}} > 1$ (11)

or $Z_{kv} = Z'_{k+1v}$, a $Z''_{\mu l} \neq Z''_{\mu l+1}$;

$$3)\ Z_{\mu v} = Z'_{kv} + \frac{0{,}5\,(x_{k+1v} - x_{kv}) - |0{,}5\,(x_{kv} + x_{k+1v}) - 10\mu|}{x_{k+1v} - x_{kv}} \times$$

$$\times (Z''_{\mu l} - Z'_{kv}), \quad (12)$$

if $Z'_{kv} = Z'_{k+1v} \neq Z''_{\mu l} = Z''_{\mu l+1}$, a $\frac{x_{k+1v} - x_{kv}}{y_{\mu l+1} - y_{\mu l}} \leqslant 1$;

$$4)\ Z_{\mu v} = Z''_{\mu l} + \frac{0{,}5\,(y_{\mu l+1} - y_{\mu l}) - |0{,}5\,(y_{\mu l} + y_{\mu l+1}) - 10v|}{y_{\mu l+1} - y_{\mu l}} \times$$

$$\times (Z'_{kv} - Z_{\mu v}), \quad (13)$$

if $Z'_{kv} = Z'_{k+1v} \neq Z''_{\mu l} = Z''_{\mu l+1}$, a $\frac{x_{k+1v} - x_{kv}}{y_{\mu l+1} - y_{\mu l}} > 1$;

$$5)\ Z_{\mu v} = Z'_{kv} + \delta \cdot \frac{0{,}5\,(x_{k+1v} - x_{kv}) - |0{,}5\,(x_{kv} + x_{k+1v}) - 10\mu|}{x_{k+1v} - x_{kv}}, \quad (14)$$

if $Z'_{kv} = Z'_{k+1v} = Z''_{\mu l} = Z''_{\mu l+1}$ and $\frac{x_{k+1v} - x_{kv}}{y_{\mu l+1} - y_{\mu l}} \leqslant 1$

and at least one of the quantities Z'_{k-1v}, Z'_{k+2}, $Z''_{\mu l-1}$, $Z''_{\mu l+2}$ is not equal to Z'_{kv};

$$6)\ Z_{\mu l} = Z'_{kv} + \delta \frac{0{,}5\,(y_{\mu l+1} - y_{\mu l}) - |0{,}5\,(y_{\mu l} + y_{\mu l+1}) - 10v|}{y_{\mu l+1} - y_{\mu l}}, \quad (15)$$

if the conditions stated in section 5 are fulfilled but $\frac{x_{k+1v} - x_{kv}}{y_{\mu l+1} - y_{\mu l}} > 1$;

in expressions (14) and (15) δ is the difference between Z'_{kv} and $\bar{Z}$, where

$$\bar{Z} \in \{Z'_{k-1v},\ Z'_{k+2v},\ Z''_{\mu-1},\ Z''_{\mu+2}\} \ \&\ \bar{Z} \neq Z'_{kv};$$

$$7)\ Z_{\mu v} = Z'_{kl}, \quad (16)$$

if all chosen field values are equal among themselves.

After making the rounds of all points, we obtain a matrix of values $\mu\nu$, which are a digital model of a 40 x 40 map board -- this digital model being reduced to generally accepted form, i.e. the values are referred to the nodes of the square grid.

If the initial map has large dimensions, it is partitioned into separate 42 x 42 map boards, which should have one common row in the region of the interface. After the reading of each map board by converter we obtain

banks of numerical information $\{\eta_{ji}\}_k$ and $\{\xi_{ij}\}_k$, where k is the map board number. These banks are put in pairs into the working storage of the computer and used to construct a digital model of the map, i.e. they make it possible to obtain field values $Z^{(k)}_{\mu\nu}$ at nodes of the square grid of map boards 40 x 40 cm in dimension on the map scale. Map boards are partitioned into four 20 x 20 squares, each of which is recorded on magnetic tape in strictly defined order.

After all matrices $\{\xi_{ij}\}_k$ and $\{\eta_{ji}\}_k$ are processed, the field is converted according to a given program. For this purpose, from the 20 x 20 squares 60 x 60 banks are formed, each having overlapping strips of 10 rows and 10 columns in interface regions.

By processing such banks, we obtain 40 x 40 cm boards of converted maps, each of which is processed for output of the counting results on the puncher.

For this purpose, row by row we determine the coordinates of the points of a row in which field values are multiples of ΔZ. The quantities ξ_{ij} are punched in the octal number system; the tag 1, 2 or 3 is assigned to them on the basis of the following conditions:

1) if $Z'_{ij} + A = \left[\frac{Z'_{ij} + A}{3\Delta Z}\right] \cdot 3\Delta Z + 0$, tag 1;

2) if $Z'_{ij} + A = \left[\frac{Z'_{ij} + A}{3\Delta Z}\right] \cdot 3\Delta Z + 1$, tag 2;

3) if $Z'_{ij} + A = \left[\frac{Z'_{ij} + A}{3\Delta Z}\right] \cdot 3\Delta Z + 2$, tag 3.

Here Z''_{ij} is the field value at point ξ_{ij}, which is a multiple of ΔZ, and A is a constant, multiple of $3\Delta Z$, making possible fulfillment of the inequality $Z'_{ij} + A > 0$.

The value of coordinate ξ_{ij} is found by linear interpolation. In conformity with the tags assigned to quantities ξ_{ij} indices of varying configuration are printed at the point with coordinate ξ_{ij}; these indices are subsequently connected by lines of equal values. At the first and last points of rows field values are derived which are used in map construction.

BIBLIOGRAPHY

1. Budnyak, A. A., and Petrenko, A. I., Mekhanizatsiya i Avtomatizatsiya Upravleniya (Mechanization and Automation of Control), 1966, 6.

2. Budnyak, A. A., Dyadyura, V. A., and Kapshuk, O. A., in the present collection of works.

COMPUTER INPUT OF GEOPHYSICAL MAPS

Metody i Ustroystva Preobrazovaniya Graficheskoy Informatsii (Methods and Devices for the Conversion of Graphic Data), 1968, pages 99-102

A. A. Budnyak, V. A. Dyadyura and O. A. Kapshuk

Information represented graphically in the form of maps of various potential fields possesses great visualizability and makes possible rapid human perception of the phenomena under study. This permits acceleration of data processing on computers through selection of the most important portion of information from a collection of experimental data which often possesses considerable redundancy.

Such information is most rapidly processable by electronic computers. However, a technical imbalance has arisen at present between the speed of modern electronic computers and the manual method of preparing technical information carriers (punched cards or perforated tape), the preparation of which for many jobs takes about 90 percent of total processing time.

Experience in making economic calculations on the computer shows that the coding and transference of primary data onto technical information carriers take up to 70-100 hours of hand labor per hour of computer operation. In the processing of graphic information, however, data preparation time may exceed that indicated above by more than one and a half or two times since the data for perforated tapes and punched cards must be obtained directly from a graphic drawing. Most often, potential field maps (for example, gravity-anomaly, magnetic and other maps) represent field information as isolines of values of a function of the form $Z + f(x, y)$.

On the one hand, the necessity of creating automatic devices which will permit automation of the process of the computer input of such maps follows from the aforecited comparison of the time required for data preparation and computer processing and, on the other hand, this necessity is evidenced by the important part played by those fields of science and production where the processing of such information is used. An automatic device can be based on an optical scanning system [2].

In reading a potential field image, most often we must determine the value matrix of potential field function $Z = f(x,y)$. This is necessary, for example, for further computer analysis.

In scanning an information carrier (potential field map) any initial message A is described by a function of a finite set of variables

$$A = F(B_1, B_2, \ldots, B_k, \ldots, B_n), \qquad (1)$$

where $B_k = f_{x_i y_i}(\omega, \nu, t)$ is a function characterizing the time variation of the intensity and spectral composition of the luminous flux received by the k-th elementary area of an observation field; x_i, y_i are the coordinates of the k-th elementary area; ω is the intensity of the elementary luminous flux; t is time; and n is the number of elementary areas in an observation field.

In other words, this expression can be regarded as the mathematical form of giving the initial message in a multidimensional space of photoresistors, from which one can then proceed to a description of the message in a multidimensional space of tags.

As a result, the expression

$$F(B_1, B_2, \ldots, B_k, \ldots, B_n) = \theta(t) \qquad (2)$$

where $\theta(t)$ is system response on conclusion of interrogation of the n-th number of elementary areas, will be found to be the mathematical model of a programmed scanning system.

In the scanning of a potential field map, the intersection (as well as tangency) of the isolines of a map with the reading beam of the scanning system is informative. This being the case, the coordinates of intersection point x_i, y_i, as well as value Z_i of the map isoline must be known. Value Z_i is most often recorded on a blank map in the form of decimal digits since this method makes possible the compact recording of a large amount of information representing value Z_i.

The use of recognition devices (often called readers) to determine value Z_i at a given stage is inefficient since their employment significantly increases the size of the hardware and lessens the reliability of the entire device (reader reliability is less than 100 percent). In addition, these devices are far from perfect, especially in case of arbitrary arrangement of digits. All this has made investigators set about searching for a simpler method of representing information about intersection points. Since the information obtained in reading a potential field was intended for subsequent computer input, it could be represented in a form having a smaller quantity of information and, by using simple computing operations, matrix Z could be obtained [1]. If we know sign ΔZ at isoline intersection and the initial value Z_{0j}, as well as the coordinates of intersection points x_{0j}, y_{0j}, we can find value Z_{ij} at these points in the form

$$Z_{ij} = \Delta Z \left[\frac{Z_{0j}}{\Delta Z} \right] + \sum_{k=1}^{i} \delta_k \Delta Z. \qquad (3)$$

where ΔZ is a cross section of isolines; $\left[\frac{Z_{0j}}{\Delta Z}\right]$ is the integer part of relation $\frac{Z_{0j}}{\Delta Z}$; $\delta_k = \frac{\text{sign } x_{i-ij} + \text{sign } x_{ij}}{2}$ and sign x_{0j} = sign Z_{0j}.

Analogously, values of Z can be found from columns (along coordinate y). If we have these data, it is a simple matter to obtain matrix Z by using one of the interpolation methods. Consequently, with this representation of information image A (an isoline in the investigated field of the scanning system) must enable the system on the basis of n tags to produce response $\theta(t)$, which has in all two values, i.e. response $\theta(t)$ can be represented by a discrete function with two values. In view of the fact that, in order to produce two values of $\theta(t)$, at least one of the functions B(k) which, as follows from (1), depend on the intensity of luminous flux and its spectrum, must vary, with this method the necessary amount of information in the event of isoline intersection will be expressed by only one bit (as compared with 5-10 bits in determining the value Z_i on isolines). One bit of information can be represented on a blank map as two values of reflection coefficient ρ or as two areas with varying spectral reflection ν .

In view of the fact that the amplitude system (variation of ρ) is very unstable, the potential-field reading device uses a method of varying the spectral composition of the reflected luminous flux, whereby elimination of the influence of variation in the intensity of luminous flux ω is possible, i.e. an additional red line is used, which jointly with the basic black isoline carries information about the sign of ΔZ.

This choice was found to be optimal in separating three zones of a map field by means of the two photoreceivers used, whose spectral characteristics do not intersect: white and red zones occur in the region of maximum spectral sensitivity of phototransistor FTG-1 (infrared region), but only a white zone occurs in the region of maximum spectral sensitivity of FEU [photomultiplier] -16 [1, 3].

Such a logic device then makes possible determination of the color of the zone in which the reading beam occurs, the sign of the variation of the function sign ΔZ at a given point, and the coordinates of the latter [1 and 2].

Determination of the value of function $Z = f(x,y)$ in nodes of the uniform grid of coordinates x and y, which is usually necessary for computer calculations of this type of information, is described in detail in [1].

BIBLIOGRAPHY

1. Bas, R. T., Budnyak, A. A., Dyadyura, V. A., Kalikhman, L. P., and Shereshevskaya, S. Ya., in the present collection of works.

2. Budnyak, A. A., and Petrenko, A. I., Mekhanizatsiya i Avtomatizatsiya (Mechanization and Automation), 1966, 6.

3. Kharkevich, A. A., Bor'ba s Pomekhami (Noise Control), State Publishing House of Literature on Physics and Mathematics, Moscow, 1965.

OSCILLOGRAM-PROCESSING ALGORITHMS FOR FORMATION OF SYSTEM OF ALGEBRAIC EQUATIONS RELATIVE TO PARAMETERS OF THE DESCRIBED PROCESSES

Metody i Ustroystva Preobrazovaniya Graficheskoy Informatsii (Methods and Devices for the Conversion of Graphic Data), 1968, pages 103-107

V. G. Chekalin

The problem of raising the accuracy and reducing the time involved in the experimental determination of the dynamic characteristics of controlled systems is very urgent [1, 3-5].

Most controlled systems can be represented in the form of a circuit, whose control action μ (t) and controlled value φ (t) can be measured. Noise n(t) is not amenable to measurement, and generally it can always be reduced to input, as shown in Figure 1.

As the result of an experimental study of the dynamic characteristics of a system, the time variations of input μ (t) and output φ (t) coordinates can be recorded (realized, for example, in the form of an oscillogram). The purpose of subsequent processing is to determine the approximating differential equation, the solution to which in a certain sense is closest to that obtained experimentally.

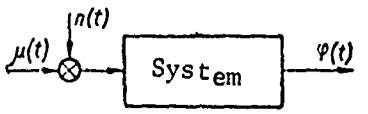

Figure 1. Control circuit

The known methods for determining the dynamic characteristics of a system either take a great deal of time, for example statistical methods [3], or require the introduction of a test signal, which is not always feasible under operating conditions. But dynamic-model systems, as a rule, can operate only under tracking conditions.

At the same time, information theory [2] shows that by employing optimum methods and taking into consideration a priori known information about the system under investigation algorithms can be created which require considerably less realization time.

For example, in cases where the structure of the operator describing the dynamic properties of a system is known or given, an effective method for forming a system of algebraic equations relative to the coefficients of this operator can be employed. Solution of the system of algebraic equations presents no great complication.

The advantage of this method, the idea of which was apparently first stated in [6], is that it is integral with an arbitrarily chosen integration limit and at the same time does not require the operation of differentiation of the monitored signals when they are processed.

The suggested method presupposes the sequential principle of the formation of a complete system of algebraic equations based on the processing of an amount of process realization equal to the number of unknown operator coefficients.

However, a complete system of algebraic equations can also be formed on the basis of processing a single realization with the use of the parallel principle.

Let the processes in the controlled system be described by a differential equation of the form

$$a_0\varphi + a_1\varphi^{(1)} + \ldots + a_n\varphi^{(n)} + \ldots = \mu(t) + n(t). \tag{1}$$

Values of coefficients a_i of this differential equation are unknown and have to be determined.

It is found possible to form a system of algebraic equations relative to unknowns a_i of the form

$$\begin{array}{l} c_{00}a_0 + c_{01}a_1 + \ldots + c_{0n}a_n = u_0; \\ c_{10}a_0 + c_{11}a_1 + \ldots + c_{1n}a_n = u_1; \\ \ldots\ldots\ldots\ldots\ldots\ldots \\ c_{i0}a_0 + c_{i1}a_1 + \ldots + c_{in}a_n = u_i; \\ \ldots\ldots\ldots\ldots\ldots\ldots \\ c_{n0}a_0 + c_{n1}a_1 + \ldots + c_{nn}a_n = u_n. \end{array} \tag{2}$$

Here
$$c_{ij} = (-1)^{i+j}\int_0^T f^{(i+j)}q\,dt, \quad u_i = (-1)^i\int_0^T f^{(i)}\varphi\,dt \tag{3}$$

Modulating function f(t) in this case must satisfy condition $f^{(k)}(0) = f^{(k)}(T) = 0$, where k = 0, 1, 2, ..., 2n - 1.

Actually, if we take initial equation (1) and differentiate it n times and then multiply each of the newly obtained equations times f(t) and integrate from 0 to T, we shall obtain the system

$$a_0\int_0^T \varphi^{(l)} f dt + \cdots + a_i \int_0^T \varphi^{(i+l)} f dt + \cdots + a_n \int_0^T \varphi^{(n+l)} f dt = \\ = \int_0^T \mu^{(l)} f dt + \int_0^T n^{(l)} f dt. \quad (4)$$

Performing integration by parts of terms which contain derivatives of φ (t) until they come out from under the sign of the integral, and taking into consideration the above-indicated property of f(t), we obtain

$$a_0(-1)^l \int_0^T f^{(l)} \varphi dt + \cdots + a_i (-1)^{i+l} \int_0^T f^{(i+l)} \varphi dt + \cdots \\ \cdots + a_n (-1)^{n+l} \int_0^T f^{(n+l)} \varphi dt = \\ = (-1)^l \int_0^T f^{(l)} \mu dt + (-1)^l \int_0^T f^{(l)} n dt. \quad (5)$$

If we assume that noise n(t) is a random stationary process with M [n(t)] = 0, then the last term given large T can be discarded and in this case expression (5) is identically equal to expression (2).

As modulating function, it is proposed to use a function of the form

$$f(t) = \sin^{2n}\omega t. \quad (6)$$

As analysis has shown, by virtue of the finite accuracy of the measuring equipment and as a result of the fact that the term $\int_0^T f^{(i)} n dt$ was not taken into consideration, the resultant system (2) can be strongly oblique-angled and even incompatible. This being the case, the solution can differ significantly from the actual solution. To reduce error to a minimum, it is suggested that the solution be found from the condition of minimum squared mismatch error, which is determined as follows:

$$e^2 = \sum_{j=0}^{n} \left[\sum_{i=0}^{n} a_i^* c_{ji} - u_j \right]^2. \quad (7)$$

Here a_i^* are the estimated values of coefficients. It can be proved that in this case the process will always be convergent.

Let us illustrate the use of the algorithms presented above with an example of the determination of coefficients of the first-order equation

$$a_0\varphi + a_1 \frac{d\varphi}{dt} = \mu(t) + n(t), \quad (8)$$

for which realizations μ (t) and φ (t) of Figure 2 were obtained. As modulating function, let us choose $f(t) = \sin^2 \omega t$. Figure 2 shows the form of the modulating function and its first two derivatives on the segment from 0 to $T = \frac{\pi}{\omega}$.

Using expression (3), we can calculate the values of coefficients c_{ji} for the example under consideration. However, in the digital computer operations are performed with quantities at discrete moments of time; therefore, in order to choose quantization time interval Δ t, let us use Kotel'nikov's theorem, according to which

$$\Delta t = \frac{\pi}{\omega c}. \tag{9}$$

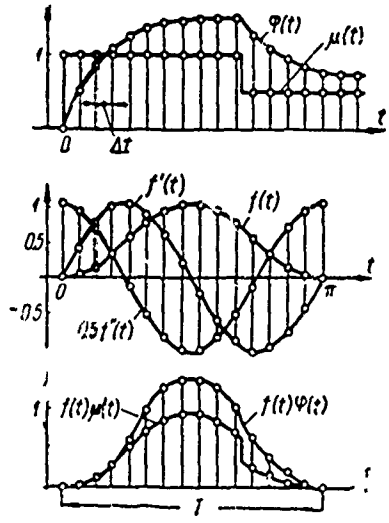

Figure 2. Graph of modulating function and its derivatives.

Lest there be information loss, the cutoff frequency ω_c must be taken for compound signal $f(t)\varphi(t)$ with it being equal to the sum of the cutoff frequency of output signal $\varphi(t)$ and modulating function f(t).

Using formulas of approximate integration, we can represent expressions (3) in the form of sums and realize the resultant algorithms on the digital computer.

Thus, using a formula of rectangles, we can write expressions for coefficients c_{ji} and u_j at moment $t = k\Delta t$ (k = 0, 1, 2, 3...) as

$$\begin{aligned} c_{ji}[k\Delta t] &\approx (-1)^{i+j}\Delta t \sum_{\nu=0}^{m} f^{(i+j)}[\nu\Delta t]\,\varphi[(k+\nu)\Delta t], \\ u_j[k\Delta t] &\approx (-1)^{j}\Delta t \sum_{\nu=0}^{m} (f^{(j)})[\nu\Delta t]\,\mu[(k+\nu)\Delta t]; \end{aligned} \tag{10}$$

here m equals T/Δ t accurate to within an integer.

More accurate results are obtained and the algorithm made negligibly more complicated if we use a formula of trapezoids. The latter was in fact used in practical calculations.

Experimental testing of the algorithms by using the example of the processing of realizations for first- and second-order systems, which were

on model MPT-9-3, showed good results. The systems of algebraic equations were solved not only by ordinary methods but also by minimization methods. The latter made it possible to obtain more accurate results in the presence of noise.

BIBLIOGRAPHY

1. Ivakhnenko, A. G., Tekhnicheskaya Kibernetika (Technical Cybernetics), State Publishing House of Technical and Theoretical Literature Ukrainian SSR, Kiev, 1959.

2. Krasovskiy, A. A., Dinamika Nepreryvnykh Samonastraivayushchikhsya Sistem (Dynamics of Continuous Self-Adjusting Systems), State Publishing House of Literature on Physics and Mathematics, Moscow, 1963.

3. Leonov, Yu. P., and Lipatov, L. N., Avtomatika i Telemekhanika (Automation and Telemechanics), 19 [?60], 9.

4. Prisposablivayushchiyesya Avtomaticheskiye Sistemy (Adaptive Automatic Systems), edited by E. Mishkin and L. Braun, Foreign Literature Press, Moscow, 1963.

5. Chinayev, P. I., Samonastraivayushchiyesya Sistemy (Self-Adjusting Systems), State Publishing House of Literature on Machine Manufacture, Moscow, 1963.

6. Control, 1964, 4, 209-210.

DIGITAL WELL-LOG CONVERTERS

Metody i Ustroystva Preobrazovaniya Graficheskoy Informatsii (Methods and Devices for the Conversion of Graphic Data), 1968, pages 123-125

A. G. Mel'nikov and K. M. Sarumova

The digital-computer processing of well logs requires their pre-conversion into digital form. Well logs recorded at wells, as a rule, are not suitable for automatic reading (due to the poor quality of the recording, the single-color coordinate grid etc.) and require time and expense to re-record them. Therefore, considering, on the one hand, the difficulty of creating an automatic well-log converter and, on the other hand, the ever growing need for a device which is inexpensive and simple to make, adjust and service, yet permits the conversion of a large amount of initial graphic data at an adequate speed, the Problem Laboratory of AzINEFTEKhIM [Azerbaydzhan Institute of Petroleum and Chemistry imeni M. Azizbekov] has developed a semi-automatic digital well-log converter (DWLC).

The converter is designed for operation with a "Minsk" or "BESM" type digital computer (with the appropriate attachment) and is supplied with a tape or card puncher.

The principal components of the device are a broaching-copying device, an angle-data transmitter, a phase-code converter and a timer. Tracking of a curve is performed by an operator shifting the edge of the master form in a vertical direction with uniform movement of logs. Deflection of the master form by a flexible coupling is converted into an angular displacement.

The angle-data transmitter is a small-sized sine- cosine rotatable transformer of the VT-3 type, which is put on a phase-shifting regime. Sinusoidal voltage is generated at the phase-shifter output, with the phase of this voltage varying relative to the phase of the reference signal in proportion to the angular increment. The phase shift of the voltages being compared by means of two zero elimination circuits is converted in the phase-code converter into the time interval filled with pulses of stable frequency (8 kc) from a special generator. The result is recorded in an eight-digit binary counter. The conversion of binary code into binary-octal code for recording parameters is performed by the electronic timer.

The DWLC provides for recording of the digital data in parts (for ease of computer input), control over the degree of log slippage, as well as enabling "characteristic" marks to be entered on punched tape (or card) during

conversion for the purpose of singling out the most interesting points of a curve from the overall information. The device uses semiconductor triodes and diodes and is characterized by the following technical data:

Maximum conversion rate	3 numbers/sec
Amplitude resolution	1 mm
Speed of log drive	2.4 and 8 m/hr
Speed of log reverse	60 m/hr
Carrier width	Up to 210 mm
Error in converting master-form deflection into code	± 1 percent
Quantization step	0.5, 1 and 2 mm of log travel
Power supply	200 v ± 10 percent, power requirement (without puncher) -- not more than 40 w

Two pilot models of the instrument have been in operation for two years at VNIIGeofizika [All-Union Scientific Research Institute of Geophysical Exploration Methods] and AzINEFTEKhIM and have proved very reliable. The instrument is being made ready for series output.

The semiautomatic well-log converter, though possessing many advantages, still fails to solve the problem of fully automating the interpretation process. Therefore, just as before, there continues to be great urgency in the question of creating an automatic digital converter suitable for reading well logs recorded at wells. The Problem Laboratory of AzINEFTEKhIM is doing work on the use of the facsimile apparatus FTA-P2 for automatic well-log conversion. One of the important problems here is the separation of a curve from a single-colored coordinate grid. To solve the question, a method is suggested which consists in having forbidden zones at moments when areas of a log containing coordinate grid lines are read. Such zones can be created by means of mechanical or electrical masks. The mechanical masks are made of a material with a reflection coefficient approximating the reflection coefficient of the carrier and are mounted between the reader and well log.

Electrical masks can be created, for example, by a generator which forms a series of pulses of a certain frequency and duration to inhibit data conversion, the pulse duration being chosen on the basis of the required width of the forbidden zone and the repetition rate on the basis of the distance between the horizontal lines of the grid. Naturally, some useful information is also lost with this method of separating the curve from the grid, but in view of the fact that the converted data are subsequently processed in a digital computer, the latter can provide a simple subroutine to restore missing sectors (for example, by means of linear interpolation).

The main advantage of the above-described method of separating a curve from a monochromatic coordinate grid is that the volume of information to be recorded and entered in the computer is significantly reduced.

In the development of digital well-log converters (automatic or semi-automatic) the question arises of choosing the optimal time quantization step, since the construction of an automatic adaptive converter is an exceedingly complex problem.

For choosing the quantization step a statistical method was tested, based on a given mean-root-square error of approximation and a certain estimate of the correlation function. The step h = 1 mm was obtained for the most characteristic curve with a given mean-root-square error of approximation of σ = 10 percent. Such a result is in satisfactory agreement with the initial curve.

GRAPHIC DATA-TO-DIGITAL CODE CONVERTER

Metody i Ustroystva Preobrazovaniya Graficheskoy Informatsii (Methods and Devices for the Conversion of Graphic Data), 1968, pages 126-129

N. S. Chakhirov, A. G. Lekvinadze, V. I. Glinkin and N. K. Gdzelishvili

The conversion and coding of graphic information (graphs, diagrams, oscillograms) are exceedingly time-consuming processes. Therefore, the automation of data reduction and preparation for computer input is an urgent problem. The Institute of Electronics, Automation and Telemechanics of the Academy of Sciences Georgian SSR has developed two types of graphic data converters, the PG-1 and PG-2.

Figure 1 gives the block diagram of the PG-1 device. Pulses go continuously from blocking oscillator 1 to ferrite-transistor switch 2, the control of which is effected from start-of-readout pickup 3, which is rigidly connected to the tape transport roller. The value of the established time interval determining the scanning step is chosen by the operator. After switch 2 is opened the pulses from the blocking oscillator begin to go to binary counter 5, which consists of series-connected statis flip-flops. As the binary counter is filled, the analog voltage increases stepwise at the output divider, the number of voltage stages corresponding exactly to the number of pulses filling the counter. The analog voltage is amplified and fed to photooptical comparator 4.

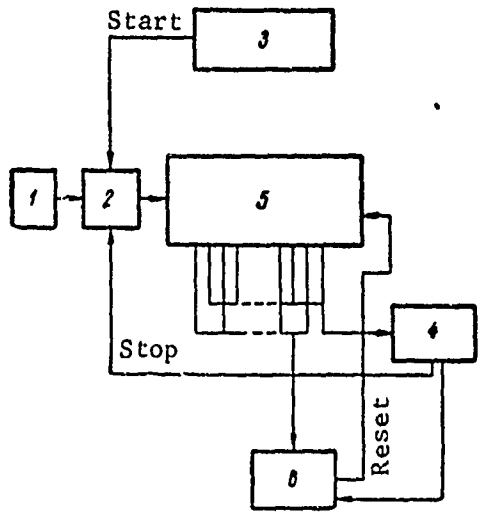

Figure 1. Block diagram of PG-1 device

The latter is a cathode-ray tube, objective and camera with photomultiplier. Striking the Y-plates of the tube (the X-plates are disconnected), the step voltage moves the beam over the tape with the graph plotted on it. At the moment the graph is intersected by the beam, a sharp drop in the illumination of the camera with photomultiplier causes receipt from the photomultiplier of a signal which closes switch 2 and thus stops the receipt of pulses by the counter. At the same time the pulse coming from the photomultiplier turns on puncher 6, and the number recorded in the counter is punched on the tape. Following the recording of the number on the punched tape the counter returns to zero position. Since the position of the beam on the tape with the graph is closely connected with the number of pulses which filled the counter, the maximum error of data-to-binary code conversion can be equal to only one discrete unit, i.e. about 3 percent for a five-digit binary counter and about 0.8 percent in case of the use of a seven-digit binary counter and seven-track punched tape.

Some of the deficiencies of the PG-1 converter were discovered during its trial run. Thus, due to the weak intensity of luminescence of the CRT and insufficiently clear focusing of its beam, completely reliable conversion of graphs with a line thickness of less than 1.0 mm is impossible with the PG-1 converter; therefore, the lines of the graphs have to be outlined with India ink. This same circumstance makes it difficult to convert graphs with an inclination of more than 80°.

The PG-2 converter does not have these deficiencies. It retains the principle of a close connection between the position of the light spot on the tape with the graph and the number of pulses filling the binary counter; however, the operating principle of this device differs substantially from the principle forming the basis of the PG-1 converter.

The PG-2 consists of three main components: an ordinate reading device, a coding device and a PL-80 puncher. The ordinate reading device, which digitizes the angle corresponding to the ordinate of a function, consists of two point light sources arranged in diametrically opposite directions (Figure 2). The first of these 1 is used to scan the tape with the graph. The light spot of the second source 2 scans bar scale 4; the number of pulses at the shaper output determines the value of the ordinate here.

The graph is pulled discretely through drum 3 perpendicularly to the rotational axis of the heads. On a common shaft with the heads of point light sources 1 and 2 is the disk of inductance pickup 5. The coding device, as usual, consists of a pulse generator, control gate (switch K) and binary counter. The tape with the graph is pulled discretely into the PG-2 by means of a special planetary mechanism. The tape transport, scanning light heads, the disk of the inductance pickup IP and the PL-80 puncher are driven off one motor M, which assures the synchronous operation of all components of the converter.

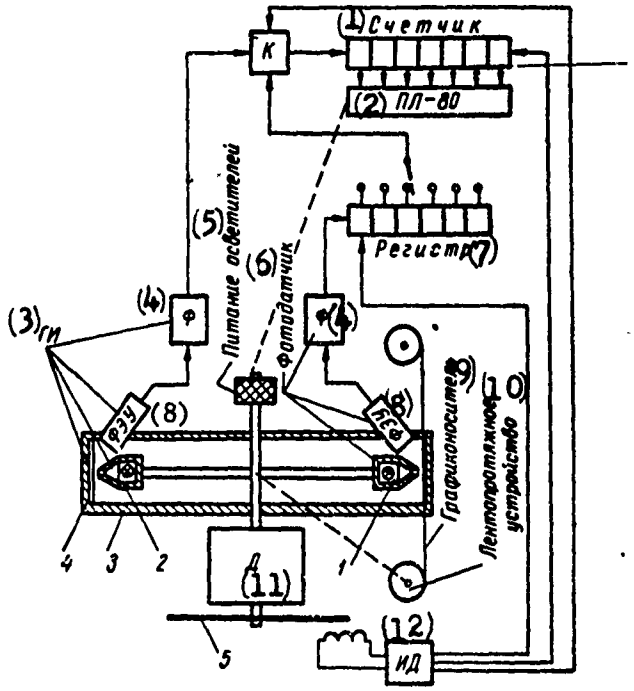

Figure 2. Block diagram of PG-2 device.

Key:
(1) Counter
(2) PL-80
(3) Pulse generator
(4) Shaper
(5) Power supply of illuminators
(6) Photopickup
(7) Register
(8) Photomultiplier
(9) Graph carrier
(10) Tape transport
(11) Motor
(12) Inductance pickup

The ordinate is measured cyclically. The conversion cycle begins from the moment a pulse is issued by the inductance pickup for resetting the counter. At the moment the light spot approaches the origin of coordinates, the inductance pickup puts out a pulse for opening the switch, and the count pulses go to the counter. If the light spot coincides with the graph line, a photopickup, consisting of a photomultiplier and shaper, puts out a pulse for closing the switch. The number of pulses going through the switch corresponds to the angle of rotation of the point light sources, i.e. the value of the ordinate; by means of the counter this number of pulses is converted to binary code. Once the scanning head is clear of the carrier, the information collected in the counter is documented by means of PL-80, which ends the cycle of reading one point of a graph.

During the punching, the tape with the graph moves a preset step. The reading of subsequent points proceeds analogously. Six nonintersecting lines can be read in the converter. The maximum tape width is 230 mm, minimum 35 mm. Tape length varies from 1 to 20 m. The maximum value of a recorded ordinate should not exceed 200 mm. The line thickness of the tape-recorded

curves is at least 0.3 mm, and the maximum slope not more than 87°. The background of the information carrier in the reading field should be kept clean, preferably white in color and transparent for motion picture tapes. The graph reading rate is 5 and 20 points/sec. The values of the issued ordinates are arbitrarily positive, reckoned from an implicit zero reference line. The discreteness step of an issued ordinate corresponds to the scale value. Systematic conversion error, reduced to the maximum ordinate, does not exceed scale value. The quantization step on the axis of abscissas is set as equal to 1, 2, 5 and 10 mm.

The PG-2 is characterized by simplicity of operation and comparatively small size with rather high accuracy. An advantage of the PG-2 instrument which distinguishes it from other such devices is the presence of a light spot of great brightness, which increases the resolution of the instrument and makes it possible to read oscillograms and diagrams without preliminarily outlining them with India ink, as well as to tune them out from grids marked on the tapes of flow meters.

SIMPLE MULTICHANNEL GRAPH READER

Metody i Ustroystva Preobrazovaniya Graficheskoy Informatsii (Methods and Devices for the Conversion of Graphic Data), 1968, pages 130-132

V. A. L'vov

At the present time a multitude of models of devices intended for reading the ordinates of recorded graphs have been developed [1, 3, 4].

Let us describe a simple reader which is a further development of a system based on facsimile transmitter FTA-P [2].

Beam scanning in the FTA-P is effected by means of an oscillating mirror which is put into oscillatory motion by a cam, while the latter is put into motion by a motor with a constant velocity up to 250 rpm. A light beam of the optical system is focused in the plane of the graph to be read, and mirror deflection takes place in such a way that the beam moves linearly over the graph with time. The beam reflected from the paper strikes a photomultiplier; if the beam intersects a line of the graph, a pulse appears at the photomultiplier output. Given uniform motion of the beam, the moment a pulse appears relative to the moment scanning begins is proportional to the value of the graph ordinate.

Let us consider the curve-reading process. Suppose that a graph has four curves. In setting one moment for the start of reading ("0") for all four curves (Figure 1,a) incomplete utilization of the maximum capacity of counters is possible since the size of each curves amounts to less than one-fourth the maximum possible value. Therefore, the accuracy of representing curve ordinates in digital form is reduced. The initial reading level must be established separately for each curve (Figure 1,b). This is accomplished by plotting on the graph a supplementary zero reference line parallel to the axis of abscissas (in the device here described both variants for designation of the reading start are envisaged). Plotting the reference lines presents no difficulties. With a common reference line, intersecting curves can be read; in this case separation of the curves takes place in an electronic computer according to a special curve-recognition program.

Figure 2 presents a block diagram of the reader. Block 5 at the beginning of the forward stroke issues an instruction to block 4 to start operations. On the arrival of pulses from the output of block 3 at the input of block 4 pulses form at the moments of line intersection on the graph, the

length of which is proportional to the magnitude of the ordinates of the curves being read. By means of these pulses block 2 is actuated and pulse trains are generated in which the number of pulses is proportional to the magnitude of the ordinate. In each train the pulses are counted up by one of four flip-flop binary-decimal counters (blocks 9-12). Ordinate code is fed sequentially through block 13 to block 14 and recorded on perforated tape.

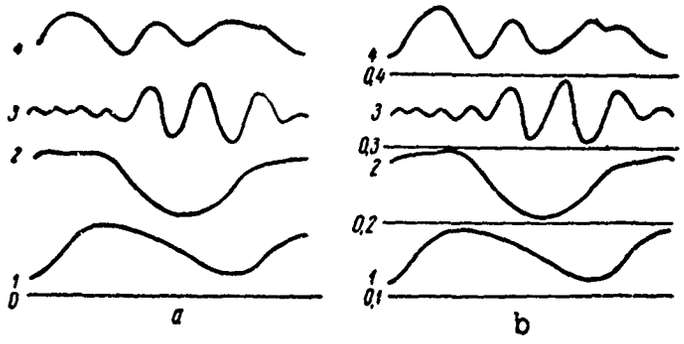

Figure 1. Graphs of curves:
a) with common base line; b) with separate base lines

The ordinate coding scale is determined by the pulse repetition rate from block 2. Block 1 makes it possible to vary the pulse repetition rate so as to obtain the necessary value of ordinate quantization level for every specific case of curves being read. This value must be selected on the following basis: the counter must not overflow if the maximum value of the ordinate is read.

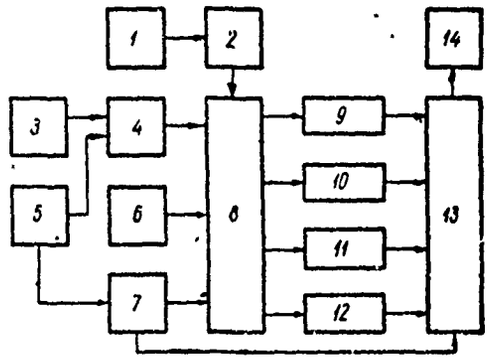

Figure 2. Block diagram of device:

1) selection of scale;	2) count-pulse generator;
3) photomultiplier;	4) shaper;
5) beam scanning block;	6) selection of reading regime;
7) scanning counter;	8) pulse distributor;
9)-12) counters 1-4;	13) output control;
14) perforator.	

By means of the above-described device the ordinates of four curves, the first two or any one curve can be read simultaneously.

The device uses the binary-decimal coding system. Every ordinate is coded in two decimal digits, which corresponds at most to 99 curve quantization levels. The ordinate value takes up two rows on the perforated tape; four ordinate values are entered per computer storage cell. The set of graph-movement elements, given step-by-step transport, is 0.25, 0.5, 1 and 2 mm.

Graph line thickness and color depend on photomultiplier quality. Completely reliable reading is obtained with line thickness not less than 0.3 mm and black (or red) line color. It is assumed that graphs are plotted on paper tape without a coordinate grid. No method of reducing noise from coordinate grid, blurs or fractures is used in the device. This simplifies the reading system but reduces operational reliability.

The device uses semiconductor elements (except for the photomultiplier and its power circuits).

BIBLIOGRAPHY

1. Bartkus, T., Budryunas, A., Meshcheryakov, V., and Tel'ksnis, L., Avtomatizatsiya Vvoda Pis'mennykh Znakov v Elektronnyye Vychislitel'nyye Mashiny -- Sbornik (Automating the Input of Written Signs into Electronic Computers -- Collection of Works), Vil'nyus, 1965.

2. L'vov, V. A., and Parinov, I. D., Tr. Uchebnykh Institutov Svyazi -- Sbornik (Transactions of Communications Schools -- Collection of Works), No. 25, Leningrad, 1965.

3. Mnogokanal'nyy Avtomat Schityvaniya Krivykh (Kratkoye Tekhnicheskoye Opisaniya) (Multichannel Automatic Curve Reader (Concise Technical Description)), Publishing House of Institute of Technical Cybernetics, Academy of Sciences Belorussian SSR, Minsk, 1965.

4. Petrenko, A. I., Preobrazovaniye Grafikov v Elektricheskiye Signaly (Conversion of Graphs into Electric Signals), State Publishing House of Technical and Theoretical Literature Ukrainian SSR, Kiev, 1964.

A GRAPH PROCESSOR BASED ON FACSIMILE APPARATUS

Metody i Ustroystva Preobrazovaniya Graficheskoy Informatsii (Methods and Devices for the Conversion of Graphic Data), 1968, pages 133-134

L. N. Bureyev and S. T. Parsadanyan

Due to the fact that there are well-developed line-scanning systems, document-feed and optical reading assembly systems in facsimile apparatus, the latter is widely used for processing graphic data of any kind. Comparatively simple logical units are required in the FA-aided processing of recorder graphs and tapes. Let us consider some of the distinctive features of a simple reader based on the facsimile apparatus.

The scheme uses for the most part standard logical semiconductor cells (flip-flops, coincidence cascades, pulse mixers, one-shot multivibrators, scaling decades) and is powered by FA rectifiers.

Minimum signal clipping used in the device makes it possible to a considerable extent to eliminate the influence of carrier grade and color, contaminants, light-struck spots etc.

Up to four nonintersecting curves are found simultaneously in the apparatus' field of vision. The logic circuit permits the selection of any curve for processing and the exclusion of signals coming from other curves.

The ordinates of a curve are measured by filling up the time interval from the start of reading to intersection with the given curve with pulses having a significant repetition rate. The following fact is of great interest: pulses are formed from the signal of the generator which powers the FA scanning motor.

The operation of the scheme is synchronized by start-of-line pulses produced in the facsimile apparatus. The sync-pulse frequency divider in the device makes it possible to vary the graph-reading step in a wide range. Filling pulses are counted up by a counter consisting of three decades of the IZ-12 type. Results go to the printer or are observed visually on the digital indicators of the counter. Counter readings are registered by digital recorder "Zoyemtron 3503" (German Democratic Republic). In order to couple the lamp control block of the printer with signals from semiconductor decades IZ-12, silicon-stabilizer matching networks are used, which make it possible to change the d-c component of a signal to the necessary level.

Owing to the noncoincidence of the code structure of the counter signal and the structure of the printer decoder slight changes are made in the scheme of the latter.

During tests of the laboratory model of the device real oscillograms of loop oscillographs were used without preliminary processing. The number of malfunctions in this case did not exceed 1 percent. After final adjustment of the scheme the number of malfunctions can be significantly reduced.

Among the shortcomings of the device must be included the fact that it is impossible to read several graphs simultaneously and the fact that there are no documents in the form of punched card or perforated tape, which hampers subsequent computer processing of reading results. It is assumed that the shortcomings noted here will be eliminated.

DEVICE FOR INPUTTING GRAPHS INTO AN ELECTRONIC COMPUTER FROM MOTION-PICTURE FILM

Metody i Ustroystva Preobrazovaniya Graficheskoy Informatsii (Methods and Devices for the Conversion of Graphic Data), 1968, pages 135-139

S. V. Gil', I. T. Parkhomenko and V. P. Chereshnyuk

Wide use is made at present of oscillography onto standard 35-mm motion-picture film with, say the MPO-2 oscillograph. Devices intended for the automatic processing of oscillograms must be made having regard for certain recording features, in particular for variation in line width of the selfsame oscillogram, the fact that there are faint line sections, fuzziness of line edges, difference in the optical density of background etc.

The design of the known graphics converters is based on the principles of follow or scanning conversion. Use of the former makes it possible to obtain high speed in the device, but malfunctions due to the above-indicated features can occur in the processing of oscillograms. To eliminate these malfunctions the equipment has to be made more complex.

In view of the fact that graph line width varies, if carrier width is narrow, following the edge of the graph line will result in significant errors. Therefore, in processing oscillograms on motion-picture film the ordinates of the graph line center must be determined. If the principle of follow conversion is used, this proves difficult to do.

Sensitivity can be increased in graphic data conversion devices by increasing the sensitivity of the photoreceiver or the brightness of the light source. In follow converters most often a light spot on a CRT screen is used as light source due to its nonpersistence although the brightness of such a source is comparatively small. Thus, when the follow-conversion principle is used, increasing the sensitivity of the photoreceiver proves to be the only resource for raising the sensitivity of the device.

Use of the scanning-conversion principle makes it possible to raise the sensitivity of the device also by using a light source of great brightness. At the same time the signal-to-noise ratio at the output of the photosensitive cell increases, and this in final analysis makes it possible to raise the sensitivity of the device. The scanning-conversion principle permits easy determination of the ordinate of the graph line center to be inputted and construction of rather simple devices for the input of several curves from a single carrier, something which proves complicated in follow converters.

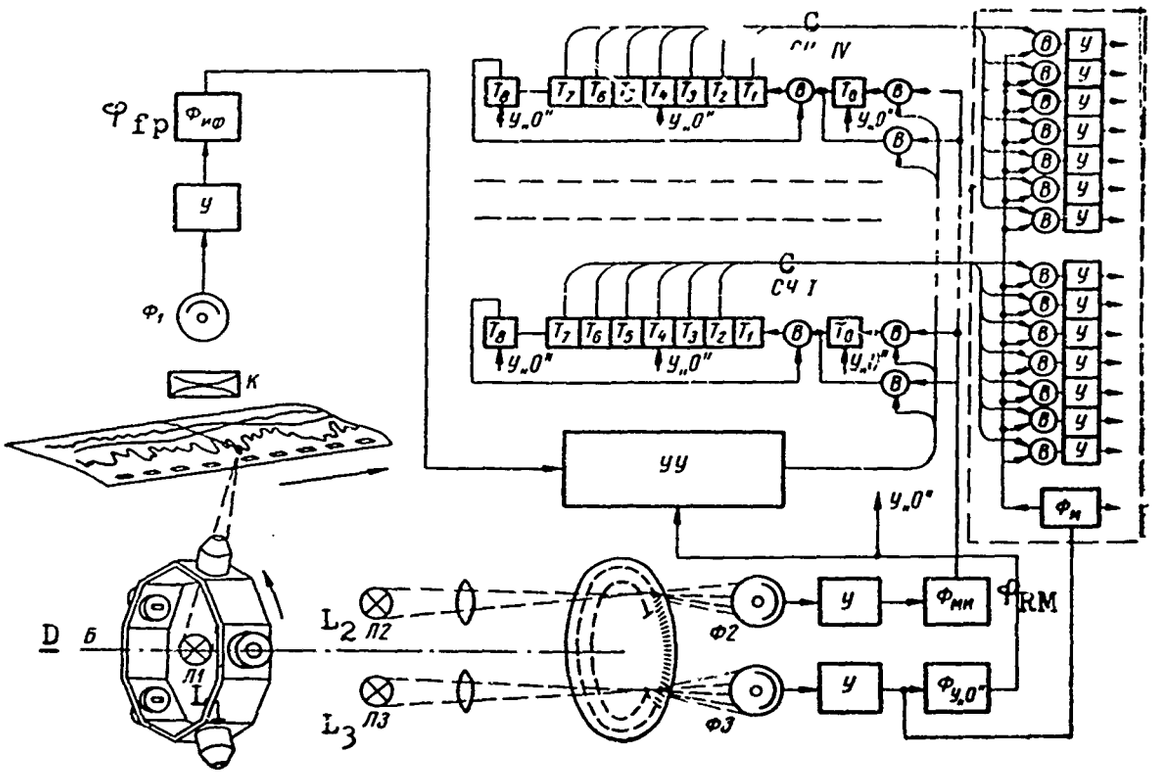

Block diagram of graph input device.

Key:

B	gate
C	counter
D	drum
FP	front pulse
K	capacitor
L	incandescent lamp
RM	range marker
T	flip-flop
Y	amplifier
Y"0"	zero setting

$\Phi_{1,2,3}$	photomultiplier
Φ_{fp}	front pulse shaper
Φ_{M}	marker shaper
Φ_{RM}	RM shaper
$\Phi_{y"0"}$	zero-setting shaper

The above-cited considerations dictated selection of the scanning-conversion principle in creating a device for oscillogram input at the Institute of Cybernetics of the Academy of Sciences Ukrainian SSR. A block diagram of this device is presented in the figure.

Graph scanning is effected by means of rotating drum D with objectives, the optical axes of which are situated along the radii in one plane. The angles between the optical axes of the objectives are equal. In the general focus of all objectives on the axis of rotation of the drum we find incandescent lamp L_1, the focused image of the filament of which is projected on the surface of the motion-picture film. As the drum rotates, a light beam, focused on the surface of the film and perpendicular to this surface at the point of incidence, moves along the line of the ordinate to be read. After the beam passes through the film, it is directed onto the cathode of photomultiplier Φ_1 via capacitor K. The basic control signals -- front pulses -- are generated at the photomultiplier output by means of the appropriate shaper Φ_{FP}.

To read the ordinate of a graph line edge at the moment the beam intersects the edge of the film with the graph, it suffices to feed a series of range markers RM to the counter input, halting the feed thereof at the moment the graph line edge is intersected. The code, recorded by the counter, expresses the value of the ordinate of the graph line edge.

To obtain the value of the ordinate of the center of line Y, the value of half the graph line width must be added to the quantity obtained, i.e. the operation

$$Y = Y_{low} + \frac{Y_{up} - Y_{low}}{2}$$

must be performed, where Y_{low} and Y_{up} are respectively the ordinate of the lower and upper line edge. The operation is executed as follows. Y is registered in the counter by counting up the RMs in the interval of time between the start of counting and the moment the moving beam intersects the graph line. At the time the beam traverses the graph line, an additional zero digit is connected to the counter. As a result, half the quantity of range markers produced during this period are inputted into the counter.

The method here considered of obtaining the ordinate of the graph line center made it possible to use one counter in the device for coding the ordinates of one curve. The shortcoming of the method here described is the fact that there is error if the number $Y_{up} - Y_{low}$ is odd, for with this method of division by two the remainder is discarded. In view of the fact that there is also a shortcoming in ordinate determination, maximum error in coding the line center reaches a value one and a half times that of the coding quantum.

The error occurring during the calculation of $\frac{Y_{up} - Y_{low}}{2}$ could be avoided by performing the calculation on the computer. But in order to transfer Y_{low} and Y_{up} into the computer, the device must have two counters for each curve. In this particular device, for the entire carrier width (25 mm) there are 100 corresponding discrete quantization levels. Maximum relative coding error is 1.5 percent.

A seven-digit counter is used for coding. Apart from the already-mentioned additional zero digit in the counter, there is an additional eighth digit, which controls the operation of the counter in the absence of a graph line. In this case overflow of the counter takes place, the flip-flop of the eighth digit is set in the "1" position by the carry pulse, and the flip-flops of the first to the seventh digits in the "0" position. At the same time the enabling potential is taken from the gate at the counter input, and the arrival of range markers at the first counter position ceases. Thus, until the start of ordinate reading the counter is set in the "0" position.

In order to obtain simultaneously the ordinates of four graphs situated on one motion-picture film there are provided in the device four identical ordinate counters, which are controlled by a four-digit binary counter, decoder and gates. RMs are produced by means of a system consisting of a rotating opaque disk with radially situated transparent marks, an incandescent lamp, objective and photomultiplier. The disk uses the photo-method, and in order to preclude error from the irregularity of rotation, it is seated on the same shaft with drum D. The signal from the photomultiplier output is amplified and shaped.

The Φ_M circuit generates signals used as marker pulses in transferring codes into the electronic computer, and the $\Phi_{y_{"0"}}$ circuit generates signals employed to set counters in the zero position (Y"0" [zero-setting]). The marks, according to which these signals are produced, are situated on the same disk with the marks of the range markers in amount equal to the number of objectives.

To shape the basic control signals of standard amplitude and duration the device employs three identical blocks, which are transistorized with tunnel diodes.

The system permits the processing of graphs with line width not less than 0.12 mm. In the event of the simultaneous reading of several curves the distance between adjacent lines must be at least 0.08 mm.

The rate of data conversion is rather high, viz. 125 cps, which is entirely adequate for use in practice. The ordinate reading step is 0.3 mm. Provision is made for changing the step by means of reducer change gears.

The realization of the electronic portion of the device is characterized by a high coefficient of structural continuity: all counters and the control assembly use standard elements of the "Dnepr-1" multipurpose control computer.

The shapers of basic control signals (RMs, FPs, Y"0" [zero-setting]) use similar circuits, which assures standardization within the given design. For communication with the computer a block is used, consisting of bit-by-bit shaper amplifiers and a marker-pulse shaper.

The device is powered by a single-phase a-c network with voltage of 220 v. Power requirement is not more than 200 va.

PHOTOELECTRIC SYSTEM FOR THE CONVERSION OF GRAPHIC INFORMATION INTO AN ELECTRIC SIGNAL BY MEANS OF A MIRROR GALVANOMETER

Metody i Ustroystva Preobrazovaniya Graficheskoy Informatsii (Methods and Devices for the Conversion of Graphic Data), 1968, pages 140-149

B. Ye. Smolyanskiy, G. V. Voyshvillo, A. M. Romanov and N. G. Vasil'yev

General Comments

At the present time extensive use is made of the recording of various processes on photographic paper (photographic film) or other carrier of graphic information. The equipment for process recording is represented by both general-purpose instruments (MPO-2, N-700, K-9-21, K-12-21) and special-purpose instruments. Analysis of the resultant recordings often requires the reconversion of the graphic realization into electric signals for input into certain automatic analyzers. However, converting equipment is practically unavailable. Series-produced converters in conjunction with an analog special-purpose computer -- of the EASP-s type, for example -- are very unstable in working with ordinary oscillograms if the latter do not have a high-contrast image of the curve or if extraneous spots, bands, scratches or other defects (noise) occur on the carrier. In addition, the EASP-s converter does not permit reading if several processes are recorded on the carrier.

The existing devices for the conversion of graphic recordings into electric voltage or current can be subdivided into two basic types: 1) following systems and 2) reading systems.

The first type includes, for example, a system with a following carriage, which possesses rather high noise immunity to extraneous signs on the carrier, but is inertial, because of which it does not provide a high rate of curve reproduction. The high inertia of the instrument is due to the use of a special carriage as the following element, which executes a linear-translational movement equal in value to the current deflection of the recording line.

The second type includes converters used in series machines of the EASP-s type, as well as instruments developed at Kiev Polytechnic Institute. The receivers used here are camera tubes (vidicons etc.) with single-line scanning or a scanning light spot obtained from an oscillographic tube or a projection kinescope with single-line scanning. Scanning is performed over the full width of the recording carrier. Such systems are comparatively complex and less noiseproof than following systems. During reading the carrier

must not have several curves, extraneous signs, spots etc. In addition, since the scanning of a spot in such systems is performed over the entire width of the carrier over a white field, the shot-noise level of the receiver is significantly higher.

The present article considers a technique for constructing a system of graphic curve reproduction by the following method which is largely free of the above-described shortcomings and is rather simple to realize. The following element used here is a mirror galvanometer which executes oscillatory motions, light-spot scanning the carrier along the recording line with an amplitude somewhat exceeding its thickness. The signal used in the system is the brightness contrast of the reflected light spot. The graphic curve following is done with the aid of electromechanical feedback from the output of the electronic block to the galvanometer. The lock-on begins from the moment the beam intersects the recording line. If the curve being reproduced has no inclinations exceeding 70°, an automatic retrieval system is feasible, to be used to lock the curve being reproduced and eliminate following failures. The moment of a following and lock-on failure is recorded by the appropriate indicator at the electronic block output. The following regime, for example, can be determined from the presence of a second harmonic in the total signal from the output of the photoreceiver.

Block Diagram of the Converter (Figure 1)

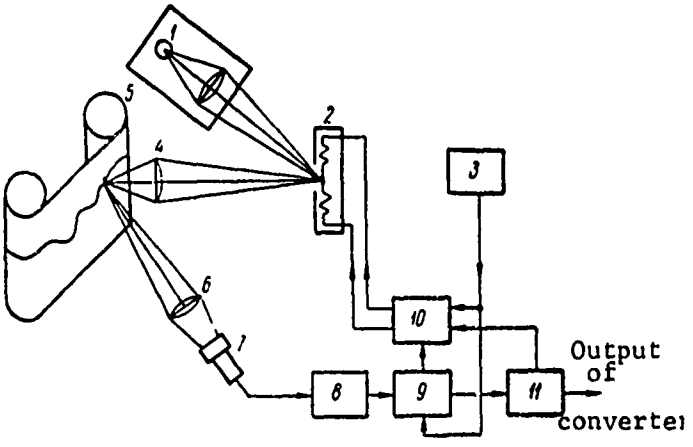

Figure 1. Block diagram of converter.

A shaped narrow light beam strikes the mirror of working galvanometer 2, which is excited by oscillator 3 through feedback amplifier 10. The amplitude of oscillation is selected from conditions that assure following with minimum reproduction error. Obviously, the greater the amplitude of oscillations of the galvanometer, the higher is the following stability (at a rationally selected depth of feedback), but the greater may be the reproduction error.

The light spot focused on the photographic paper executes oscillatory motions, intersecting the recording line. The reflected light modulation

occurring here creates a pulsating light signal. The latter goes to photomultiplier 7, to whose output is connected resonance amplifier 8, which is tuned to the oscillation frequency of the galvanometer, and then goes on to phase demodulator 9.

As the light spot moves across the recording line with a frequency f, a phase-modulated periodic signal appears at the photomultiplier output. The time dependence of this signal is determined by the shape of the spot and the phase is proportional to the shift between the equilibrium position of the galvonometer beam and the curve ordinate. The latter, in which the equilibrium position of the oscillating spot coincides with the center of the recording line, is the reference point.

To reduce the shot-noise level of the photomultiplier to an acceptable value, appropriate limiting of the amplifier pass-band is used. Switching voltage is fed to phase demodulator 9 from the same oscillator 3 which is used to excite the galvanometer.

A signal goes from the phase detector output through low-pass filter 11 to the feedback amplifier and galvanometer. The closed feedback loop assures curve following.

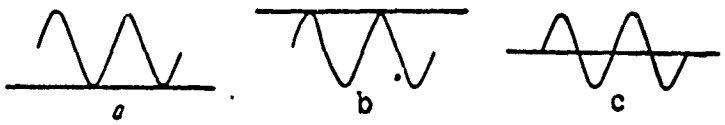

Figure 2. Following regimes:
a) and b) one intersection; c) two intersections.

During operation of the device the light spot can have three characteristic positions. In Figure 2, a and b the light spot intersects the recording once, creating signals with a beam oscillation frequency of F = f, dephased by 180°. In Figure 2, c the signal has a modulating frequency of F' = 2f, since the light spot intersects the recording line twice in the same time. In all other positions the signal contains the corresponding frequencies F = f and F' = 2f; the component with frequency F may vary in phase here by 180°.

If a recorded curve is situated symmetrically relative to the oscillating light spot, the signal frequency F' = 2f. As soon as the recording curve begins to deflect in some direction, error voltage appears as a result of the presence of a signal with frequency F = f at the input of photomultiplier 7. This signal is sent through the feedback loop to the galvanometer, deflecting the mirror in such a way that the peak-to-peak amplitude of its oscillations is symmetric with respect to the recording curve.

Optical Circuit (Figure 3)

The light flux from electrode-light lamp (elektrodosvetnaya lampa) of the DVT-6 type is collected by condenser 2 in the plane of diaphragm 3, which

assures definition of the boundaries of the light spot on the carrier by eliminating the halo from the bulb of the lamp, condenser etc. Diaphragm 3 is projected by lenses 4, 5, 7 and mirror 6 on the recording carrier. Lens 5 together with mirror 6 constitutes a single structural element of the optical system of the permanent-magnet galvanometer.

The angle between the axes of the light beams passing through lens 5 in mutually opposing directions does not exceed 9°. The emergent light beam, which diverges in the meridian plane, is focused on the photographic paper by lens 7. Situated in front of the photographic paper is semitransparent plate 8. In order to assure focusing of the beam within the width of the oscillogram (H = 120 mm), lens 7 is made cylindrical.

The light diffusely reflected from the photographic paper and mirror-reflected from semitransparent plate 8 is collected by lens 11 in different sectors of the lens of collective 13 depending on the location of the spot

AUTOMATIC CONVERTER OF CLOSED-CURVE GRAPHS INTO NUMERICAL CODE

Metody i Ustroystva Preobrazovaniya Graficheskoy Informatsii (Methods and Devices for the Conversion of Graphic Data), 1968, pages 150-153

D. I. Vigdorov and B. M. Sukholutskiy

Day-to-day monitoring of the operation of deep-pumping wells is accomplished by means of dynamometer cards, which represent a graph, plotted to scale, showing the stress on the polished rod as a function of the distance traveled. The analysis of dynamometer cards is performed on the field by an interpreter-engineer, and the quality of the analysis depends on his experience and skill. Therefore, the use of computer equipment to analyze dynamometer cards holds great promise. Electronic digital computers are widely used at present to process diverse graphic information.

One of the principal questions which determines the feasibility of digital-computer study of dynamometer cards is the development of a simple and reliable automatic device for the conversion of dynamometer-card graphs into digital code. The specificity of the device is due to the fact that the graph of a dynamometer card is a closed curve with a given zero line. Conversion has to be sequential along the contour of the graph in a clockwise direction (Figure 1).

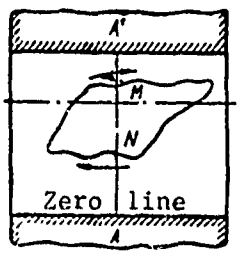

Figure 1. Arrangement of graph on drum.

We present below a description of an automatic converter developed at AzINEFTEKhIM [Azerbaydzhan Institute of Petroleum and Chemistry imeni M. Azizbekov].

The instrument is based on the scanning-conversion principle with the use of an electromechanical scanner. The latter is a drum with a transparent window to which tracing paper with a graph is attached in such a way that the zero line coincides with the window edge. A photodiode is firmly attached in the drum cavity, and on the outside is a light source with an optical focuser.

The drum, which is steadily rotated by a synchronous motor, simultaneously executes a translational motion along the shaft. When the lines of the graph and the borders of the window intersect the light flux, pulses which control the circuit operation appear at the photodiode output.

The instrument employs a principle which permits a significant simplification of both the electromechanical part and the logic circuit. The latter is so constructed that, regardless of the direction of drum rotation, the time interval between the two pulses corresponding to the border of the drum window and the first graph line intersected by the beam is fixed. Thus, if the drum rotates clockwise (moves from right to left), a time interval proportional to segment A'M (Figure 1) is fixed, while if it rotates counterclockwise (moves from left to right), an interval proportional to the segment AN is fixed.

The defined time intervals are filled with stable-oscillator pulses, the number of which (m and n respectively) is recorded by an eight-digit binary counter. However, the ordinate of point M actually equals the segment AA' — A'M, to which the number of pulses a-m should correspond (a is proportional to window width). If the oscillator frequency chosen is such that in the time interval corresponding to the distance between the window borders maximum counter filling occurs, i.e. the setting of ones in all its digits, then the number m will express the ordinate of point M in one's complement. The transition to true representation is accomplished in the circuit by switching outputs of the counter flip-flops by means of relay contacts of the drum motor reverse.

The above-described method possesses the following advantages:

1. The converter design is simplified since the direction of the translational motion is changed by simple reversal of the drum.

2. The selfsame logic circuit is used to convert both the upper and lower parts of a graph since there is no need to separate third pulses.

3. The instrument is calibrated against readings of the counter (the instrument proves to be calibrated if in the absence of a graph on the drum during a single reading ones are set in all positions).

A functional diagram of the converter is presented in Figure 2. Signals from the photodiode output are shaped by an asymmetrical flip-flop and sent to a differentiating circuit. A series of pulses is observed at the output of capacitor C_1 in each cycle, viz. a negative pulse corresponding to the beginning of the window, a positive pulse corresponding to the end of the window, and pairs of pulses -- positive and negative -- corresponding to the moment a beam intersects the graph line. Polar selection of pulses is performed by diodes Д 1, Д 2, Д 3.

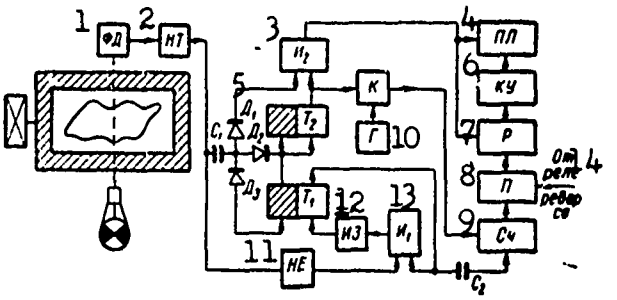

Figure 2. Functional diagram of converter.

Key: (1) Photodiode
(2) Asymmetrical flip-flop
(3) Inverter
(4) Perforator
(5) Diode
(6) Code amplifiers
(7) Distributor
(8) Switch
(9) Counter
(10) Oscillator
(11) NOT
(12) Integrating unit
(13) Inverter
(14) From relay [illegible] erse

The principal logic elements of the circuits are flip-flops T_1 and T_2. In the initial position at the right one output of T_1 is zero potential, and at the one output of T_2 negative potential. Key K is closed in this case, and the input of the eight-digit binary counter does not receive pulses from the filling oscillator. After sending the first negative pulse flip-flop T_1 goes over into the one position and flips flip-flop T_2 into the zero state.

Key K is opened, and filling of the counter begins, which goes on until the input of flip-flop T_2 receives the first positive pulse through diode $И_2$. The flip-flop is reset, and filling of the counter halts. Thus, the number on the counter is proportional to the distance between the beginning of the window and the first line of the graph. Upon the arrival of the next positive pulse through the diode, which results from intersection of the second graph line or window edge by a beam, the perforator circuit is triggered, since the other input of the coincidence circuit is sent potential from the output of flip-flop T_2. The circuit of $И_2$ is necessary to prevent the triggering of the perforator in case there are no graph line intersections by a beam.

The perforator control circuit consists of a noncontact switch, which switches the output of the counter flip-flops according to the direction of rotation of the drum and the distributor, which converts parallel binary code of the counter to series-parallel code and sends the corresponding pulses to code amplifiers of the perforator. Special pulses are formed in this same circuit for punching on the tape the number tags and recording tags necessary for the group input of data into a digital computer. The operator cycle of the perforator ends in one revolution of the drum.

The NOT circuit is designed to reset flip-flop T_1 after the entire window is traversed by a beam. The integrating unit prevents the triggering of a flip-flop by short noise pulses. Before the start of each new cycle the counter is set in the zero position by a pulse from flip-flop T_2 through capacitor C_2.

Let us give a brief characterization of the instrument.

Conversion rate	3 conversions/sec
Work field	85 x 70 mm
Error	1.5 percent
Voltage supply	220 v ($\pm$ 15 percent)
Power requirement	111 w
Dimensions	450 x 370 x 220
Weight	15 kg

THE INPUT OF GRAPHS INTO A "URAL-2" DIGITAL COMPUTER

Metody i Ustroystva Preobrazovaniya Graficheskoy Informatsii (Methods and Devices for the Conversion of Graphic Data), 1968, pages 154-156

L. M. Ganich and V. V. Krasovskiy

The solution of many problems, particularly problems in harmonic analysis, requires the input of graphs into the store of a digital computer.

The device proposed by the authors is designed for the input of ordinates of graphs of single-valued functions into the working storage of a "Ural-2" computer, with the input possible directly from a blank without preliminary processing of the graphs. Used as the reader is the scanning mechanism and photo-optic system of the "Rekord" facsimile apparatus (FA).

Operating Principle of the Device

The graph is placed on the drum of the FA, which reciprocates relative to the immobile photooptic system. Pulses received from the reference line and graph line control the program which effects the input of ordinates into the computer memory.

The value of an ordinate is determined by the time interval which elapses between these pulses.

The principal elements of the device are: a sensor -- the FA optomechanical system with photomultiplier FEU-20 and preamplifier stage; circuits which determine the switching on or off of the sensor; pulse-amplification and -shaping circuits; a counter for separating pulses of the reference line from pulses of the graph line; univibrators; circuits for entering instructions "22a" in the instruction register IR and circuits for blocking the entry of other information in the IR.

A block diagram of the device is given in Figure 1. Pulses received from FA go to block Y_1, consisting of the shaper and univibrator. The pulse width is regulated by means of the univibrator; this makes possible the entry of curves with an inclination angle of up to 85-87° for individual sectors. The shaped pulses after Y_1 go to the counter, which consists of flip-flops T_1 and T_2. Flip-flop T_2 is reset according to the leading edge of the first pulse from Y_1, and T_1 is set in the one position according to the trailing edge. The pulses from the flip-flop are inverted, triggering the univibrators Un, which limit pulse duration to a quantity commensurable with the

machine cycle value. A pulse of Un_1 according to machine clock pulse P15 permits entry of instruction "22a" in the IR through valve K_3 and at the same time through valve K_4 blocks the entry of any other instructions in the IR during the entry of instruction "22a."

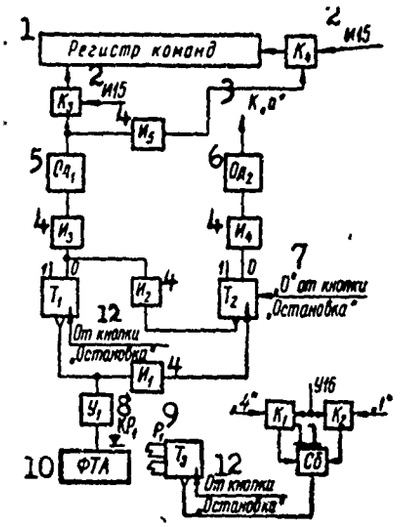

Figure 1. Circuit of graph input device.

Key:
(1) Instruction register
(2) P15
(3) To "a"
(4) Inverter I_1, I_2 etc.
(5) Un_1
(6) Un_2
(7) "0" from "Stop" button
(8) Switching relay
(9) Relay
(10) Facsimile apparatus FA
(11) Reset
(12) From "Stop" button

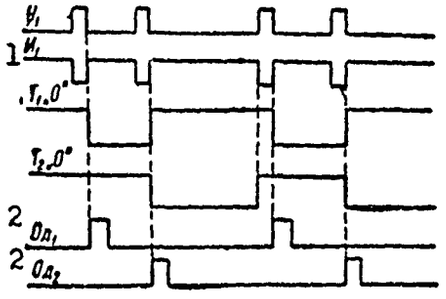

Figure 2. Time diagrams.

Key: (1) Inverter I_1 (2) Un_1, Un_2

At the unconditional-transfer-of-control instruction "22a" control is transferred to cell "a," beginning with which the machine memory contains the ordinate input program.

The program sums codes until the moment a pulse is received from Un_2 from the graph line. At the pulse from Un_2 a signal is generated, and a conditional-transfer-of-control instruction transfers control for ordinate entry in the memory. On receipt of the next ordinate values address modification occurs and they are entered in a consecutive series of memory cells. The reading step and the number of read ordinates is preset by the program. The scale of an ordinate is determined by the summation code value.

Several graphs can be entered simultaneously. For this purpose the graphs are arranged on the drum parallel to one another. The circuit is cleared from the "Stop" button on the machine panel. The device is switched on or off at the instruction PSM-40 (signal Y16); the "on" tag is "1" and the "off" tag "4." The on-off switching is controlled by flip-flop T_3 with anode resistors replaced by built-in RSM-type relays, one of which P_1 switches the phase-electromagnet circuit of the FA (KP_1).

Figure 2 presents time diagram of the device and Figure 3 a specimen of an inputted curve.

Figure 3. Specimen of curve entered in "Ural-2" memory.

Let us give the technical data of the device.

Drum rotation rate — 2 rps
Placement capacity — minimum ordinate step 0.2 mm
Size of blank — 220 x 150 mm, useful field 200 x 150 mm
A program takes 32 memory cells.
Maximum ordinate value — 18 binary digits of adder
The device uses standard "Ural-2" cells (number of cells: 20).

FOLLOWING A GRAPH OF ARBITRARY SHAPE

Metody i Ustroystva Preobrazovaniya Graficheskoy Informatsii (Methods and Devices for the Conversion of Graphic Data), 1968, pages 157-163

Yu. A. Zaborovskiy

Amid the great stream of graphic information being recorded on diagram tapes and photographic film, a special place belongs to records representing multivalued functions. Examples of such information are the recordings of two-coordinate recording potentiometers, which record on a rectangular diagram the graphs of functional dependences of two quantities converted into electric voltages, the recording of vectorcardiographs, for example in medicine in the study of cardiac activity and diagnosis.

The last few years have witnessed considerably increased interest in two-dimensional followers in connection with the possibility of employing contour following for electronic metal analysis and in homing guidance and orientation systems.

Let us formulate the requirements to be met by devices for the conversion of graphs of multivalued dependences. Reading devices must provide the following: 1) the conversion of initial graphic images without preliminary preparation for reading (we have in mind the thickening of lines, the transfer of data to another type of carrier, blackening part of a graph, the making of profiling masks; 2) the processing of graphs represented as closed and open functions; 3) the maximum speed of graphic data processing with the possibility of representing the coordinates of contour points in digital form with minimum error.

Analysis of the known reading algorithms has shown that the most important factor influencing the structure of the device and determining its block diagram is the mode of segregating the error voltage. Therefore, devices which effect the following of a multivalued function represented as a line and a blackened drawing can be subdivided.

1. Converters with the spectral method of obtaining error voltage, based on segregating the harmonic components of a train of notch pulses and comparing their phases with reference voltages.

These devices are characterized by such deficiencies as reduced speed of response and the impossibility of reading graphs represented as open dependences.

2. Converters with the aperture method of segregating error voltage, based on the light flux recorded by a photosensitive cell being dependent on the area of light spot shading.

A device based on this method permits the reading of simple closed figures whose contour represents a single-valued dependence relative to a circular time axis. Such a limitation narrows the range of solvable problems; therefore, this method is not universal and cannot be used to read multivalued graphs.

3. Converters with the analog method of segregating error voltage, based on storage of the instantaneous values of local scanning voltages at the moments a reading beam intersects a contour line, possess a higher speed of response than devices of the first group. Of the converters based on the analog method, special note should be taken of the Loève following algorithm, which is best suited for the reading of multivalued functions. However, in the Loève device during the following of a graph line a beam, in addition to the basic movement along the contour, executes local movements in a direction opposite to the direction of the circuit, which prevents optimum use of time for the local scan of the next regular point of the graph and leads to a lower speed of response. Therefore, investigations aimed at improving existing devices have naturally been directed towards perfecting the Loève following algorithm, which is the most effective for graph processing. The speed of graphic data processing will increase significantly if a device is designed in which there is no return motion of the reading beam and optimum use is made of the local scanning time.

The posed problem is satisfied by a device for the reading of multivalued dependences in which, during the following of a contour curve, the spot moved along the arcs of circles which are conjugated at moments of graph line intersection. The circuit path of a sector of the graph being read is presented in Figure 1,a, from which it can be seen that after each intersection the beam executes a subsequent move only in the direction of the circuit, i.e. the local scan of the next regular graph point coincides with the advance of the spot along the contour line. Two-dimensional graphs of arbitrary shape can be followed by means of the described circuit path, since for two adjacent local paths there always exists a common tangency point at the moment the light spot is intersected by the curve of a graphic dependence. Two operations must be performed to move the beam along the path indicated in Figure 1,a. First, at the moment of intersection the X- and Y-plates must be sent voltages out of phase by 180° with respect to the initial scanning voltages, i.e. $\sin(\omega t - 180°)$ and $\cos(\omega t - 180°)$.

As can be seen from Figure 1,b, with commutation of the scanning voltages the beam goes instantaneously from point a along the diameter of the circular path to point b. Unless in the process the coordinates of the center of the scanning arc change, the arc sequences are superimposed on each other.

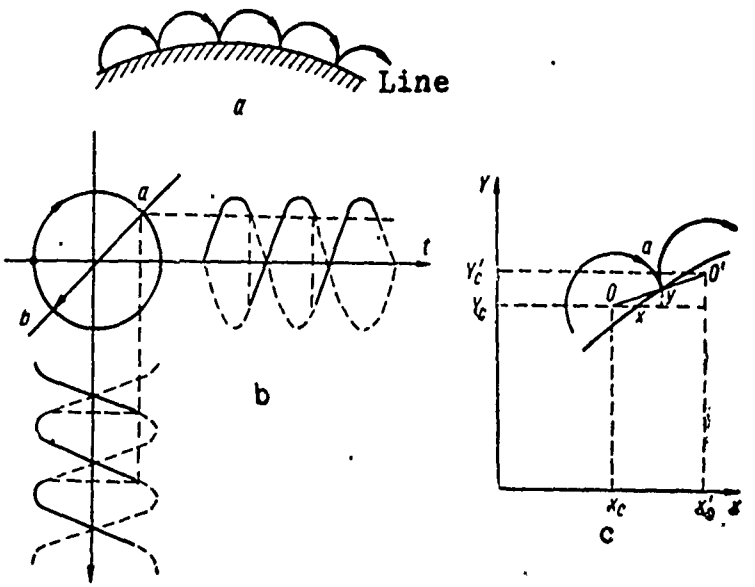

Figure 1. Path of spot and shape of scanning voltages in device with commutation of scanning voltages.

Second, to assure a uniform circuit of the image curve simultaneously with commutation of the scanning voltage phase, the center of the scanning arc must be shifted to set-forward point 0 according to the curve slope. The quantity of the displacement of the scanning arc center is determined from the condition of smooth conjugation of circular paths (Figure 1,c) and is expressed by the formulas

$$\begin{aligned} X' &= X_c + 2x; \\ Y' &= Y_c + 2y. \end{aligned} \tag{1}$$

Here X_c, Y_c are the initial coordinates of the center of the scanning arc; x, y are coordinates of the point of intersection of the scanning arc with the curve of the image, measured with respect to its center.

The coordinates of the contour points, also generated in channels X and Y in accordance with the expressions

$$\begin{aligned} X_a &= X_c + x, \\ Y_a &= Y_c + y. \end{aligned} \tag{2}$$

go to the output of the device in the form of analog voltage or digital code. As a graph converter with commutation of scanning voltages reads curves with monotonically increasing or monotonically decreasing curvature (spiral of Archimedes), the end of the advance vector leaves the graph line, and in the n-th scanning cycle there develops the risk of a following failure due to error accumulation in determining the coordinates of the points of the set-forward center. It should be noted that error in the determination of the set-forward center does not increase the error in finding the coordinates of

the points of the set-forward center. It should be noted that error in the determination of the set-forward center does not increase the error in finding the coordinates of the contour points, since only the values of the increments x and y depend on the choice of origin, while the absolute values of the coordinates calculated according to expression (2) remain unchanged.

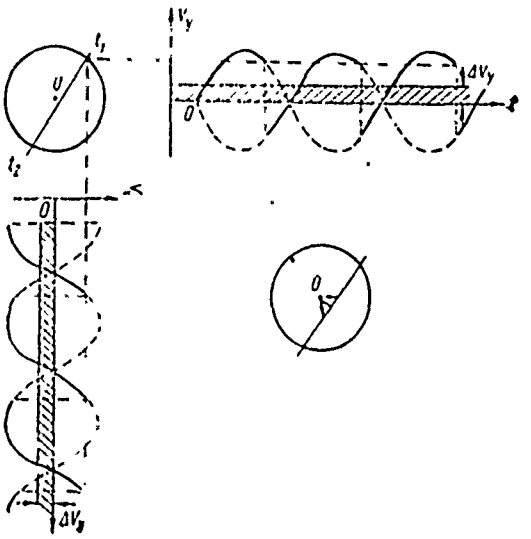

Figure 2. Centering of scan during following.

The effect of error accumulation can be eliminated by means of a scan centering block, which works to isolate the first harmonic component of the notch pulse train. However, it was found possible to use the direct components of the scanning voltages being commutated for this purpose. The commutated voltages are sent from the phase commutator output through a transmission RC network with specially selected parameters to the X- and Y-plates of the tube. The principle of centering for some position on a sector of the curve of the graph being read is illustrated by voltage diagrams (Figure 2). The illustration isolates the direct components ΔV_x and ΔV_y, which appear at the output of the phase commutators. Alternating scanning voltage is superimposed on a certain constant plate level, which determines the position of the center of the scanning arc on the CRT screen. The direct components ΔV_x and ΔV_y are lost as a result of the presence of a coupling capacitor, which causes the appearance of an additional vector for the displacement of the center of the scanning arc towards the contour line and eliminates the error accumulation effect. There is a four-fold increase in the processing speed in a graph converter with scanning voltage commutation as compared to a Loéve device, since in a circular scanning half-cycle the beam travels the quantity 2r (r being the radius of the circular scan). Technically a device with scanning voltage commutation is realized according to the functional diagram given in Figure 3. The converter includes: a photooptical device PD (all blocks are designated by broken lines), a synchronization block SB, a beam scanning block BSB, two beam control blocks BCB_x and BCB_y in channels

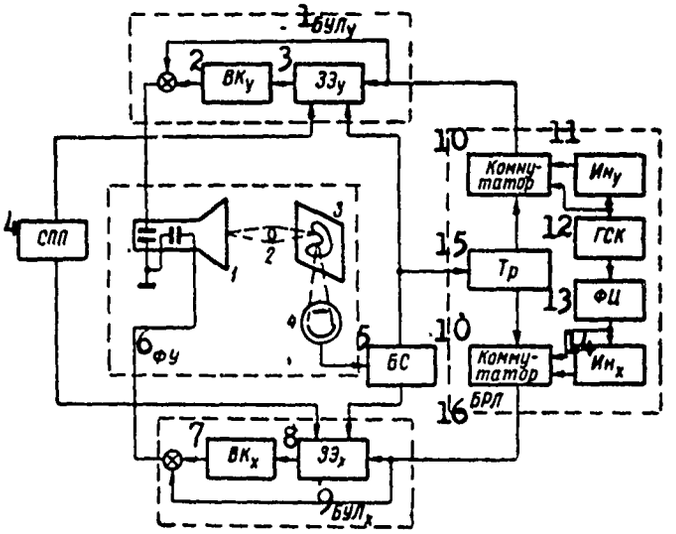

Figure 3. Block diagram of device with commutation of scanning voltages.

Key
(1) Beam control block BCB_y
(2) Output stage OS_y
(3) Storage element SE_y
(4) Initial scanning system ISS
(5) Synchronization block SB
(6) Photooptical device PD
(7) Output stage OS_x
(8) Storage element SE_x
(9) Beam control block BCB_x
(10) Commutator
(11) Inverter In_y
(12) Sinusoidal oscillator SO
(13) Phase-shift circuit PC
(14) Inverter In_x
(15) Control flip-flop
(16) Beam scanning block BSB

X and Y respectively, an initial scanning system ISS. The PD consists of a cathode-ray tube 1, which is used as a point light counter to scan a carrier with a graph, and an unusual inertialess actuating element in the following portion of the device. Optical system 2 is used to project the screen image on the surface of the carrier with graph 3, and photomultiplier 4 is used to record the moments of intersection of light spot with contour line. The SB by means of special processing converts the notch pulses taken from the photomultiplier into pulses of a strictly defined amplitude and duration, to be used to synchronize the operation of the entire device. Local scanning is formed by the BSB, which includes: a sinusoidal oscillator SO and phase-shift circuit PC, from whose outputs the voltages $U_m \sin \omega t$ and $U_m \cos \omega t$ are used to move a beam around a circle. At the same time these same voltages are fed to inverters In_x and In_y, from whose outputs are taken voltages out of phase by 180°. Harmonic signals $U_m \sin \omega t$ and $U_m \sin (\omega t - 180°)$ in channel X, as well as $U_m \cos \omega t$ and $U_m \cos (\omega t - 180°)$ in channel Y go to the inputs of the phase commutators, which are controlled by control flip-flop TP, which operates under scaling conditions and is triggered by each incoming notch pulse. The commutated scanning voltages are sent to two identical beam control blocks BCB_x and BCB_y, which include zero-order storage elements SE_x and SE_y, which are controlled by the SB and store the instantaneous values of the local scanning voltages which come from the beam scanning block.

The potentials fixed in the reservoir capacitors of the storage circuits and determining the position of the center of the scanning arc are sent to the inputs of output stages OS_x and OS_y.

ELECTRONIC PLANIMETRY WITH CIRCUIT ALONG THE CONTOUR

Metody i Ustroystva Preobrazovaniya Graficheskoy Informatsii (Methods and Devices for the Conversion of Graphic Data), 1968, pages 164-169

V. G. Polyakov

The operation of moving around a figure along the contour has long been used for manual planimetry although in principle it is not obligatory. Such a simple instrument as a curvometer enables the area to be measured if the entire part of the plane occupied by the figure is drawn sequentially (line by line). But the loss of time in doing this is so great that a considerably more complex planimeter with a movable pin for tracing the contour is preferred.

An analogous situation arises with the transition to electronic image scanning. In element-by-element (for example, line) scanning of the entire area of a figure the computing part of the planimeter will obviously be extremely simple. Automatic tracing of the contour at the very same forward speed of the beam reduces the measuring time, but only one store (integrator) will no longer do in this case for calculating the area.

An attempt to find a simpler, technically convenient scheme of analog planimetry led to the result described infra [1].

The most popular system of following scanning with phase detection of video signal in feedback channel also proves the most suitable. The figure presents the block diagram of a device using a pulse-position variant of scanning with beam rotation. No special changes are required in the scanning circuit (it fills the top part of the drawing). A circular-sweep oscillator generates voltages which rotate the reading beam of the photoelectronic converter round a circle of small radius with the frequency ω . The position of the center of the circle in the field of vision is determined by integrators, whose output voltages x and y are added by means of summing amplifiers to the circular-sweep voltages. The shaping video amplifier, at whose input the white level gives way to a black level with the frequency ω (the circle intersects the contour), marks as a short "advance" pulse at the output that moment when the beam x goes from black to white, but not vice versa (we shall assume that the beam rotates counter-clockwise). The advance pulse opens the keys for a moment, and the circular-sweep voltages are found to be applied to the input of the integrators for this short time interval. As a result the output potentials of the integrators receive increments, which abruptly shift the circular-scan center towards the point of beam transition from black contour to white field.

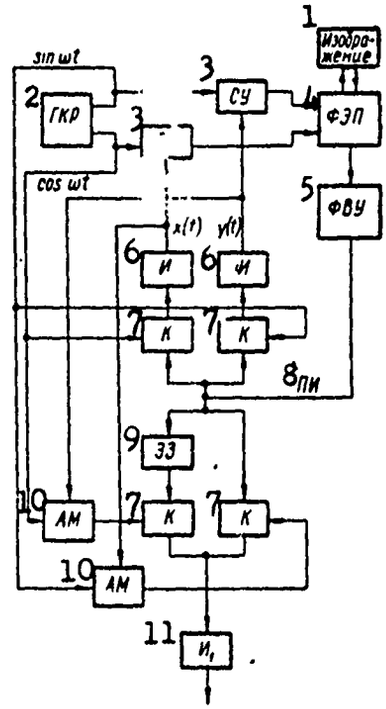

Block diagram of the device

Key: (1) Image
(2) Circular-sweep oscillator
(3) Summing amplifier
(4) Photoelectronic converter
(5) Shaping video amplifier
(6) Integrator
(7) Key
(8) Advance pulse
(9) Delay element
(10) Amplitude modulator
(11) Final integrator

The phase angle of each advance pulse, measured with respect to the cosinusoidal circular-scan component, is identical to the angle of inclination of the corresponding scanning step to the horizontal axis of tube deflection. The keys in conjunction with the sinusoidal and cosinusoidal reference voltages form a square-law pulse-position detector, which we shall designate "internal."

The central element of the computing part of the planimeter is the "external" phase detector, whose input is connected in parallel with the input of the internal detector. However, some changes are made in the "external" detector. The key of the "horizontal" branch of the detector, i.e. the one which receives the cosinusoidal reference voltage, is opened only after the half-cycle of the driving voltage following the moment of the appearance of the advance pulse (consequently, following the opening of the "vertical" branch key). This means that the system of coordinates proper of the "external" detector represents a mirror image (about the vertical axis) of the coordinate system of the "internal" detector. During following separately along each axis of the coordinate system of the "external" detector the

linear scale changes; along the vertical axis the scale depends on the current horizontal coordinate of the contour, and along the horizontal axis on the vertical coordinate. The scale is controlled by means of two amplitude modulators AM, in the first of which the cosinusoidal reference voltage of the "external" detector is modulated by the potential y(t) of the integrator for vertical deflection of the follow scan. In the second the sinusoidal reference voltage is modulated by the potential x(t) of the horizontal deflection integrator. Voltage proportional to the area of the figure being read is generated by the end of a complete circuit by its scan at the output of the single storage, which receives increments alternately via both keys.

Now let us consider the operation of the circuit in greater detail. Each scanning step, if it is sufficiently small, gives the current trajectory coordinates (as well as the potentials of the follow-scan integrators) small increments, but in the time interval which elapsed between the two steps the reference voltages go through the entire period of their variation. Consequently, in our case, as usually happens with AMs, the carrier frequency is considerably greater than the modulating frequencies. Let us assume that the sensitivity (the relation between the shift of the beam on the tube screen and the increment in the integrator potential causing this shift, henceforth designated as q) of both follow-scan deflection systems is the same. Then the parameters of the amplitude modulators should also be the same. The entire possible range of potential variation of the scanning integrators (from $-U_0$ to U_0 along any axis of coordinates), corresponding to the limiting peak-to-peak amplitude of beam deflection on the tube screen, should be placed in the linear sector of the modulation characteristic of the modulators.

Using the generally accepted formula for the recording of AM oscillations and considering the carrier amplitude to be unit, we shall have to represent the reference voltages received by the external detector as

$$\left[1 + m\frac{x(t)}{U_0}\right]\sin\omega t,$$

$$\left[1 + m\frac{y(t)}{U_0}\right]\cos\omega t,$$

where m is the depth of modulation and a constant. Assume that at the i-th step from the beginning of tracing, at moment of time t(i) at the detector input the next regular advance pulse appears, the scanning beam comes at the point of the contour with coordinates $\tilde{x}_i$, $\tilde{y}_i$ and the potentials of the scanning integrators take the values x_i, y_i, respectively. The advance pulse immediately unlocks for a short time the key of the external detector which is left in the circuit, and the final integrator N_1 receives a voltage increment $(\Delta U_i)_1$ proportional to the instantaneous value of the sinusoidal reference voltage at moment t_i

$$(\Delta U_i)_1 \quad \Delta S\left(1 + m\frac{x_i}{U_0}\right)\sin\omega t_i = \Delta S\left(1 + m\frac{x_i}{U_0}\right)\sin\alpha_i.$$

But before a new, (i + 1)-th advance pulse is received from the scan (and this will happen at least after three-fourths of the driving voltage), the potential of the final integrator will receive a second increment $(\Delta U_i)_2$; the right gate of the circuit will be opened with a delay for the time interval π/ω with respect to the left gate (the delay element is designated in the circuit as $\exists 3$).

Thus

$$(\Delta U_i)_2 = \Delta S\left(1 + m\frac{y_i}{U_0}\right)\cos\omega\left(t + \frac{\pi}{\omega}\right) = -\Delta S\left(1 + m\frac{y_i}{U_0}\right)\cos\alpha_i.$$

Thus, the total increment in the potential of the final integrator at the i-th step

$$\Delta U_i = (\Delta U_i)_1 + (\Delta U_i)_2 = \Delta S\left[\left(1 + m\frac{x_i}{U_0}\right)\sin\alpha_i - \left(1 + m\frac{y_i}{U_0}\right)\cos\alpha_i\right],$$

and by the moment of completion of a complete circuit of the contour the total accumulation of potential will be

$$U = \sum_i \Delta U_i = \sum_i \left[\left(1 + m\frac{x_i}{U_0}\right)\sin\alpha_i - \left(1 + m\frac{y_i}{U_0}\right)\cos\alpha_i\right]\Delta S =$$

$$= \sum_i \left[\left(1 + m\frac{x_i}{U_0}\right)\Delta y_i - \left(1 + m\frac{y_i}{U_0}\right)\Delta x_i\right].$$

Assuming that the scanning step is small, let us express the result in the form of a line integral (let us designate the contour being traced by the letter C)

$$U \approx \oint_C \left(1 + m\frac{x}{U_0}\right)dy - \left(1 + m\frac{y}{U_0}\right)dx.$$

Let us now partition this integral into two parts

$$\therefore U = \oint_C dy - dx + \frac{m}{U_0}\oint_C xdy - ydx.$$

of which the first quite obviously is identically equal to zero. As for the second addend, it is distinguished only by the proportionality factor from the integral

$$\oint_C \tilde{x}d\tilde{y} - \tilde{y}d\tilde{x},$$

which, as is known, gives the doubled area S_c, bounded by the contour C.

Thus,

$$U = 2\frac{mq}{U_0}S_c.$$

Let us note that too small a depth of modulation makes the planimeter crude. The fact is that the potential accumulated at the output of the final integrator, as we have seen, is expressed by the sum of the two addends, of which the first vanishes identically, while the second is less, all other things being equal, the smaller the depth of modulation. But in a real device

the first addend never proves exactly equal to zero; leakage of the integrators, imperfections in the keys and amplifiers, drift of the phase angles of the reference voltages and other causes disturb the ideal course of calculations. However, the deeper the modulation, the less is the relative weight of the remainder of the first addend obtained by the end of the circuit and the more precise is the planimeter. The appearance of the first addend is not inevitable; it can be eliminated by replacing ordinary amplitude modulators with balanced modulators, at whose output there is no carrier frequency. To be sure, the advisability of such a replacement is questionable, since precisely functioning balanced modulators prove exceedingly complex.

The procedure which has been considered should be regarded as a particular case of planimetry in the broad sense of the word: the selfsame circuit is suitable for calculating moments not only of zero order, but also of higher orders. Usually the central two-dimensional moment of n order of the part of the plane D, bounded by closed contour C, is represented as an integral with respect to the entire area of the figure, i.e. as

$$M_n' = \iint_D (x^n + y^n)\,dxdy.$$

However, this double integral can be converted to a line integral by means of Green's formula

$$M_n' = \frac{1}{n+1} \oint_C x^{n+1}\,dy - y^{n+1}dx.$$

It now becomes obvious that the circuit presented in the figure can be used with equal success to calculate the central moment of any order n if analogs of the functions x^{n+1} and y^{n+1} are used as the pair of modulating voltages. In this case devices for raising the voltage to the power n + 1 must be included between the scan integrators and amplitude modulators. But if a separate integrator is connected to the output of each branch of the external detector, the pair of axial moments of the same order n will prove to be calculated.

It is significant that in scanning the entire area of a plane figure element by element and calculating the moment of n order directly as a double integral, it is necessary to raise the voltage level of the scan integrators to the n-th rather than the (n + 1)-th power. The alternative, as can be seen, is still the same, viz. either planimetry with a circuit along the contour, or the longer (but involving a certain simplification of the calculations) way of element-by-element scanning of the entire surface of the figure.

BIBLIOGRAPHY

1. Polyakov, V. G., "Author's Certificate 189,228," Byulleten' Izobreteniy (Bulletin of Inventions), 1966, 23.

THE READING OF ARBITRARY CONTOUR IMAGES WITH THE AID OF FOLLOW SCANNING

Metody i Ustroystva Preobrazovaniya Graficheskoy Informatsii (Methods and Devices for the Conversion of Graphic Data), 1968, pages 170-173

G. G. Vaynshteyn

By contour images we mean double-gradation images composed of lines whose thickness is as small as possible for the given resolution of a reading device. As is known [3, 4], a good, adequate way to read such images is follow scanning -- scanning along the contour, which makes it possible to receive a signal close to the minimum in volume during reading, thereby reducing the frequency band of the communication channel or the storage capacity.

However, the operation of following alone is insufficient to process arbitrary contour images, whose contours can form an extremely complex maze of lines. The reader in this case should also store sectors of the contour already covered and look for new ones. One of the known ways to solve this problem is based on image erasure during reading [2]. Prerecording of the image on the target of a storage camera tube can be used for this purpose [5, 6]. Another way of reading is to use the working storage of a digital computer.

Methods involving storage apparently are the only ones possible when an image is read once. In some cases continuous real-time reading is required, for example when a contour image changes and these changes need to be recorded. An analogous situation is also created when the contour image must be reproduced on the screen of an ordinary cathode-ray tube for visual observation.

In real-time operation it is possible, for example, periodically to record an image on the camera-tube target and then read it by means of follow scanning with simultaneous erasure. In this case all points of the image are transmitted many times in one way or another, and storage of the image on the target merely assures the exact periodicity of the frames. The foregoing of periodicity considerably simplifies the reading procedure since no image storage at all is required.

Such a procedure may be based on the reading of an image by individual fragments taken randomly from different parts of a frame. The size of the fragments and their choice must satisfy the following requirements: 1) all

points of a contour image must be read on the average with the same frequency; 2) for each point of the contour the spread of time intervals between successive moments of the incidence of the reading beam must be as small as possible. The latter is due to the fact that the foregoing of exact periodicity means a partial loss of the benefit obtained as a result of the use of statistical peculiarities of contour images.

Thus, in scanning fragments of the image the scanning point moves over the field of the frame according to random law. The scanning process should possess certain statistical characteristics to fulfill the above-cited requirements. At a constant speed of motion the direction of the motion, as well as the coordinates of the scanning point should be distributed uniformly. After intersection the point moves along the contour; a contour fragment of standard length is read in this case. The mean frequency of scanning-point incidence on some element of the contour per unit of time (mean equivalent frequency of frames) is determined by the expression

where A and B are dimensions of a frame; V the scanning velocity; L the total length of all contours; l the length of a fragment.

This kind of procedure was checked experimentally with the aid of a "flying-spot" reader. The scanning process represented movement of the scanning point over the frame field with mirror reflection from its borders (Figure 1). Such a variant sufficiently satisfies the scanning process requirements and at the same time permits the construction of a simple scanning control circuit. In addition, continuous coordinate signals convenient for transfer or storage in analog form may be received [1]. However, such a scanning variant is not the only one possible nor the best. Good results can be obtained by using a pseudorandom dot pattern for the scan.

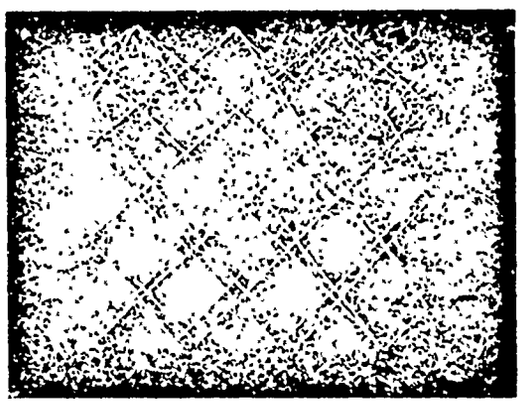

Figure 1. Process of scanning on screen of monitor tube

According to the foregoing, after striking the contour the follow scan begins to function, the beam moves along the border between black and white and reading of the fragment occurs. The length of the latter is determined

by the size of the fine image details and can be selected experimentally. The images being read were observed on the screen of a monitor long-persistence tube. Photographs taken of the screen are depicted in Figure 2 (the original image is also given for comparison).

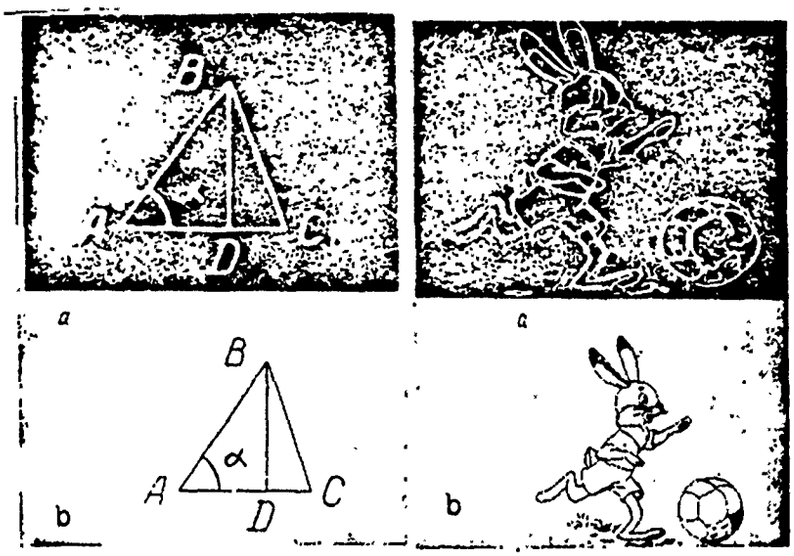

Figure 2. Sample of read image: a) read image; b) original.

Figure 3. Image which was not prepared for reading: a) read image; b) original.

The results of the experiment show that the use of random scanning offers certain advantages, viz. the system proves resistant to isolated scanning malfunctions and the resultant control circuit is rather simple. This kind of stability makes it possible to read rather complex images which have not been prepared ahead of time (Figure 3).

In principle it is also possible to contour half-tone images. The inadequacy of random scanning manifests itself in the flicker of the image points when observed on the CRT screen, as well as in reduced accuracy when restoring a moving image from random readings.

BIBLIOGRAPHY

1. Vasil'yev, V. K., and Vaynshteyn, G. G., Izvestiya Vuzov (Radiotekhnika) (Bulletin of Higher Educational Institutions (Radio Engineering)), 1966, 5.

2. Garmash, V. A., Vlasov, V. N., and Kirillov, N. Ye., Authors' Certificate No. 122,764, Byulleten' Izobreteniy (Bulletin of Inventions), 1958.

3. Kharkevich, A. A., Elektrosvyaz' (Electrocommunication), 1958, 5.

4. Foy, W., IEEE Trans. on Inform. Theory, 1964, IT-10, 2.

5. Sezaki, N., and Katagiri, H., Proc. of the IEEE, 1965, 5.

6. Sezaki, N., Katagiri, H., and Kaneko, T., Proc. of the IEEE, 1965, 53, 10.

THE USE OF PHOTOPOTENTIOMETERS FOR THE READING OF GRAPHIC INFORMATION

Metody i Ustroystva Preobrazovaniya Graficheskoy Informatsii (Methods and Devices for the Conversion of Graphic Data), 1968, pages 174-180

V. M. Kvasov and S. V. Svechnikov

The principle of the conversion of graphic information into electric voltage by means of slide-wire potentiometers has long been known although actual converters with operation based on this principle have limited use. The trouble is that in such converters, as a rule, the potentiometer slider has to be mechanically moved along the line of the graph that is being converted.

However, potentiometric graph converters are characterized by an important advantage over other converters in that the mechanical movement of the slider along the graph line is at once converted into analog electric voltage which has a common law of time variation with the graph being read.

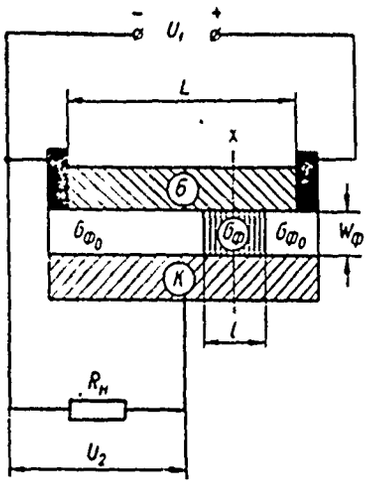

Figure 1. Design and operating principle of photopotentiometer.

New possibilities for the conversion of graphic information into electric voltage are opened up by photopotentiometers, whose operating principle and design are shown in Figure 1 [1]. A photoconductive layer with a width of W_ϕ is applied between resistive layer σ and collector K. The layer

has a conductivity of σ_ϕ in the region of the light probe with a width of l and σ_{ϕ_0} in the shunting regions thereof, with multiplicity of the ratio $\frac{\sigma_\phi}{\sigma_{\phi_0}} = \gamma \gg 1$. As a result, the lines of the current passing into load R_H contract into a narrow region limited to the probe width l. Therefore, during movement of the light probe along the length L of the photolayer the magnitude of the output voltage U_2 depends on the coordinate of the center of the light probe x.

The above-described property of photopotentiometers can be used to create a graph converter in which the functions of an instrument sensitive to variations in the graph line ordinate are performed by a photopotentiometer. The technique of graph conversion by means of photopotentiometers has the qualitative advantage that elements of a graph are projected directly on the photopotentiometer by optical means. This obviates the necessity for mechanically connecting the potentiometer slider with the line of the graph being read, as happens in known potentiometric graph converters.

The photopotentiometric technique of graphic data conversion possesses many other advantages as a result of the following factors: a long service life due to the absence of wiping contacts, high sensitivity to variations in the ordinate of the graph being read, a high conversion speed, simplicity of design and potting, the absence of resonant frequencies and hysteresis phenomena.

The operating principle of a photopotentiometric graph converter is shown in Figure 2. Here 1 is the light source, 2 an opaque image carrier with a transparent graph line 3, 4 the diaphragm and 5 the photopotentiometer. The realization of this principle necessitates either having an optical system protecting the graph image on the photopotentiometer, or arranging the photopotentiometer and image carrier in the immediate vicinity of each other.

During the movement of the image carrier along the axis x the variation in ordinate Y of the graph line element being isolated by diaphragm 4 is analogous to the variation in the coordinate of the center of light probe x (see Figure 1). Consequently, the magnitude of the output voltage U_2 is functionally related to the graphically given function. The character of this relation is determined by the operating regime of the photopotentiometer.

In order for ordinate Y of the graph line element being read to be linearly related to the output voltage U_2, the photopotentiometer must be used in a potential regime [2] in which the potential of the resistive layer is practically linear over the entire length of the photopotentiometer (Figure 3,a).

Work [2] shows that the most effective operating regime for a photopotentiometer is a forward regime where the probe region has a conductivity higher than the shunting regions. This regime is characterized by high transconductance S of output voltage U_2

$$S(y) = \frac{L}{U_1}\left|\frac{dU_2(y)}{dy}\right|, \quad (1)$$

and, consequently, by high values for the sensitivity and resolution of the photopotentiometer (Figure 3,b).

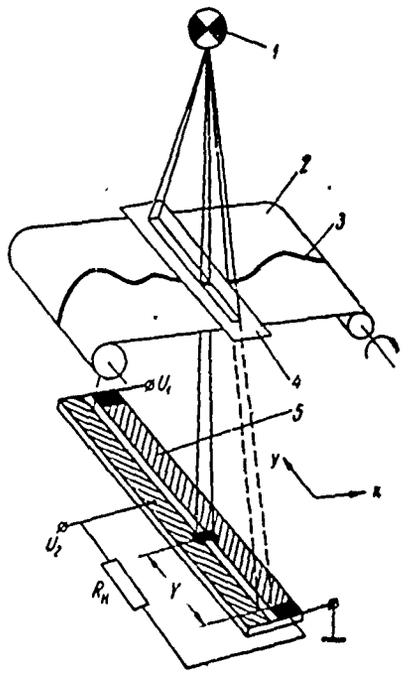

Figure 2. Operating principle of photopotentiometric converter.

A reverse-potential operating regime [2], in which, unlike the forward-potential regime, the output voltage U_2 drops with an increase in y (Figure 3,c), in principle can be used to read a graph line plotted against the bright background of the image carrier (paper, photographic film etc.). However, the reverse-photopotentiometer regime is characterized by a lower output transconductance than the forward regime $U_2 = F(Y)$, which makes the use of this regime for graph conversion unpromising.

The forward-potential photopotentiometer operating regime can also be used to read graphs from opaque image carriers if the graph line is plotted in colors which emit light at the moment of conversion.

This photopotentiometer operating regime is determined by two alternative inequalities [1]

$$\left|\frac{\frac{R_{\Phi_0}}{Y}}{R_н}\right| \gg R_0, \quad (2)$$

where $R\phi_0$ is the total leakage resistance through the photolayer, determined by conductivity σ_{Φ_0} and the geometric dimensions of the photolayer; R_0 is the total resistance of the resistive layer.

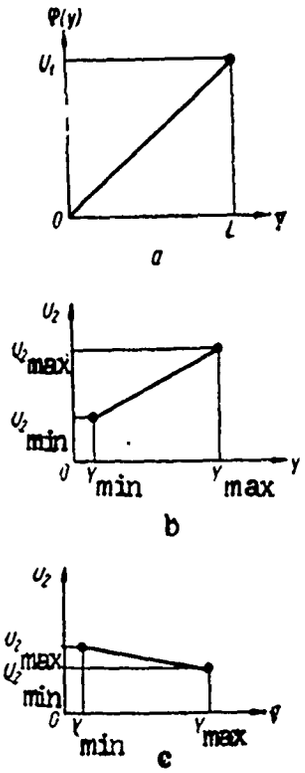

Figure 3. Choosing the photopotentiometer operating regime.

It follows from inequalities (2) that the potential regime can be achieved either by increasing the ratio $R\phi_o / \gamma$ or, as in the case of slide-wire potentiometers, by increasing the load resistance R_H. Then, as shown in [2], the output voltage linearly depends on the coordinate of the light probe (see Figure 2).

$$U_2 = U_1(A + BY). \qquad (3)$$

Parameters A and B, being functions of the quantities $\sigma\phi_o$, $\sigma\phi$, γ, l, L, $W\phi$ and R_H, can be calculated with the requisite accuracy [2] in order for the parameters of the photopotentiometer as a whole to correspond to its optimal characteristics under graph reading conditions.

It is especially necessary to dwell on the influence of the graph line slope angle θ (Figure 4) on the photopotentiometric conversion error. Let us assume the graph line within the limits of photolayer width $W\phi$ to be linear. This limitation is not very strict since real specimens of photopotentiometers have the quantity $W\phi < 1$ mm. With a change in slope angle θ the region of the light probe on the photolayer, by changing its outline from a rectangle to a parallelogram, as it were shifts up (given $\frac{\pi}{2} > \theta > 0$) or down (given $0 > \theta > -\frac{\pi}{2}$) from point 0, whose ordinate is taken to be the

true ordinate of the graph line element being read. It must be assumed that these changes and shifts in the light probe region will affect the output voltage U_2 given Y = const and in the final analysis the statistical conversion error.

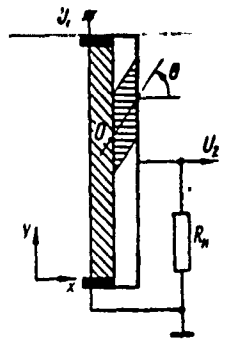

Figure 4. Influence of graph line slope angle on conversion error.

For this purpose an EGDA-9/60 integrator was used to construct models of the potential fields for various values of the quantity Y, $\beta = \frac{W\phi}{l}$ and θ with the electrode arrangement according to Figure 5,a and b. An analysis of these fields showed that the problem of determining the influence of slope angle θ on the field of currents in the photopotentiometer photolayer has no convenient analytic solution. This necessitates limiting oneself to qualitative or approximate estimates of the influence of slope angle θ on conversion accuracy.

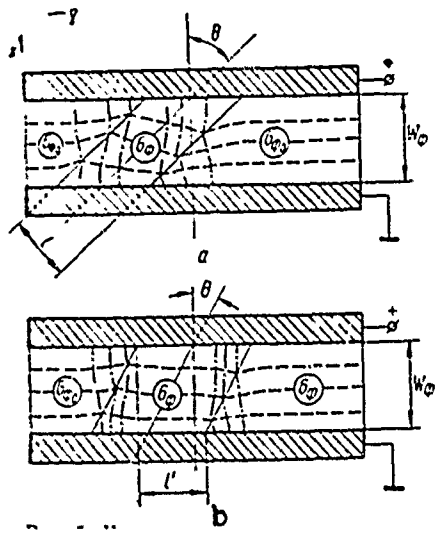

Figure 5. Configuration of field in photopotentiometer.

The photolayer resistance in the light probe region R_ϕ is connected in series with the load resistance R_H. Therefore, any changes in quantity R_ϕ will cause corresponding deviations of output voltage U_2 from the values which determine the true line graph ordinates.

If the light probe width $l < W_\phi$, i.e. $\beta < 1$, then with an increase in slope angle θ (Figure 5,a), beginning with certain angles

$$\theta_0 = \arcsin \beta, \tag{4}$$

there will be no regions on the photolayer which are struck by the light probe over the entire width W_ϕ along the x axis. Therefore, given large multiplicities of the photoconductivity ($\gamma \gg 1$) with an increase in the slope angle there will be an increase in the resistance R_ϕ and, consequently, a decrease in the output voltage U_2, which will cause negative conversion error.

In order to reduce the influence of fluctuations in the quantity R_ϕ on the output voltage U_2, the ratio R/R_ϕ must be increased either by increasing the resistance R_H or by decreasing the resistance R_ϕ. One of the ways of decreasing the resistance R_ϕ is to reduce the photolayer width W_ϕ.

To compensate for technological inhomogeneities of the quantities $\sigma_{\phi 0}$ and σ_ϕ over the length of the photopotentiometer L the light probe must be made as wide as possible.

In view of the foregoing, it may be asserted that fulfillment of the relation $\beta > 1$ will be more typical of photopotentiometric graph converters. Then for any slope angles there will be a region on the photolayer which is struck by the light probe over the entire width W_ϕ along the x axis (Figure 5,b). The width of this region l' is determined from the expression

$$l' = l \sec \theta - W_\phi \operatorname{tg} \theta. \tag{5}$$

Analyzing expression (5) for extremum, it is not difficult to establish that for slope angles θ equal to

$$\theta_m = \arcsin \frac{1}{\beta}, \tag{6}$$

the quantity is minimal and equals

$$l'_m = \frac{1}{\sqrt{\beta^2 - 1}} (l\beta - W_\phi). \tag{7}$$

The quantity l'_m will approach l with the growth of β.

For slope angles θ large in absolute value

$$\theta_k = \arccos \frac{\beta^2 - 1}{\beta^2 + 1}, \tag{8}$$

the quantity $l' > l$.

Analysis of the potential field models for $\beta > 1$ showed that even at $Y > 10$ the greater part of the current flowing through the probe region from resistor to collector is accounted for by the region l'. Therefore, for an approximate estimate of the influence of the slope angle θ on conversion error, the values of the output voltage U_2 as a function of θ can be determined from formula (3) by replacing the parameter l entering into this formula with the effective probe width l', obtained from expression (5). It must be borne in mind here that the range of slope angle θ variation depends on the Y ordinate. It is obvious from Figure 4 that the maximum slope angle

$$|\theta_m| \approx \arccos \frac{l}{2Y}. \tag{9}$$

Given $Y \to 0$ or $Y \to 1$ the range of slope angle θ variation will approach zero. Consequently, it is at the edges of the photopotentiometer, where variations in the quantity l' would cause especially significant deviations of the output voltage U_2 [2], that the slope angle θ because of its small value will have an insignificant effect on the conversion accuracy.

Given uniform movement of a graph with the speed v' along the x axis (see Figure 4), the graph line scans the photopotentiometer photolayer with the speed

$$v = v' \operatorname{tg} \theta. \tag{10}$$

The influence of the slope angle θ and velocity v' on the dynamic conversion error can be determined by using a photopotentiometer kinetic equation which reflects the dependence of the output voltage U_2 on the scanning velocity v.

Let us describe some of the possibilities of using photopotentiometric converters. By varying the graphically given functions, it is possible by means of the selfsame photopotentiometric converter to generate electric voltages of arbitrary shape. By cascading photopotentiometers which read two graphically given functions simultaneously, the operation of multiplication can be performed simultaneously with the conversion process. If the photopotentiometers are positioned at the requisite distance from each other along the axis of abscissas of the graph, there will be the simultaneous reading of its ordinates corresponding to different moments of time, which can be used for the direct determination of autocorrelation functions of graphically represented random processes. By positioning photopotentiometers along two graphically given random processes the simultaneous reading of ordinates can be used for the direct determination of cross-correlation functions of these random processes.

BIBLIOGRAPHY

1. Zyuganov, A. N., and Svechnikov, S. V., Radiotekhnika i Elektronika (Radio Engineering and Electronics), 1965, 7.

2. Zyuganov, A. N., and Svechnikov, S. V., Tezisy Dokladov Vsesoyuznogo Soveshchaniya po Poluprovodnikovym Soyedineniyam A^2B^6 i Ikh Primeneniyu -- Sbornik (Summaries of Papers Presented at the All-Union Conference on Semiconductor Connections A^2B^6 and Their Application -- Collection of Works), "Naukova Dumka," Kiev, 1966.

INTERROGATION OF PHOTORECEIVERS DESIGNED FOR CONVERSION OF GRAPHIC DATA

Metody i Ustroystva Preobrazovaniya Graficheskoy Informatsii (Methods and Devices for the Conversion of Graphic Data), 1968, pages 181-185

V. M. Kvasov, B. N. Malinovskiy and V. P. Skuridin

Often, for example in statistical investigations of random processes, input into digital computers requires graphic-data to digital-code converters which, having in all several quantization levels, are simple and reliable in operation within the limits of variation of the quantity under study. Worthy of attention in this connection are photoelectric graph to digital-code converters, whose graph line ordinates are determined by means of photoreceivers situated along the entire width of the image storer [2]. The graph line, depending on the kind of background against which it is plotted -- dark or light, illuminates or darkens the photoreceivers situated on a given ordinate being read, thus increasing or decreasing their conductivity. Variations in the conductivity of the photoreceivers act upon the corresponding electronic devices. Let us call the electronic devices intended for determining the ordinates of graph line elements to be read interrogators.

Regardless of the type of photoreceivers used or the block diagram of the interrogator, the latter must have one or more threshold elements sensitive to the pertinent variations in the conductivity of the photoreceivers.

The choice of a particular principle of interrogator design depends on many factors, among which the following play a special role: relative position of photoreceivers in a line (lineyka); required accuracy and conversion rate; complexity of the threshold element.

When a line of photoreceivers (Figure 1), situated at every one of N quantization levels with gaps d between the light-sensitive surfaces of adjacent photoreceivers which are greater than graph line width l, are used in a photoelectric graph converter, the interrogator must be constructed according to the block diagram presented in Figure 1. The line graph, as it moves along the X axis, acts at certain moments of time upon the photoreceivers, changing the states of threshold elements to the opposite states. The state characterized by the switching of one of N threshold elements is converted by code converter into binary code, which is stored in its output register. The principle of simultaneous interrogation of photoreceivers of the line provides the maximum speed of response since the conversion rate in final analysis is determined by the transition characteristics Φ [photoreceiver], threshold element and code converter. But the very fact that

$d > 1$ does not permit the use of such photoelectric converters to read immobile graphs. Moreover, in the use of structurally complex, highly sensitive threshold elements and a considerable number of quantization levels N the complexity of the photoelectric converter as a whole increases, and its operating characteristics, for example the adjustment speed of threshold elements, deteriorate.

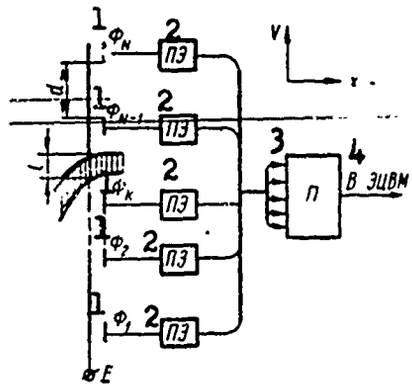

Figure 1. Arrangement of photoreceivers in a line.

Key: (1) Ф = photoreceiver
(2) threshold element
(3) Converter
(4) To electronic digital computer

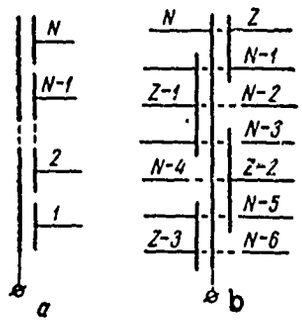

Figure 2. Line of photoreceivers with small gap between them

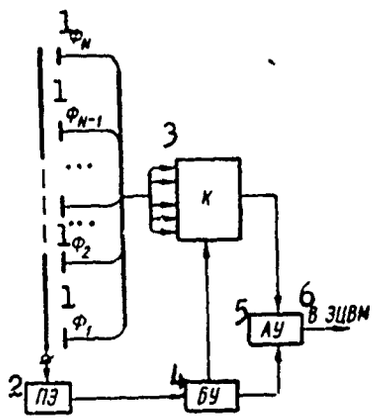

Figure 3. Block diagram of interrogator
Key: (1) Ф = photoreceiver
(2) threshold element
(3) commutator
(4) control block
(5) arithmetic unit
(6) to electronic digital computer

Work [1], using film photoresistors as an example, shows that, in order to eliminate illegibility of readout and to decrease the number of photoresistors in a line with accuracy of conversion remaining the same, it is preferable in photoelectric converters to use lines of photoresistors in which the gap between adjacent photoresistors is either quite small $d < l$ (cf. Figure 2,a and Figure 1) or absent altogether (Figure 2,b). Depending on the relation between level quantization step Δ_{level} and graph line width l, as well as on the slope angle of the graph line θ, the graph line can illuminate (darken) simultaneously two or more photoresistors out of total number Z. Therefore, in using lines with the arrangement of photoreceivers shown in Figure 2,a and b one must employ the appropriate interrogators which react requisitely to simultaneous illumination (darkening) of several adjacent photoreceivers.

Figure 3 shows the block diagram of the interrogator for the lines of photoreceivers depicted in Figure 2,a. Commutator K, consisting of a binary counter and decoder, sequentially interrogates the photoreceivers in accordance with signals from the control block. The threshold element, which signals the presence of an illuminated photoreceiver at the interrogated level, is connected to the common vertical busbar of the line of photoreceivers. After interrogation of the first illuminated (darkened) photoreceiver the threshold element issues a signal via the control block for the registration of the contents of the counter of commutator K into the adder of arithmetic unit AY. If the next photoreceiver is unilluminated (undarkened), interrogation comes to a halt, and the adder of the arithmetic unit will store the value of the illuminated (darkened) level $M_{initial}$ which is proportional to the ordinate of the graph element being read

$$Y = kM_{initial}.$$

If the next photoreceiver is illuminated, ordinates M of both illuminated photoreceivers are entered in the register of the arithmetic unit until an illuminated (undarkened) photoreceiver is interrogated. In this event, in accordance with commands from the control block the arithmetic unit AY adds the contents of the register containing the values of the final level M_{final} to the contents of the adder where the value of the initial level $M_{initial}$ is stored, and the result of the addition is shifted one position to the right, i.e. the expression

$$Y = k\left(\frac{M_{initial} + M_{final}}{2}\right)$$

is realized.

However, it is considerably more difficult to realize the above-described algorithm in the case of interrogation of lines whose photoreceivers are arranged with mutual overlap (Figure 2,b). The number of photoreceivers Z in such lines is less than the number of quantization levels N, which gives rise to certain difficulties in the determination of values $M_{initial}$ and M_{final}.

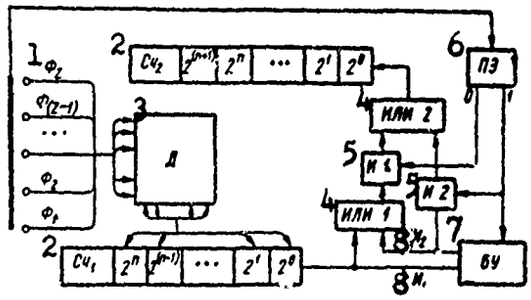

Figure 4. Reading of signals from photoreceivers.

Key: (1) Photoreceivers
(2) Counter
(3) Decoder
(4) OR 1, 2
(5) AND 1, 2
(6) Threshold element
(7) Control block
(8) Pulse P_1, P_2

Figure 4 shows the block diagram of an interrogator for lines of photoreceivers arranged according to Figure 2,b, for any number of photoreceivers illuminated (darkened) by the graph line. There are two counters: counter C_{41} for sequential interrogation of photoreceivers via decoder Д and counter C_{42} for recording interrogated levels. The initial position of these counters is zero in all positions. The first photoreceiver Φ_1 is interrogated. The control block generates odd pulses P_1 and even pulses P_2. P_1 go to the input of counter C_{41} for sequential interrogation of the photoreceivers. Until an illuminated (darkened) photoreceiver is interrogated, the threshold element is in the "0" state, and pulses P_1 and P_2 arrive at the input of counter C_{42} via assembly OR 1, AND 1 gate and assembly OR 2. Interrogation of an illuminated (darkened) photoreceiver and, consequently, the one state of the threshold element generates an inhibit for one of the inputs of the AND 1 gate and permits passage of pulses P_2 to the input of counter C_{42} via the AND 2 gate and assembly OR 2. As soon as the threshold element again returns to the zero state, the control block ceases the production of pulses P_1 and P_2 and issues a signal for a readout of the readings of counter C_{42} either directly into the digital computer or into the memory unit.

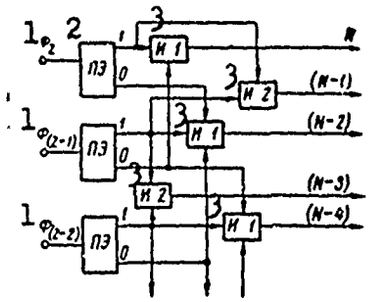

Figure 5. Block diagram of parallel-interrogation unit

Key: (1) Photoreceiver (2) Threshold element (3) AND 1, 2

The interrogation unit here described can also be used to interrogate lines with the arrangement of photoreceivers shown in Figure 2,a. In this event, considerable simplification of the interrogator is achieved in comparison with the device depicted in the block diagram in Figure 3.

Figure 5 presents the block diagram for the simultaneous interrogation of all photoreceivers of a line whose graph line can illuminate (darken) one or a maximum of two adjacent photoreceivers. The operating principle of such a device is clear from Figure 5. Let us note only that the codes obtained from the outputs of gates AND 1 and AND 2 require conversion into binary code, analogously to the block diagram depicted in Figure 1.

BIBLIOGRAPHY

1. Kvasov, V. M., Malinovskiy, B. N., and Skuridin, V. P., Tezisy Dokladov VIII Vsesoyuznoy Konferentsii po Avtomaticheskomu Kontrolyu i Metodam Elektricheskikh Izmereniy -- Sbornik (Summaries of Papers Presented at the Eighth All-Union Conference on Automatic Control and Methods of Electric Measurements -- Collection of Works), Publishing House of the Siberian Department, Academy of Sciences USSR, Novosibirsk, 1966.

2. Rozenberg, I. M., Obzor Inostrannykh Patentov -- Sbornik (Survey of Foreign Patents -- Collection of Works), Publishing House of Central Scientific Research Institute of Patent Information and Technical and Economic Research, Moscow, 1964.

SELECTING THE NUMBER AND QUANTITY OF READ CURVES IN THE PROCESSING OF MULTICHANNEL RECORDINGS

Metody i Ustroystva Preobrazovaniya Graficheskoy Informatsii (Methods and Devices for the Conversion of Graphic Data), 1968, pages 186-188

Yu. A. Rymakov and Ye. I. Skvortsova

The circuit here described is used in the "Grafik" (Graph) device, which is designed for the computer input of medicobiological test data represented in the form of recordings of a multichannel recorder.

The maximum number of channels is nine, of which any number of curves can be chosen for investigation. The recording of the graphs is accomplished on a paper carrier 210 mm wide in ink of a single (any) color. The metric grid of the carrier differs from the graph line in the shade of color. The graph lines do not intersect and have nc clearly pronounced location zones. The distance between converging lines does not exceed 1 mm, with a line width of 0.25 mm.

The "Grafik" is a scanning-type device with step movement of the raster element and carrier. Concurrent with the selection of the number and quantity of curves to be read, the circuit makes it possible to monitor the number of curves on the carrier so as to eliminate the influence of random contamination or fractures in the graph lines on the operation of the device.

When the reading beam intersects a graph line, a standard notch pulse controlling the operation of the device is generated in the photoelectric block. The functional diagram of the block for selecting the number and quantity of curves to be read, shown in the Figure, consists of a binary standing-on-ones carry counter employing four flip-flop and three amplifier stages of the "Dnepr" computer, two comparison circuits employing potential stages, by means of which the necessary logical operations are performed, and amplifier stages for shaping standard pulses.

Before the start of operation the switch "Quantity of Curves" is set to a position corresponding to the quantity of curves on the carrier, and of nine "Curve Number" toggle switches those whose numbers correspond to the curves chosen for study are switched on. For example, to study the first, fourth and eighth curves toggle switches 1, 4, 8 are put in the "On" position.

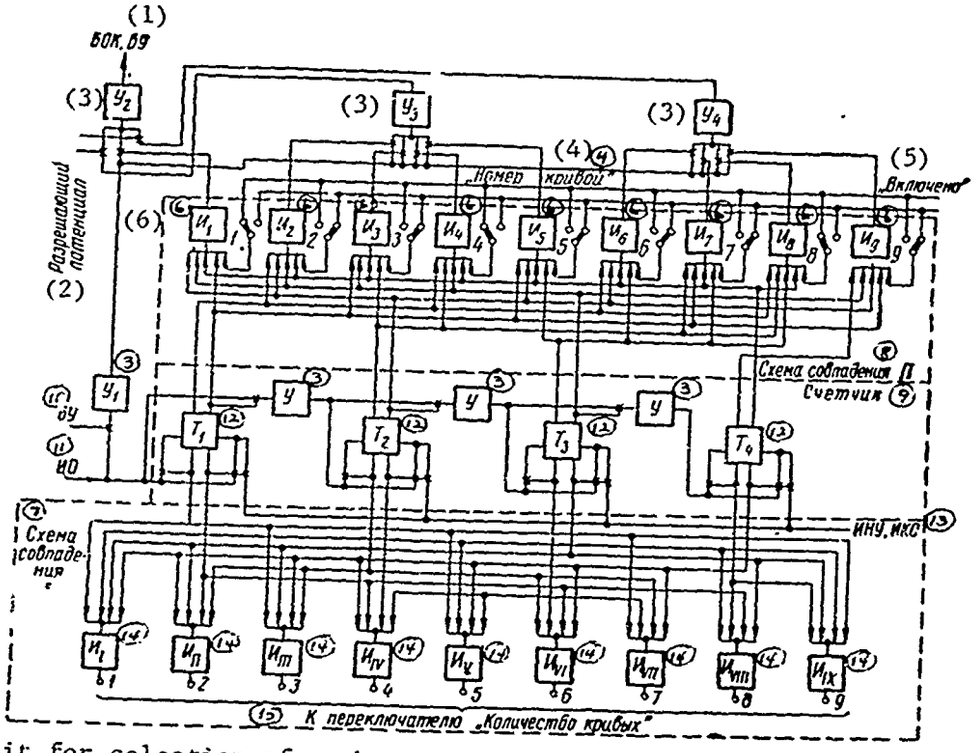

Symbolic circuit for selection of number and quantity of curves to be read.

Key:
(1) Coordinate determining block, control block
(2) Enabling potential
(3) Amplifier
(4) "Curve number"
(5) "on"
(6) Potential stage
(7) Coincidence circuit I
(8) Coincidence circuit II
(9) Counter
(10) Control block
(11) Notch pulse
(12) Flip-flop
(13) Initial set pulse, end-of-line pulse
(14) Potential stage
(15) To "Quantity of Curves" switch

If the instrument begins to operate with a forward motion, the notch pulses go only to the counter input and not to the control block or the coordinate determining block since there is no permission for notch pulses to go through amplifier Y_1. Permission comes after a check and agreement between the quantity of curves on the carrier and the position of the "Quantity of Curves" switch.

After the forward motion of the beam (line) ends, an end-of-line pulse resets the counter. The return motion of the beam begins. The quantity of arriving notch pulses is recorded in binary code in the counter. The outputs of the counter flip-flops are connected to the inputs of the potential stages ($И_I$ - $И_{II}$) of coincidence circuit I through potential gates. Coincidence at the input of the appropriate stage indicates that there has turned out to be the expected quantity of lines on the carrier. In this case enabling potential goes from the output of the potential stage through the "Quantity of Curves" switch to the control block. The step scanning motor continues to function, and the enabling potential generated in the control block is fed to the potential input of amplifier Y_1, and as the beam moves forward notch pulses go through amplifier Y_2 to the control block and coordinate determining block. The selection of curves and hence the selection of notch pulses from these curves is performed as follows. During the forward motion of the beam the notch pulses go to the counter input. The outputs of the counter flip-flops are connected to the inputs of the potential stages (Y_1-Y_9) of coincidence circuit II through the potential gates. Coincidence at the input of the appropriate potential stage can occur only by switching on the appropriate "Curve Number" toggle switch. Potential appears at the stage output, and this is fed as enabling potential to one of the inputs of amplifiers Y_2, Y_3, Y_4. The pulse inputs of the amplifiers are connected to the outputs of Y_1. Thus, the only notch pulses going through Y_2, Y_3, Y_4 are those for which enabling potentials have been sent from the outputs of the corresponding stages. The initial setting of all circuit elements is effected by a special set pulse.

PLACEMENT OF SINGLE-PULSE CODES IN DIGITAL COMPUTER MEMORY FOR PULSE DRIVE CONTROL

Metody i Ustroystva Preobrazovaniya Graficheskoy Informatsii (Methods and Devices for the Conversion of Graphic Data), 1968, pages 189-192

Yu. A. Romanenko, M. L. Shemyakin and D. I. Kunin

After preparing an array of coordinates for the beginning and end of rectilinear segments which constitute the path of a two-coordinate step-pulse (SPD), single-pulse instructions can be uniformly placed as follows with the aid of a digital computer. Let us find the necessary number of steps along the x and y axis (η^x and η^y respectively) needed to move the SPD from the beginning of a given rectilinear segment to the end. Subsequently instructions for the completion of these steps must be placed in such a way that when an instruction is put on magnetic tape, for example, signals for positive movement along the x axis are on the first code track, signals for negative movement along the x axis on the second code track, signals for positive and negative movement along the y axis on the third and fourth tracks respectively. To move the SPD in a positive direction along the x axis it is possible, for example, in one of the magnetic tape rows to place the code h^{+x} (Figure 1), in which the one (within the limits of this row) is placed only in the first position on the right. The codes h^{-x}, h^{+y} and h^{-y}, in which the one is placed in the second, third and fourth positions on the left respectively, will serve as signals for movement in the remaining directions (-x, +y, -y). Figure 2 shows possible signal combination variants which correspond to movements of the drive in different quadrants.

With allowance for the rate of magnetophone code recording ω and the rate of SPD operation Ω the magnitude of control signal rarefaction

$$\Delta A = E\left(\frac{\omega}{\Omega w}\right) + 1,^{*} \tag{1}$$

where ΔA is a whole number of cells, the multiple quantity of rows w necessary for placing the codes of a single cell.

The recording of all control signals of a given rectilinear segment requires the following quantity of cells:

$$M_q = \Delta A H\left|\eta_q^x \vee \eta_q^y\right|,^{**} \tag{2}$$

where q = 1, 2, ..., l is the number of the rectilinear segment.

---

*E(A) denotes the integral part A.

**$H\left|A \vee B\right|$ and $\overline{H}\left|A \vee B\right|$ are the greater and lesser values of the modulus of the two numbers $\left|A\right|$ and $\left|B\right|$.

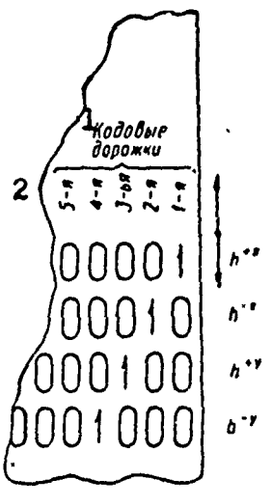

Figure 1. Possible variant of code placement on computer tape.

Key: (1) Code tracks
(2) 5th, 4th, 3rd, 2nd, 1st

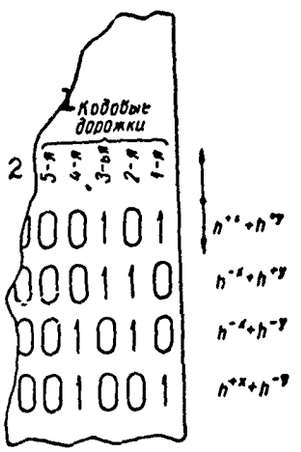

Figure 2. Possible combinations of signals.

Key: (1) Code tracks
(2) 5th, 4th, 3rd, 2nd, 1st

The numbers of the cells in which the quantity M_q of signals is recorded are determined from the expressions

$$N_q^l = N_{q-1} + l\Delta A; \quad l = 1, 2, \ldots, H\left|\eta_q^x \vee \eta_q^y\right|, \tag{3}$$

where N_{q-1} is the position of the last control signal of the $(q-1)$-th rectilinear segment.

If the lesser quantity of control signals for movements along one coordinate is a multiple of the greater number of their movements along another coordinate, the position of the control signals is determined from the expression

$$N_q^g = N_{q-1} + g\Delta A \frac{H\left|\eta_q^x \vee \eta_q^y\right|}{\bar{H}\left|\eta_q^x \vee \eta_q^y\right|}, \tag{4}$$

where $g = 1, 2, \ldots, \bar{H}\left|\eta_q^x \vee \eta_q^y\right|$.

If $H\left|\eta_q^x \vee \eta_q^y\right|$ is not a multiple of $\bar{H}\left|\eta_q^x \vee \eta_q^y\right|$ but the quantity of rows $M_q w$ necessary to record the volume of information determined from expression (2) is such a multiple, then control signals are sent to the following row numbers:

$$\varepsilon_q^g = N_{q-1}\ w + gE\left(\frac{M_q w}{\bar{H}\left|\eta_q^x \vee \eta_q^y\right|}\right) \text{given } 1, 2, \ldots, \ldots, \bar{H}\left|\eta_q^x \vee \eta_q^y\right|. \tag{5}$$

But if the opposite is true, then

$$\varepsilon_q^g = \begin{cases} N_{q-1}w + g\left[E\left(\frac{M_q w}{\bar{H}\,|\eta_q^x \vee \eta_q^y|}\right) + 1\right] \text{given} g = 1, 2, \ldots, \bar{l}; \\ N_{q-1}w + gE\left(\frac{M_q w}{\bar{H}\,|\eta_q^x \vee \eta_q^y|}\right) \text{given} g = \bar{l}, \bar{l}+1, \ldots, \bar{H}\,|\eta_q^x \vee \eta_q^y|, \end{cases} \tag{6}$$

where $\bar{l} = M_q w - E\left(\frac{M_q w}{\bar{H}\,|\eta_q^x \vee \eta_q^y|}\right)\bar{H}\,|\eta_q^x \vee \eta_q^y|.$

Using expression (5) or (6), one can easily find the corresponding cell number

$$N_q^g = \begin{cases} E\left(\frac{\varepsilon_q^k}{w}\right) + 1, & \text{if} \quad \varepsilon_q^g - E\left(\frac{\varepsilon_q^g}{w}\right) = \nu \neq 0; \\ E\left(\frac{\varepsilon_q^g}{w}\right), & \text{if} \quad \varepsilon_q^g - E\left(\frac{\varepsilon_q^g}{w}\right) = \nu = 0. \end{cases} \tag{7}$$

When instructions are placed according to the cell numbers found from expression (7), the control signal codes are shifted the following number of positions:

$$b = (\nu - 1)\left[1 + E\left(\frac{\theta}{w}\right)\right], \quad \nu = 1, 2, \ldots, w-1, \tag{8}$$

where θ is the number of bits per memory cell of the digital computer.

If $\nu = 0$, then

$$b = (w-1)\overline{\left[1 + E\left(\frac{\theta}{w}\right)\right]}. \tag{9}$$

Each time after the determination of N_q^f or N_q^g the numbers found are compared with the number determined from the formula

$$N = N_0 + S \tag{10}$$

where S is the storage space used to place the instructions and N_0 and N are the numbers of the initial and final cells used to place the instructions.

If $N < N_q^f$ and $N < N_q^g$, then there is no further placement of signals and all control signals are outputted, for example, to the magnetic tape or directly to the SPD.

MECHANISM WITH TWO-COORDINATE STEP-PULSE DRIVE

Metody i Ustroystva Preobrazovaniya Graficheskoy Informatsii (Methods and Devices for the Conversion of Graphic Data), 1968, pages 193-196

E. L. Yemel'yanov and K. P. Kashcheyev

For the final adjustment of systems for automatic and semiautomatic input of graphic data into a computer, as well as a system for automatic data output from a computer in graphic form, staff members of the Siberian Department of the Academy of Sciences USSR and the Siberian Scientific Research Institute of Geology, Geophysics and Mineral Raw Materials designed and made a mechanism with a two-coordinate step-pulse drive.

Principal Technical Data:

maximum width of information carrier	1000 mm;
type of step electric motors	ShD-4;
linear movement along each of the coordinate axes per control pulse	0.1 mm;
pickup of drive	800 cps;
dimensions of mechanism	
length	1430 mm;
width	530 mm;
height	635 mm

Principal Parts and Components of Mechanism (Figure):

left rack;	axle;
right rack;	eccentric clamp;
base;	step motor of carriage;
step motor of drum;	reducing gear of carriage;
reducing gear of drum;	pinion;
pinion of drum;	pulley;
driving drum;	belt;
claw clutch;	carriage;
clamping device;	tightener;
driven drum;	guides

Description of Design

All parts and components of the mechanism are mounted on two racks 1 and 2, secured to base 3. The left rack holds the reducing gears and motors

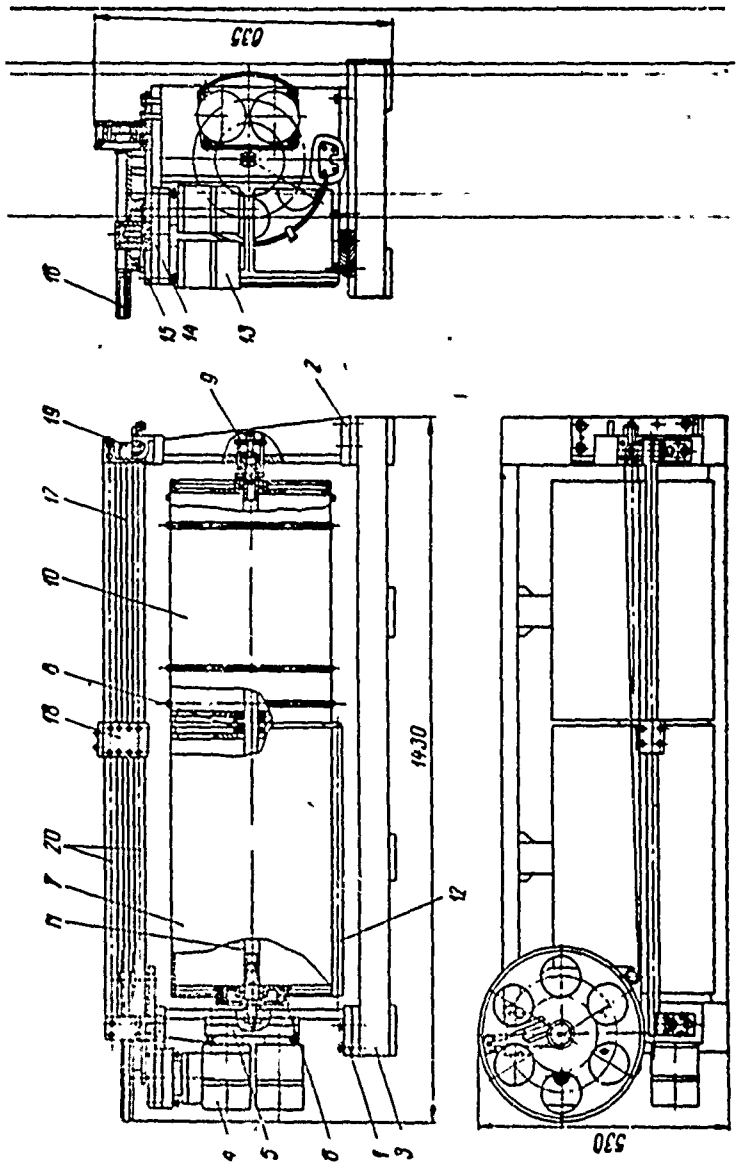

Mechanism with step-pulse drive

for driving the drums and carriage. The information carrier (card or paper tape) is secured to drum 7 by means of eccentric clamps 12. Moving parallel to the generating line of the drum on cylindrical guides 20 is carriage 18. The drum drive consists of step motor 4, which rotates pinion 6, attached to drum 7, through playless reducing gear 5. The overall gear ratio from the output shaft of ShD-4 to drum equals 40. Driven drum 10 can be connected up to driving drum by means of claw clutch 8 and clamping device 9.

Such a design permits the use of one drum if the information carrier has a width of up to 500 mm and two drums for a width of up to 1000 mm. The diameter of the drums is selected so as to secure an information carrier up to 1000 mm long to their surface.

The processing of long tape diagrams is done sequentially in sectors 1 meter long, with the replacement of the sectors being performed manually; however, the point at which processing of the preceding sector ends is retained, so that no additional adjustment is needed when changing a sector. Both drums rotate on ball bearings around axle 11, secured to racks 1 and 2. the carriage drive consists of step motor 13, which rotates pulley 16 through playless reducing gear 14 and pinion 15.

The rotation of the pulley is converted into the translatory motion of carriage 18 by means of a belt transmission. Smooth metallic belt 17 is rigidly fixed to the pulley by wedge clamps. The belt is stretched by tightener 19. The pulley diameter equals the diameter of the drums and, since linear movements per control pulse along both coordinates are the same, the designs of the reducing gears and driving pinions have been standardized. Carriage 18 moves over two cylindrical guides 20 on ball bearings. Part of the ball bearings are mounted on eccentric axles to take up slack and for carriage control.

Depending on the experiments being staged, the carriage has fastened to it a photoelectric indicator for the automatic graphic data input system or a sighting device for the semiautomatic graphic data input system or an automatic six-position recorder for the automatic data output system. Mobile terminal switches are provided along both coordinates to limit movements. The step motors are operated from series-produced control blocks BU-1-60.

The above-described mechanism is now in pilot operation to determine the magnitude of error in the final adjustment of movements for different frequency relations of control signals.

THE USE OF A FOLLOWING STROBE IN GRAPH CONVERTERS

Metody i Ustroystva Preobrazovaniya Graficheskoy Informatsii (Methods and Devices for the Conversion of Graphic Data), 1968, pages 197-203

V. G. Abakumov and V. V. Tatarinov

The noise immunity and operational reliability of automatic graph converters in many respects depend on the proper choice of a regime for the sensitive elements of the photoelectric assembly (photomultipliers, camera tube), the quality of the graphs to be converted and the method of processing output signals of the photoelectric assembly.

The question of the proper choice of a regime for the photoelectric assembly elements has been covered in sufficient detail in the literature; the gist of the recommendations that have been made is that it is necessary to assure a given (maximum) signal-to-noise ratio, whereby the number of errors per unit of time caused by signal and background fluctuations does not exceed a certain preset quantity. Graph converters are usually made so that if an output signal exceeds a certain threshold U_0, it is taken to mean the presence of a signal from the graph line. In accordance with this, background fluctuations can be reduced to converter malfunctions -- short-duration failures which occur when the established threshold is exceeded by noise with the highest amplitude. A consequence of signal fluctuations may be blanks (the signal proves to be less than the threshold) or repeated responses (Figure 1).

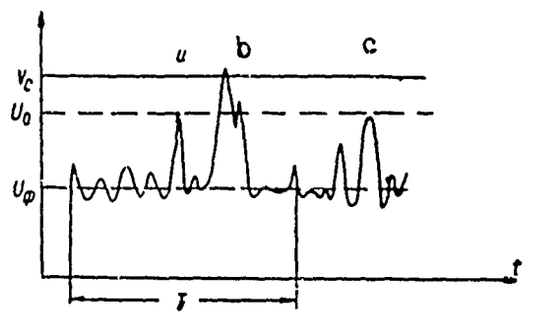

Figure 1. Signal of photoelectric assembly and character of errors:
a) short-duration failure;
b) repeated response;
c) blank

The significance of error of a particular type is determined by the circuit of the converter and its purpose. Thus, in multichannel converters a short-duration failure or repeated response can cause improper channel distribution of the graph ordinates, while in single-channel devices a repeated response is often unimportant.

If noise distribution is governed by the normal law, the mean trouble-free operating time T is determined from the formula

$$T = \frac{1}{N},$$

where N is the admissible number of errors per unit of time, equal to the sum total of errors due to background fluctuations N_b and signal fluctuations N_s.

The value of N proves to be related to the value of the threshold U_o [1]

$$N = \frac{\Delta f}{\sqrt{3}}\left(\frac{t_o - \tau}{T} e^{-\frac{1}{2}\psi_b^2} + \frac{\tau}{T} e^{-\frac{1}{2}\psi_s^2}\right), \quad (1)$$

where Δf is the width of the passband of the photoelectric assembly amplifiers, t_o is the observation interval, T the duration of the reading line, τ the signal duration, $\psi_b = \frac{U_o - U_b}{\sigma_b}$, σ_b is the effective value of the noise at the background level, $\psi_s = \frac{U_s - U_o}{\sigma_s}$, σ_s is the effective value of noise at the signal level.

In expression (1) the first addend characterizes errors due to background fluctuations, the second errors due to signal fluctuations. Naturally, the number of errors declines with an increase in the signal-to-noise ratio.

In addition, the number of errors can be reduced by cutting the observation interval down to τ. This requires using a strobe with the duration τ_{str}, the center of which is continuously or discretely made coincident with the position of the notch pulse from the graph line. In view of the fact that $\tau_{str} < t_o$, the number of short-duration failures $N_{str} < N$ and will be determined by the expression

$$N_{str} = \frac{\Delta f}{\sqrt{3}}\left(\frac{\tau_{str} - \tau}{T} e^{-\frac{1}{2}\psi_b^2} + \frac{\tau}{T} e^{-\frac{1}{2}\psi_s^2}\right). \quad (2)$$

The strobe is made coincident with the notch pulse by means of analog or digital equipment, depending on the manner of representing the output data of the converter. In particular, in converters with analog output the strobe is controlled by means of output analog voltage. Regardless of the method of strobe control, maximum reduction of the observation interval with time is fundamental. Sometimes the observation interval decreases with space. Only a small sector of the carrier in the vicinity of the graph line is considered here.

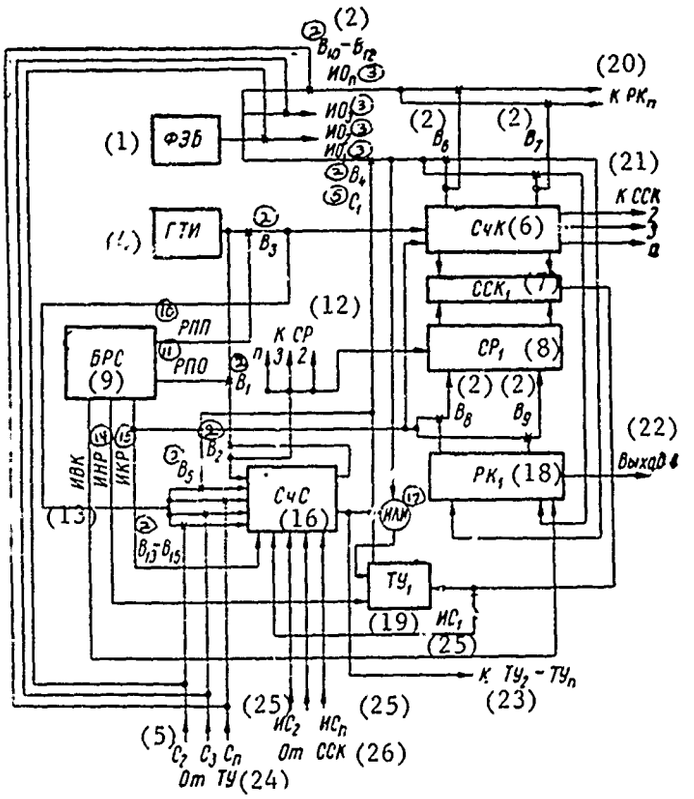

Figure 2. Block diagram of the device.

Key:
(1) Photoelectric block
(2) Gate
(3) Notch pulse NP_1, NP_2, etc.
(4) Timing generator TG
(5) Strobe signal S_1, S_2, etc.
(6) Coordinate counter CC
(7) Code comparison circuit CCC
(8) Register-counter R-C_1
(9) Scan and synchronization block SSB
(10) Forward-motion enabling potential FMEM
(11) Enabling potential signal EPS
(12) To register-counter R-C
(13) Code output pulse COP
(14) Start-of-scan pulse SOSP
(15) End-of-scan pulse EOSP
(16) Strobe counter SC
(17) OR
(18) Coordinate register CR_1
(19) Control flip-flop CFF_1
(20) To coordinate register CR_n
(21) To code comparison circuit CCC
(22) Output
(23) To control flip-flops CFF_2 - CFF_n
(24) From control flip-flop CFF
(25) Comparison pulse CP_1, CP_2, etc.
(26) From code comparison circuit CCC

The limit to which t_0 can be reduced without disturbing the operation of the device is set according to the character of the function being converted and the value of the discreteness step Δx along the axis of abscissas. In the choice of the value of Δx from the condition of approximation of the function being converted by a first-degree polynomial the spatial width of the strobe h will be determined by the expression

$$h = 2Y'_m \sqrt{\frac{8\varepsilon}{Y''_m}}, \tag{3}$$

where Y'_m and Y''_m are the maximum values of the first and second derivatives of the function to be converted and ε is the admissible error of approximation; the duration of the strobe pulse with uniform movement of the raster element will equal $\tau_{str} = \frac{h}{v}$, where v is the velocity of travel of the raster element (scanning element).

Here any possible variation in the function to be converted on the sector Δx proves to be within the limits of the strobe width; with a lesser strobe width a following failure is possible on sectors with a higher rate of change in the output function Y(x). Good results can be obtained with additional control of the strobe width according to the law of variation of the first derivative Y' (decrease in the number of errors) or regulation of the discreteness step Δx according to the law of variation of the second derivative (elimination of information redundancy).

In constructing a graph converter it is most important to control the position of the strobe according to the trend of the function to be converted and its width according to the law of variation of the first derivative (in case a strobe of variable width is used).

Let us consider below one of the possible variants of a multichannel graph converter with a following strobe whose width is chosen in accordance with what has been set forth above. Strobe control is effected by means of digital devices.

Figure 2 gives the block diagram of a single channel together with elements of the strobe control system. Assume that numbers which are determined by the value of the ordinates of the graphs being read are entered in coordinate registers CR (for example, in CR_1 the number m_1, corresponding to the ordinate Y_1). On completion of the scanning cycle the coordinate counter CC and strobe counter SC are set to "0" by means of the end-of-scan pulse EOSP, and the code corresponding to the Y_1 ordinate is transferred from the coordinate register CR_1 to register-counter $R\text{-}C_1$. There are analogous code transfers from registers CR_i to counters $R\text{-}C_i$. During the return motion of the scan, the scan and synchronization block SSB generates an enabling potential signal, designated in the diagram as EPS; the pulses of the timing generator TG go to the input of SC and $R\text{-}C_i$ through two gates B_1 and B_2, which are fed enabling potentials. The number of pulses going to the input of $R\text{-}C_i$ will be determined by the number m, given which gate B_2 will be sent an enabling potential. This number will also determine the width of the half-strobe in

the numerical range of variation of the input quantity M. The quantities m and H are interrelated by the relation

$$m = \frac{hM}{2Y_m} \qquad (4)$$

where M is the number corresponding to the maximum value of Y_m of the input quantity being converted.

Thus, during the return motion of the scan the inputs of the register-counters, or, to be more precise, the subtraction buses of these counters are fed m pulses, as a result of which by the beginning of the forward motion of a scan the number $m_i - m$, corresponding to the beginning of the strobe in the numerical range, will be entered in $R\text{-}C_i$.

During the forward motion of the scan a start-of-scan pulse SOSP is formed in the SSB, as well as a forward-motion enabling potential FMEM, which is sent to gate B_3. The SOSP resets the control flip-flops CFF_i in each channel (they should be in the initial state when the device works normally). At the same time scanning of the carrier with a light spot begins; a video signal is formed at the output of the photoelectric block PEB, and the CC makes a count of the clock pulses coming from the TG through B_3. The CC forms a code, which goes to the code comparison circuits CCC of each channel. The CCCs are used to compare the code in the R-C with the CC code. These codes are compared at certain moments of time (first in the first channel, then in the second channel etc.). During the first comparison a short comparison pulse CP_1 is formed at the CCC output; this pulse acts on control flip-flop CFF_1 and sets the counter SC at "0." CFF_1 is used to form strobe signal S_1 and to open gate B_4, which assures passage of notch pulse NP_1 from the PEB output for the entry of code from CC into CR_1, and gate B_5, through which TG pulses go to the zero digit place of the SC. B_4 and B_5 will be open until the SC sets the number m, which will correspond to 2m TG pulses, since they are sent to the zero digit place. If there is no carry from CC to CR_1 during the passage of 2m TG pulses which is possible if there is a recording gap and no NP_1, then control flip-flop CFF_1 will be reset by a pulse generated by SC when the number m is set in it. Gates B_4 and B_5 will be closed.

If, however, there is no recording blank, a new number will be entered in CR_1, and CFF_1 will be reset by notch pulse NP_1 and gates B_4 and B_5 will be closed. This will evidently be followed by the comparison of codes in CCC_2 and the formation of signal CP_2, the zero setting of SC, and by means of CFF_2 the formation of the signal S_2, which acts on gates B_{10} and B_{13}. In this case the zero digit place of SC will be sent clock pulses (via B_{13}) and gate B_{10} in the circuit for entering code from CC in CR_2 will be opened. After the arrival of notch pulse NP_2 or the reading of 2m pulses by the SC counter, control flip-flop CFF_2 will be reset. The cycle will subsequently be repeated until codes are entered in all the CR registers. It can easily be seen that the pulses generated by SC on the reading of the number 2m can change the state only of the flip-flop belonging to the channel in which the code comparison took place. The rest of the flip-flops are unaffected by this signal.

The output of codes from the registers CR_i is effected by a special pulse COP, generated by SSB. It should be noted that the code output can be organized differently according to the manner of representing the output data of the graph converter, the number of channels and the documenting device that is used. In considering the circuit operation, we assumed that originally codes were set in the CR which correspond to the ordinates of the graph lines in each channel. But when the device is turned on, zeros are set in all the counters and registers. The question of strobe control is solved if there are data on the graph ordinates. Therefore, it is advisable to introduce the two regimes "Tape Mounting" and "Operation" in the device. In the first regime the tape is mounted in the tape transport and initial data are entered in the coordinate registers CR. The input can be performed automatically with an immobile carrier during the mounting of the tape. In this case with the aid of the "Tape Mounting" switch a ring counter is formed of CFFs to distribute notch pulses over the channels according to the time principle (SC, CCC and R-C are switched off). The corresponding numbers are entered in CR. Automatic input of the initial data complicates the commutation of the device.

The initial setting of the CR can also be effected manually from the control panel of the device. This method was preferred by us, since usually a graph converter is supplied with a hand punching panel, by means of which different service combinations can be set up and entered on punched tape. In the instant device the input of the necessary data in the CR is effected from the hand punching panel in the "Tape Mounting" regime.

A converter employing the above-described circuit possesses considerable resistance to hand corrections and service marks not in the immediate vicinity of a graph line. In addition, when there are recording blanks, the output of the device receives a numerical expression of the preceding value of the read ordinate, which is stored in the register. Naturally, any improvement in the operating characteristics of the converter makes the device more complicated (register-counters, a strobe counter, a CCC are introduced). However, such a circuit lacks a channel commutator, whose role is performed by the CFF, CCC and SC.

The introduction of R-Cs is not indispensable and the functions of the R-Cs and CR can be combined, which simplifies the circuit somewhat. In conclusion, it should be noted that by making the circuit more complex it is possible to control not only the position, but also the width of the strobe according to the character of the functions to be converted. However, in so doing difficulties arise due to the fact that the character of the processes recorded over various channels is different and the strobe width required likewise differs. This necessitates adjusting the strobe width in each channel and makes the device considerably more complex.

BIBLIOGRAPHY

1. Krasil'nikov, N. N., Pomekhoustoychivost' Televizionnykh Ustroystv (Noise Immunity of Television Sets), State Scientific and Technical Power-Engineering Publishing House, Moscow, 1961.

METHODS AND DEVICES FOR AUTOMATIC RECOGNITION OF GRAPH LINE COLOR

Metody i Ustroystva Preobrazovaniya Graficheskoy Informatsii (Methods and Devices for the Conversion of Graphic Data), 1968, pages 204-210

V. A. Fesechko
V. F. Smeshko

The capabilities of devices for the automatic processing of graphic data can be significantly expanded if graph lines are executed with different colorants. The processing of such graphs does not require reproduction of the color of the lines. All that is necessary is to distribute the signals corresponding to the different colorants by channels. Therefore, the problem of automatic colored-line recognition is more simply solved than the colorimetric problem of color measurement.

The color recognizer must consist of a color-description analysis block and a decoding block. The former block, which includes light-sensitive cells, optical filters and mirrors, and spectrum analyzers, extracts signals which are proportional to the most informative attributes of chromatic radiation. Let us call these chromaticity signals. Their subsequent processing and color recognition are accomplished by means of the latter block, where on the basis of one of the recognition algorithms a determination is made whether a point of the color under investigation belongs to a certain decision domain embracing one or more points of a two-dimensional or multidimensional color space.

Recognition is effected according to the coincidence or proximity of points or vectors in the multidimensional space.

Depending on the method adopted, the distance and decision algorithm are determined by the expressions

$$\rho = \sqrt{\sum_{i=1}^{n} (a_i - b_i)^2} \leqslant \rho_j \cdot \max \qquad (1)$$

or

$$\rho = \sum_{i=1}^{n} |a_i - b_i|^2 \leqslant \rho_l \cdot \max, \tag{2}$$

where a_i, b_i are components of the points of the color under investigation and the standard color. The proximity of vectors is characterized by the magnitude of the angle between them and is determined by the expression

$$\varphi_{AB} = \arccos \frac{\overline{A}\overline{B}}{|\overline{A}||\overline{B}|} = \arccos \frac{\sum_{i=1}^{n} a_i b_i}{\sqrt{\sum_{i=1}^{n} a_i^2 \sum_{i=1}^{n} b_i^2}} \leqslant \varphi_l \cdot \max, \tag{3}$$

where $\overline{A}$ and $\overline{B}$ are respectively the vector of the color under investigation and the vector of the standard color.

The above-described method is called the correlation method.

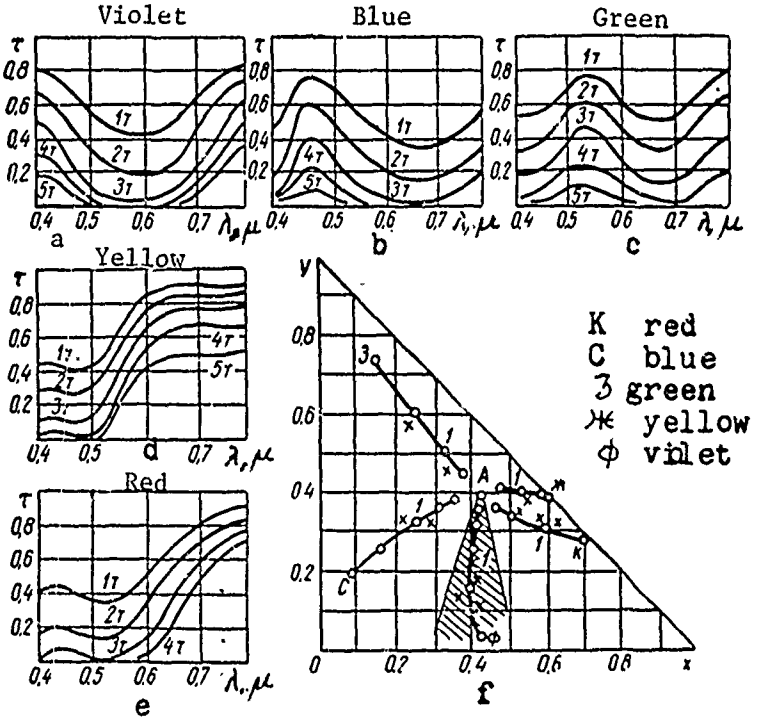

Fig. 1. Spectral reflection characteristics (a, b, c, d, e) and position of points of a color on CIE color plane (f).

In using expressions (1) and (2) the decision domain has the shape of a circle or square with maximum dimensions $2\varphi_{j\cdot max}$, and in using expression (3) it has the shape of a wedge-shaped zone with apex angle $2\varphi_{j\cdot max}$.

Let us dwell on the character of the shift of the point of a graph line color on the color plane in relation to the structure of colorant coating, its thickness and density. In the event of variation in the density and thickness of colorant application, i.e., in the event of so-called subtractive mixing of two colored media, the result can be determined by means of Beer and Bouguer's well-known law in colorimetry. Figure 1, a-e, shows spectral reflection characteristics for different colorants used to record graphs, which are taken at different density values. Figure 1, f, depicts calculated and experimental points on a color plane. The points of one graph line color are located within a wedge-shaped zone (except for lines with great colorant density). That is why the correlation method is more convenient for recognizing the color of a graph line.

The color-recognition problem can be simplified somewhat (Fig. 2).

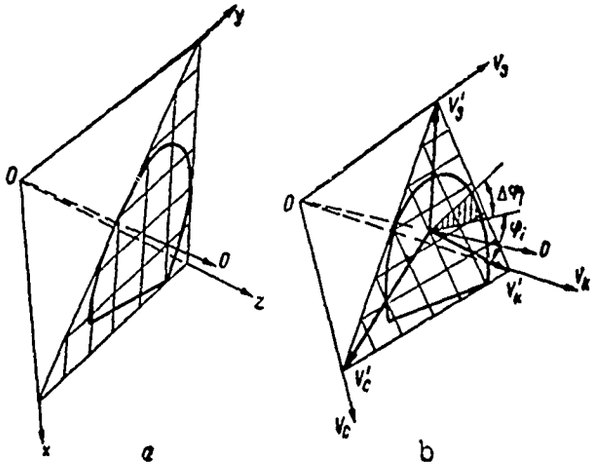

Fig. 2. Transformations of a color space.

Key: Subscript C = blue
Subscript K = red
Subscript 3 = green

A color plane of the CIE system is shown in the three-dimensional chromaticity-signal space (Fig. 2, a). Vector $\overline{z}$ is perpendicular to the plane, and vectors $\overline{x}$ and $\overline{y}$ intersect it at an angle of 30°. The white-color point corresponds to the centroid of the triangle. The properties of the plane are well-known.

Another choice of color space is possible, in particular that depicted in Fig. 2, b. Here all chromaticity vectors V_{red}, V_{green}, V_{blue}, V'_{red}, V'_{green}, V'_{blue} are situated identically relative to each other. The color plane is perpendicular to the white-color line. In view of the linearity of the transformation here effected of the spaces, the new color plane is equivalent to the initial CIE color plane. This can also be proved by using the color-difference coordinate system.

In the color decoder considered below, chromaticity signals modulate high-frequency oscillations with phase shift of 120°, and the color of graph lines is recognized from the phase of the resultant sum oscillation.

On the basis of what has been set forth above, a color-separating assembly has been devised which is part of the "Luch"* device intended for the automatic computer input of multichannel well logs.

Figure 3 shows the overall functional diagram of the color-separating assembly.

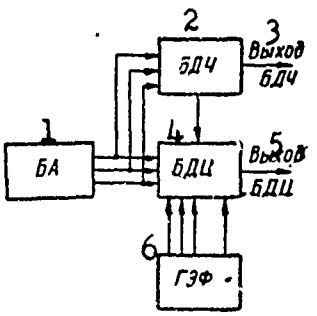

Fig. 3. Block diagram of color-separating assembly.

Key: 1. Analysis block AB
2. Black-line decoding block BDB
3. BDB output
4. Colored-line decoding block CDB
5. CDB output
6. Phase standard oscillator PSO

Analysis block AB is designed to use dichroic mirrors and correcting optical filters. The receivers are FEU-55 photomultipliers, which have a practically plane spectral characteristic in the visible region of the spectrum. In addition, the block includes special electronic chromaticity-signal shaping circuits which make possible the elimination of the influence of background transients on the line, as well as the influence of the

*The designation is tentative.

short duration of the analysis process. Output signals have the form of steep square pulses somewhat delayed relative to input signals. The amplitudes of input and output signals are equal to each other. This is achieved by means of holding circuits with capacitor storage. The shaped chromaticity signals go to the colored-line decoding block CDB and the black-line decoding block BDB. High-frequency oscillations are fed to the CDB from the phase standard oscillator PSO.

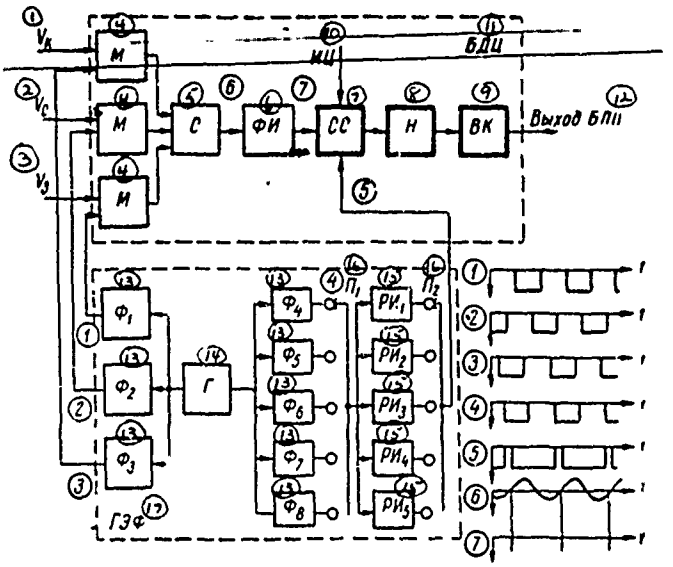

Fig. 4. Block diagram of colored-line pulse decoder.

Key:
1. V_{red}
2. V_{blue}
3. V_{green}
4. Modulator M
5. Adder A
6. Pulse shaper PS
7. Coincidence circuit CC
8. Storage circuit SC
9. Output stage OS
10. Chromaticity pulse
11. Colored-line decoder block CDB
12. CDB output
13. Phase-shift circuit Φ_1, etc.
14. High-frequency oscillator O
15. Enabling pulse EP_1, etc.
16. Switch S_1, S_2
17. Phase standard oscillator PSO

Figure 4 presents a more detailed functional diagram of colored-line decoding and some oscillograms. By means of high-frequency oscillator O and phase-shift circuits Φ_1, Φ_2, Φ_3 high-frequency square-wave periodic signals with time shift 1/3 T, 2/3 T are produced. This corresponds to a 120 and 240° shift of the first harmonics; f = 75 kc. These signals go to modulators M and are amplitude-modulated in accordance with input chromaticity signals V_{red}, V_{green}, V_{blue}. The first harmonics are extracted from the modulated signals and summed in adder A. The resultant oscillations

are amplified and limited, and short pulses 0.3 microsecond in duration are shaped at the "0" crossover points. The time position of these pulses relative to pedestal pulses coming from the master oscillator corresponds to the phase shift of the color vector relative to a certain constant direction.

From oscillator 0 oscillations also go to phase-shift circuits Φ_4, Φ_5, Φ_6, Φ_7, Φ_8, and then via switch S_1 to enabling-pulse EP shapers. At the output of the latter the voltage is of the type depicted in Fig. 4, (5). The delay of enabling pulses φ_i is established by circuits Φ_4-Φ_8 and has four fixed values and one adjustable value; the duration of enabling pulses is established by EP_1-EP_5 stretchers and also has four fixed values and one adjustable value. Fixed values φ_i and $\Delta\varphi_i$ correspond to the position and aperture angle of the wedge-shaped decision domain on the color plane and are determined during setting or learning. Graph lines can be used directly as standards.

Shaped enabling pulses are sent to coincidence circuit CC, and in the event of their coincidence with pulses of the shaper PS the latter enter the storage circuit SC, which represents recognition of a given line color. In addition, the BDB sends a no-black-recognition signal. A pulse signal is produced in the SC only after at least 10-12 pulses come continuously from the CC. Such a procedure rules out malfunctions due to transients in the decoding block. The output stage OS shapes a signal for reading a line of a given color.

Switching of the choice of colors is accomplished by means of switches S_1 and S_2.

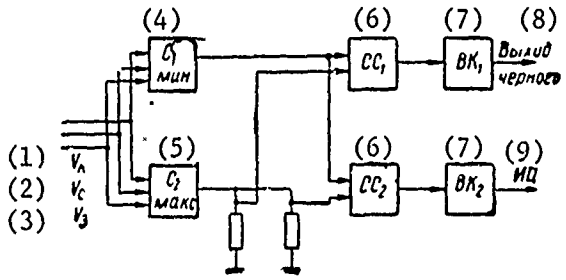

Fig. 5. Block diagram of black-line pulse decoder.

Key:
1. V_{red}
2. V_{blue}
3. V_{green}
4. Minimum search circuit $SchC_1$
5. Maximum search circuit $SchC_2$
6. Comparison circuit CC_1, CC_2
7. Stage output SO_1, SO_2
8. Black color output
9. Chromaticity pulse

Figure 5 shows the functional diagram of the block for the decoding of pulses from black lines BDB. The block operates provided the chromaticity

signals on black lines are initially equal. During operation minimum and maximum values of chromaticity signals are compared; in the reading of black-colored lines these values differ little from each other.

Input signals go to the inputs of minimum and maximum search circuits $SchC_1$, $SchC_2$, and then part of the maximum signal (usually 0.8-0.9) is compared with the minimum signal by means of comparison circuits CC_1 and CC_2. If the minimum signal exceeds 90 percent of the maximum signal, comparison circuit CC_1 is triggered and a black-color recognition signal appears at stage output SO_1, which is connected with the CC.

If the minimum signal is less than 90 percent of the maximum signal, comparison circuit CC_2 is triggered and a presence-of-colored-line signal (chromaticity pulse CP) appears at stage output SO_2. The presence-of-colored-line signal goes to the color-decoding block as an enabling signal.

In the "Luch" device, which uses the optical system of the FTA-PM facsimile apparatus with dichroic mirrors and FEU-55 photomultipliers, there are five fixed positions of the color switch, viz.: red, green, blue, violet, black. The device also permits manual setting to any given color.

TRANSIENT CHARACTERISTICS OF GRAPH-READING SCAN SYSTEMS

Metody i Ustroystva Preobrazovaniya Graficheskoy Informatsii (Methods and Devices for the Conversion of Graphic Data), 1968, pages 211-219

S. V. Denbnovetskiy
G. F. Semenov

The scan-reading (dynamic-compensation) method is widely used in devices for the conversion of graphic data into electric signals. Use is made of the graphic representation of continuous signals on paper and motion picture tape in the form of a black-and-white or colored line, as well as on the target of a storage cathode-ray tube in the form of a potential pattern line [1, 2].

The main source of error in scan conversion is inaccuracy in the determination of the time position of the notch pulse -- inaccuracy which in many respects is dependent on pulse shape, i.e., on the transient characteristic of the scan system, and on the method of time tie-in of notch pulse and noise level.

There is great interest in the investigation of the transient characteristics of scanners, as well as in the determination of the shape of the notch pulse and the establishment of its connection with conversion parameters and procedure. When noise level is known, one can select a method of time tie-in, estimate time tie-in error and find methods of lessening it, as well as proceed to an estimate of scanner resolution as defined by this error.

It is advisable to consider the reading of graphs from paper or motion picture tape, as well as of potential pattern lines from the target of a storage tube. In the latter case it is important to take into consideration the distinctive features of recording (halftone, bistable) and reading (capacity-discharge, grid-control) regimes.

To analyze the interaction of reading aperture and graph line, let us couple mobile coordinate system x', y' with the center of the scanning

spot, and immobile coordinate system $\overline{x}$, $\overline{y}$ with the point of intersection of the scanning line -- with the axis of the line being read (Figure 1).

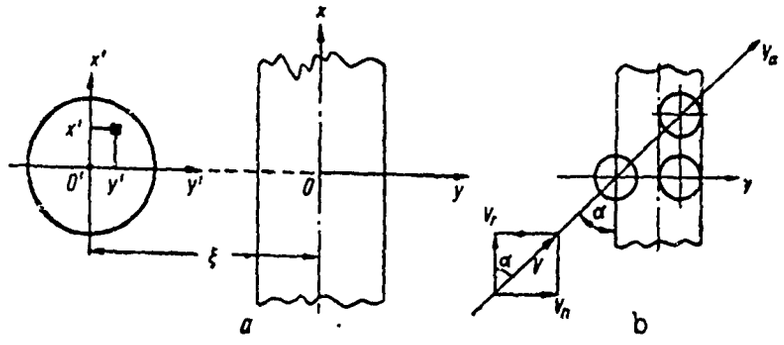

Figure 1. Reading aperture and graph line:
a) $\alpha = 90°$; b) $\alpha \neq 90°$.

Then

$$y' = y - \xi \tag{1}$$

and

$$\frac{y'}{R} = u - a, \tag{2}$$

where R is reading-spot radius.

If the spot hits the graph line, either the reflected light flux Φ or reading current I changes. Per elemental area of the spot ds this change will amount to

$$d\Phi = F_{\text{light}}(x, y, t)\, ds \tag{3}$$

for a light beam, and to

$$dI = F_{\text{electron}}(x, y, t)\, ds, \tag{4}$$

for an electron beam, where F(x,y,t) is a function of the interaction of reading spot with carrier and graph line; ds = dx'dy' is elemental area of the spot.

The form of function $F_{\text{light}}(x,y,t)$ is dependent on reflection or transmission characteristics of the carrier and graph line for the light spot, while $F_{\text{electron}}(x,y,t)$ is dependent on capacity-discharge processes on the target.

The transient characteristic is determined by integrating (3) or (4) with respect to the area of the scanning spot

$$\Phi(t) = \iint_{(s)} F_c(x, y, t)\, ds, \quad * \tag{5}$$

$$I(t) = \iint_{(s)} F_э(x, y, t)\, ds. \quad * \tag{6}$$

For the light spot

$$F_c = \sigma(y) B(x', y') \Omega, \tag{7}$$

where

$$B(x', y') = B_0 e^{-\frac{x'^2 + y'^2}{R^2}} \tag{8}$$

denotes Gaussian brightness distribution in the reading spot (if there are efficient aperture stops B (x',y') = B = const; B_0 is brightness in the center of the spot; R -- effective radius of the spot reckoned at level $\frac{1}{e}$; Ω -- the solid angle at which luminous intensity is constant; σ (y) -- the dependence of reflection (transmission) coefficient for the light spot.

For a sharply defined line one must distinguish σ_{line} (line characteristics) and $\sigma_{carrier}$ (carrier characteristics).

For a line with fuzzy edges it holds true that

$$\sigma(y) = (\sigma_н - \sigma_л) e^{-\frac{y^2}{R_r^2}} \quad ** \tag{9}$$

where R_r is the effective halfwidth of the line at level $\frac{1}{e}$).

For the electron spot it holds true that

$$F_э = j(x', y') \varphi |V(x, y, t)|, \tag{10}$$

where φ [V(x, y, t)] is volt-ampere characteristic of the target; j(x', y') is current density distribution in the spot which, depending on properties of the electron gun, can be considered Guassian

$$j(x', y') = j_0 e^{\frac{x'^2 + y'^2}{R^2}} \tag{11}$$

*Here and hereinafter the Russian subscript c = light, and э = electron.

**Here and hereinafter the Russian subscript н = carrier, and л = line.

uniform (in a round spot of radius ρ)

$$j(x', y') = \text{const} \tag{12}$$

or triangular (in a round spot)

$$j(x', y') = j(y') = \frac{j_{max}}{2\rho}(\rho - y'), \tag{13}$$

which represents the limiting case of deviation of maximum current density from center.

The volt-ampere characteristic of the target is dependent on the character of physical processes during the interaction of the reading spot with the potential pattern line.

For capacity-discharge reading of a step in the potential pattern by Gaussian beam we obtained

$$\varphi[V(x, y, t)] = \lambda V(y) \exp\{\gamma e^{-g^2}[1 - \Phi(u - a)]\}, \tag{14}$$

where λ is the inclination of the linear segment of target secondary-emission characteristic;

$\frac{y}{R} = u$, $\frac{x}{R} = g$, $\frac{\xi}{R} = a$ are relative coordinates;

$\gamma = \frac{\sqrt{\pi} R \lambda j_0}{2 C_0 v}$ is effectiveness of commutation; (15)

$V(y) = V_0$ is depth of pattern of potential track;

v is rate of travel of beam.

Under conditions of bistable capacity-discharge reading with complete sampling of secondary electrons by a collector

$$\varphi[V(x, y, t)] = \sigma - 1. \tag{16}$$

In grid-control reading under linear conditions

$$\varphi[V(x, y, t)] = \frac{V(y) - V_0}{V_{max} - V_0}; \quad V(y) < V_{max}, \tag{17}$$

under upper cut-off conditions

$$\varphi[V(x, y, t)] = \frac{V(y) - V_0}{V_{max} - V_0} \text{ given } \rho^0 \leqslant y \leqslant \rho^*. \tag{18}$$

$$\varphi[V(x, y, t)] = 1 \text{ given } 0 < y \leqslant \rho^0.$$

Here V_0, V_{max} are lower and upper cut-off voltage*

$$\rho^0 = R_з \sqrt{\ln \frac{\delta_з}{V_{max}}} \quad * \tag{19}$$

and

$$\rho^* = R_з \sqrt{\ln \frac{\delta_з}{V_0}} - \quad * \tag{20}$$

are the effective width of potential track for upper and lower collector-current cutoff respectively; $\delta_{recording} = \gamma_{recording} V_{0recording}$ is commutation efficiency during recording.

Transient characteristics obtained on the basis of expressions (5) and (6) can be represented as follows in relative units.

For the light spot, Gaussian brightness distribution, and sharp line boundary (represented by the broken line in Figure 2)

$$\frac{\Phi(a)}{\Phi_{max}} = \frac{1-k}{2}[\Phi(a+m) + \Phi(m-a)], \tag{21}$$

where $k = \frac{\sigma_{line}}{\sigma_{carrier}}$ is contrast; $m = \frac{\rho}{R}$ is the ratio of line halfwidth to spot radius;

$$\Phi_{max} = \Omega B_0 \sigma_{max} \pi R^2; \tag{22}$$

$$\Phi(a) = \frac{2}{\pi} \int_0^a e^{-a^2} da \quad \text{is probability integral.} \tag{23}$$

Notch pulse amplitude

$$A_. = (1-k)\Phi(m) \tag{24}$$

depends on contrast and the ratio of line width to spot radius.

The notch pulse is symmetric to the origin of coordinates x, y, i.e., the position of its tip corresponds to the intersection of the center of the reading spot with the graph-line axis. Pulse shape depends on m; it varies from bell-shaped to trapezoidal with an increase in m from 0.2 to 4.0.

If the line boundary is blurred (represented in Figure 2 by a solid line), then

*The Russian subscript *з* = recording.

$$\frac{\Phi(a)}{\Phi_{max}} = \frac{1-k}{\sqrt{m_r^2+1}} \exp\left[\frac{m_r^2 a^2}{1+m_r^2}\right], \tag{25}$$

where $m_r = \frac{R_r}{R}$ is the ratio of effective line halfwidth to effective spot radius.

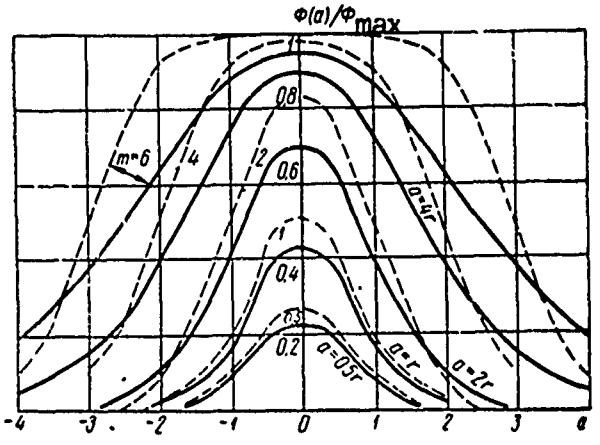

Figure 2. Transient characteristics during light-spot reading of graph line and bistable capacity-discharge reading of potential track by electron spot.

Notch-pulse amplitude

$$A_{cr} = \frac{1-k}{\sqrt{1+m_r^2}}. \tag{26}$$

The pulse is symmetric, but its edges are prolonged. The edge time from level 0.1 to tip is

$$\tau_\Phi^* = \frac{1}{m_r}\sqrt{(m_r^2+1)\ln\frac{10}{\sqrt{1+m_r^2}}}. \tag{27}$$

During capacity-discharge reading of a potential relief line with sharp boundaries [3] (Figure 3)

$$\frac{I(a)}{I_{max}} = \frac{\Phi(m+a)+\Phi(m-a)}{[2.4-\gamma[1-\Phi(m-a)]][2.4-\gamma[1+\Phi(m+a)]]}, \tag{28}$$

where $I_{max} = 2{,}88\,\lambda V_0 I_n$.

*The Russian subscript ϕ = edge.

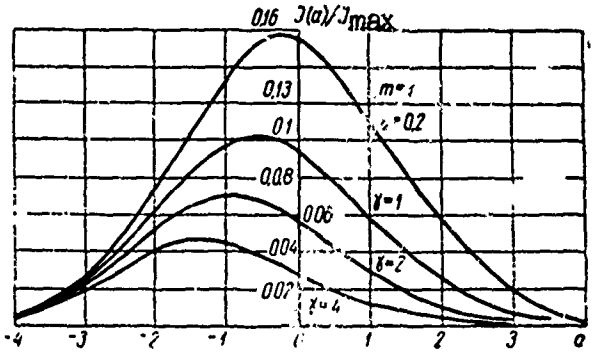

Figure 3. Transient characteristics during capacity-discharge reading of potential track.

Pulse amplitude depends on γ, m and I_{max}. The pulse is asymmetric, its tip is shaped prior to intersection of the reading-beam center with pattern-line axis; this shows up especially clearly given large γ, when potential pattern is erased by sections of the spot with small relative current-density values. The magnitude of the pulse-tip shift depends on electrical conditions and can be constant if they are stabilized.

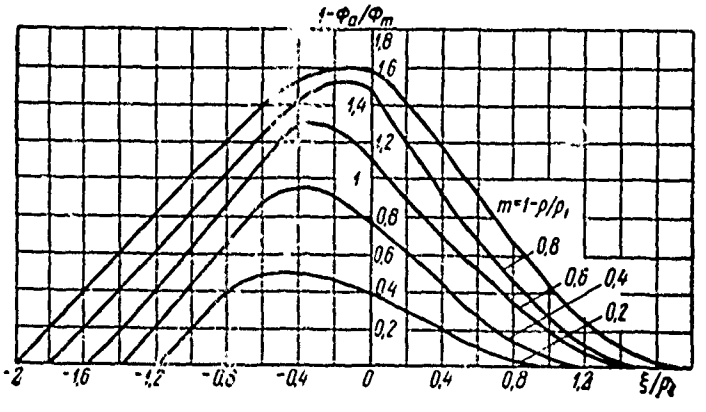

Figure 4. Transient characteristics during potential track reading by electron spot with "triangular" distribution of current density.

During bistable capacity-discharge reading of a step of potential pattern by Gaussian beam

$$\frac{I(a)}{I_{max}} = 1 - \frac{1}{2}[\Phi(m+a) + \Phi(m-a)]; \qquad (29)$$

$$A = 1 - \Phi(m). \tag{30}$$

Pulse amplitude is A; its shape is symmetric and depends on m. If current-density maximum shifts relative to spot center ("triangular"-beam reading; Figure 4), then

$$\frac{I(a)}{I_{max}} = 1 - \left\{\frac{1}{2}a_1\sqrt{1-a_1^2} + \frac{1}{2}\arcsin a_1 - \frac{1}{3}\sqrt{(1-a_1^2)^3} - \right.$$
$$\left. - \frac{1}{2}a_2\sqrt{1-a_2^2} - \frac{1}{2}\arcsin a_2 + \frac{1}{3}\sqrt{(1-a_2^2)^3}\right\}. \tag{31}$$

The notch pulse is asymmetric; its maximum shifts relative to the origin of coordinates x,y in a direction opposite to the direction of spot motion. In the operating range of values of m the shift of the maximum does not exceed 0.22 ρ_1 (ρ_1 is the radius of the reading spot).

During grid-control reading under linear conditions

$$\frac{I(a)}{I_{max}} = -A[\Phi(m-a) + \Phi(m+a)] + 2BC, \tag{32}$$

while with upper cutoff

$$\frac{I(a)}{I_{max}} = A[\Phi(m-a) + \Phi(m+a)] + 2BC \pm$$
$$+ \frac{1}{2}[\Phi(n-a) + \Phi(n+a)], \tag{33}$$

where

$$m = \frac{\rho^*}{R}; \quad n = \frac{\rho^*}{R}; \tag{34}$$

$A = \frac{V_0}{V_{max} - V_0}$ & $B = \frac{\gamma}{\sqrt{\pi}R(V_{max} - V_0)}$ are regime functions (35)

$C = \int_{-\rho^*}^{+\rho^*} e^{-\frac{v^2}{R^2} - \frac{(v-v')^2}{R_1^2}}$ is an integral determined by the numerical method.

The notch pulse is symmetric; its amplitude depends on electrical conditions.

If graph-line reading takes place at angle $\alpha < 90°$ (see Figure 1, b), then

$$\xi_\alpha = \frac{\xi}{\sin\alpha}. \tag{36}$$

i.e., pulse shape and the relation between pulse ordinates are preserved; the scale along the time axis varies. Pulse edges are stretched $\frac{1}{\sin \alpha}$ times; tip shift increases the same number of times in those cases where it occurs.

The analysis here made showed that in the case where the distribution of reading spot intensity is constant or symmetric relative to its center and the spot has no effect on the properties of the graph line, notch pulses are symmetric and the position of their tip corresponds to the intersection of reading-spot center with graph-line axis. In this case the tie-in with pulse tip assures minimum reading error and optimum resolution of the converter. Error is dependent on noise level and edge time of the notch pulse. In the event of a decrease in reading angle, error increases as a result of an increase in edge time.

Notch-pulse shape depends on the ratio between graph-line width and reading-spot radius m. Given large m's, notch-pulse shape becomes trapezoidal. Asymmetry of the distribution of reading-spot intensity entails a shift of the tip towards the leading edge of the notch pulse, the shift being dependent on conditions and its magnitude amenable to estimate.

With a change in graph-line parameters in response to the influence of the spot (capacity-discharge reading of potential pattern), the notch-pulse tip shifts towards the leading edge the more markedly, the greater the intensity of commutation. The constancy of such a shift can be assured by stabilization of reading conditions. In order to eliminate asymmetry and give trapezoidal pulses a shape suitable for tie-in to the tip, the use of filters is recommended.

BIBLIOGRAPHY

1. Petrenko, A. I., Preobrazovaniye Grafikov v Elektricheskiye Signaly (Conversion of Graphs into Electric Signals), "Tekhnika" (Technology), Kiev, 1965.

2. Petrenko, A. I. and Denbnovetskiy, S. V., Masshtabnovremennyye Preobrazovateli Impul'snykh Signalov (Scale-time Pulse-signal Converters), "Tekhnika" (Technology), Kiev, 1965.

3. Ryftin, Ya. A., ZhTF (Journal of Technical Physics), 1957, 27, 8.

STORAGE CRT AS CARRIER OF GRAPHIC INFORMATION

Metody i Ustroystva Preobrazovaniya Graficheskoy Informatsii (Methods and Devices for the Conversion of Graphic Data), 1968, pages 220-225

S. V. Denbnovetskiy

The target of a storage cathode-ray tube SCRT can be represented as a two-dimensional information carrier [7] having two geometrical and one physical dimension. For the geometric dimensions there are corresponding coordinates of target points, while for the geometric dimension there is a corresponding depth of potential pattern at the given point. Depending on the number of dimensions used per target, first-, second-, or third-order images can be obtained.

Input signal U(t) can be represented as a graph; in this case two geometric target dimensions are used and a second-order image Y(x) is formed.

Such a representation of the input signal is employed not only in oscillography [2], when a graphic image recorded on a potentialscope screen with a visible image is presented to the operator for analysis, but also in automatic measurements. In the latter case the signal oscillogram is usually read on the basis of the scanning method [8] and its readout values are represented in digital or analog form. A change in the time interval between readings permits an increase or decrease in the length of the output signal, i.e., accomplishment of the scale-time conversion [5] necessary to match the time parameters of the fast broadband signals under investigation with the parameters of the automatic apparatus. Scale-time conversion makes possible a redistribution of the flow of information contained in the input signal without a change in the total volume of information. In addition, time and parameter adaptations are easily introduced in the scale-time converter during reading of the fixed signal [5]. The number of discrete time readings [1] or the number of amplitude quantization levels, moreover, vary in conformity with the current tendency of a signal in such a way that the volume of output information decreases while the prescribed accuracy of conversion is preserved.

Use of the SCRT with visible image and internal reading of the fixed signal makes it possible to include information filters in the scale-time converter, thus significantly cutting down the volume of output information. The operator evaluates the character of the input signal according to its visible image on the SCRT screen and selects its parameters carrying useful information about the phenomenon under study. They are automatically determined during reading of the signal from the target and are inputted into a unit for further processing. Redundant information contained in other parameters is destroyed or filtered.

In determining the information characteristics of a scale-time converter it is important to calculate the information capacity and resolution of the SCRT target under conditions for recording the graphic image of an input signal.

We must distinguish target resolution in a horizontal direction along the x axis, corresponding to the time axis of the input signal, from that in a vertical direction along the y axis, corresponding to the axis of amplitude values. y-Resolution is determined by the number N_y of discrete signal-ordinate levels which can be distinguished in the process of conversion with allowance for errors made in recording and reading. A distinctive feature of the SCRT is the fact that, in contrast to other signal converters with intermediate graphic representation, signal-recording and reading processes are here combined in one instrument. This makes it possible to avoid many conversion errors which occur in cases where recorders and readers are independent complexes. In addition, it is possible to discern errors made by the cathode-ray converter and assign the appropriate value of resolution to the storage target as information carrier.

Let us divide into two groups the components of amplitude error which appear in a system containing an SCRT and operating under conditions for recording the input-signal oscillogram with subsequent reading thereof according to the scan method. In the first group let us include errors arising outside the cathode-ray converter, and in the second group errors due to SCRT features.

The first group will include: distortions caused by the input-signal amplifier and notch-pulse amplifier, as well as error from the nonlinearity of scanning in the reading and conversion of notch-pulse time position into digital or analog equivalent. The use of methods for raising the accuracy of scanning converters makes it possible to reduce components of the first group to a minimum. Let us designate total amplitude error of this type, reduced to target, as δ_0. In the general case the law of its probability distribution is arbitrary. In work [7] it is shown that any error with an arbitrary distribution law can be replaced by an equivalent error with uniform discribution

$$\Delta = k_0 \delta_0, \qquad (1)$$

where k_0 is proportionality coefficient dependent on distribution law of δ_0. For the normal law $k_0 = 2.07$ [4].

If we assume that the input amplitude discreteness interval equals Δ, we obtain the number of such intervals in the absence of error introduced by the SCRT

$$N_\Delta = \frac{Y_м}{\Delta}, \qquad (2)$$

*

where Y_{target} is the vertical target dimension.

In the second group let us include the components of amplitude conversion error introduced by the cathode-ray storage tube: nonlinearity of deflection systems, noncoaxiality of the electron guns in double-beam tubes, aperture distortions, error in notch-pulse timing. With careful final adjustment of storage-tube design the principal role here will be played by deflection of the time position of notch-pulse tip from the moment the center of the reading pulse passes through the potential pattern axis at the reading point, as well as by error in the timing of the notch-pulse tip.

Both error components are determined by the shape of the transient characteristic of the tube during scan reading, while timing error depends also on the noise level in the notch-pulse processing channel and the timing method. Timing according to the position of the notch-pulse maximum at the output of the matched filter makes it possible to obtain the least error, close to the minimum theoretically attainable [3]. The signal-to-noise ratio at the output is maximal and, apart from maximum accuracy, assures maximum reliability. Therefore, in determining resolution we must proceed from precisely this method. Thus, for a notch pulse in the shape of an isosceles trapezoid mean-square error reduced to target is

$$\delta = \frac{\sqrt{N_0 \tau_\phi v_{сч}}}{A_c \sqrt{2n}}, \qquad **$$

where N_0 is the spectral density of noise at the input of the matched filter; A_c is notch-pulse amplitude; τ_{edge} is notch-pulse edge time; n the number of pulses used to determine time position; v_{read} velocity of travel of the reading spot.

---

*Here and hereinafter the Russian subscript M = target.

**The Russian subscript сч = read.

Reduced error with a uniform distribution law, which allows for a shift of notch-pulse tip and tie-in error, just as before is

$$\gamma = k\delta. \tag{3}$$

If we assume γ to be equal to the range of variation in the error of notch-pulse timing, we find

$$N_\gamma = \frac{\gamma_M}{\gamma}. \tag{4}$$

Thus, the notch-pulse tip can be represented as an analyzer, with the help of which the discrete input-signal levels, established in the form of point ordinates with the plotted potential pattern, can be distirguished on the target. The fact that the analyzer has a dead zone decreases the number of different levels and decreases the amount of information which can be converted in a single signal reading value.

Let us introduce the ratio between input-signal quantization interval Δ and range of error variation γ

$$n = \frac{\Delta}{\gamma} \tag{5}$$

and determine the resolution of SCRT target as its equivalent number of divisions N_y. By N_y we shall understand the number of discrete signal-ordinate levels distinguishable on the target of an SCRT which does not introduce conversion error and permits the same amount of information to be obtained per ordinate reading value as in the given tube

$$N_y = N_\Delta e^{-H_\Delta(n)} = N_\gamma e^{-H_\gamma(n)}, \tag{6}$$

where H_Δ, H_γ are the upper limits of conditional entropy due to error γ. The values H_Δ (n) and H_γ (n) can be found from the graph presented in [6].

The x-resolution is determined by the number of reading values of ordinates N_X which can be obtained in a given tube. At the same time we must distinguish between SCRTs with one-time and multiple reading. In the former case the interval Δx between two adjacent reading lines is determined by the permissible lowering of notch-pulse amplitude due to partial erasure of pattern at the given point during reading at the preceding point. A decrease in the signal-to-noise ratio should not cause appreciable deterioration of conversion accuracy.

In tubes with multiple reading no reciprocal influence of adjacent lines shows up, and the interval Δx can be made arbitrarily small. This is convenient during further approximation of a continuous signal from discrete readings. In cases where readings are represented in digital form,

Δx must be so selected that every subsequent interval differs from the preceding one by not less than Δy, i.e.,

$$\Delta x = \Delta y \operatorname{ctg} \alpha,$$

where α is the slope angle of the patvern line at the reading point. Obviously,

$$N_x = \frac{X_м}{\Delta x}, \tag{7}$$

where X_{target} is the horizontal target dimension.

Work [5] shows that the width of the signal spectrum which can be processed in an SCRT-containing system is

$$\Delta F^{*}_{вх} = \frac{v_з}{2\Delta x N_y}^{*}, \tag{8}$$

where $v_{recording}$ is the maximum recording rate on the tube target.

Taking expression (6) into consideration for the equivalent number of divisions N_y, we can write the following relation:

$$\Delta F_{вх} = \frac{v_{зс} H_\Delta(n)}{2\Delta x N_\Delta} = \frac{v_{зс} H_y(n)}{2\Delta x N_y}. \tag{9}$$

The resultant expression makes it possible to establish the connection of the broadband character of the SCRT with its recording rate and resolution.

The number of readings for a signal of length τ_{input} in conformity with Kotel'nikov's theorem will be

$$N_r \geq \tau_{вх} 2\Delta F_{вх} = \tau_{вх} \frac{v_{зс} H_\Delta(n)}{\Delta x N_\Delta}, \tag{10}$$

where $\tau_{вх} \frac{v_{зс} H_\Delta}{N_\Delta} = X_м$ is the necessary horizontal target dimension given a particular resolution value.

The method here set forth of determining y-resolution through the equivalent number of divisions with the use of information characteristics of the instrument, having regard for the parameters of processing circuits, also holds true for other scanning conversion systems.

*Here and hereinafter the Russian subscript ВХ = output, з = recording.

BIBLIOGRAPHY

1. Denbnovetskiy, S. V., and Zinchenko, V. Ya., Mnogoznachnyye Elementy i Struktury -- Sb. (Multivalued Elements and Structures -- Collection of Works), "Sovetskoye Radio" (Soviet Radio), 1967.

2. Denbnovetskiy, S. V., Mudrak, Yu. N., and Petrenko, A. I., Avtomatika i Priborostroyeniye (Automation and Instrument Manufacture), 1963, 3.

3. Mityatshev, B. N., Opredeleniye Vremennogo Polozheniya Impul'sov pri Nalichii Pomekh (Determination of the Time Position of Pulses in the Presence of Noise), "Sovetskoye Radio" (Soviet Radio), Moscow, 1962.

4. Novitskiy, P. V., Izmeritel'naya Tekhnika (Measurement Techniques), 1966, 7.

5. Petrenko, A. I., and Denbnovetskiy, S. V., Masshtabnovremennyye Preobrazovateli Impul'snykh Signalov (Scale-time Pulse-signal Converters), "Tekhnika" (Technology), Kiev, 1965.

6. Rabinovich, V. I., and Tsapenko, M. P., Izmeritel'naya Tekhnika, 1963, 6.

7. Temnikov, F. Ye., Avtomaticheskiye Registriruyushchiye Pribory (Automatic Recorders), State Scientific and Technical Publishing House of Literature on Machinery Manufacture, Moscow, 1961.

8. Temnikov, F. Ye., Teoriya Razvertyvayushchikh Sistem (Theory of Scanning Systems), State Scientific and Technical Power-Engineering Publishing House, Moscow, 1963.

9. Temnikov, F. Ye., Tr. MEI -- Sb. (Works of Moscow Paper Engineering Institute -- Collection of Works), No 52, Publishing House of Moscow Power Engineering Institute, Moscow, 1963.

SOME QUESTIONS RELATING TO THE DYNAMICS OF FOLLOW SCANNING SYSTEMS

Metody i Ustroystva Preobrazovaniya Graficheskoy Informatsii (Methods and Devices for the Conversion of Graphic Data), 1968, pages 226-230

G. G. Vaynshteyn

The measuring element in follow scanning systems determines graph-line position relative to the scanning point. Systems can be subdivided into three types depending on the completeness of the information obtained regarding line position [4].

In systems of the first type graph-line position is determined precisely. Thus in some devices the reading beam moves around the scanning circle, and both points of this circle's intersection with the graph line are fixed. Line direction and magnitude of deflection from the contour are then calculated.

In systems of the second type position is measured by just one graph point, for example, one of the points of intersection with the scanning circle. The scanning point moves towards a known graph point. Deflection from the contour and rate of motion along it are not directly controlled.

In systems of the third type there is no auxiliary scanning and direction towards the graph line is not measured. Motion of the beam is corrected by varying the curvature of its path at line crossings. In such systems, called extrapolative systems, control is effected according to curvature.

Let us dwell on the dynamics of systems with incomplete information about contour position.

Calculation of Path in a System of the Second Type

The analysis made here may be of interest in determining following error in electromechanical systems. In the general case, every coordinate channel in such systems is described by the linear equation

$$L_n(u_2) = a_0 \frac{d^n u_2}{dt^n} + \cdots + a_{n-1} \frac{du_2}{dt} + a_n u_2 = u_1,$$

where u_1 and u_2 are input and output action respectively.

The equations of motion will then assume the following form [2]:

$$L_n\left(\frac{dx}{dt}\right) = X(s) - x$$

and

$$L_n\left(\frac{dy}{dt}\right) = Y(s) - y,$$

where quantity s is implicitly given by the expression

$$[X(s) - x]^2 + [Y(s) - y]^2 = r^2.$$

Here x and y are the coordinates of the center of the scanning circle; r is its radius; X(s) and Y(s) are coordinates of the contour line as a function of arc length. The order of the equations equals 2(n + 1).

It can be shown that the path of motion depends only on contour shape and is not dependent on its situation in the coordinate system [1]. Such invariance makes it possible to reduce the equations of motion to a form more convenient for path calculation by eliminating x, y and t from them. Moreover, input action on the system can be represented by the dependence of curvature K of the line being followed on arc length s, with the latter emerging as an independent variable. Output quantities are velocity w of the scanning circle's point of intersection with the contour, and angle θ between the tangent to the contour at this point and the radius of the scanning circle. The transformed equations will assume the following form:

$$f_1(w, w', \ldots, w^{(n)}, \theta, \theta', \ldots, \theta^{(n+1)}, K, K', \ldots, K^{(n)}) = 0;$$
$$f_2(w, w', \ldots, w^{(n)}, \theta, \theta' \ldots, \theta^{(n+1)}, K, K', \ldots, K^{(n)}) = r.$$

The order of the equations is one less because quantity w itself is a derivative.

Let us examine as examples an inertialess system and a system in which the coordinate channel is an aperiodic circuit. Let us write the transformed equations

given n = 0

$$\theta' + \frac{1}{r}\sin\theta - K = 0,$$

$$aw\cos\theta = r;$$

given n = 1

$$a_0 K w\cos\theta + a_0 w'\sin\theta + a_1\sin\theta - a_1 rK + a_1 r\theta' - a_0 rw'K + \\ + a_0 rw'\theta' - a_0 rwK' + a_0 rw\theta' = 0,$$

$$a_0 ww'\cos\theta - a_0 w^2 K\sin\theta + a_1 w\cos\theta + a_0 rw^2 K^2 + \\ + a_0 rw^2(\theta')^2 - 2a_0 rw^2 K\theta' = r.$$

To obtain steady-state equations, all derivatives must be equated with zero and the assumption made that curvature is constant. By solving the equations the error in motion around a circle with arbitrary radius can readily be found.

Let us note that the first equation of an inertialess system is a modification of the general Riccati equation. Substitution of

$$\operatorname{tg}\frac{\theta}{2} = u$$

yields

$$u' = \frac{K}{2}u^2 - \frac{u}{r} + \frac{K}{2}.$$

Motion of Extrapolative System with Simplest Law of Control

Let the graph line coincide with the x axis and the velocity of the scanning point be a constant equal to v. The vertical velocity component

$$y' = v\sin\varphi,$$

where φ is the angle between the horizontal axis and the direction of motion. Let us take as given the following law of control:

$$\varphi' = -cy,$$

where c is a constant coefficient of amplification. If we eliminate y, we obtain the well-known pendulum equation

$$\varphi'' + cv\sin\varphi = 0.$$

The solution of this equation and the path of the point can be written by means of Jacobi's elliptic functions and zeta function.

Let us note that

$$k^2 = \frac{\omega_0^2}{4cv} + \sin^2 \frac{\varphi_0}{2},$$

where $\omega_0 = \varphi_3'$ and φ_0 are the initial conditions. Given $k < 1$ (oscillatory motion), path equations will assume the following form:

$$x(t) = vt\left(2\frac{E}{K} - 1\right) + 2\sqrt{\frac{v}{c}}\,\mathrm{zn}\,(t\sqrt{cv});$$

$$y(t) = 2k\sqrt{\frac{v}{c}}\,\mathrm{cn}\,(t\sqrt{cv}).$$

Here E and K are complete elliptic integrals. The first term in the expression for x(t) is mean velocity of motion

$$w = v\left(2\frac{E}{K} - 1\right).$$

Depending on initial conditions, three case are possible:

1) $w > 0$ (motion without loops); $2E > K$; $0 < k < 0.909$.
2) $w = 0$ (closed cycle); $2E = K$; $k \approx 0.909$.
3) $w < 0$ (motion with loops); $2E < K$; $0.909 \ldots < k < 1$.

The first regime is most suitable for line following. In calculating a real system allowance must be made for the nonlinearity of aperture characteristic, inertia of individual assemblies, and path curvature. The system needs stabilization. Apart from a differentiator [3], any parametric devices which give phase lead can be used for this purpose. The equalizer can, for example, after every intersection of the contour alter the coefficient of amplification in accordance with a certain declining law, with path curvature decreasing at the same time. This is the stabilization method which was used in a discrete extrapolative system [2].

One more regime can be obtained given $k > 1$ (rotary motion). The equations of motion have the following form:

$$x(t) = vt\left[1 + 2k^2\left(\frac{E}{K} - 1\right)\right] + 2k\sqrt{\frac{v}{c}}\,\mathrm{zn}\,(tk\sqrt{cv});$$

$$y(t) = 2k\sqrt{\frac{v}{c}}\,\mathrm{dn}\,(tk\sqrt{cv}).$$

The path forms loops and does not intersect the x axis. The regime resembles the operation of systems with a scanning circle and can be used

for following. The system described in work [5] can be considered from this viewpoint.

Time Optimization with Limited Acceleration

A smooth curve is given by the dependence of curvature on arc length K(s); $0 \leqslant s \leqslant S$. Maximally permissible acceleration is also known. We must establish the character of the change in velocity v(s), given which the scanning point shifts from the point s = 0 to s = S in the minimum segment of time.

It is assumed that before and after motion the scanning point is in a state of rest.

It can be shown that the optimum law must satisfy the following conditions: curve v(s) is continuous, and all its points where the derivative is finite satisfy the equation

$$(vv')^2 + v^4 [K(s)]^2 = A^2.$$

The derivative v'(s) is piecewise continuous, and all its discontinuities are such that at discontinuity point s* the following relations take place:

$$|v'(s^* + 0)| = |v'(s^* - 0)|; \quad v'(s^* + 0) < 0; \quad v'(s^* - 0) > 0.$$

These conditions make it possible to synthesize the optimum law from curve segments conforming to the above-cited equation. The second condition must be observed at the salient points.

The written expression is reduced to an Abel equation of the first kind by substituting

$$\lambda = \frac{v}{2v'}; \quad 2vv' = \sqrt{\frac{4A^2}{1 + 4K^2\lambda^2}}; \quad v^2 = \lambda \sqrt{\frac{4A^2}{1 + 4K^2\lambda^2}}.$$

In the general case only a numerical solution is possible, but in the particular case, given K = const = $\frac{1}{R}$, we obtain the optimum law of acceleration and deceleration on a circle

$$v(s) = \sqrt{AR \sin \frac{2s}{R}}.$$

BIBLIOGRAPHY

1. Vaynshteyn, G. G., Tr. MEI -- Sb. (Works of Moscow Power Engineering Institute -- Collection of Works), No 58, Publishing House of Moscow Power Engineering Institute, 1965.

2. Kovalevskiy, V. A., and Semenovskiy, A. G., Avtomatika i Priborostroyeniye (Automation and Instrument Manufacture), 1960, 1.

3. Pereverzev-Orlov, V. S., Opoznavaniye Obrazov. Teoriya Peredachi Informatsii -- Sb. (Pattern Recognition: Theory of Information Transmission -- Collection of Works), "Nauka" (Science), Moscow, 1965.

4. Petrenko, A. I., Preobrazovaniye Grafikov v Elektricheskiye Signaly (Conversion of Graphs into Electric Signals), State Publishing House of Technical and Theoretical Literature of the Ukrainian SSR, Kiev, 1964.

5. Greanias, E. C., Meagher, P. F., Norman, R. J., and Essinger, P., IBM J. of Research and Devices, 1963, 7, 1.

MAGNETIC-TAPE RECORDING OF OBSERVATION DATA FOR COMPUTER INPUT

Metody i Ustroystva Preobrazovaniya Graficheskoy Informatsii (Methods and Devices for the Conversion of Graphic Data), 1968, pages 231-232

V. V. Kalinin

A device for the magnetic-tape recording of analog quantities in binary code, based on electronic digital recorder ETsR-1, consists of a digital voltmeter ETsV-3, commutator block KB-1, and electronic blocks employed in the BESM-2M digital computer (Figure). Data are recorded on magnetic tape in binary code in a manner analogous to the recording of machine words on the BESM-2M.

The ETsV-3 is a multirange high-speed high-accuracy voltmeter with a completely automated measurement process. Commutator block KB-1 makes it possible to issue command synchronizing pulses connecting voltmeter ETsV-3 to twenty different sources of the voltage being measured.

Let us describe the operation of the device as a whole. On arrival of a crigger pulse measurement is made of the voltage in the first channel, which is connected to the voltmeter input. On completion of measurement the measurement result is read and registered. The ETsV-3 voltmeter issues the following information in parallel binary-decimal code: 1) measurement result in 16 binary digits; 2) sign "+" or "-" in one binary digit (sign 4); 3) exponential order of a number in two binary digits (0_1 and 0_2).

Prior to magnetic-tape recording a 19-digit word is first received in the number register in parallel code and then after 39 clock shift pulses is recorded on magnetic tape in sequential code. The output of clock write pulses is effected by "Counter 40."

During recording the magnetophone is started up from the control console, and some time later the ETsV-3. At the same time the voltage fed to the ETsV-3 input from a particular channel is measured. Afterwards the result of measurement appears in binary-decimal code at the ETsV-3 output.

The end-of-measurement pulse transmits the result from ETsV-3 to flip-flops of the number register and starts "Counter 40," which issues clock pulses for recording the number on magnetic tape. Synchronizing pulses SP are recorded on magnetic tape simultaneously with the code.

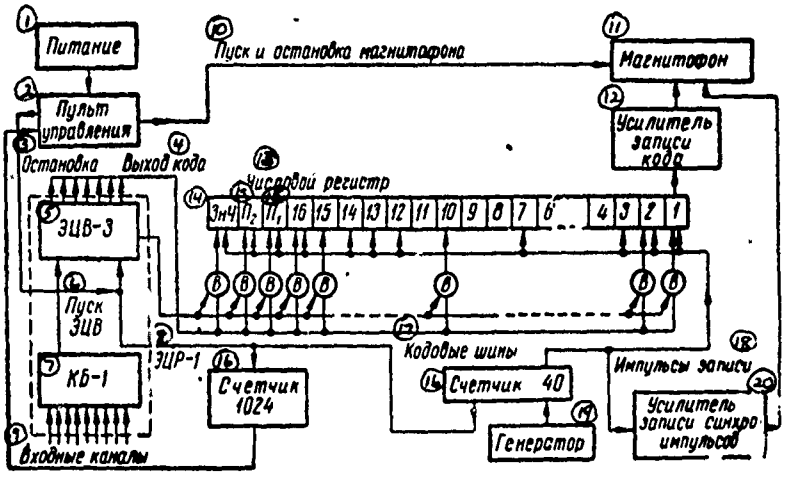

Block diagram of device.

Key:
1. Power supply
2. Control console
3. Stop
4. Code output
5. Digital voltmeter ETsV-3
6. Digital-voltmeter start
7. Commutator block KB-1
8. Electronic digital recorder ETsR-1
9. Input channels
10. Magnetophone start-stop
11. Magnetophone
12. Code-recording amplifier
13. Number register
14. Sign 4
15. Exponential order of a number in two binary digits 0_1 and 0_2
16. Counter
17. Code buses
18. Write pulses
19. Oscillator
20. Sync-pulse recording amplifier

After one number is recorded, "Counter 40" is automatically cleared, actuating voltmeter ETsV-3 for further measurements. The number of recorded numbers is fixed by "Counter 1024," which is part of the general block diagram. After the recording of 1024 codes the magnetophone stops, and measurements cease.

The array, consisting of 1024 numbers, is recorded without group number and is read on the computer with zero number. The recorded array of numbers is processed according to a special program, and the numbers are reduced to a form suitable for use by the BESM-2M computer.

HOLOGRAPHIC METHOD OF GRAPHIC DATA PROCESSING

Metody i Ustroystva Preobrazovaniya Graficheskoy Informatsii (Methods and Devices for the Conversion of Graphic Data), 1968, pages 233-238

L. D. Bakhrakh
G. A. Sobolev
G. Kh. Fridman
Ye. R. Tsvetov

The development of the techniques of optical data processing and holography makes possible the performance of complex computing operations, including pattern recognition [1], key-word retrieval in information materials and machine translation. The progress achieved in this field is explained by the simplicity of manufacturing optical matched filters for composite signals. Optical systems with matched filters can perform independent computing operations, as well as form part of complex integrated systems along with electronic digital computers. Great interest attaches to the use of optical machines for digital-computer input and output of graphic data.

In the technology of optical data processing use is made of the ability of a thin lens to perform Fourier transformation. Let an object with amplitude transparency f(x,y) be in the first focal plane of a thin spherical lens and let it be illuminated with a plane monochromatic wave. Here complex field amplitude in the second focal plane is expressed by the relation

$$F\left(k\frac{\xi}{f},\ k\frac{\eta}{f}\right)=\iint_{an} f(x,y)\exp\left[\frac{2\pi i}{\lambda}\left(\frac{\xi}{f}x+\frac{\eta}{f}y\right)\right]dxdy,$$

where integration is performed with respect to the illuminated aperture; $k=\frac{2\pi}{\lambda}$; f is focal distance of the lens; x, y and ξ, η are coordinates in the first and second focal plane of the lens respectively.

With the introduction of generalized coordinates u, v, instead of $k\frac{\xi}{f}$ and $k\frac{\eta}{f}$ we obtain a symbolic representation of the Fourier transformation performed by the lens,

$$F(u, v) \leftarrow f(x, y).$$

Matched filtration consists in the signal's being modified by a filter with a complex frequency characteristic, which is the conjugate of the signal spectrum and which is inversely proportional to the noise spectrum.

Such a filter can be implemented in the set-up shown in Figure 1, a. From a light source a plane wave is formed, illuminating an image (letter, word) placed in the first focal plane of spherical lens L. Part of the light is used to form a reference coherent beam. The second focal plane of the lens registers the matched filter (for example, on a photoplate).

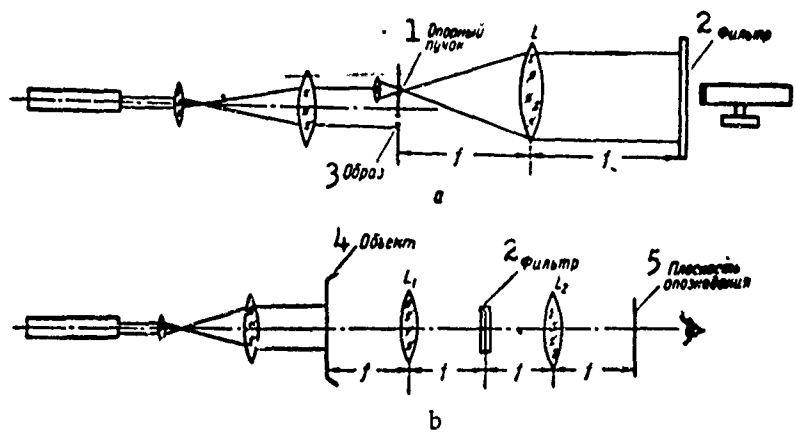

Figure 1. Block diagram of the set-up.

Key: 1. Reference beam
2. Filter
3. Image
4. Object
5. Recognition plane

The complex amplitude of a light wave in the registration plane equals M(u,v) for the image, and $A_0 \exp [i(bu + v)]$ for the reference wave. Total complex amplitude amounts to $H(u,v) + A_0 \exp [i(bu + v)]$, and the intensity registered by the film to

$$I(u, v) = [|H(u, v)|^2 + A_0^2] + H(u, v) \exp [-i(bu + v)] + \\ + M(u, v) A_0 \exp [i(bu + v)].$$

During the processing of a plate up to $\gamma = 2$ its amplitude transparency is $\tau \approx I$ (u,v). The filter thus made is inserted into the frequency plane of the correlator depicted in Figure 1, b.

Let the object possess transparency f(x,y) and have spectrum F(u,v) in the plane of the filter. The luminous flux passing through the filter then has the form

$$F(u, v) I(u, v) = F(u, v)[|H(u, v)|^2 + A_0^2] + \\ + F(u, v) H(u, v) A_0 e^{-i\Phi} + F(u, v) H(u, v) A_0 e^{i\Phi}.$$

Lens L_2 performs an inverse Fourier transformation, and in the recognition plane we obtain three spatially separated light signals.

The signal along the optical axis has the following form:

$$f(u, v) \vee T[|H|^2 + A_0^2].$$

Signals displaced in both directions from the optical axis have the following form respectively

$$A_0[f \vee h]_x + b_1 y$$

and

$$A_0[f \vee h]_x - b_1 y,$$

where V denotes convolution, and $\vee$ correlation.

Useful information about the image to be recognized is contained in the former of these signals.

The advantage of the recognition method here under consideration is its insensitivity to a shift of the image over the entire input plane and small variations in scale and rotations, as well as noise-immunity and high recognition speed determined by the sensitivity of the recorder.

Matched filters were obtained holographically for many objects (including digits, letters, symbols of words and portraits), by means of which pattern-recognition experiments were conducted using transparencies.

Figure 2 shows the results of the recognition of the digit "5" by reference to a table consisting of 16 digits and letters. Two "5" digits were correctly identified, and one "3" digit was incorrectly identified. The error is explained by the fact that the patterns were drawn by hand with a 30-percent variation in scale.

Figure 3 shows the result of the retrieval of the word golografiya (holography) on a typescript page. All six words [illegible] correctly recognized. It is noted that in recognition no distinction i[illegible] between words with different endings, for example, golografiya [n[illegible]e singular] and golografii [genitive, dative, locative singul[illegible]. [illegible]he text to be

recognized is rotated $\pm$ 15° around the optical axis, the output signal is above noise level. In the case where there is a threshold circuit at the output of the optical device, recognition can reliably take place despite such rotations. But if retrieval has to be conducted in a wider range, a filter must be rotated around the optical axis (if the necessary threshold unit is present).

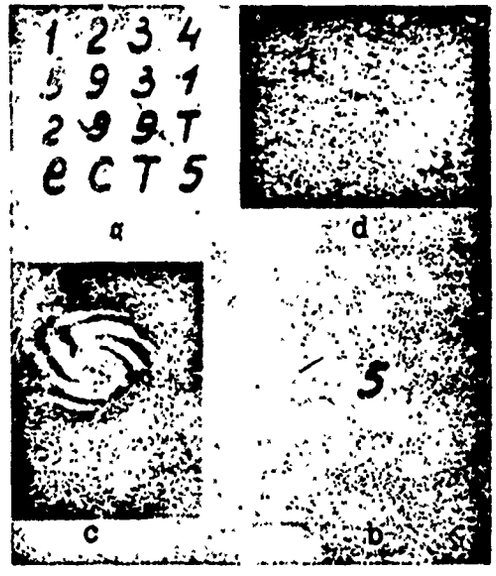

Figure 2. Recognition of digit "5":

a -- Table; b -- digit "5"; c -- matched filter for digit "5"; d -- recognition result (bright spots stand for recognized images).

Matched filters were also made for the retrieval of different symbols and portraits, and the experiments conducted with these filters yielded the same results.

Criticalness to rotation and variation in size depends on the specific pattern (its symmetry, etc.). In enumerating the possible applications of machines using the principles here set forth, we should point out key word retrieval from information materials, machine translation, data input and output devices for electronic digital computers. Moreover, the capabilities of optical machines can be increased by the introduction of object search by orientation, by the introduction of many optical channels, as well as by filter replacement.

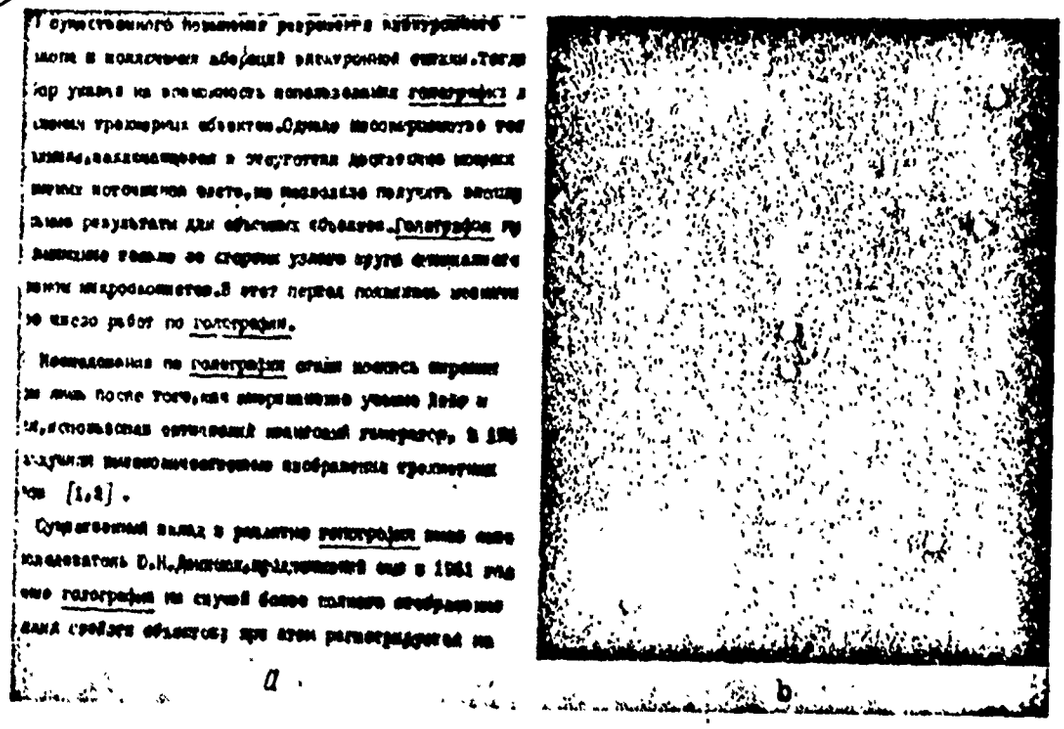

Figure 3. Retrieval of reference word:

a -- text; b -- recognition result. [Translator's note: The underlined word throughout is holography.]

Evidently it is most practical to use such machines in conjunction with electronic digital computers to perform the necessary logical operations.

Further improvement of optical machines should aim towards the use of associative-memory principles [2]. In response to a displayed pattern the machine should read out the pattern in its own "language" without scanning. The creation of a large-capacity associative memory involves the development of three-dimensional storage units, for example, solid-state units (alkali halide crystals, photochromic glasses, thick-film emulsions, etc.).

The authors conducted experiments with models of such a system using a photoplate memory. A simple associative memory was created holographically. On the display of one of the patterns to the machine, it read out the corresponding associated pattern.

Improvement of such systems with an increase in the complexity of their memory should result in the creation of optical machines to perform

complex operations without scanning (for example, machine translation, translation of information from machine language to language comprehensible to an operator, and vice versa).

BIBLIOGRAPHY

1. Van der Lugt, A., IEEE Trans. on Information Theory, 1964, 10.

2. Van Heerden, P. I., Appl. Optics, 1963, 2.

ILLUMINATION-ENGINEERING CALCULATION OF FLYING-SPOT PICKUP EMPLOYING CATHODE-RAY TUBE AND PHOTOMULTIPLIER

Metody i Ustroystva Preobrazovaniya Graficheskoy Informatsii (Methods and Devices for the Conversion of Graphic Data), 1968, pages 239-242

Yu. A. Zaborovskiy

Despite the research under way on the use of vidicons and dissectors to read graphic images the flying-spot pickup, due to its simple construction, relative simplicity of adjustment and minimal cost, remains as before the principal device for receiving information signals. The flying-spot pickup for sequential scanning of points of a carrier uses the light spot of some light source. Electromechanical devices for the processing and conversion of graphic data in the main employ incandescent lamps to form the reading beam. But electronic devices, which possess high speed, use the light spot of a cathode-ray tube (CRT) as a point light source, and a photomultiplier (PM) in order to register variations in luminous flux.

Studies of the flying-spot pickup employing a CRT and PM are known which investigate the image-"smearing" effect at the receiving end of a facsimile system as a result of the time constant of the phosphor of the CRT screen. The present article analyzes the transient dynamic characteristic of the flying-spot pickup employing a CRT and PM with application to graph reading. The error in graph conversion here depends to a significant extent on a proper estimate of the moments of the taking of reading values since, due to the finiteness of the size of the reading spot (aperture), the signal on the light-sensitive cell will not vary instantaneously as it approaches the boundary of contrast transition, but in accordance with a certain law, called the transient characteristic. The shaded area, normalized relative to the entire area of the spot as a function of its displacement, is represented by the graph depicted in Figure 1, while the analytically indicated dependence is described by the equation

$$S_{от}^{*} = \frac{S_{з}^{*}}{\pi r^2} = \frac{2\alpha - \sin 2\alpha}{2\pi}, \qquad (1)$$

*The Russian subscripts OT = relative; З = shaded.

where S_{shaded} is the shaded part of the spot;

$$\alpha = \arccos\left(1 - \frac{x}{r}\right) \text{ given } 0 < \alpha < \frac{\pi}{2}.$$

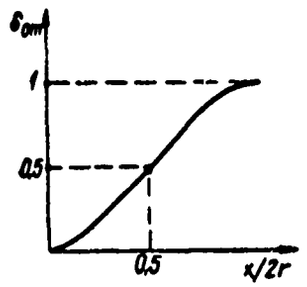

Figure 1. Static transient characteristic for case of cylindrical illumination distribution in spot.

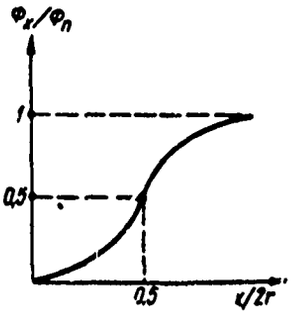

Figure 2. Static transient characteristic for case of normal illumination of distribution in spot.

With cylindrical illumination distribution of the light spot the transient characteristic will duplicate the form of dependence (1), shown in Figure 1, if we assume that the light-sensitive cell in the entire range of variation of luminous flux operates under linear conditions, i.e.,

$$U_{outputPM} = k\Phi_{flux}, \tag{2}$$

where Φ_{flux} is the integrated luminous flux incident on the photocathode; and k is coefficient of proportionality.

However, as research [1] has shown, the illumination of the CRT spot along its radius is described by an exponential dependence of the form

$$E = E_n e^{-\left(\frac{x}{r}\right)^2}. \tag{3}$$

Then the total luminous flux radiated into a space by the CRT spot will be defined as

$$\Phi_n^* = \iint_s E_n e^{-\frac{x^2+y^2}{r^2}} dxdy. \tag{4}$$

*Here and hereinafter the Russian subscript n = flux.

Under static conditions and at low reading speeds, i.e., when the time constant of phosphor persistence can be disregarded, the form of the transient characteristic can be estimated through calculation of the double integral described by formula (4). This dependence is represented in the graph in Figure 2 as a function of the shift of the center of the spot relative to the contrast-transition line.

Usually the operating point is selected in the middle of a linear segment which corresponds to the moment of finding the center of the spot on the contrast-transition line, on the assumption that the contrast transition itself is represented by a step function.

Under dynamic conditions due to the time constant of tube screen persistence T_{screen} an additional luminous flux $\Delta\Phi$ appears, which has a significant influence on the shape of the transient characteristic of the photooptical assembly as a whole.

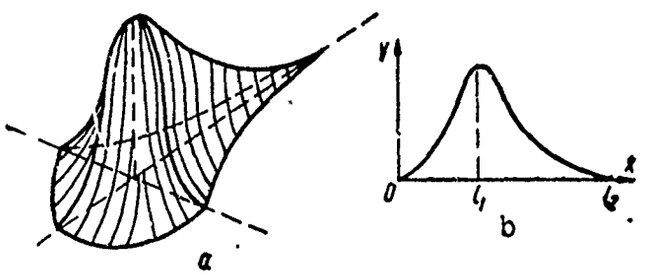

Figure 3. Shape of dynamic reading spot of cathode-ray tube:

a -- shape of spot; b -- law of brightness distribution.

For many phosphors the persistence characteristic obeys exponential law; for any moment of time the luminous flux from a point of the screen will be defined as

$$\Phi_t = \Phi_{n\text{flux}} e^{-\frac{t-t_0}{T_э}}, * \qquad (5)$$

where Φ_{flux} is the luminous flux excited by an electron beam at moment of time t_0.

Thus the given contrast transition is scanned by a CRT light spot, which is characterized by a complex law of illumination distribution (Figure 3, a, b). From the figure it can be seen that the shape of the spot is asymmetric in the xy plane, with illumination from 0 to l_1 obeying normal law, but from l_1 to l_2 exponential law; for a given phosphor time

*$T_э$ = T_{screen}

constant T_{screen} the magnitude of segment $l_1 l_2$ depends on the spot's rate of travel.

Analytic determination of the dynamic transition characteristic is a fairly complex and cumbersome problem; therefore, it is often solved by graphic computation. If we superpose static and dynamic characteristics on one graph (Figure 4), it is easy to find the magnitude of error Δl in the determination of contrast-transition coordinate, which error arises from disregarding T_{screen}.

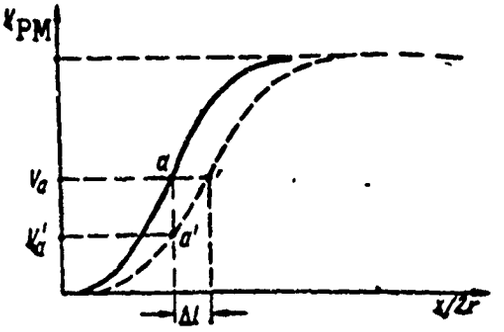

Figure 4. Determination of operating point of photooptical assembly.

To reduce this error to zero, information must be taken regarding the contrast-transition line at point a'.

Usually when the voltage on the PM reaches the magnitude V_a, a standard pulse generator is triggered, whose output signals are used to synchronize the entire device, it being given that

$$V_{trigger} = kV_a, \tag{6}$$

where k is the coefficient of amplification of stages situated between PM load and pulse generator. When the value of V'_a has been determined graphically, it is easy to find the necessary value of k'

$$k' = \frac{V_{trigger}}{V'_a}, \tag{7}$$

at which conversion error in the case of the given reading speed v and persistence time constant of the tube used T_{screen} will be minimal.

BIBLIOGRAPHY

1. Ryftin, Ya. A., ZhTF (Journal of Experimental Physics), 1953, 23, 7.

A METHOD OF CONVERTING CARTOGRAPHIC DATA FOR DIGITAL-COMPUTER INPUT

Metody i Ustroystva Preobrazovaniya Graficheskoy Informatsii (Methods and Devices for the Conversion of Graphic Data), 1968, pages 243-246

I. N. Krylov
Yu. B. Sadomov
L. M. Khokhlov

In the engineering practice of cartographic data processing the search for optimal solutions for the choice of routes of railroads, highways and gas pipelines, as well as the solution of other problems, as a rule, require the processing of large volumes of cartographic material, analysis of which is extremely time-consuming. The advisability of employing electronic computers for these purposes is obvious although their adoption in practice is delayed due to the lack of simple and efficient means for formalizing the process of cartographic data coding and computer input of the data.

The difficulties in the coding of cartographic material are due to the following causes: 1) the complexity of analytic representation of cartographic data (relief profiles, area contours) and the necessity of coding in a three-dimensional space; 2) the necessity of giving the qualitative characteristic (attribute) of a surface point (forest, water, field); 3) the particularly individual character of the operation of coding each separate map.

The following premises were used in the choice of a method. 1) A method for retrieving the map sectors needed for reading had to be chosen which did not involve sorting the material stored in the machine's memory. 2) The coding method had to meet the condition of minimum word-length. The importance of this condition is due to the principle of using a magnetic drum (MD) as the carrier of cartographic information. This limitation follows, firstly, from the fact that the information characterizing a map element is taken from one head of the MD in the form of a pulse train and therefore requires varying computer run time depending on word-length and, secondly, that the word-length characterizes the volume of cartographic material which can be put onto the MD.

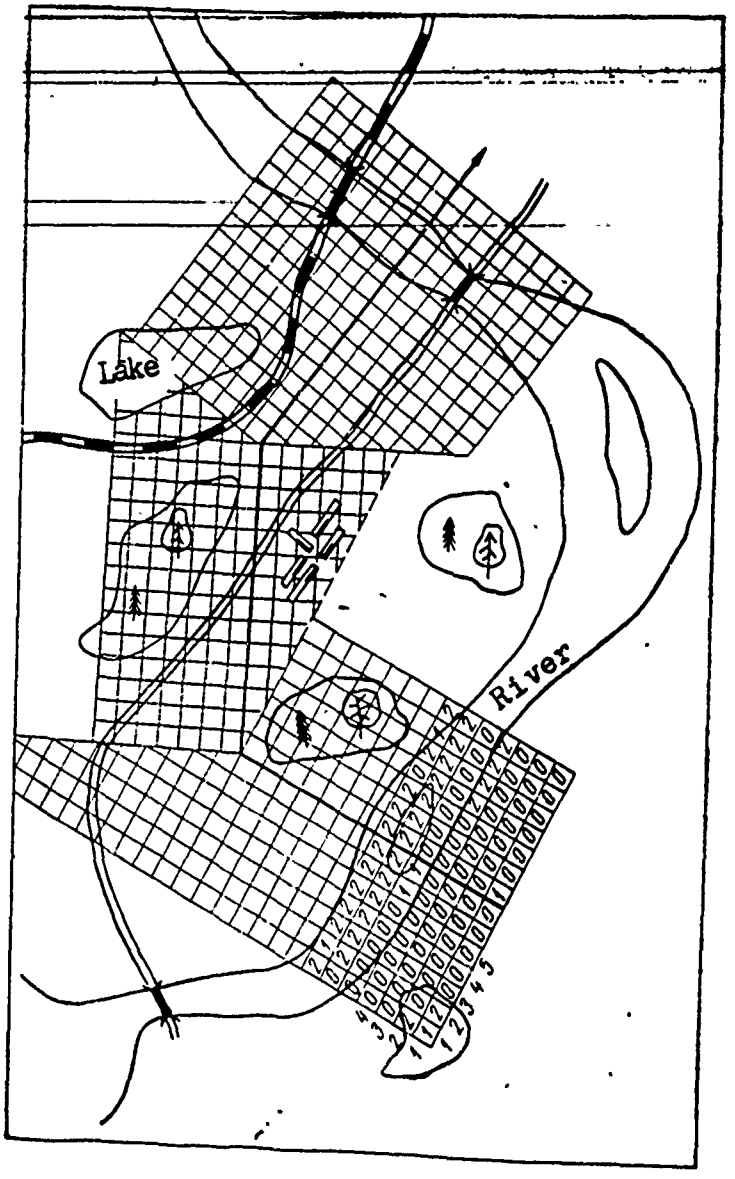

Figure 1. Discretization of map.

It is these circumstances which occasioned the necessity of employing the one-word coding principle, which determines map coordinates, terrain elevation and character for every terrain element. Subsequently it was possible to reduce the number of coding tags to two (terrain elevation and character). As for word-length, it is determined primarily by the prescribed accuracy of the investigation, diversity of the relief, and qualitative tags of the cartographic information.

Cartographic material is coded at the first stage on the basis of the foregoing methodological considerations. In the process the map is covered with a rectangular grid (Figure 1). Each cell of the grid is assigned a specific value of relative contrast or relative elevation of the relief. The contrast or elevation quantization range is selected in accordance with terrain character and the prescribed accuracy of the investigation. Thus the grid is filled with numbers from 0 to n-1 (n is the adopted number of gradations) and carries information accurate within a unit of the division. The information carried by the grid is coded by dividing each row into (n-1) parts with lines parallel to the reading lines and by arranging the numbers ("0" or "1") thus obtained in the cells (Figure 2). The numbers are arranged so that the sum of the ones, taken for (n-1) cells of the recording grid inside one cell of the original grid, is equal to the relative-contrast or relative-elevation value assigned to the given terrain sector. In view of the minimum word-length requirement in the principle selected, a capability must be sought whereby the same digits selected for characterizing relative terrain contrast or elevation can be used for coding terrain character. The positional arrangement of zeroes and ones inside the original grid is used for this purpose. For example, for the value "3" given n = 4 the arrangement of zeroes in the upper and lower cells characterized "water," zeroes in the first and third position a "forest," etc.

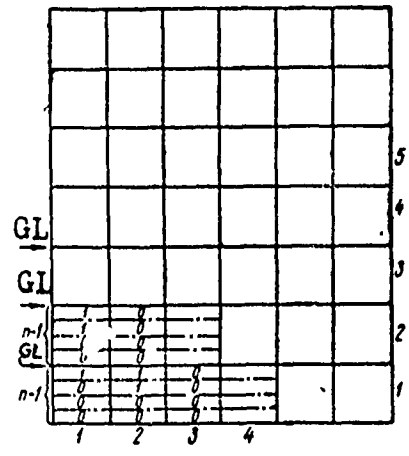

Figure 2. Arrangement of numbers in cells:

GL = grid line.

Obviously, further use of coded cartographic material -- its transfer onto the magnetic drum -- has to be effected by the digital computer itself in the usual way with arrangement of the zeroes and ones of the recording grid on their drum tracks and with rows along the generatrix of the cylinder.

Analysis of the advantages and deficiencies of this method is an exceedingly laborious task, for at present we have at our disposal an extremely limited arsenal of other technical means acceptable for the solution of analogous problems. However, the feasibility in principle, illustrated by the example here, of using existing magnetic stores which make possible the storage and digital-computer input of cartographic material in large volume by comparatively simple means, without any additional devices, indicates the necessity of a further serious search for methods applicable to specific problems in the digital-computer processing of cartographic data.

CORRECTION OF LINE FOLLOWING BY MEANS OF MULTISECTOR PHOTOHEAD

Metody i Ustroystva Preobrazovaniya Graficheskoy Informatsii (Methods and Devices for the Conversion of Graphic Data), 1968, pages 247-249

D. I. Kunin

One method of graphic data reading consists in line following: in the event of intersection of curves the center line of a given curve must be followed rather than its boundary. Due to variation in the curve slop angle, velocity errors and backlash of the servomechanism, the photohead PH leaves the curve being followed. In order to make the appropriate correction in the motion (return the PH and alter the following direction), we must know the direction of PH departure from the lines, i.e., their mutual positioning.

Let us consider a method of following whereby the PH makes no motion (scanning, turn of the head) other than a following motion. The image of a segment of a curve (for example, a circle with diameter approximately equal to line thickness) is broken into elements (sectors), with the photosignal from every element of the image striking its own photosensor. The breakdown can be made with the help of a mirror pyramid or position-sensitive photodiodes. The entire PH "field of vision" is divided by commutation of photosensor signals into two regions (accurate within half the dimension of a single element), left and right relative to the following direction. If the PH "field of vision" is divided into n sectors, commutation of the photosensors takes place with a 360° change in the following angle α_{fol}. Thus, one of the two groups of photosensors corresponds to each of the two regions of the PH "field of vision." The signals of individual photosensors making up a given group are summed, and the difference between the sum signals of groups is compared with reference voltage. The reference voltage sets the threshold at which a record is made if a PH goes beyond a line. Thus the comparison result is determined solely by PH shift relative to the center line of the curve and does not depend on line thickness. The sign of the difference between signals of the groups determines the direction of drift: If the signal of photosensors of the left group is

larger than the signal of photosensors of the right group ($U_{left} > U_{right}$), this means that the PH has moved to the left (relative to the course of motion) and the slope angle of the center line of the curve is smaller than the following angle, i.e., the PH must be brought to the right (relative to the course of motion), and the following angle decreased. If $U_{right} > U_{left}$, the converse holds true.

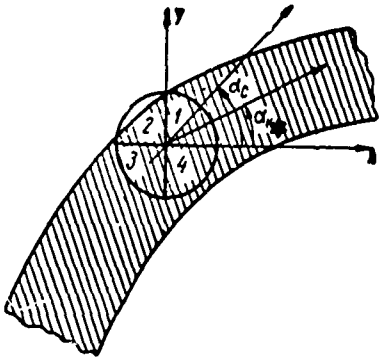

Figure 1. Schematic diagram of working principle of photohead.

Let us consider by way of example the construction of a photohead with a "field of vision" divided into four equal sectors, the boundaries of the latter coinciding with the coordinate axes (Figure 1). For such a PH, given following angles $315° \leqslant \alpha_{fol} \leqslant 45°$, the first and second photosensors belong to the left group, the third and fourth to the right group. In the event of an increase in the following angle at point $\alpha_{fol} = 45°$ the first photosensor is switched into the right group, and the third photosensor into the left group. In all there are four commutation points:

$$\alpha_{commutation} = 45° \pm \frac{\pi}{2} k \qquad (k = 0; 1; 2; 3).$$

If the following angle is in a range $315° < \alpha_{fol} < 45°$ and the signal of the left group is greater than the signal of the right group, the PH must be brought along y, and the following angle decreased. But if the following angle is in a range $45° < \alpha_{fol} < 135°$ and $U_{right} > U_{left}$, the PH must be brought along x, and the following angle increased, etc.

The construction of the PH is shown schematically in Figure 2. Due to the lack of position-sensitive photodiodes with the necessary properties a tetrahedral mirror pyramid and four photodiodes are used. The projection of the mirror surface of a pyramid onto a plane perpendicular to the optical axis of the PH is a circle. For visual monitoring the image is projected

(with the help of a cube with a semitransparent layer) onto a ground-glass screen.

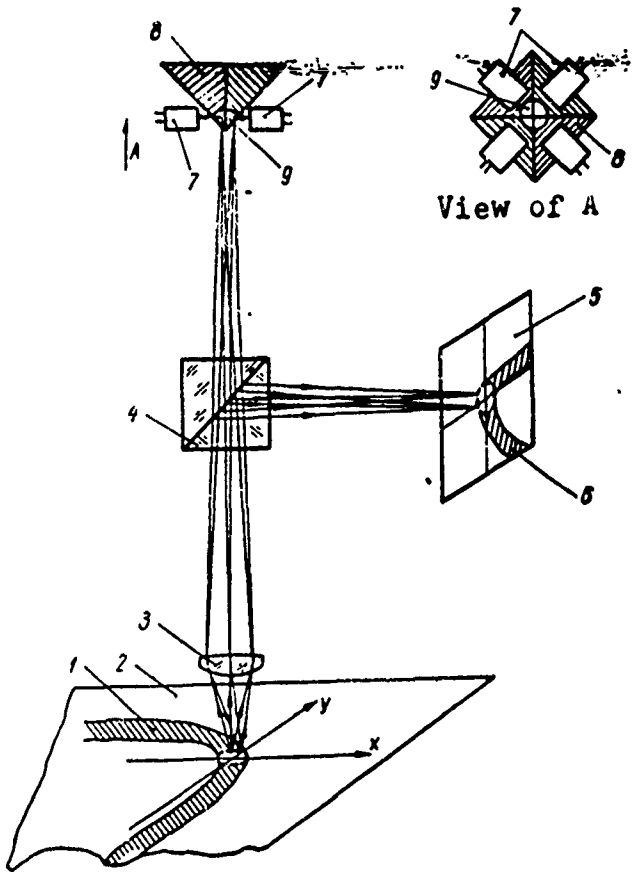

Figure 2. Construction of multisector photohead:

1 -- line being followed; 2 -- carrier (map, graph); 3 -- objective; 4 -- cube with semitransparent layer; 5 -- ground-glass screen with network of filaments parallel to coordinate axes, and with a circle within which light reflected from the carrier strikes the photosensors; 6 -- image of line on screen; 7 -- photosensors; 8 -- tetrahedral pyramid; 9 -- mirror surface of pyramid.

RATIO OF GATES IN MULTISECTOR PHOTOHEADS OF ELECTROMECHANICAL FOLLOWIN^ SYSTEMS

Yu. A. Romanenko

Metody i Ustroystva Preobrazovaniya Graficheskoy Informatsii (Methods and Devices for the Conversion of Graphic Data), 1968, pages 250-253

The magnitude and direction of the displacement of a system with a center curve line are determined by means of optoelectrical heads of electromechanical following systems, which perform the following of intersecting curves of multiple-valued functions. In some head designs this problem is solved by using an electromechanical scanning system and by rotating the photohead at an angle equal to the slope angle of the curve. In other cases the magnitude and direction of the displacement are found by projecting a curve segment in the form of a circle onto multisector position-sensitive photodetectors of varying construction [1, 2]. Electronic recognition systems, which analyze the signals from every sector photoelectric pickup, unambiguously determine not only the direction of photohead drift away from the curve being followed, but also the following angle α, which corresponds to the slope angle of the line being followed at the point of departure. Area S of the photohead's departure beyond the line is proportional to the sum signal of drift E of the photodetectors. To determine E, use can be made of the formula [3]

$$S = \pi R^2 \arccos\left(1 - \frac{h}{R}\right) - h(R-h)\sqrt{1 - \frac{h}{R}}, \qquad (1)$$

where R is the radius of a round multisector photodetector; h is the height of a segment formed by part of the photodetector outside the image of the curve boundary.

Thus, for a given sum threshold signal of drift E_0 there is a corresponding segment height $h = h_0$, strictly constant for all following angles α, which is equal to the admissible value of photohead displacement from the curve being followed. The reading of α is effected in

counterclockwise fashion, beginning with the bissectrix of the first sector.

In order to analyze drift signals e_n (n = 1, 2, ..., k is the number of the sector photodetector), it is more convenient to represent the circle with radius R (Figure) on a plane in the form of a dependence $\alpha = f\left(\frac{R}{h}\right)$. It is possible on this plane to select the value of h_o at which maximum error $\Delta\alpha$ will be constant for the case of the recording of departure by means of one photodetector ($E_o = e_n$) or several photodetectors simultaneously (for example, $E_o = e^*_{n,\_1} + e^*_{n\pm1,n}$).

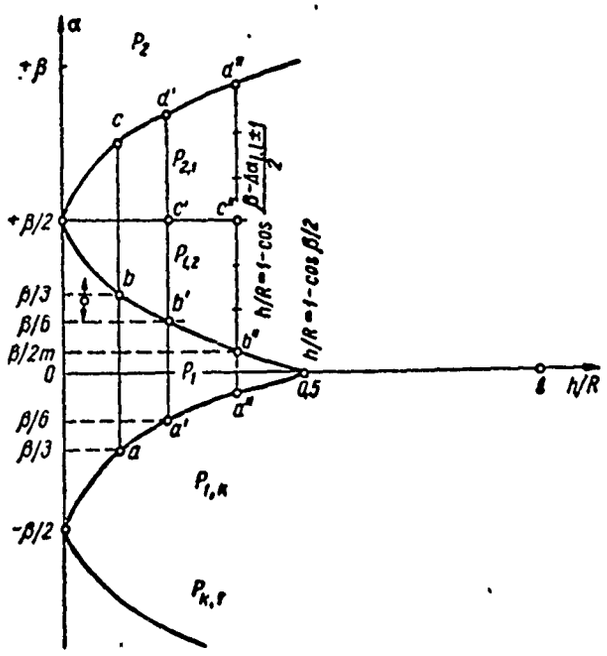

Graph of the dependence of quantity α on relation $\frac{h}{R}$.

If $0 \leqslant \frac{h}{R} < 1 - \cos\frac{\beta}{2}$, then maximum error $\Delta\alpha_n$ in the determination of following direction (recording of one-sector drift) equals maximum error $\Delta\alpha_{n,n+1}$ (recording of two-sector drift) in the case where ab = bc. Greater accuracy in the determination of α can be attained if we use not only the information about drift of any two detectors beyond the line boundary, but

*Here and hereinafter the second, third, etc., indices at the lower right indicate the number of the sectors which also issue drift signals.

also the result of a comparison of drift signals with each other. In this case the magnitude of maximum error will be equal on all following intervals if we take that ratio $\frac{h_0}{R}$ at which a'b' = b'c' = c'd'. The following angle is determined even more accurately by comparing each of the signals $e_{n,n\pm1}$ and $e_{n\pm1,n}$ with certain threshold levels and by identifying the slope angle of the curve as a function of the number of the threshold levels coinciding with the gate signals of individual sectors.

In compiling a table of threshold gate levels, the following expression can be used for the sector area corresponding to the gate signal of each of two photodetectors (for the sake of brevity in exposition, here presented without derivation)

$$S_{n,n\pm1} = \frac{\pi R^2}{180}\left[\arccos\left(1-\frac{h}{R}\right)+\beta\frac{1\pm2(n-1)}{2}\mp\alpha\right]-$$

$$-\frac{R^2}{2}\left(1-\frac{h}{R}\right)\left\{1-\frac{h}{R}+\sqrt{\frac{h}{R}\left(2-\frac{h}{R}\right)}\operatorname{ctg}\left[\beta\frac{1\pm2(n-1)}{2}\mp\alpha\right]\right\}, \qquad (2)$$

n = 1, 2, ..., k; k + 1 = 1; n - 1 = k given n = 1.

Let us designate as m the number of threshold quantization levels of signal e_n. Consequently, within region $P_{n,n+1}$ the maximum error in the determination of line boundary position is determined by the quantity

$$\Delta\alpha_{n,n\pm1} \leqslant \frac{\beta}{m}. \qquad (3)$$

By selecting the appropriate value of $\frac{h_0}{R}$ we can achieve fulfillment of the condition of equality of the maximum value of error in the determination of the angle in region P_n and region $P_{n,n-1}$ or $P_{n,n\pm1}$

$$\Delta\alpha_n = \Delta\alpha_{n,n\pm1} = \frac{\beta}{m}. \qquad (4)$$

The following direction at the point of departure from the curve is determined from the following expressions

$$\alpha = \begin{cases} (n-1)\beta, \text{ if } e_n = E_0;\ e_1 = e_2 = \dots = e_{n-1} = e_{n+2} = \dots = e_k = 0; \\ (n-1)\beta + i\frac{\beta}{m}, \text{ if } e_{n,n+1} + e_{n+1,n} = E_0;\ e_1 = e_2 = \dots = e_{n-1} = e_{n+2} = \dots = e_k = 0; \\ (n-1)\beta - i\frac{\beta}{m}, \text{ if } e_{n,n-1} + e_{n-1,n} = E_0;\ e_1 = e_2 = \dots = e_{n-2} = e_{n+1} = \dots = e_k = 0. \end{cases} \qquad (5)$$

Here i is the number of the threshold level (i = 1, 2, ..., m) coinciding in magnitude with the level of signal $e_{n,n\pm1}$.

BIBLIOGRAPHY

1. Belanov, A. P., and Maslovskiy, F. N., Primeneniye Poluprovodnikovykh Elementov v Vychislitel'noy Tekhnike -- Sbornik (Use of Semiconductor Elements in Computer Technology -- Collection of Works), "Sovetskoye Radio" (Soviet Radio), Moscow, 1965.

2. Gorbach, T. Ya., Krolevets, K. M., and Savelov, V. N., Avtomatika i Priborostroyeniye (Automation and Instrument Manufacture), 1964, 4.

3. Maslovskiy, F. N., Poluprovodnikovaya Tekhnika i Mikroelektronika (Semiconductor Technology and Microelectronics), "Naukova Dumka" (Scientific Thought), Kiev, 1966.

SEMICONDUCTOR AMPLIFIERS WITH SILICON PHOTODIODES FOR REGISTRATION OF SMALL LIGHT SIGNALS

Metody i Ustroystva Preobrazovaniya Graficheskoy Informatsii (Methods and Devices for the Conversion of Graphic Data), 1968, pages 254-258

L. Ye. Chevychalov
E. G. Saprykin

To amplify light signals for the purpose of reading graphic data by means of a multisector photohead and for the purpose of recording light-pip movements by raster-type pickups, photoamplifier circuits were developed at SNIIGGIMS [Siberian Scientific Research Institute of Geology, Geophysics and Mineral Raw Materials], which are distinguished by varying methods of connecting silicon photodiodes of the KFDM type.

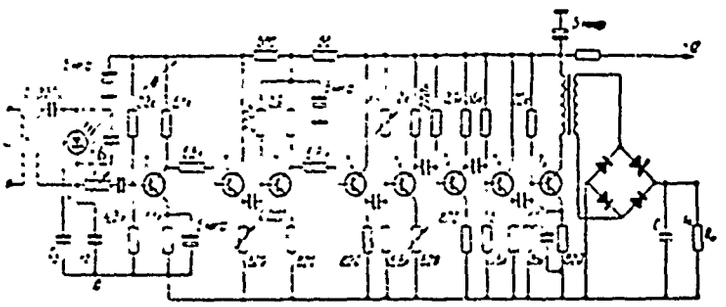

Figure 1. Schematic diagram of photoamplifier.
Key: MKϕ = microfarad

The photoamplifier, assembled according to the diagram shown in Figure 1, can be employed in the case of an illumination drop of 2-3 lx, with maximum value up to 4 lx. A photodiode, connected in parallel circuit, is used as a photovaricap, varying the capacitance of the p-n junction according to the illumination. The circuit is tuned to a pump oscillator frequency in such a way that with a variation in illumination the circuit

voltage varies according to intensity of the light signal. Capacitor C_1 separates inductance and varicap according to direct current.

As is known [1], in every semiconductor diode, in addition to the capacitance C_b of the p-n junction there is leakage resistance R_R of the junction and series resistance R_S. At low frequencies R_S can be disregarded. For silicon photodiodes R_R is large; therefore C_b is not able to recharge with an increase of frequency. Consequently, with the above-indicated scheme for cutting a photodiode into the circuit the upper cutoff frequency is determined by the expression

$$\tau = C_b R_R, \tag{1}$$

where τ is the discharging circuit constant of equivalent semiconductor diode; C_b is barrier capacitance of photodiode; R_R is leakage resistance of photodiode.

Barrier capacitance of photodiodes of the KFDM type has a magnitude of the order of several hundred picofarads, R_R of the order of several megohms, while upper cutoff frequency in this case has a magnitude of the order of 100 hertz. Accordant connection of the circuit to transistor amplifier input is effected with the aid of a capacitive divider formed by capacitors C_b, C_2 and C_3. To calculate circuit output resistance at points a, b, let us make use of the expression

$$C_{a,b} = C_2 + \frac{C_b C_3}{C_b + C_3}, \tag{2}$$

where $C_{a,b}$ is the equivalent capacity of the input part of the amplifier. If pumping frequency f = 500 kc, $C_2 = C_3 \approx 20$ picofarads, then output resistance of the circuit does not exceed 10 kohm.

The amplifier is mounted on eight transistors of the P415 type. Every pair of transistors forms a follower amplifier cell consisting of an amplifier and an emitter follower; this makes possible good matching of stages and stability of the entire amplifier channel. The third cell uses variable resistor R_{15} to limit the signal for setting the zero level, which corresponds to the minimum illumination of the photodetectors. The output transformer stage is mounted on triode T_8. The transformer is wound on a core of the SB-2a type. The transformer output is connected to a bridge rectifier using diodes of the D9B type. Output voltage on a load of 1 kohm varies from 0 to 2.5 v for positions of the photohead on the line and white field of the carrier respectively.

The photoamplifier, assembled according to the diagram depicted in Figure 2, is designed to amplify light pips which follow with a frequency of 0-10 kc and are produced by a raster-type pickup of angular displacements. The light pips are characterized by an illumination drop of 5 lx with maximum illumination of 30-40 lx. Stability requirements caused the

selection of a circuit with the conversion of the photosensor illumination signal into high-frequency alternating voltage. The carrier frequency taken was equal to 150 kc. For signal conversion a differential photosensor circuit diagram was devised which permits regulation of the initial amplification level. The necessary correction of the frequency characteristic of the photosensor is made in the output stage after extraction of the converted signal envelope. Stability of the coefficient of amplification is achieved by the employment of deep negative feedback.

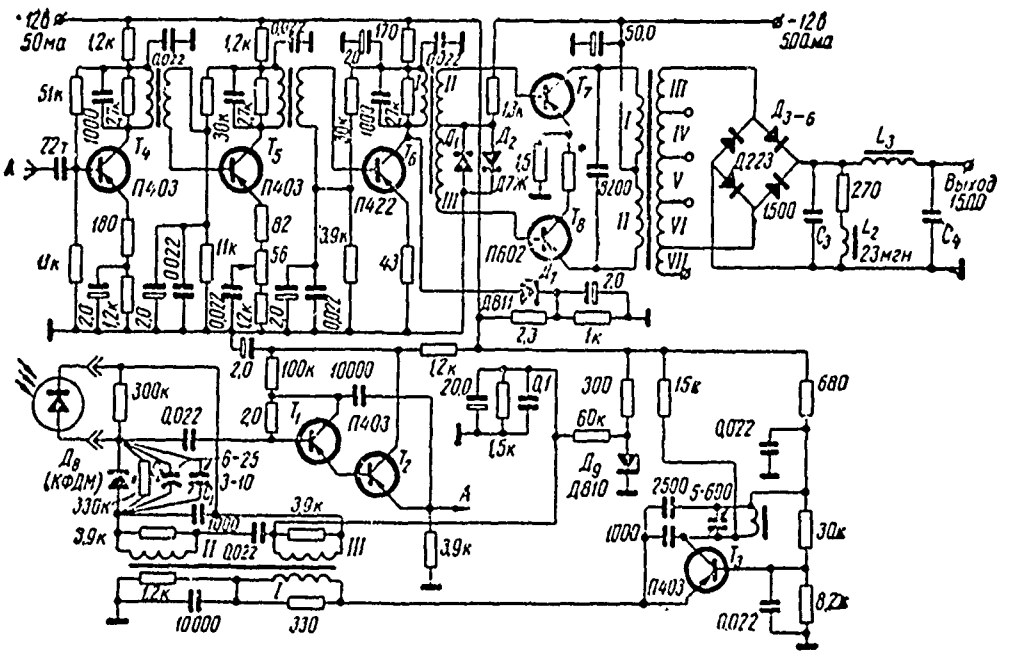

Figure 2. Schematic diagram of photoamplifier of signals from raster-type sensor.

Key: В = volt; Д(кфдм) = diode (of the KFDM type); Выход = output; Мгн = millihenry; Д = diode; п = follower

The input part of the amplifier is a differential measuring device DMD, one of the circuits of which includes a silicon photodiode installed in a raster-type pip sensor. In the event of the equality of capacitances in the DMD circuits the output signal equals zero. In the event of change in KFDM parameters as the result of illumination at the circuit output an unbalance signal appears, the magnitude of which is estimated according to the formula

$$U_{output} = \frac{1}{2} U_{pumping} \frac{\Delta C}{C} , \quad (3)$$

where C is capacitance in the DMD circuit; ΔC is variation in capacitance with illumination; $U_{pumping}$ is pumping voltage. The DMD is powered by a generator mounted on triode T_3 according to capacitance Hartley oscillator circuit. Precise zero balancing of the circuit is achieved by connecting the photodiode to the second DMD circuit analogously to the circuit in the sensor, by selecting shunt resistances and by supplying cutoff voltage to photodiodes. Balancing of the input circuit, i.e., selection of the initial reading level of the light signal to be amplified, is effected by capacitor C_1. Precise zero balance is additionally achieved on the initial adjustment of an amplifier by selecting photodiode-shunting resistances.

The unbalance signal goes from the DMD to an emitter follower which is mounted on transistors T_1 and T_2 and distinguished by high input resistance. From the output of the emitter follower the unbalance signal is fed to the input of a band-pass amplifier with a pass-band not less than 20 kc at level 0.9. The band-pass amplifier consists of three resonance stages, mounted on transistors T_4, T_5 and T_6. To widen the amplifier pass-band the circuits are shunted by the resistance and detuned relative to average pass-band frequency. Stages are assembled in accordance with a common-emitter circuit. Amplification stabilization is achieved by having each stage provided with deep negative d-c and a-c feedback. Amplification control is accomplished by potentiometer R_1 in the negative feedback circuit of the second stage. The output stage is assembled according to a push-pull common-emitter circuit using transistors T_7 and T_8.

For temperature stabilization displacement to triode bases is supplied from germanium diode D_1. The voltage going to the final stage is limited by stabilitron tube D810. Modulating illumination voltage is separated by the bridge detection circuit at the output of the band-pass amplifier. Suppression of carrier frequency voltage is achieved by a low-frequency pi-section filter $C_3L_3C_4$. The output stage operates on a mismatched load. The necessary rise in frequency characteristic at high modulating frequencies is effected by varying the load resistance of the output stage. The resistance of correcting inductance L_3 increases with an increase in modulating frequency; output voltage also increases.

Phase shifts due to correction inductance and the low-frequency filter have unlike signs and are partially compensated. As a result the phase shift does not exceed 0.15 π.

BIBLIOGRAPHY

1. Berman. A. S., Varikapy (Varicaps), "Energiya" (Energy), Moscow-Leningrad, 1965.

WIDENING THE DYNAMIC RANGE OF OSCILLOGRAMS

Metody i Ustroystva Preobrazovaniya Graficheskoy Informatsii (Methods and Devices for the Conversion of Graphic Data), 1968, pages 259-261

O. K. Skikevich

One of the shortcomings of the beam graphic recording of processes is the dependence of the width and density of the recorded trace on the velocity of travel of the light indicator. This phenomenon is especially perceptible at extremal values of the beam's velocity of travel and, all things remaining equal, depends on beam intensity. Thus, great illumination of the light spot and high velocities of its travel assure continuity of the curve being recorded, but at low velocities loss of the high-frequency component of the process being recorded occurs due to significant widening of the recorded trace and blurring of its edges. Conversely, with low illumination of the light spot the high-frequency section of the spectrum is recorded relatively well, but at the same time fractures in the recorded trace occur due to insufficient exposure of elemental areas of the carrier.

The above-described shortcoming shows up most markedly during the recording of irregular processes having wide frequency and dynamic ranges. Therefore the oscillograms obtained often require considerable effort on the part of the operator during visual processing, and this lowers labor productivity. In addition, the oscillograms obtained frequently prove unsuitable for reproduction or computer input. As a result, the extent of travel of the light indicator must be limited, i.e., the dynamic range of oscillograms must be curtailed.

To improve the information characteristics of oscillograms a method was suggested for automatically regulating the intensity of the writing beam approximately proportionately to its velocity of travel. The first version of a device based on the above-described principle was developed by the author of the present article in 1958. The device uses a diaphragm of parallel slits, through which the light beam of a lamp, reflected by a

galvanometer mirror, illuminates a photocell, creating in the circuit pulses with a repetition rate proportional to the beam's velocity of travel. Pulses are used to control the lamp's filament current by means of a simple electronic circuit with appropriate correction for the lamp's nonlinear conversion. In the second version of the device, developed in the United States in 1959, the input signal goes via a cathode follower to d-c amplifier and differentiator, then to phase inverter, modulator, voltage amplifier and power amplifier. The lamp of the galvanometer illuminator is connected to the power amplifier output, and the recorded signal goes to the frame of the galvanometer.

The production of oscillograms with traces of uniform density and width made it possible to separate and recognize intersecting curves because it became possible to register the third axis of measurement with a physical dimension (the initial filament current of illuminator lamps can be set differently for each channel).

However, the devices here under consideration did not find wide application in view of the fact that they did not permit realization of the principal advantage of the light-beam recording of processes -- simplicity, reliability and ready feasibility of recording a practically unlimited number of channels. Moreover, due to the thermal inertia of the incandescent lamp filament the frequency control band was limited at best to tens of cps, whereas with the help of modern frame galvanometers frequencies of 10 kc or more can be recorded.

In view of what has been set forth above, we undertook the attempt to develop a method of modulating the intensity of a light indicator in proportion to its velocity of travel for any number of recording channels without complicating the oscillographic instruments with electronic circuits. For this purpose use was made of a special light modulator, made of photochromic material (of the spiropyran type in polymeric films). A distinctive feature of photochromic systems is the reversible change of their coloration and the direct effect, which eliminates the necessity of "wet" chemical development.

Photochromic film is placed between the collector cylindrical lens and the photosensitive layer of the recording medium, in immediate proximity to it, in such a way that a streak of light, gathered into a spot, passes through the film before hitting the photosensitive layer. The radiation of the ultra-high-pressure mercury lamp used in the illuminator has a characteristic line spectrum consisting of a number of lines in the UV and visible regions. In simplified form, we can visualize the light indicator containing radiations $h\nu_1$ and $h\nu_2$ to which the photoch omic modulator and recording medium respectively are actinic. The kinetic characteristic of the process of coloration of the elemental area of photochromic film is described in first approximation by exponential law, the transition from initial state to colored state taking place comparatively rapidly (fractions of a second), and the rate of increase in density with low radiation flux $h\nu_1$ being close to linear.

During the travel of the light indicator over the photochromic film a trace forms on it, the density of which is clearly determined by the rate of travel of the light spot. By appropriately selecting the characteristics of photochromic film and recording medium, as well as the intensity and spectral composition of the light indicator conditions can be achieved whereby the intensity of the radiation $h\nu_2$ acting upon the recording medium is controlled by the photochromic system in proportion to the light indicator's velocity of travel. Spontaneous transition of the photochromic system to the initial state (dark reaction) takes place slowly (tens of minutes). Therefore, in order to prevent repeated influence of the light indicator which travels along only one ordinate, the photochromic film is given a certain constant velocity in the direction of the axis of abscissas.

In construction the oscillograph with a photochromic modulator does not differ from known types -- for example, from oscillograph N-107, because photochromic film is easily wound on a reel into a roll together with the recording medium and drawn by the tape transport included in the design of the instrument. The photochromic film can be used several hundred times repeatedly.

The modulator suggested here makes it possible with the simplest hardware to improve the information characteristic of oscillograms in the entire range of frequencies recorded by light-beam instruments for practically any number of recording channels.

GENERAL-PURPOSE LIGHT-BEAM ELECTROGRAPHIC RECORDER EFR

Metody i Ustroystva Preobrazovaniya Graficheskoy Informatsii (Methods and Devices for the Conversion of Graphic Data), 1968, pages 262-263

A. K. Skikevich

Electrophotographic recorder EFR is intended for light-beam visible graphic recording of various physical and geophysical processes under steady-state conditions.

The operation of the recorder is based on the principle of obtaining an electrographic reversed image on paper coated with a layer of a photo-semiconductor, formed by fine particles of zinc oxide dispersed in a dielectric binder. Semiconductive paper becomes light-sensitive in the process of electrostatic sensitization, which consists in the deposition of negative electric charges on the surface of the semiconductive coating. After passing through a charger, the paper, moved along by a tape transport, arrives in the exposure zone. Here, in places hit by light beams the resistance of the semiconductive coating of the paper decreases, and a potential pattern forms on it. The latent electrostatic image is visualized by a developer consisting of a liquid (a mixture of carbon tetrachloride and gasoline or freon) possessing high specific resistance, in which is dispersed a colorant (experimental printing ink No. 1), which acquires a negative charge during triboelectrification. Under nominal operating conditions of the instrument development is followed by a black-line recording on a bright carrier background -- rose or white (depending on the type of paper used). The liquid rapidly evaporates, and an oscillogram -- resistant to external influences -- of the recorded process forms on the tape.

Structurally, the device consists of several separate blocks interconnected by electric cables. By combining these blocks it is possible to obtain various performance characteristics of the device, and this explains its general-purpose capability. A distinctive feature of the EFR is its

ability to record processes in the 0-25 cps frequency range by light indicator with optical-lever length of 2,000 mm at recording amplitudes up to 100-150 mm. For comparison let us point out that the electrographic oscillograph of type N001 has an optical-lever length of 300 mm and permits the recording of processes in the 0-3 cps frequency range with recording amplitude of 15-20 mm.

An increase in the optical lever of light-beam recorders involves several difficulties: 1) the illumination of the writing spot of the light indicator drops in proportion to the square of the length of the optical lever (for the present case this is extremely important since the sensitivity of a semiconductor carrier is at least an order of magnitude lower than the sensitivity of the oscillograph photographic paper); 2) with an optical lever over 800-1,000 mm the phenomenon of diffraction shows up, as manifested in a widening of the recorded trace and blurring of its edges. However, these limitations have been eliminated in the EFR by using a special high-transmission illuminator with an ultrahigh-pressure mercury-vapor lamp DRSh-100-2. The illuminator consists of a combination of a double projection condenser and a cylindrical lens which functions as an illuminating slit and transforms the optical image of the luminous body of the lamp into a segment of a thin (10-12 mm) horizontal line. Working length of the segment: up to 700 mm. This makes it possible to lay out a sufficient number (several tens) of recording channels. During optical adjustment of the device the vertically positioned cylindrical lens can be removed, thereby creating additional accommodations for installing system elements on the optical axis which they have in common. The prism block permits installation of the illuminator in the immediate vicinity of the recorder or its removal 4,000 mm away from the light-beam deflection systems. In view of the fact that at such a distance the magnetic fields created by the power circuits of the DRSh-100-2 lamp are insignificant, it became possible for the first time to record variations in the earth's magnetic field electrographically.

Let us cite the principal characteristics of the EFR recorder:

Width of recording medium	300 mm;
Type of carrier	semiconductive paper EFO-1, EFO-2, EFM-1;
Capacity of feed reel	250 m;
Rate of carrier transport	2 and 10 mm/sec;
Capacity of tank containing liquid developer	3 liters;
Power from a-c (50 cps) power supply network	220 v;
Power requirement	up to 270 w;
Weight of recorder block	17 kg;
Weight of electric power block	28 kg.

A pilot model of the EFR has been constructed by staff members of IZMIRAN [Institute of Terrestrial Magnetism, the Ionosphere and Radio Wave Propagation of the Academy of Sciences] USSR.

USE OF DIGITAL COMPUTER TO PROCESS HALFTONE IMAGES

L. P. Yaroslavskiy

Metody i Ustroystva Preobrazovaniya Graficheskoy Informatsii (Methods and Devices for the Conversion of Graphic Data), 1968, pages 264-[last page or pages missing]

Process simulation on general-purpose digital computers is an extremely efficient way of developing and investigating methods of image transmission and processing. Obviously, the use of digital computers for these purposes is not feasible without appropriate image-input and output devices. It should also be noted that the use of image-input and especially image-output devices goes beyond the limits of the above-mentioned problems and significantly widens the scope of digital-computer utilization in scientific research.

Image Discretization

For a halftone image to be put into a digital computer it must undergo discretization, i.e., must be converted into a sequence of digits. From the viewpoint of most efficient computer utilization it is, of course, always advisable to decrease the number of binary digits representing an image. The minimum number of binary digits describing an image equals the ε-entropy of an image, and this quantity can be attained with so-called generalized quantization, i.e., quantization of an image space taking into account the prescribed fidelity criterion and image statistics.

The methods and results of generalized quantization depend essentially on the fidelity criterion used and the statistics of the image ensemble to which the problem to be solved belongs. The realization of any method of generalized quantization in image input-output devices will significantly narrow down the range of problems solvable through the use of these devices. Therefore, it is advisable to base the design of image input-output devices on another, less efficient, but withal more universal principle of discretization -- that of so-called elementwise quantization.

It takes place in two stages. To begin with, an image representing a continuous two-coordinate brightness function is replaced by a two-dimensional set of brightness readings -- image elements. The brightness value of each image element is then quantized, i.e., is replaced by one of the values of a discrete set.

In the use of elementwise quantization the number of binary digits necessary to describe an image depends on the number of image elements and the number of image-element brightness-quantization levels. Therefore, one must use methods of breaking images down into elements and quantizing image-element brightness which, while preserving the prescribed quality of reproduction, permit reduction to a minimum of the number of image elements and the number of brightness-quantization levels.

As for the break-down of an image into elements, the following can be noted. In accordance with Kotel'nikov's theorem the number of readings per unit area of an image cannot be less than $4S_{x,y}$, where $S_{x,y}$ is the area occupied by the spectrum of image spatial frequencies on the plane of spatial frequencies. This quantity can be approximated with a reciprocal arrangement of readings (image elements) on the image plane such that there is dense packing of the image spectrum on the plane of spatial frequencies [1]. However, if the spectrum of spatial image frequencies is limited to a rectangle, the readings must be arranged in points of a rectangular lattice.

This method of discretization is most prevalent at present. However, the actual devices to create images, for example, optical instruments, beam aperture of cathode-ray tube, etc., are isotropic, and therefore the spectrum of real images is limited not to a rectangle, but a circle. In this case the arrangement of readings (image elements) at points of a perfect hexagonal lattice corresponds to optimum spectrum packing. It is calculated that this method of discretization makes possible approximately a 15-percent reduction in the number of image elements as compared with a rectangular lattice [1].

During the quantization of image-element brightness values the required number of quantization levels can be reduced if the value to be quantized is nonlinearly predistorted prior to uniform quantization. The type of optimum nonlinearity depends on the permissible accuracy of quantization, which in turn is determined by the character of the problem to be solved. In order to quantize halftone images intended for human inspection, permissible quantization accuracy is determined by the Weber-Fechner law, according to which error in the transfer of brightness B of image element ΔB must not exceed a magnitude proportional to the brightness of the element

$$\Delta B \leq \delta B,$$

where δ is the threshold of contrast sensitivity.

Thus, the limitation to relative quantization error

$$\frac{\Delta B}{B} \leqslant \delta.$$

is given. It is easily shown that in this case logarithmic predistortion must be employed before quantization, i.e., the value of quantity f(B), determined by the following equation:

$$\frac{f(B) - f_{min}}{f_{max} - f_{min}} = \frac{\ln \frac{B}{B_{min}}}{\ln \frac{B_{max}}{B_{min}}} \qquad (1)$$

must undergo uniform quantization. The number of quantization levels, moreover, must be equal to

$$L = \frac{\ln \frac{B_{max}}{B_{min}}}{\delta} \qquad (2)$$

Requirements Set for Image Input-Output Devices for General-Purpose Digital Computers

The quality of image input and output devices is characterized by the number of scanning elements, by the kind of light-signal characteristic of the device for image input into a general-purpose digital computer and by the kind of inverse signal-light characteristic of the device for image output from the computer, as well as by the number of signal quantization levels and speed of response. Devices are also characterized by the method of communication with the machine: in some cases an intermediate carrier in the form of punched cards or perforated tapes is used, in another case direct image input into and output from a general-purpose digital computer takes place.

Halftone image-input and output devices must satisfy the highest requirements. Let us consider the requirements set for the characteristics of these devices.

The number of image elements determines the size, or scale, of the image under study. Therefore, in choosing the necessary scanning standard one must proceed from the character of the problems contemplated. Experience shows that to model image transmission channels and solve many pattern recognition problems one can be satisfied with a standard of 256 x 256 elements, and sometimes with an even smaller standard. To reduce the amount of information to be put into the computer it is desirable that image input-output devices for computers be able to create a "hexagonal pattern."

It was shown above that with prescribed error logarithmic predistortion before quantization proves optimal. Correspondingly, the signal-light characteristic of the image-output device must be exponential. Let us determine the number of quantization levels necessary for input-output devices for halftone images intended for human inspection.

In "crude" quantization specific distortions show up on the image in the form of "false contours," the degree of noticeability of which is determined by contrast and size. Under usual illumination conditions "false contours" of maximum length will be unnoticeable unless their relative contrast exceeds 4-5 percent; therefore, δ in formula (2) should equal 0.04-0.05. With the use of photographic materials image contrast $\frac{B_{max}}{B_{min}} = 100$ can be obtained. With these quantities given, let us determine the necessary number of quantization levels if there is logarithmic predistortion before quantization.

$$L = \frac{\ln\frac{B_{max}}{B_{min}}}{\delta} = \frac{2.3 \cdot 2}{0.04} = 115.$$

The operating speed of image input-output devices determines the efficiency of experiments. It is desirable that the operating speed of the devices should not be less than the operating speed of the computer in use.

High-Speed Image Output Device for "Minsk-1" Electronic Digital Computer

The high-speed image output device for the "Minsk-1" electronic digital computer developed at the Institute of Information Transmission Problems of the Academy of Sciences USSR has the following characteristics: maximum number of scanning element with rectangular pattern -- 256 x 256 (switch to standards of 128 x 128 elements with rectangular and hexagonal pattern is possible); number of quantization levels -- 128; signal-light characteristic during photographic-plate and film recording -- exponential.

The device can be used with three indicators: indicator using cathode-ray tube 18LK2B for recording on photographic plate or film; indicator using long-persistence tube 13L036V; and indicator using a dark-trace storage cathode-ray tube (of the skiatron type).

Maximum output speed during recording on a cathode-ray tube for direct observation is 10,000 elements per second. Output speed in the event of the recording of high-quality images on photographic plate or film is limited by the time lag of the magnetic deflecting system and equals 50 elements per second.

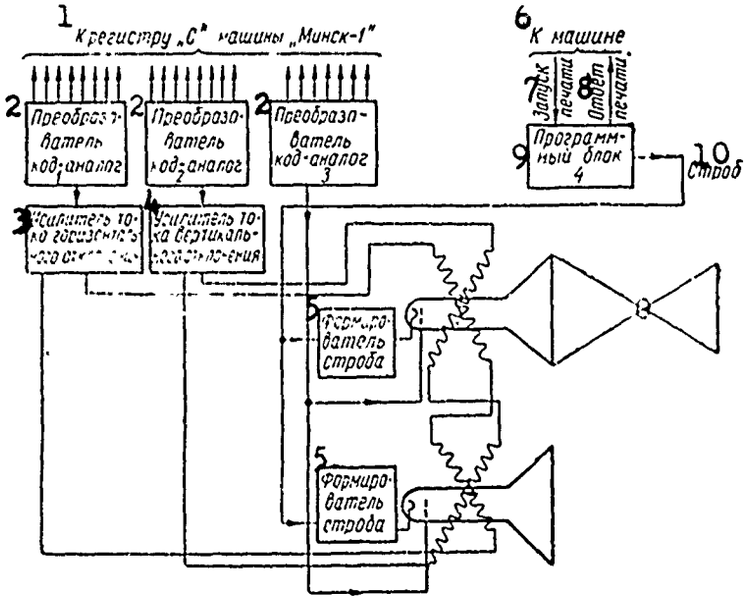

Figure 1. Block diagram of output unit.

Key: 1. To "C" register of "Minsk-1" computer
2. Code-to-analog converter 1, 2, 3
3. Horizontal-deflection amplifier
4. Vertical-deflection amplifier
5. Strobe shaper
6. To computer
7. Printer start-up
8. Printer response
9. Program block
10. Strobe

The device provides for two regimes: 1) autonomous elementwise scanning of rectangular patterns consisting of 256 x 256 elements and 128 x 128 elements and hexagonal pattern consisting of 128 x 128 elements; and 2) control from a digital computer.

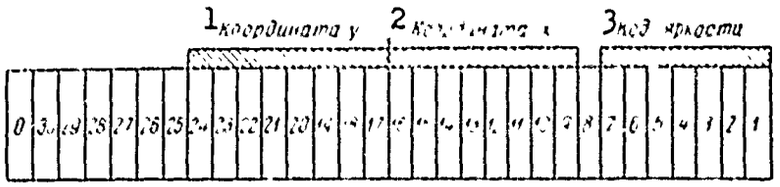

Figure 2. Code distribution in output register of "Minsk-1" computer.

Key: 1. Coordinate y
2. Coordinate x
3. Brightness code

During the output of high-quality halftone images the device must be synchronized with the power network in order to eliminate the influence of pickup from the network. In the event of the lack of synchronization, pickup will cause the appearance of extraneous markings on the image, which will cause significant deterioration in the quality of the reproducible image.

Figure 3. Output image of device.

A block diagram of the halftone image-output device under conditions of computer scanning control is shown in Figure 1. Eight-digit code-to-analog converters 1 and 2, connected to the output register of a "Minsk-1" computer, serve to convert the codes of the coordinates of the point which is to be displayed into the current of the deflecting coils of the indicator tubes.

[Remainder of source text missing.]